REGULATION OF MEDULLARY HOMEOSTASIS BY THYMIC EPITHELIAL CELLS

By

NICHOLAS IAN MCCARTHY

A thesis submitted to the University of Birmingham
For the Degree of DOCTOR OF PHILOSOPHY

The Institute of Immunology and Immunotherapy
College of Medical and Dental Sciences
University of Birmingham

August 2016

Abstract

The development of αβ T-cells is a step-wise process guided by unique stromal microenvironments within the thymus, which results in the formation of T-cells with a highly diverse repertoire of T-cell receptors (TCRs). In the latter stages of development, T-cell tolerance is established through the selective deletion of cells expressing auto-reactive TCRs, in addition to the generation of $Foxp3^+$ regulatory T-cells (T-Reg), which suppress autoimmune T-cell responses.

Central tolerance induction is mediated by interaction with functionally heterogeneous medullary thymic epithelial cells (mTEC), including distinct subsets expressing CCL21 and Aire. The aim of this study was to search for further mTEC-expressed functional molecules involved in medullary homeostasis and central tolerance. Here we identify two novel mTEC populations; cells expressing osteoprotegerin (OPG), a negative regulator of Rank-mediated mTEC maturation, and inducible nitric oxide synthase (iNOS), an immune-active enzyme catalysing the production of nitric oxide.

By investigating the impact of these molecules using knockout mouse models, we found OPG to restrict the size of the mTEC compartment, which in contrast to previous findings had no impact on T-Reg production, and instead limited the influx of peripheral lymphocytes to the thymus. In contrast, iNOS appears to play only a minor role in the maturation of single positive thymocytes in the medulla.

These findings identify novel heterogeneity within mTEC, and highlight the importance of functionally distinct mTEC compartments in maintaining medullary homeostasis.

Acknowledgements

Wholeheartedly, I would like to thank my supervisor Professor Graham Anderson for his guidance and support over the course of my PhD, and for mentoring me through the entirety of my fledgling scientific career to this point. I would also like to extend my thanks to my second supervisor, Doctor William Jenkinson, as it was Graham and Will's obvious enthusiasm and approachability during BMedSci seminars that inspired my interest in research.

I would also like to say a massive thankyou to all members of the T-cell Development group, past and present, who have always been there for me with help, advice and (occasionally) sympathetic ears! In particular, I would like to thank Sonia Parnell, Andrea White, Jennifer Cowan and Kyoko Nakamura, as well as Song Baik and Beth Lucas, who have all at times been fundamental to my lab work, and eating of biscuits. Equally, I wish the best of luck to Kieran James and Emilie Cosway, who are next up on the thesis chopping block!

Lastly, I would like to thank my friends, my parents, my brothers Connor and Colin, and my girlfriend Clare, for their continual support during the rough and the smooth of my PhD, and for making my life away from the lab that bit brighter!

TABLE OF CONTENTS

LIST OF FIGURES AND TABLES

LIST OF ABBREVIATIONS

()L	(Receptor) Ligand
aa	Amino acid
AID	Activation induced cytidine deaminase
Aire	Autoimmune regulator
aly	Alymphoplasia
APC	Antigen presenting cell
APECED	Autoimmune polyendocrinopathy candidiasis ectodermal dystrophy
Atg5 ; Atg7	Autophagy protein 5 ; 7
B220	B-cell isoform of 220 kDa
Bcl2 ; BclXL	B-cell lymphoma protein 2 ; extra-large
BCR	B-cell receptor
BFA	Brefeldin A
BrdU	Bromo-deoxyuridine
CCL (XCL)	Chemokine receptor ligand
CCR (CXCR)	Chemokine receptor
CD	Cluster of differentiation
cDNA	Complimentary DNA
CHOP	CCAAT-enhancer-binding protein homologous protein
Cld3,4	Claudin 3, 4
Clec16A	C-type lectin 16A
CLIP	Class-II associated invariant chain peptide
CLP	Common lymphoid progenitor
CRE	Causes recombination (recombinase)
cTEC	Cortical thymic epithelial cell
CTV	Cell trace violet
D	TCR gene diversity region
Da	Dalton
DAPI	4'6-diamidino-2-phenylindole
DC	dendritic cell
DETC	Dendritic epidermal T-cell
dGuo	2'deoxyguanosine
DKO	Double knockout
Dl4	Delta like ligand 4
DN	Double negative
DNA	Deoxyribonucleic Acid
DP	Double positive
E(n)	Embryonic day of development (n)
eNOS	Endothelial nitric oxide synthase
ETP	Earliest thymic progenitor
FACS	Fluorescence activated cell sorting

Fezf2	Fez family zinc finger 2
Fl	Flanked by LoxP site
Flt3	Fms-like tyrosine kinase 3
Foxn1	Forkhead box protein N1
Foxo1	Forkhead box protein O1
Foxp3	Forkhead box family transcription factor 3
FTOC	Fetal thymic organ culture
GFP	Green fluorescent protein
GITR	Glucocorticoid induced tumor necrosis factor receptor
GMP	Guanosine monophosphate
GOI	Gene of interest
HEL	Hen egg lysozyme
i.p.	Intraperitoneal
ICAM	Intercellular adhesion molecule 1
IFN	Interferon
IFNAR	Interferon alpha receptor
Ii	Invariant chain
IL	Interleukin
IL(n)R	Interleukin (n) receptor
iLNs	Inguinal lymph nodes
iNKT	Invariant natural killer T-cells
iNOS	Inducible nitric oxide synthase
ITAM	Immunoreceptor tyrosine-based activation motifs
J	TCR gene joining region
KIT	c-Kit receptor CD117
Klf2	Kruppel-like factor 2
Lck (p56Lck)	Lymphocyte specific protein tyrosine kinase
LFA-1	Lymphocyte function associated antigen 1
LMPP	Lymphoid primed multipotent progenitor
LoxP	Locus of crossing P1
LPS	Lipopolysaccharide
Ltbr	Lymphotoxin beta receptor
Lti	Lymphoid tissue inducer cell
M1	Mature stage 1 SP
M2	Mature stage 2 SP
MACS	Magnetic-activated cell sorting
MFI	Mean fluorescence intensity
MHC	Major histocompatibility complex
mRNA	Messenger Ribonucleic Acid
mTEC	Medullary thymic epithelial cell
MyD88	Myeloid differentiation primary response gene 88
NFATC3	Nuclear factor of activated T-cells 3
NFkB	Nuclear factor kappa B

NIK	NFkB-inducing kinase
NK cell	Natural killer cell
NLR	Nod-like receptor
nNOS	Neuronal nitric oxide synthase
NO	Nitric oxide
NOD	Non-obese diabetic
NOS1 ; 2 ; 3	Nitric oxide synthase 1 ; 2 ; 3
Notch-1	Notch-receptor family member 1
NT	Nitrotyrosine
Nur77	Nerve growth factor IB/77
OPG	Osteoprotegerin
OT-I	Ovalbumin transgenic TCR MHC-I restricted
OT-II	Ovalbumin transgenic TCR MHC-II restricted
OX40	Tnfrsf member 4, CD134
PAMP	pathogen associated molecular patterns
PBS	Phosphate buffered saline
PCR	Polymerase chain reaction
PI	Propidium iodide
Plet1	Placenta expressed transcript 1
Plt	Paucity of lymph node T-cells
pMHC	Peptide-MHC complex
POU6F1	POU class 6 homeobox 1 protein
PRR	pattern recognition receptors
PSGL1	P-selectin ligand 1
PUMA	p53 up-regulated modulator of apoptosis
Qa2	Qa lymphocyte antigen 2
Rag 1; Rag2	Recombinase activating gene 1; 2
Rank	Receptor activator of NFkB
RelB	Rel-like domain containing protein B
RIP	Rat insulin receptor
RLR	Rig-1-like receptor
RORγt	RAR-related orphan receptor gamma (thymic variant)
rRNA	Ribosomal Ribonucleic Acid
RTE	Recent thymic emigrant
Runx3	Runt-related transcription factor 3
S1P	Sphingosine 1 phosphate
S1P1	Sphingosine 1 phosphate receptor 1
SCF	Stem cell factor
SM	Semi mature SP
SNAP	S-nitroso-N-acetly-DL-penicillamine
Socs1	Suppressor of cytokine signalling 1
SP	Single positive
SP4	CD4+8- single positive

SP8	CD8+4- single positive
SSEA-1	Stage-specific embryonic antigen 1
T-Conv	Conventional T-cell
T-Reg	Regulatory T-cell
Tap	Transporter associated with antigen processing
TCR	T-cell receptor
Tdt	Terminal deoxynucleotidal transferase
TEC	Thymic epithelial cell
TGFβ	Transforming growth factor beta
Th1	T-helper cell type 1
Th17	IL-17-secreting T-helper cell
Th2	T-helper cell type 2
ThPOK	T-helper inducing POZ/Krueppel-like factor
TIR	Toll interleukin receptor homology domain
TLR	Toll-like receptor
TNF	Tumor necrosis factor
TNFRSF	Tumor necrosis factor receptor superfamily
TRA	Tissue restricted antigen
Traf6	TNF receptor associated factor 6
TRIF	Tir-domain-containing adapter-inducing interferon-beta
TSA	Tissue specific antigen
Tssp	Thymus specific serine protease
UPR	Unfolded protein response
V	TCR gene variable region
Xbp1(s)	X-box binding protein 1 (spliced)
YFP	Yellow fluorescent protein
Zap70	Zeta chain of TCR associated kinase 70kDa

1. INTRODUCTION

1.1. Function of the immune system

The immune system is the collective term for the body's mechanisms of defence against infection by pathogenic organisms such as bacteria, viruses, fungi and parasites, and from tumours and malignancies. Constant co-evolution alongside pathogens has led to the establishment of distinct co-operating compartments of immune cells, which co-ordinate to launch inflammatory responses to control and clear infection in mammalian organisms (Chaplin, 2010). Two distinct arms of the immune system operate to control infection: the innate system (Beutler, 2004), and the adaptive system (Romagnani, 2000). Adaptive immune responses require the activation and amplification of rare cell types, and hence require a period of 4-7 days post-infection to begin to launch a powerful, targeted immune response (Germain, 2001). However adaptive immune cells have the capacity for immunological memory – the formation of long-lived pathogen-experienced cells that can become rapidly activated and expanded in the instance of recurrent infection by the same pathogen (Ahmed and Gray, 1996, Gray, 1993). The early stages of infection are hence controlled by the immediate activity of innate immune cells, which are abundant, and activated in a comparatively non-specific manner (Janeway and Medzhitov, 2002). The makeup and function of both compartments varies with age – in infancy, the adaptive immune system is inexperienced to infections, and can only launch slower primary responses, and hence memory responses against life threatening childhood infections are routinely supplemented by vaccination (Plotkin, 2010, Anderson and May, 1985). The process of aging however slows the new

production of adaptive immune cells, and causes loss of function of the innate immune system, leaving the very elderly essentially immuno-compromised (Miller, 1996, Dorshkind et al., 2009, Shaw et al., 2010). The make-up and function of the immune system as a whole is strikingly similar between humans and mice, and hence much of our understanding of immune responses has been formed through observations in mouse models of cancer, infection and auto-immunity.

1.1.1. Innate immunity

Innate immunity is conferred by three broad mechanisms that act in largely non-specific terms to prevent and resolve infection - these mechanisms can be physical, chemical or cellular. Physical protection from infection comes from the maintenance of stromal barriers at external surfaces that physically impede the invasion of pathogens into the tissues to establish infection (Elias, 2007, Peterson and Artis, 2014). The effectiveness of this approach is demonstrated by the benign occupation of the human gut by an estimated 500-1,000 bacterial species (Sekirov and Finlay, 2009, Hooper et al., 2012), which are capable of causing devastating peritoneal infections on perforation of the intestinal wall. Specialization of epithelial cells present in external barriers also contributes to innate immunity directly. In the lungs, goblet cells produce viscous mucous capable of trapping bacteria, which is physically expelled by the beating cilia of the respiratory epithelium (Rogers, 2003, Williams et al., 2006). At these surfaces, bacteria are also targeted for direct killing by chemical anti-microbial mechanisms. The low pH of the skin renders it inhospitable to the

majority of potentially pathogenic organisms, while the production of digestive acids in the stomach limits the survival of bacteria to reach the lower gastro-intestinal organs. The paneth cells lining the crypts of the small intestine also secrete an array of non-specific anti-microbial peptides, such as defensins, which cause cytotoxicity through disruption of bacterial cell membrane integrity (Ayabe et al., 2000, Ganz, 2003).

The cells of the innate immune system are derived from haematopoiesis in the bone marrow. Innate cells include largely secretory populations, such as mast cells, basophils and eosinophils, as well as broadly phagocytic cells, including monocytes - which continually differentiate into macrophages in residence in the tissues - neutrophils and dendritic cells (DC), which capture and present antigen for the priming of the adaptive immune system (Janeway and Medzhitov, 2002, Paul, 2011). Upon activation, macrophages and neutrophils can contribute to direct killing of bacteria from the early stages of infection, through their uptake into the cell by phagocytosis (Nagl et al., 2002), production of toxic reactive oxygen and nitrogen species (Robinson, 2009, MacMicking et al., 1997, Forman and Torres, 2002), and the generation of neutrophil extracellular traps (Brinkmann et al., 2004).

The activation of innate immune cells is characterised by recognition of pathogen associated molecular patterns (PAMPs): specific bacterial or viral components that trigger signalling through receptors common to multiple sub-types of innate immune cells (Bianchi, 2007). PAMPs include key structural or replicative microbial components that cannot be altered structurally without severely impacting fitness, and hence have persisted to allow for the evolution of specific pattern recognition receptors (PRRs), which are constitutively expressed

by innate immune cells (Kimbrell and Beutler, 2001). Bacterial PAMPs are not unique to pathogenic strains, and are abundant in the normal flora. Hence compartmentalization of innate cells by epithelial barriers is thought to be essential to prevent unwanted activation of innate cells through PRR triggering in steady state conditions.

PRRs include intracellular and extracellular trans-membrane receptors, such as the toll-like receptor (TLR) family (Hemmi et al., 2000, Hoshino et al., 1999, Takeuchi et al., 1999, Hayashi et al., 2001), as well as free cytoplasmic receptors, including NOD-like (NLR) and RIG-like (RLR) receptor family members (Chen et al., 2009, Yoneyama and Fujita, 2007, Yoneyama et al., 2004). Engagement with PAMPs causes recruitment of adapter proteins (MyD88 or TRIF) via homotypic Toll/interleukin receptor domain interactions (O'Neill and Bowie, 2007), triggering downstream signalling events resulting in the production and release of inflammatory mediators known as cytokines. Cytokines are small 5-20kDa proteins released by cells that can modulate the activity of local cell populations through the binding of receptors. The effects of cytokines can be pro- or anti-inflammatory (Paul and Seder, 1994, Arai et al., 1990, Dinarello, 1997), and chemotactic cytokines (chemokines) can induce targeted trafficking of immune cells by the process of chemotaxis (Rot and von Andrian, 2004, Luster, 1998). PRR activation of macrophages and DCs triggers the production of pro-inflammatory cytokines, including interleukins, such as IL-1β, IL-6, IL-8, IL-12 and TNFα, although the exact cytokine profile can depend on the receptor route of activation (Dinarello, 2000). Through release of pro-inflammatory cytokines, activated innate cells can act systemically to cause fever and a lowered pain threshold, as well as modifying the local environment, triggering vasodilation and endothelial expression of chemokines

and cell adhesion molecules (Ley and Kansas, 2004, Miyasaka and Tanaka, 2004), and allowing continual recruitment of phagocytes to the site of infection.

1.1.2. Adaptive immune responses

In a similar vein to innate immune cells, the cells of the adaptive immune system, B- and T-lymphocytes, can become activated upon receptor engagement with specific components of pathogenic organisms. Unlike innate receptors, the structures of which are conserved to engage with a restricted range of viral and bacterial components, adaptive immune receptors are formed by a series of random gene recombination events, providing extensive variation in structure (Schatz, 2004, Tonegawa, 1983). Hence, although individual B-cells and T-cells express a single clonal receptor (Brezinschek et al., 1995, Arstila et al., 1999), the total pool of adaptive immune cells has the theoretical capacity to specifically recognise any component of an invading pathogen. Such components, "antigens", are recognized differentially between B- and T-cells. B-cells express the B-cell receptor (BCR), which is surface-expressed by immature B-cells, becoming activated on engagement with 3-dimensional structures on whole antigens known as epitopes (Reth, 1992, Amit et al., 1986). B-cells hence have the capacity to become activated by proteins, lipids or saccharides (Stein, 1992, Haji-Ghassemi et al., 2015). Upon activation, B-cells differentiate to form memory B-cells (McHeyzer-Williams and McHeyzer-Williams, 2005), as well as plasma cells with the capacity to secrete antibody (Dal Porto et al., 1998), a form of the BCR lacking the integral membrane domain required for tethering to the cell membrane (Honjo, 1983, Williams and Barclay, 1988). Through antibody

secretion, B-cells act to target pathogens and infected cells directly, triggering antibody-mediated cell death through activation of serum complement proteins (Kay et al., 1977), as well as indirectly by opsonisation, the process of facilitating phagocytosis by innate immune cells (Aderem and Underhill, 1999). In addition, B-cells have the unique capacity to modify their receptor through two processes involving the activation induced cytidine deaminase (AID) protein – class switching, and somatic hypermutation (Muramatsu et al., 2000). Class switching involves switching the conserved heavy chains to alter the properties of the antibody, allowing B-cell clones with identical receptor specificities to produce antibodies with different properties (Jung et al., 1993). Somatic hypermutation requires B-cells to form structures known as germinal centres, in which they undergo AID-induced point mutations to the BCR gene, which subtly alter the antigen specificity of their receptor (Bernard et al., 1978, Rogozin and Kolchanov, 1992).

In contrast to the BCR, the T-cell receptor (TCR) can become activated only on engagement with short peptide sequences, and hence is restricted to recognising protein antigens. Moreover, T-cells cannot engage with antigen in it's native capacity, and require proteins to be processed into short peptides and loaded into major histocompatibility complexes (MHC), before presentation on the surface of antigen presenting cells (APCs) (Iwasaki and Medzhitov, 2010). The antigen specificity of the TCR is hence for peptide-MHC complexes (pMHC), rather than peptide alone, and the capacity for T-cell activation is equally determined by the context of antigen presentation (Reinherz et al., 1999). As MHC alleles are highly polymorphic, an identical peptide presented by cells with a differing MHC haplotype may not invoke TCR activation (Zinkernagel and

Doherty, 1997, Zinkernagel and Doherty, 1979). There are two classes of MHC molecules involved in antigen presentation to conventional T-cells; MHC class I (MHC-I), which is expressed ubiquitously, and MHC class II (MHC-II), expression of which is largely restricted to professional APCs, including B-cells, macrophages, and most importantly dendritic cells (DCs), which are highly effective in promoting T-cell activation (Schwartz, 1985, Sallusto et al., 1995).

1.1.3. The structure of the T-cell receptor

The TCR is a multimer comprised of two regions – one conferring antigen specificity, and a second aiding in signal transduction to trigger T-cell activation. Antigen specificity is determined by a surface-bound heterodimer consisting of TCR α, β, γ or δ chains. The focus of this study will be conventional T-cells, which pair the α and β chains, however comparatively rare subsets of innate-like cells express γδ TCRs that have been shown to become activated in an unconventional manner in response to molecules related to stress responses (Raulet, 1989). The structure of the TCR α and β genes consists of four regions; a leader region of 18-29amino acids, a variable segment (V) of 88-98aa, a joining segment (J) or 14-21aa, and a final diversity segment (D), which shares structural homology to immunoglobulin constant regions (Malissen et al., 1984, Davis and Bjorkman, 1988). Gene recombination events result in pairing of either V-J or V-D-J regions to form a functional TCR gene. Many copies of the V, D and J segments appear within the gene locus of both TCRα and TCRβ, and hence random recombination events have been predicted to be able to form genes coding up to $2.9x10^{22}$ unique viable receptors (Lieber et al., 1988, Bassing et al., 2002). This is

supplemented further by the action of terminal deoxynucleotidal transferase (Tdt), an enzyme which catalyses the addition of random nucleotides to the junctions between V-D-J regions (Gilfillan et al., 1993). Interestingly, gene recombination can only yield one productively rearranged TCRβ allele, as a result of a process known as allelic exclusion (Malissen et al., 1992, Levelt et al., 1995). In the majority (60%) of developing T-cells, rearrangement is only attempted on a single allele, and if performed successfully, this gene is exclusively expressed for the formation of the αβ TCR. However, in the remaining 40% of instances, T-cells possess two rearranged alleles, where one is non-productively rearranged, suggesting that re-arrangement of the second only occurs in the event that the first attempt failed to yield a functional TCR chain (Michie and Zuniga-Pflucker, 2002). The TCRαβ dimer associates with the CD3 complex, a signal-transducing complex formed of four transmembrane proteins; CD3γ, δ, ε and ζ. The products of the CD3 γ, δ and ε genes are members of the immunoglobulin superfamily, and are hence structurally similar, possessing negatively charged amino acids in their transmembrane domains that allow for stable association with the TCRαβ dimer (Clevers et al., 1988, van der Merwe and Dushek, 2011). CD3ζ is structurally unrelated to the other CD3 complex components, and consists of a short external region, a transmembrane domain, and a cytoplasmic tail. The cytoplasmic domain of CD3ζ contains multiple conserved immunoreceptor tyrosine-based activation motifs (ITAMs), which are accessible for phosphorylation by $p56^{Lck}$ kinase after conformational changes caused by TCR-pMHC engagement (Irving and Weiss, 1991, Weiss and Littman, 1994). Doubly phosphorylated ITAMs on CD3ζ can recruit and activate the

kinase Zap70, which is sufficient to initiate the downstream portions of the TCR signalling cascade (Love and Hayes, 2010).

1.1.4. Antigen presentation

Peptide antigen is displayed for recognition by the TCR in MHC molecules on the surface of antigen presenting cells. MHC-I is expressed by all nucleated cells, and consists of a heterodimer between the MHC-I heavy chain, and the ubiquitously expressed polypeptide β2-microglobulin (Natarajan et al., 1999, Koller et al., 1990, Zijlstra et al., 1990). The heavy chain consists of three regions – an extracellular section consisting of α1, α2 and α3 domains, a transmembrane region, and a short cytoplasmic tail (Schwartz, 1985). The α1/2 domains form the peptide-binding groove, allowing for presentation of antigens between 8-10aa in length (Engelhard, 1994, Falk et al., 1991). MHC-II molecules are heterodimers of class II α and β chains (Kaufman et al., 1984), which are similarly structured to the heavy chain of MHC-I, with their extracellular domains allowing the presentation of slightly longer peptides (13-24aa) (Engelhard, 1994, Falk et al., 1991). Peptides bound in MHC-I and MHC-II are targeted by two distinct populations of T-cells defined by differential expression of the co-receptors CD4 and CD8, which act to strengthen TCR-MHC interactions, as well as recruiting the kinase Lck to the TCR signalling complex (Weiss and Littman, 1994, Cantrell, 1996). The β2 domain of MHC-II features a binding site for CD4, which acts as a co-receptor for TCR binding in $CD4^+$ "helper" T-cells (Janeway, 1992), which strengthen and direct the immune response through secretion of cytokines, and expression of co-stimulatory molecules (Rahemtulla

et al., 1991). Conversely, the α3 domain of MHC-I enables binding of the co-receptor CD8 (Kern et al., 1998), which is expressed by "cytotoxic" T-cells, which release perforins, granzymes and granulysin to contribute to the direct killing of tumour cells, as well as those infected by intracellular pathogens (Koller et al., 1990).

The antigens displayed in MHC-I/II differ in source. As MHC-I is ubiquitous, and hence expressed by non-professional APCs without explicit mechanisms for the uptake of antigen from the cytosol, antigens are largely newly produced endogenous peptides derived from proteins in the cytoplasm. Misfolding of these proteins during production results in their ubiquitination; that is, the covalent attachment of the small 8.5kDa protein ubiquitin (Pickart, 2001). This acts as a tag which directs unwanted proteins to the proteasome, a cytoplasmic macromolecular structure with a 20S cylindrical core capable of catalysing cleavage of polypeptides (Groll et al., 1997). The core consists of 2 outer rings, and 2 inner rings, each consisting of 7 subunits; α1-7 and β1-7 respectively (Groll et al., 1997). Of these, β1, β2 and β5 are catalytically active, and display preferences to cleave polypeptides after acidic, basic and hydrophobic residues to produce short peptide antigens for loading (Rock et al., 1994). Furthermore, peptides are loaded to the endoplasmic reticulum by the transporter associated with antigen processing (TAP) protein, wherein they are loaded into the binding groove of MHC-I by association with a loading complex (Ortmann et al., 1994). pMHC complexes are then surface presented via the golgi pathway (Peters et al., 1991). Although cross-presentation of exogenous antigens derived from phagocytosis does occur, the majority of MHC-I-presented peptides

are hence endogenously derived. Hence, MHC-I is utilised to display cytoplasm-derived antigens for the detection of infected cells by cytotoxic T-cells.

By contrast, professional APCs are known to internalise exogenous antigens for MHC-II presentation through an array of mechanisms, such as phagocytosis, micropinocytosis, and receptor-mediated endocytosis, including uptake via the C-type lectin receptors of DCs, and the B-cell receptor. MHC-II dimers are loaded into the endoplasmic reticulum where they associate with the invariant chain (Ii), the cytoplasmic tail of which targets them for export via the endocytic pathway. In this process, Ii is cleaved, leaving only a small peptide (CLIP in mice) occupying the peptide binding groove, and hence abrogating antigen loading (Katz et al., 1996, van Bergen et al., 1997). In immature APCs, the surface expression of MHC-II is very low as a result of the constant recycling of MHC-II from the cell surface, and endosomal degradation (Cella et al., 1997). In addition, the majority of MHC-II in immature cells remains occupied by the CLIP peptide (Bodmer et al., 1994). Upon activation, CLIP peptides are unloaded form MHC-II as a result of degradation by the enzyme cathepsin, and assistance of the invariant MHC-II molecules H2-M and H2-O, which facilitate subsequent binding of peptides produced by the endosomal proteases (Hsing and Rudensky, 2005, Denzin et al., 2005, Neefjes et al., 2011). In addition, the synthesis and surface half-life of MHC-II is increased in activated APCs (Boes et al., 2002), and thus efficient loading in the endosomal pathway allows for the presentation of both endogenous and exogenous peptides in professional APCs.

1.1.5 T-cell activation

As non-professional APCs constitutively express MHC class I on their cell surface, and so pMHC complexes are often present under steady state conditions, the presence of antigenic pMHC alone is hence insufficient to determine the requirement for adaptive immune responses. T-cells therefore require assistance in contextualizing their antigen, and are reliant upon the detection of a danger signal through PRR engagement by APCs (Iwasaki and Medzhitov, 2004). In the case of professional APCs such as dendritic cells, this triggers their chemokine receptor 7 (CCR7)-dependent migration to the lymph nodes from the site of infection (Forster et al., 1999), and acquisition of an activated phenotype. Regardless of cell type, the first interaction between T-cells - termed "naive" as a result of their antigen inexperience - and APCs occurs as a result of non-specific binding of adhesion molecules, such as LFA-1 and ICAM-1/3 (Shaw and Luce, 1987). This allows the physical association of cells while the naïve T-cell scans the APC cell surface for specific pMHC molecules. If antigen-specific TCR triggering occurs, subsequent T-cell "activation" is entirely dependent on the presence of a secondary signal. Co-stimulatory molecules, such as CD80 and CD86, are conditionally up-regulated by APCs upon PRR engagement, and through triggering of the receptor CD28 on T-cells provide essential co-stimulation for the full activation of T-cells, and the launching of an adaptive immune response (June et al., 1990, Lenschow et al., 1996). Activated helper T-cells can subsequently up-regulate CD40L, which in turn can activate $CD40^{+}$ professional APCs, leading to amplification of the response (Elgueta et al., 2009, Parker, 1993). The same mechanism also promotes T-cell dependent class

switching in B-cells (Kawabe et al., 1994). In addition, activated APCs express IL-1, which drives activated T-cells to up-regulate expression of the high-affinity IL-2 receptor CD25, allowing them to receive autocrine IL-2 signalling, which drives their proliferation and amplification (Willerford et al., 1995, Lichtman et al., 1988). In the absence of co-stimulation, pMHC engagement and TCR triggering doesn't activate T-cells, and can lead to tolerance. The activation phenotype of DCs is dictated by the specific pathogen, and the environment in which it is encountered, and cytokines produced by DCs have been shown to skew the phenotype and cytokine profile of activated $CD4^+$ helper T-cells. Helper T-cells are broadly categorized depending on this cytokine profile into T-helper 1 (Th1) cells and Th2 cells (Mosmann and Sad, 1996). Th1 cells secrete interferon-γ (IFNγ) together with tumour necrosis factor β (TNFβ), which are effective at resolving infections by intracellular bacteria and protozoa (Mosmann and Coffman, 1989). Th2 cells secrete interleukin family member proteins, such as IL-4, IL-5 and IL-13, which control parasitic infections such as those by helminths, and have also been implicated in allergic responses (Yazdanbakhsh et al., 2002). The specific pathway of DC activation can lead to their production of IL-12, IL-23, IL-27 and type 1 IFN - cytokines which skew T-helper cells to assume a Th1 phenotype on activation (Hsieh et al., 1993, Trinchieri, 1995, Oppmann et al., 2000, Pflanz et al., 2002), or alternatively CCL2 and OX40L, which are thought to promote Th2 responses (Gu et al., 2000, Ito et al., 2005). More recent work has focussed on the balance of the cytokines transforming growth factor β (TGFβ) and IL-6, which control the skewing of naïve T-helper cells towards an autoimmune or tolerant phenotype. Regulatory T-cells (T-Reg) are a T-helper subtype expressing anti-inflammatory cytokines such as IL-10

(Hara et al., 2001), as well as exerting contact-dependent control over inflammatory T-cell responses (Tai et al., 2005, Sakaguchi et al., 1995). In addition to their formation in the thymus (see section 1.2), T-Reg can be induced peripherally via DC secretion of TGFβ, as well as IL-10 and retinoic acid (Chen et al., 2003, Sun et al., 2007, Coombes et al., 2007). In contrast, IL-17-producing Th17 cells have been shown to play active roles in autoimmune responses and asthma (Tesmer et al., 2008). Th17 cells are similarly induced peripherally upon TCR-triggering in an environment supplemented with DC-derived TGFβ and IL-6 (Veldhoen et al., 2006). The context of antigen presentation is hence not only an important go/stop control for the adaptive immune system, but also acts to dictate the nature of the immune response through factors secreted by APCs activated in the context of infection.

1.2. Stages of intrathymic T-cell development

1.2.1. Thymus structure and function

Developing B and T lymphocytes share a pool of precursors; namely lymphoid-primed multipotent progenitor (LMPP) and common lymphoid progenitor (CLP) derived from haematopoiesis (Adolfsson et al., 2005, Yoshida et al., 2006). However, the development of T-cells is distinct in that it requires particular developmental signals that can only be provided by the stromal populations of the primary lymphoid organ known as the thymus (Anderson et al., 1993, Owen and Raff, 1970). The thymus is a bi-lobed structure located in the anterior superior mediastinum, into which T-cell precursors from the fetal liver or adult bone marrow enter from the blood stream (Lind et al., 2001, Foss et al., 2001). Histologically, the thymus is commonly divided into two regions, the cortex and medulla, which are occupied by distinct stromal networks capable of fostering sequential stages in the lifecycle of developing T-cells, or "thymocytes" (Takahama, 2006)(summarized in Figure 1.1). Stromal populations include thymic epithelial cells (TEC) and mesenchymal cells, in addition to an array of haematopoiesis-derived cell types, including macrophages, dendritic cells, eosinophils and NK cells (Takahama, 2006). In particular, the following study will focus on the thymic epithelial cells – a population distinct to the thymus, and indispensible at multiple stages of thymocyte development (Anderson et al., 1993, Takahama, 2006). The TEC occupying the cortex and medulla are functionally and phenotypically distinct, however both mediate MHC-dependent selective processes on developing thymocytes in order to prevent contribution of non-functional, or potentially autoreactive T-cells to the peripheral pool (Surh

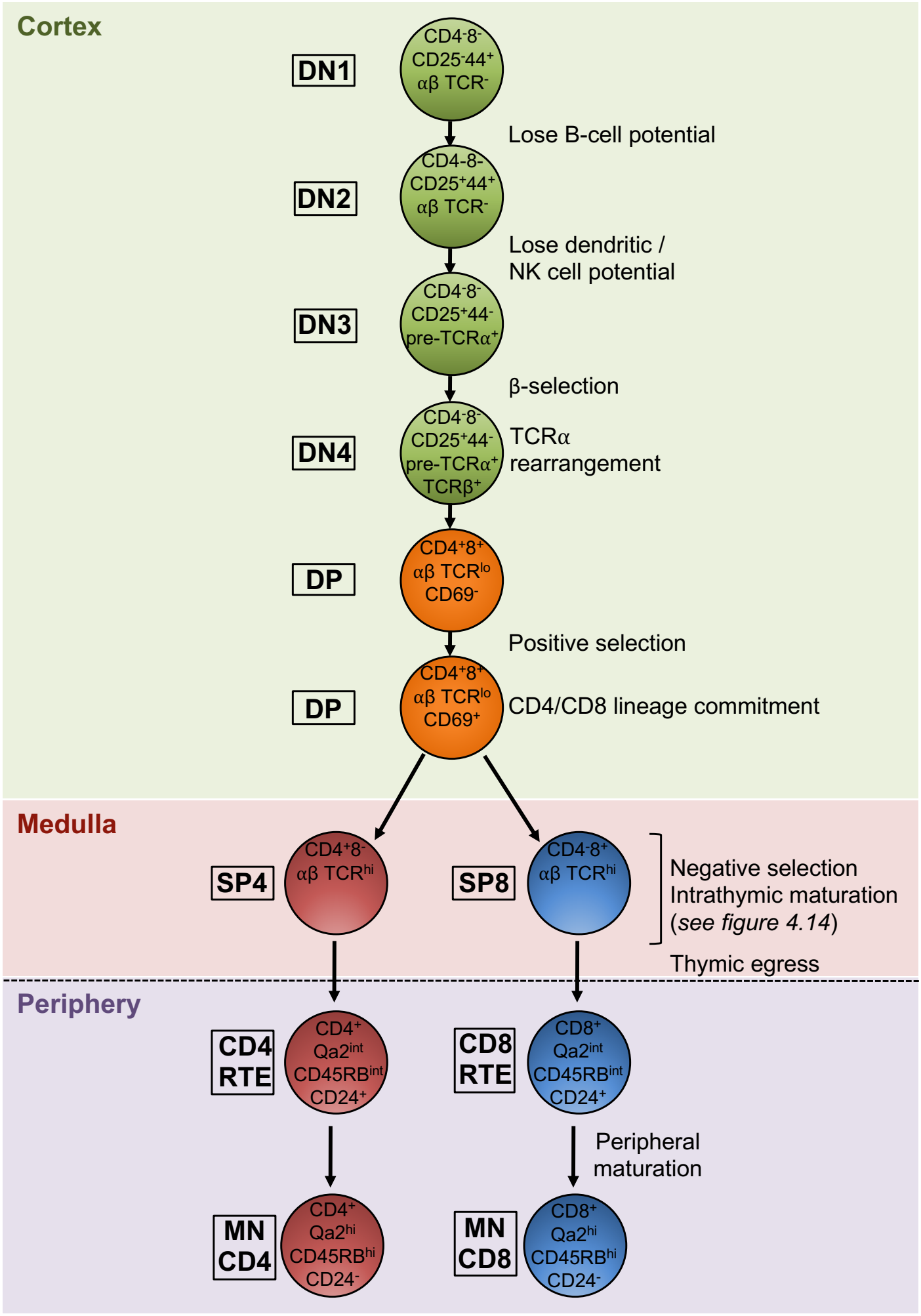
Cortex
DN1
CD4-8-
CD25-44+
αβ TCR-
Lose B-cell potential
DN2
CD4-8-
CD25+44+
αβ TCR-
Lose dendritic /
NK cell potential
DN3
CD4-8-
CD25+44-
pre-TCRα+
β-selection
DN4
CD4-8-
CD25+44-
pre-TCRα+
TCRβ+
TCRα
rearrangement
DP
CD4+8+
αβ TCRlo
CD69-
Positive selection
DP
CD4+8+
αβ TCRlo
CD69+
CD4/CD8 lineage commitment
Medulla
SP4
CD4+8-
αβ TCRhi
SP8
CD4-8+
αβ TCRhi
Negative selection
Intrathymic maturation
(see figure 4.14)
Thymic egress
Periphery
CD4
RTE
CD4+
Qa2int
CD45RBint
CD24+
CD8
RTE
CD8+
Qa2int
CD45RBint
CD24+
Peripheral
maturation
MN
CD4
CD4+
Qa2hi
CD45RBhi
CD24-
MN
CD8
CD8+
Qa2hi
CD45RBhi
CD24-

Figure 1.1: T-cell development and maturation

T-cells develop in the thymus, where they traffick through sequential stages of development defined as DN1, DN2, DN3, DN4 and DP, wherein they commit to either the SP4 or SP8 lineage depending on TCR reactivity to either MHC-I or MHC-II during positive selection in the cortex. SP thymocytes then migrate to the medulla to undergo antigen-dependent deletion (negative selection), before egressing the the periphery, where further functional and phenotypic maturation occurs.

and Sprent, 1994, Starr et al., 2003). Cortical thymic epithelial cells (cTEC) form the niche for the early stages of T-cell development, and hence contribute signals for precursor commitment to the T-cell lineage, before mediating "positive selection", a process whereby survival signals are issued to thymocytes producing a functional, in-frame TCR capable of recognizing MHC-bound peptide antigens (Huesmann et al., 1991, Kisielow et al., 1988). Medullary thymic epithelial cells (mTEC) are dispensable for the production of conventional T-cells (Weih et al., 1995, Burkly et al., 1995); however they, together with medullary dendritic cells, mediate "negative selection", a process whereby late-stage thymocytes bearing auto-reactive TCRs are actively deleted within the thymus (Surh and Sprent, 1994, Laufer et al., 1996). These processes are thought to contribute to the intrathymic apoptosis of 97-99% of cells to enter T-cell development (Tough and Sprent, 1994), but are essential in maintaining the production and export of functionally competent T-cells capable of responding in an antigen-specific manner to pathogenic challenge, and yet remaining tolerant to endogenous stimuli.

1.2.2. Early T-cell development

T-cell progenitors have been shown to enter the thymus from the circulation in distinct waves mediated by chemokine receptor (CCR) signalling (Savino et al., 2004). To this end, thymic epithelial cells express CCL25, the ligand for the CCR9 receptor (Zlotoff et al., 2010, Krueger et al., 2010), CXCL12, the CXCR4 ligand (Calderon and Boehm, 2011), as well as CCR7 ligands CCL19/21 (Misslitz et al., 2004), with the former also periodically expressed together with

P-selectin ligand 1 (PSGL1) by the endothelial cells of the thymus (Gossens et al., 2009, Rossi et al., 2005). Observations in fetal (Liu et al., 2006, Calderon and Boehm, 2011) and adult (Krueger et al., 2010, Zlotoff et al., 2010) thymic tissues in mice lacking expression of CCR7 and/or CCR9 have shown the colonization of the thymus to be reliant on signalling through both receptors; however, the CCR7 appears to be the predominant receptor for seeding of the pre-vascularized thymus (Liu et al., 2006), whereas *Ccr9*$^{-/-}$ mice have a more severe defect in the entry of thymic progenitors in the adult thymus, which is slightly compounded by the absence of CCR7 (Krueger et al., 2010, Zlotoff et al., 2010). In addition, parabiosis experiments have revealed the degree of chimerism within the thymus of a joined wildtype to be greatly reduced if thymic progenitors are deficient in P-selectin (Rossi et al., 2005), suggesting a similar importance of this pathway in progenitor homing in adult mice.

The earliest thymic progenitor (ETP) population is identifiable through expression of high levels of the adhesion molecule CD44, as well as a small array of receptors implicated in lineage commitment and survival at this precursor stage, including Notch-1, IL7Rα, KIT, and Flt3 (Yui and Rothenberg, 2014). Upon entry into the thymus, these cells are signalled to initiate the T-cell development programme, which is characterised by changes in the expression of transcription factors, together with that of cell surface proteins. At the earliest stages of their development, thymocytes are termed double negative (DN) - as they lack expression of TCR co-receptors CD4 or CD8 - and progress linearly through multiple stages of development defined by their expression of CD44, as well as the IL-2 receptor alpha chain CD25 (Godfrey et al., 1993); namely, DN1 ($CD44^{+}CD25^{-}$), DN2 ($CD44^{+}CD25^{+}$), DN3 ($CD44^{-}CD25^{+}$) and DN4 ($CD44^{-}CD25^{-}$).

Throughout early developmental progression, $CXCR4^+$ DN cells traffick from the cortico-medullary junction to the subcapsular zone of the cortex until the DN3 stage (Plotkin et al., 2003), at which point cells become dependent on signalling through the pre-TCR complex for subsequent progression (Trigueros et al., 2003). Contrastingly, stages DN1 to DN3a require Notch-1 receptor triggering by Delta-like ligand 4 (Maillard et al., 2008), which is expressed in the cortex by cTEC (Fiorini et al., 2008). Together with IL-7 and SCF, Delta-like ligand signalling facilitates repeated proliferation of early thymocytes (Moore et al., 1996, Krueger et al., 2010, Magri et al., 2009) which counters the high rate of apoptosis among DN cells (Surh and Sprent, 1994), and compensates for the low rate of thymic seeding by ETP (Kyewski, 1987). Subsequently, receipt of Notch signalling triggers precursor commitment to the T-cell lineage (Wilson et al., 2001). Firstly, thymocytes fade out expression of genes required for maintenance of their progenitor status (KIT, IL2Rα and FLT3) and hence lose the capacity to enter the dendritic, myeloid, natural killer, and innate lymphoid cell lineages, becoming committed, lymphocyte progenitors (Balciunaite et al., 2005, Masuda et al., 2007). Secondly, the expression of T-cell specific genes is initiated - the TCR gene locus is opened, allowing commencement of TCR gene recombination driven by recombination-activating gene proteins 1 & 2 (RAG1 & RAG2), and expression of components of the TCR signalling complex (CD3, LCK, ZAP70) and required for pro-T-cell survival (IL7Ra) ensues (Taghon et al., 2006, Taghon et al., 2005). Depending on the nature of recombination events, the result is surface expression of either the pre-TCR, consisting of a recombined β-chain paired with invariant pre-TCRα, or alternatively the TCRγδ heterodimer (Aifantis et al., 1998, Fehling et al., 1995). Cells of the latter fate form cells of the

innate-like γδ-T-cell lineage, the development of which is thereon distinct from conventional αβ-T-cells (Saint-Ruf et al., 2000).

Expression of the pre-TCR complex endows DN3 thymocytes with the capacity to receive MHC-dependent TCR signals in a process known as β-selection (Michie and Zuniga-Pflucker, 2002), from which point cells begin to phase out dependence on Notch signalling for subsequent development (Ciofani et al., 2006). Thymocytes at the DN3a stage remain quiescent during TCRβ recombination (Palacios and Weiss, 2007, Hoffman et al., 1996), but successful gene re-arrangement allowing signalling through the pre-TCR acts to both trigger proliferation, and rescue cells from apoptosis through expression of anti-apoptotic proteins (Falk et al., 2001). Two recent publications have demonstrated a role for CXCR4, implicated in initial sub-capsular localization of DN thymocytes, as an essential co-stimulatory molecule in β-selection, as DN cells with a conditional deletion of *Cxcr4* stall in development between DN3 and DN4, and fail to up-regulate Bcl2-A1 – an effect that cannot be overcome through artificial TCR stimulation (Trampont et al., 2010, Janas et al., 2010). In passage from DN3 to DN4, thymocytes up-regulate the T-cell lineage defining transcription factors NFATC3, POU6F1, Aidos and RORγt, the latter of which contributes to survival during TCRα recombination by inducing expression of another anti-apoptotic protein in BclXL (Rothenberg et al., 2008). Notch signalling is redundant for subsequent development, and expression of Notch-dependent, DN3 specific, and phase 1 genes is completely terminated (Ciofani et al., 2006). In addition, thymocytes progress beyond DN development, and initiate expression of both CD4 and CD8 to become double positive (DP) thymocytes (Shinkai et al., 1993, Mombaerts et al., 1992), although up-regulation of CD8

precedes that of CD4, yielding a transient immature CD8 single-positive (ISP8) phase (Schilham et al., 1998).

DP thymocytes undergo repeated and sequential attempts at TCRα recombination, and cells successful in this undertaking gain surface expression of the TCRαβ heterodimer (Capone et al., 1998). TCR expression renders DP thymocytes susceptible to two distinct MHC-dependent processes: 1. Positive selection by cTEC, a quality control process in which thymocytes receive survival signals upon expression of a functional TCR; 2. Negative selection by medullary antigen presenting cells, wherein thymocytes bearing expression of auto-reactive TCR specificities are deleted to establish tolerance to peripheral tissues (Starr et al., 2003). In wildtype mice, DP thymocytes are restricted to the cortex, but are highly motile within this region (Bousso et al., 2002), allowing for many repeated engagements with cortical antigen presenting cells. For a given T-cell, the outcome of positive selection is influenced by multiple factors, including TCR specificity for specific peptide-MHC complexes (Marrack and Kappler, 1987), as well as the timely receipt of γ-chain cytokine signalling (McCaughtry et al., 2012). Co-expression of CD4 and CD8 renders DP thymocytes the capacity to engage with peptide-loaded MHC-I or MHC-II complexes on the surface of cTEC via their TCR, wherein successfully interacting cells receive positively selecting signals for their survival and differentiation (Klein et al., 2009). As will be addressed later, negative selection is a highly antigen-dependent process, with a clear proportional relationship between TCR affinity for self-peptide MHC complexes, and thymocyte deletion (Palmer and Naeher, 2009). Although of evident importance, the involvement of peptide antigens in positive selection is less clear-cut. Outcomes of positive selection are dependent on the MHC-specificity of

a given T-cell receptor. Interaction with MHC-I yields the down-regulation of CD4 to form CD8 single-positive (SP8) thymocytes with a "T-cytotoxic" profile (Fung-Leung et al., 1993). Contrastingly, MHC-II engagement triggers loss of expression of CD8, resulting in the formation of CD4 single-positive (SP4) thymocytes with a "T-helper" phenotype (Rahemtulla et al., 1991). The loss of either co-receptor is thought to be compounded by epigenetic changes (Zou et al., 2001), meaning commitment to either helper or cytotoxic lineage is likely to be imprinted permanently during positive selection. Early studies on positive selection of HY-TCR transgenic cells, which are activated by H-2D^{b} loaded male antigen, demonstrated positive selection of exclusively SP8 thymocytes in both male and female mice of the H-2D^{b} allotype, but not their H-2D^{d+} counterparts, suggesting the process to be driven by MHC-specificity, rather than that for antigen (Scott et al., 1989).

Exactly how such lineage commitment is instilled in positive selection remains uncertain. This had been proposed to be dictated by the strength of TCR signalling received in positive selection, as the cytoplasmic tails of CD4 and CD8 have differing affinities for the Src family kinase Lck, a key mediator in TCR signal transduction (Turner et al., 1990, Hernandez-Hoyos et al., 2000). Qualitative differences between CD4-dependent and CD8-dependent TCR triggering during positive selection are exemplified by the instantaneous down-regulation of CD8 mRNA - but not that of CD4 - post-TCR engagement, which ensures a shortened duration of MHC-I:TCR interactions relative to those involving MHC-II (Stepanek et al., 2014). However, the so-called "instructive model" has been cast into doubt by studies involving mice with transgenic CD4 incapable of interaction with Lck, wherein SP4 thymocytes continued to be

formed (Germain, 2002). If this process does indeed occur, it is hence likely to occur independently of Lck. An alternative possibility is the "stochastic model", in which the down-regulation of either CD4 or CD8 by DP thymocytes occurs in a random manner after positive selection, with SP thymocytes only receiving essential secondary survival signals on the condition that the TCR MHC-specificity is matched by expression of the correct co-receptor (Davis et al., 1993). This model has similarly been disproven, as the positive selection efficiency of some TCR-transgenics has been calculated to be up to 90%, suggesting co-receptor down-regulation to be specific and targeted rather than random (Itano and Robey, 2000). Equally, thymocytes with mismatched TCRs and co-receptors have been shown to develop into mature T-cells, and emigrate to the periphery (Sarafova et al., 2005), and hence post-selection survival does not seem dependent on TCR-co-receptor pairing.

Recent evidence suggests the formation of SP8s from positive selection to have a unique requirement for secondary signals provided by ϒ-chain cytokines. Mice in which the *Il7ra* gene is deleted in thymocytes after the DN stage of development yielded a 3-fold reduction in SP8 thymocytes, wherein the production of SP4s was unimpeded (McCaughtry et al., 2012). This effect could be replicated by conditional deletion of Socs1, a negative regulator of ϒ-chain cytokine signalling induced in DP thymocytes upon positive selection by MHC-II (Chong et al., 2003). Hence, the most recent perspective on the factors determining T-cytotoxic versus T-helper lineage commitment during positive selection is the "kinetic signalling model", which suggests that positive selection is a distinct event from lineage commitment, consistently resulting in the termination of CD8 expression by DP thymocytes (Singer et al., 2008). As CD8 is

required for TCR signalling by MHC-I-restricted thymocytes, TCR signal persists only in MHC-II-restricted cells, skewing thymocytes towards the expression of Socs1, together with the T-helper lineage defining transcription factors Gata3 and ThPOK (Egawa, 2015). In the absence of such a signal, commitment to the CD8 lineage predominates in response to unimpeded IL-7 receptor signalling, with cells expressing the Runx3 transcription factor critical to adoption of the cytotoxic phenotype (McCaughtry et al., 2012).

In addition to the direction of lineage commitment by TCR MHC-I/II tropism, the outcome of positive selection has been shown to be equally dependent on the avidity (i.e. ligand availability x TCR affinity) of antigen-specific TCR engagement by developing thymocytes (Palmer and Naeher, 2009). It has been postulated that there are two potential mechanisms determining the strength of TCR engagement an individual T-cell receives during interaction with an antigen-presenting cell. The serial triggering model suggests that the level of TCR stimulation is dependent on the number of serial TCR-pMHC interactions of comparable strengths occurring within a given time (Valitutti and Lanzavecchia, 1997). The kinetic proofreading model suggests that TCR signalling strength is instead determined by the length of individual TCR-pMHC interactions – the dwell time – where higher affinity interactions would take longer to dissociate, and hence increase the level of TCR signalling received (McKeithan, 1995). In either instance the affinity of TCR-pMHC interaction clearly governs the fate of DP thymocytes, and peptide ligands capable of positively selecting both MHC-I and MHC-II restricted T-cells have been identified through mass spectrometry of isolates from cell lines derived from B cell lymphoma, thymoma and TEC (Ebert et al., 2009, Lo et al., 2009, Hu et al., 1997). Again in contrast to T-cell negative

selection, which is driven by high affinity antigen recognition, the process of positive selection is driven by engagement with MHC loaded with peptides that are either partially agonistic or antagonistic to mature peripheral T-cells (Hogquist et al., 1994). Indeed, fully agonistic peptides have been demonstrated to trigger positive selection in whole fetal thymic organ cultures (FTOC) (Yachi et al., 2006), however the function of the SP thymocytes produced is impaired. By screening 95 MHC-II displayed self-peptides via their introduction into TCR-transgenic FTOC, 6 peptides were discovered to positively select 5C.C7-TCR transgenic thymocytes, whereas only 1 peptide could induce positive selection of SP thymocytes from AND-TCR transgenics (Ebert et al., 2009). This finding is notable, as not only were multiple peptides capable of triggering selection of TCR-transgenic T-cells, but both transgenic receptors have specificity for the same antigen, MCC (Ebert et al., 2009). The pool of peptides positively selecting 5C.C7 T-cells included peptides related to and distinct from the structure of MCC, suggesting a wide degree of promiscuity in ligands capable of positive selection for a given T-cell clone. This fact is supported by an array of studies of mouse strains wherein MHC-I/II is loaded with a single peptide. Findings vary between models, but the observation of positive selection of a varied polyclonal pool of thymocytes is common to each (Ebert et al., 2009, Lo et al., 2009, Hu et al., 1997), albeit this pool is limited in both size and clonal variation relative to that seen in wildtype thymus.

1.2.3. Late-stage T-cell development

Effective positive selection in the cortex produces a pool of thymocytes with useful TCR specificities, which are capable of reacting functionally in the instance they engage their peptide antigen. Although this is a positive outcome in terms of immune competency, this process also enables the selection of a high proportion of thymocytes with auto-reactive TCRs capable of initiating autoimmune disease (Laufer et al., 1996). This is countered in the thymic medulla through negative selection, a process involving the deletion of self-antigen specific single positive thymocytes by mTEC and DC. The outcome of negative selection is dependent on the level of TCR signalling that a given T-cell clone receives – high levels over a certain threshold induce apoptosis, whereas lower levels allow the escape of SP thymocytes (Stritesky et al., 2013), which emigrate from the medulla after a residence of 4-5 days (McCaughtry et al., 2007). In order to achieve this, mTEC are programmed with the quite unique capacity produce an array of antigens that are normally restricted in their expression to limited tissues or cell types, termed "tissue restricted antigens" (TRA) (Anderson et al., 2002). Hence, mTEC are able to present a pool of antigens that effectively mirrors those available to T-cells in the periphery. SP thymocytes strongly reactive to these antigens hence receive strong TCR signals in the medulla, sufficient to induce their apoptosis, whereas thymocytes incapable of activation on encounter with self-antigens receive only low-level TCR signals below the threshold of deletion (Stritesky et al., 2013).

The initial relocation of post-positive selection thymocytes to the medulla occurs as a result of switching of the expression of chemokine receptors.

Selected DP thymocytes are distinguishable by their expression of the activation marker CD69 (Yamashita et al., 1993), and it is at this stage that cells lose expression of the cortex-homing receptor CCR9, and up-regulate CCR4, rendering them susceptible to signalling from medullary-derived chemokines CCL5, CCL17 and CCL22 (Cowan et al., 2014, Campbell et al., 1999). Expression of CCR4 in newly generated SP thymocytes is only transient, however, and is superseded by surface expression of CCR7 (Cowan et al., 2014) – the ligands for which, CCL19 and CCL21, are highly expressed by mTEC (Ueno et al., 2002) - with their progressive maturation. Models involving *Relb*$^{-/-}$ thymic stroma, in which development of the mTEC lineage is blocked, have demonstrated engagement with the medulla to be a redundant process in the development of SP thymocytes (Cowan et al., 2013). However, mice exposed to T-cells selected in a *Relb*$^{-/-}$ thymus confer severe autoimmune disease to their host (Burkly et al., 1995, Cowan et al., 2013). Similarly, *Ccr7*$^{-/-}$ mice, in which SP thymocytes accumulate in the cortex, have been shown to develop spontaneous autoimmunity (Kurobe et al., 2006), demonstrating the importance of engagement of developing thymocytes with the medulla for the establishment of T-cell tolerance.

In comparison to positive selection, the nature of TCR-pMHC interactions facilitating negative selection is relatively well understood. TCR triggering over a certain threshold induces apoptosis in thymocytes, whereas sub-threshold levels of stimulation allow escape from negative selection in the thymus (Stritesky et al., 2013), and have a known importance in T-cell homeostasis and function peripherally (Houston and Fink, 2009). The first observation of clonal deletion in the thymus was achieved through tracking of Vβ17a^{+} thymocytes, which are

reactive to the class II MHC molecule I-E, with the monoclonal antibody KJ23a (Zuniga-Pflucker et al., 1989, Cazenave et al., 1990). Although present in peripheral T-cells in many mouse strains, Vβ17a^{+} T-cells were reduced or absent in I-E^{+} mice beyond the immature stages of thymocyte development, suggesting their deletion within the thymus (Cazenave et al., 1990). Furthermore, the deletion of T-cell clones recognising endogenous antigens, such as those possessing the HA or C5 TCRs, has been observed in a variety of different mouse models (Starr et al., 2003). Recently, reporter mice in which the intensity of TCR signalling is measurable through the expression of the downstream mediator Nur77 (Nur77^{GFP}) have allowed the measurement of the affinity of TCR-pMHC interactions in individual thymocytes (Moran et al., 2011). Nur77^{GFP} thymocytes lacking the pro-apoptotic regulator Bim are unable to undergo apoptosis, allowing for the detection of T-cells that would normally undergo deletion (Stritesky et al., 2013) - a feat made challenging through detection of apoptotic markers, as thymocytes are known to be cleared by phagocytic cells rapidly on initiation of cell death (Dzhagalov et al., 2013). In this model, clonally deleted thymocytes were seen to express very high levels of GFP (Stritesky et al., 2013). Somewhat surprisingly, negative selection was observed not only among SP thymocytes in the medulla, but also DP thymocytes, which accounted for up to 75% of clonally deleted cells (Stritesky et al., 2013).

On a per cell basis, the occurrence of negative selection has been suggested to be dictated by the "Lck come&stay/signal duration" model (Stepanek et al., 2014). Early hypotheses included a "kinetic proofreading" model, wherein apoptosis is triggered by specific strong TCR-pMHC interactions, involving high affinity ligands, as well as a "serial triggering" model, where the

threshold for deletion is reached via the accumulation of many TCR-pMHC interactions, allowing lower affinity antigen to negatively select on the condition it's availability is higher (Palmer and Naeher, 2009). Although both may occur to a degree, the "Lck come&stay/signal duration" model is a refinement on the former model. CD4 and CD8 co-receptors engage the activated form of the Src kinase family member Lck, which is required to phosphorylate elements of the TCR complex, allowing Zap70 recruitment (Stepanek et al., 2014). As only low percentages of CD4 and CD8 bind active Lck (6.8% and 0.6% respectively), and co-receptors are constantly cycled in their association with TCR complexes, the probability of CD4 or CD8 carrying active Lck binding, and hence allowing TCR signalling is determined by the half-life of the TCR-pMHC interaction, which is in turn dictated by antigen affinity (Stepanek et al., 2014). Hence, high-affinity interactions have a greater chance of initial TCR triggering, and a greater chance of prolonged TCR-pMHC binding continuing after the initiation of the TCR signal to facilitate a stronger level of stimulation, above the threshold of deletion. In this way, high affinity ligands are suggested to be essential for negative selection, as low affinity ligands with a half-life of ~0.6s cannot negatively select even at very high concentrations in FTOC (Stepanek et al., 2014). Studies involving mice transgenically expressing antigen under control of the Rat Insulin Promoter (RIP), which is active in mTEC under control of the transcription factor Aire (Jolicoeur et al., 1994), have reaffirmed this understanding by demonstrating reliance on the medullary expression of high affinity self-antigens for the deletion of specific TCR clones. When Hen egg lysozyme (HEL) is expressed in a RIP/Aire dependent manner, HEL-specific T-cells are deleted intrathymically,

whereas in the absence of Aire and HEL expression, these cells persist to cause pancreatic auto-immunity (Liston et al., 2003).

Regulatory T-cell Selection

Although the majority of auto-reactive thymocytes are deleted via negative selection, this process is inefficient, as auto-reactive T-cells are known to be present in the periphery of wildtype mice (Yan and Mamula, 2002, Bouneaud et al., 2000). However, that these mice remain free of measurable auto-immunity alludes to a second mechanism by which T-cell tolerance is mediated in the thymic medulla; the production of $CD4^+$ regulatory T-cells (T-Reg) (Fontenot and Rudensky, 2005). T-Reg have the capacity to suppress conventional αβ T-cells through secretion of anti-inflammatory mediators (IL-10) (Hara et al., 2001), as well as via contact dependent mechanisms (CTLA-4) (Tai et al., 2005). Interestingly, expression of the co-stimulatory molecule CTLA-4 has been shown to render T-Reg with the capacity to sequester CD80/86 from the surface of antigen presenting cells, preventing auto-reactive T-cells receiving sufficient co-stimulation for their activation (Qureshi et al., 2011). T-Reg were originally characterised by their constitutive expression of the activation marker CD25 - the high affinity IL-2Rα chain (Sakaguchi et al., 1995). Transfer of CD25-depleted T-cells into immuno-compromised mice was shown to confer severe auto-immunity that was only abrogated on restoration of the $CD25^+$ population (Sakaguchi et al., 1995). More recently, the forkhead box transcription factor family member Foxp3 has been identified to define the T-Reg lineage, as expression is both required for the T-Reg suppressive phenotype, and sufficient to confer suppressive capabilities to conventional T-cells (Fontenot et al., 2003,

Hori et al., 2003). Foxp3 mutant (*scurfy*) mice develop fatal multi-tissue auto-immune disease only a few weeks post-partum (Godfrey et al., 1991a, Godfrey et al., 1991b), demonstrating the essential nature of their presence in the periphery for immune tolerance.

Although Foxp3 expression can be induced under certain conditions in the periphery (Coombes et al., 2007, Round and Mazmanian, 2010), acting to maintain tolerance against exogenous antigens such as those derived from the normal flora, the majority of T-Reg are thought to develop intra-thymically. Thymic T-Reg arise from an intermediate stage of SP4 development, as defined by surface expression of CCR7 and CD69 (Cowan et al., 2013), and two pre-cursor populations to $CD25^{+}Foxp3^{+}$ T-Reg have so far been defined; namely, $CD25^{+}Foxp3^{-}$ (Lio and Hsieh, 2008) and, more recently, $CD25^{-}Foxp3^{+}$ SP4 thymocytes (Tai et al., 2013). Relative to that of conventional αβ T-cells, T-Reg development has a unique set of signalling requirements, and is known to depend on the level of TCR ligation, receipt of co-stimulatory signals, and the provision of γ-chain cytokines (Sakaguchi et al., 2008). Analysis of $Nur77^{GFP}$ mice has demonstrated thymic T-Reg to express higher levels of GFP relative to conventional SP4 thymocytes, with $CD25^{+}$ precursors uniformly GFP bright, suggesting they are induced through high-affinity TCR-pMHC interactions, marginally below the threshold for negative selection (Moran et al., 2011). As CD25 expression renders T-Reg precursors responsive to IL-2 signalling, which drives acquisition of Foxp3 expression, T-Reg generation in the thymus had until recently been viewed as a defined two-step process (Lio and Hsieh, 2008). However, more recent research has highlighted the essential nature of co-stimulation during T-Reg development. Initial formation of $CD25^{+}$ T-Reg

precursors is equally dependent on CD80/86 co-stimulation via the receptor CD28 (Lio et al., 2010), which subsequently induces the surface expression of an array of other TNF receptor superfamily members – including GITR, TNFR2 and OX40 - signalling through which also acts to mediate efficient conversion of these cells to mature Foxp3$^+$ T-Reg (Mahmud et al., 2014). More recently, Foxp3$^+$ T-Reg precursors have been shown to overcome distinct hurdles in their own development. Foxp3 expression alters the balance of expression of mitochondrial regulators of apoptosis, inducing expression and activation of pro-apoptotic PUMA and Bim, and reducing the level of expression anti-apoptotic Bcl-2 (Tai et al., 2013). Hence, the intrinsic apoptotic tendency of Foxp3$^+$ precursors is overcome through co-stimulation via CD27 (Coquet et al., 2013), and IL-2 signalling (Tai et al., 2013), with the production of CD25$^+$Foxp3$^+$ T-Reg from both pathways likely limited under normal circumstances by the availability of IL-2. Two recent papers have suggested this to be a circumstance regulated to a degree in the adult thymus by the re-circulation of peripheral T-Reg back to the thymus, wherein through CD25 they sequester local DC-derived IL-2, thereby forming a negative feedback loop to limit their own production (Thiault et al., 2015, Weist et al., 2015). For the maintenance of peripheral tolerance, there lies importance not only in the quantity of T-Reg production within the thymus, but also their clonal specificity. Although T-Reg are known to mediate suppression in a non-TCR specific manner (Thornton and Shevach, 2000), TCR specificity is vital to the tissue localization and expansion of antigen specific T-Reg (Malchow et al., 2013, Rosenblum et al., 2011). As T-Reg generation in the thymus maps to strong TCR ligation, both production and specificity are highly regulated by the expression of TRAs by thymic epithelium,

as will be discussed in detail later. However, evidence suggests that the capacity to form a full T-Reg repertoire intrathymically may be dictated by early stages of thymocyte development. In NOD mice, which spontaneously develop autoimmune diabetes, normal numbers of thymic and peripheral T-Reg are present; however the conversion from DN1 to the DN2 stage is inefficient, and thymocyte numbers recuperated later through additional rounds of proliferation (Ferreira et al., 2014). Despite quantity being restored, the TCR repertoire of NOD-deficient T-Reg is greatly altered (Ferreira et al., 2014), and has been suggested to lead to the absence of T-Reg protective of the pancreatic islets that would normally prevent autoimmune development.

1.2.4. Thymic egress and peripheral maturation

Single positive thymocytes lay in residence within the medulla for a period of 4-5 days prior to their emigration to the periphery (McCaughtry et al., 2007). In this time, they are known to undergo negative selection by medullary APCs, as well as extensive phenotypic maturation. An early approach used to elucidate the maturational process of SP cells involved sorting populations based on surface marker expression, and tracking them on injection into a congenically marked thymus (Jin et al., 2008). These experiments revealed semi-mature SP thymocytes to have the surface phenotype $Qa2^{lo}CD69^{hi}CD62L^{lo}CD24^{hi}$; semi-mature cells could subsequently mature to become $Qa2^{hi}CD69^{lo}CD62L^{hi}CD24^{lo}$ cells, the most mature subset immediately prior to thymus egress (Jin et al., 2008). Alternatively, these populations can be mapped through changes in the expression profile of CCR4, CCR7 and CCR9 (Cowan et al., 2014). This finding has

been solidified with a newer model, wherein a GFP reporter for the *Rag2* gene, which is transiently expressed prior to the SP stage of development, allows the determination of the age of thymocytes via the level of GFP expression (RAG-2p-GFP mice) (Monroe et al., 1999). Although requiring further research, the importance of intrathymic SP maturation has been stressed through analysis of the functional capacity of semi-mature and mature thymocytes. Semi-mature cells undergo apoptosis on TCR triggering, whereas mature SPs, although not insensitive, instead largely undergo rounds of proliferation (Kishimoto and Sprent, 1997). Interestingly, intrathymic maturation is thought to be possible independent of antigen engagement, as Qa2 up-regulation is induced in the presence of MHC-II-deficient APC (Dong et al., 2013), and is unaffected by the absence of mTEC in $Relb^{-/-}$ fetal thymic tissue (Cowan et al., 2013). Post-maturation, exit of SP thymocytes to the periphery depends on signalling through the receptors KLF2 and S1P1, expression of which is induced by the transcription factor Foxo1 (Fabre et al., 2008, Kerdiles et al., 2009). Foxo1 DNA binding is repressed in semi-mature cells through TCR triggering, and hence on the completion of interaction with medullary APC, SP thymocytes mature to express KLF2 and S1P1, and become sensitive to exit signals (Fabre et al., 2008, Kerdiles et al., 2009). It has been likewise suggested that CD69, expressed by semi-mature cells, can directly bind and inhibit the S1P1 receptor (Shiow et al., 2006). These processes are likely of great importance in dictating the order in which SP thymocytes can exit to the periphery, as controlling S1P1 and KLF2 expression ensures that only the most mature cells which have undergone negative selection – the so-called "conveyor belt" mechanism (Savino et al., 1996,

McCaughtry et al., 2007) - and hence only populations depleted of autoreactive thymocytes can escape the medulla.

The RAG-2p-GFP model is now routinely used to identify recent thymic emigrants (RTE) – T-cells that have recently been output from the thymus to peripheral tissues, which retain a GFP signal (Monroe et al., 1999). Through analysis of GFP^{high}, GFP^{low} and GFP negative fractions of peripheral T-cells, it has become apparent that peripheral maturational processes also occur (Boursalian et al., 2004). These have been visualised as alterations to the expression of surface proteins, as RTE are $CD24^{hi}Qa2^{lo}CD45RB^{lo}IL\text{-}7R\alpha^{lo}TCR^{hi}CD3^{hi}$ relative to non-RTE in the periphery (Boursalian et al., 2004). As in the thymus, maturational events in the periphery also correlate with functional changes. RTE have reduced capability to produce IL-2 and IFNγ on stimulation than mature cells (but increased IL-4 production) (Berkley et al., 2013, Boursalian et al., 2004), and a greater propensity for survival and proliferation on activation (Friesen et al., 2016). Finally, RTE have a greater tendency to form $Foxp3^{+}$ T-Reg in response to TGF-β stimulation in vitro (Paiva et al., 2013). In conclusion, maturation events occur both within the thymic medulla as well as the periphery to produce phenotypically and functionally mature T-cell populations.

1.3. Control and function of thymic stromal populations

The epithelial stroma of the thymus is highly specialized to allow for the development and antigen-specific selection of thymocytes, and exerts control measures from initial commitment to the T-cell lineage until the egress of mature cells to the periphery (Takahama, 2006). The importance of thymic epithelium has been evident since the 1960's, where the discovery of mice bearing a natural mutation in the Foxn1 gene – dubbed *nude* mice as a result of their failure to develop body hair – which have greatly impaired development of thymic epithelium (Pantelouris, 1968, Flanagan, 1966). These mice fail to produce mature αβ T-cells (Schedi et al., 1975), and hence have hugely defective adaptive immunity. Thymic epithelium is broadly categorized as cortical (cTEC) or medullary (mTEC), and these subtypes have been shown to be distinguishable through differential expression of protein markers (summarized in Figure 1.2), including Ly51 (Pillemer et al., 1984), CD205 (Kraal et al., 1986) and cytokeratins (Farr and Braddy, 1989), as well as the capacity to bind lectins, such as the fucose binding lectin UEA-1 (Farr and Anderson, 1985), which have all proven useful tools to identify the requirements and functional capacity of the two distinct lineages. cTEC have been shown to regulate the early stages of T-cell development, playing a major role in the production of immature thymocytes with a re-arranged TCR, as well as inflicting positive selection, a quality control measure for the removal of non-functional thymocytes (Kisielow et al., 1988). In contrast, mTEC play a largely redundant role in thymocyte development (DeKoning et al., 1997). When grafted under the kidney capsule of a host mouse, fetal tissues deficient for Relb - a transcription factor vital for the formation of

	mTEC	cTEC
Surface and cytoplasmic epithelial markers	UEA-1 ligand	Ly51
	Cytokeratin 5	Cytokeratin 8
		CD205
Co-stimulatory	CD80/86	Delta-like ligand 4
	CD70	
	OX40L	
Chemokine receptor ligands		Cxcl12
	Ccl21	Ccl25
Antigen production	Aire	β5t
	Fezf2	Tssp
TNFRSF members	Rank	
	Ltbr	
	OPG?*	
	iNOS?*	

Figure 1.2: Phenotypic distinction of cTEC and mTEC

cTEC and mTEC can be distinguished for analysis by flow cytometry and confocal microscopy through differential expression of a host of cell surface markers, co-stimulatory molecules, chemokine receptor ligands, TNFRSF members, and markers relating to the expression of genes and degradation of proteins involved in peptide antigen production.

mTEC – produce normal numbers of mature T-cells (Cowan et al., 2013). However, the medulla does play a vital role in negative selection – the process of deleting auto-reactive T-cells in a manner depending on antigen specificity (Laufer et al., 1996). Both positive and negative selection require specific peptide ligands to be presented to developing thymocytes – however, TEC have very poor phagocytic capabilities in comparison to other APC subtypes (Eshel et al., 1990), and hence cTEC and mTEC have evolved mechanisms to produce their own distinct arrays of antigen for this purpose (Klein et al., 2009).

1.3.1. cTEC specializations for positive selection of functional thymocytes

In addition to this role in facilitating the survival and development of early thymocyte populations, cTEC are unique mediators of positive selection of DPs within the cortex (Starr et al., 2003). Although the lineage commitment of individual DP cells is for the most part dictated by the tropism of their newly formed TCR to either MHC-I or MHC-II, recent evidence suggests the outcome of positive selection, in terms of both the survival and functional maturation of SP thymocytes, is heavily dependent on antigen specific interactions within the cortex (Nitta et al., 2010, Murata et al., 2007). To this end, although other cell types are capable of inducing positive selection of thymocytes in culture, cTEC are uniquely specialized to produce and present peptide antigens for the positive selection of highly polyclonal $CD4^+$ and $CD8^+$ T-cell populations within the thymus (Takada and Takahama, 2015).

Cathepsin-L and TSSP: cortex specific proteases

Prior to endosomal/lysosomal relocation, the peptide-binding groove of MHC-II molecules is occupied by the invariant Class II-associated invariant chain peptide (CLIP), which is degraded by cysteine proteases to facilitate the binding of peptide antigens (Lee and McConnell, 1995). cTEC express Cathepsin-L, a lysosomal cysteine protease unique to the cortex (mTEC and DC express the variant Cathepsin-S), which is integral to cTEC antigen loading, as the majority of MHC-II molecules in Cathepsin-L deficient cTEC retain CLIP (Farr et al., 1996, Nakagawa et al., 1998). The thymus of *Ctsl*$^{-/-}$ mice has a 60-80% reduction in the number of SP4 T-cells, with an equivalent loss of peripheral CD4s, suggesting the capacity of cTEC to present an array of endogenous peptides to be essential for the positive selection of MHC-II restricted T-cells (Nakagawa et al., 1998, Honey et al., 2002). Interestingly, the cellularity of SP4 thymocytes is restored in *Ctsl*$^{-/-}$ mice that lack expression of MHC-II on thymic dendritic cells, suggesting that in strict numerical terms, the positive selection of cortical thymocytes is not impaired in the absence of Cathepsin-L – rather, the TCR specificity of positively selected thymocytes is biased towards types that are deleted in negative selection within the medulla (Honey et al., 2002). The product of the Prss16 gene - the Thymus-specific Serine Protease (TSSP) – is also specific in it's expression to cTEC (Carrier et al., 1999). The importance of this protease is however less clear-cut. The production of SP thymocytes is unaltered in *Prss16*$^{-/-}$ mice, however close examination of the Vβ repertoire of SP4 has revealed it to be skewed relative to that seen in wildtype thymocytes (Gommeaux et al., 2009). Studies on Non-obese diabetic (NOD) mice deficient in TSSP have shown that TSSP is necessary for the diabetic phenotype (Viret et al., 2011a, Viret et al.,

2011b). *Prss16*$^{-/-}$ cTEC have reduced surface presentation of the pancreatic islet auto-antigen IA-2β, and hence diabetes-triggering CD4^{+} thymocytes likely fail to be positively selected in the thymus of these mice (Viret et al., 2011a, Viret et al., 2011b). The expression of specific endosomal/lysozomal proteases by cTEC therefore appears to be a crucial factor in the production and loading of positively selecting peptide ligands.

The Thymoproteasome

In the tissues of adult mice, the expression of the transcription factor Aire, and the proteasomal sub-unit β5t are distinct to the thymic medulla and cortex respectively (Zuklys et al., 2000). However, Aire is expressed in embryogenesis within the genital ridge and by oocytes (Bin et al., 2012), and is only detectable from the emergence of functionally mature mTEC in the thymus at day 16 of embryonic development (E16, where birth occurs around E20) (Zuklys et al., 2000), leaving β5t to stand alone as a defining factor of thymus functional specialization; β5t is expressed in the thymic primordium from E12.5, and is expressed exclusively by TEC from embryonic development through to adulthood (Ripen et al., 2011, Murata et al., 2007). Together with β1 and β2, β5 subunits represent the enzymatically active constituents of the core of the proteasome (Groll et al., 1997). All three subunits are constitutively expressed in all cell types, however upon IFN-stimulation, immune cells are induced to express the variants β1i, β2i and β5i, which together form the "immunoproteasome" (Tanaka, 1994). β5i has enhanced chymotrypsin-like activity, and hence has greater efficiency at producing peptides for MHC-I loading in the event of viral infection (Nussbaum et al., 1998, Zanker et al., 2013).

Expression of β5t by cTEC allows the formation of the unique "thymoproteasome", which is essential for the production of peptides capable of positively selecting MHC I-restricted T-cells. β5t-deficient *Psmb11*$^{-/-}$ mice have a 70-80% reduction in the number of SP8 thymocytes in spite of the maintenance of cTEC cellularity and surface MHC expression, and hence peptides produced by the degradation of endogenous proteins by the constitutive and immunoproteasomes (as β5i expression predominates in cTEC in the absence of β5t), are insufficient to maintain the cortical production of CD8 T-cells (Murata et al., 2007, Nitta et al., 2010). The remaining fraction of CD8^{+} T-cells present in *Psmb11*$^{-/-}$ mice again had highly altered Vβ chain composition relative to their wildtype counterparts, as well as higher levels of expression of CD5 and the TCR signal transducer Nur77 (Xing et al., 2013, Takada et al., 2015), both indicative of strong TCR ligation during positive selection, and potentially suggesting that higher affinity selection events occur in the absence of β5t.

In contrasting fashion to β5i, β5t possesses a lower degree of chymotrypsin-like activity, but it's function is not dependent on competitive inhibition of β5/β5i variants, as specific inhibitors of these two subunits fail to re-capitulate cTEC function in it's absence. Instead, it appears likely that β5t is required for the production of unique positively selecting ligands by cTEC. The potential for this requirement has been demonstrated by the addition of antigenic OVA peptides with altered C-terminal amino acids to OT-I FTOC cultures (Daniels et al., 2006, Stepanek et al., 2014). In this instance, none of the peptide variants tested were capable of inducing positive selection, suggesting the generation of unique peptides by cTEC may be essential for the selection of specific T-cell clones. In monoclonal models, reliance on cTEC β5t expression has

been shown to be dependent on specific TCR clonality (Xing et al., 2013). For instance, HY TCR-transgenic thymocytes fail to undergo positive selection in *Psmb11*$^{-/-}$ thymus, however selection of OT-I T-cells does not require β5t (Xing et al., 2013). This effect has been shown to have some, albeit imperfect correlation with the strength of TCR signalling in positive selection of a given clone, with cells expressing high levels of CD5 post-selection tending towards β5t-independence, and clones with lower post-selection CD5, indicative of low–level TCR triggering, having a tendency to be β5t-dependent, perhaps suggesting that β5t is required for the production of specific partially agonistic or antagonistic peptides known to influence positive selection (Xing et al., 2013). A recent study by Takada et al. (Takada et al., 2015) has shown for the first time that β5t is not only required for the screening of TCR functionality among DP thymocytes, but also plays an important role in functionally educating T-cells at the DP stage. Isolated naïve CD8^{+} T-cells from β5t-deficient mice have reduced responsiveness to TCR triggering, and fail to highly up-regulate the activation markers CD25 and CD69, as well as displaying smaller increases in cellular expansion and calcium flux upon anti-CD3 stimulation (Takada et al., 2015). Indeed, OT-I T-cells selected in *Psmb11*$^{-/-}$ thymus have been demonstrated to be incompetent in controlling sub-lethal influenza infections in mice, and in this study failed to respond to infection by OVA-expressing Listeria Monocytogenes, producing short-lived effector T-cells upon engagement with antigen, in contrast to the memory cells formed on activation of wildtype-derived OT-I T-cells (Takada et al., 2015).

Macroautophagy

A final interesting function of cTEC is their constitutively high capacity to undergo the process of macro-autophagy (Nedjic et al., 2008), in which small (~1um^3) volumes of cytoplasm are encapsulated within a double membrane, which fuses with endosomal/lysosomal compartments, resulting in the degradation of the cytoplasmic contents (Yang and Klionsky, 2010). This process is believed to play critical roles in the homeostasis of some cell types via the removal of misfolded proteins and unwanted developmental features from cells, however the deletion of autophagy-related protein Atg5 has revealed no such reliance by cTEC for their integrity and survival (Nedjic et al., 2008). Although not unique to cTEC in the thymus – 60% of cTEC present with high numbers of auto-phagosomes, compared to 10% of MHC-II^{hi} mTEC – cTEC as a population hence possess a distinctly high capacity for autophagy, which is also absent from thymic dendritic cells (Nedjic et al., 2008). Surface presentation of the MHC II-derived I-E$\alpha_{52\text{-}68}$ peptide was found to be greatly increased in the cTEC of kidney capsule grafted *Atg5*$^{-/-}$ fetal lobes, suggesting that under normal conditions, autophagy is required for the provision of MHC II-presented peptides for positive selection (Nedjic et al., 2008). The exact extent of the impediment to presentation of a full array of cTEC peptides is comparatively difficult to assess however, as the low cellular yield from thymic enzymatic digestion, and the loss of cTEC-specific genes in culture preclude isolation of sufficient cTEC for analysis via mass spectrometry.

Unlike β5t-deficient mice, the development of SP thymocytes in *Atg5*$^{-/-}$ fetal thymic lobes was unaffected; however, TCR-transgenic models showed a clone-specific defect in the efficiency of positive selection of CD4 T-cells, with the

DP to SP4 transition of both HA and SEP T-cells effected (Nedjic et al., 2008). A more recent publication by Schuster et al. (2015) has revealed similar findings in a mouse model where the autophagy related component Clec16A is knocked down in TEC. Interestingly, as well as preventing the diabetes development in NOD mice, Clec16A knock-down produces CD4 T-cells with reduced responsiveness to in vitro TCR-triggering, as revealed by reduced phosphorylation of downstream TCR signalling components relative to cells selected by wildtype thymus (Schuster et al., 2015). Hence, it may be that autophagic processes in cTEC create a peptide repertoire capable of both positively selecting and functionally educating MHC II-restricted T-cells in the same vein as β5t regulates these processes in $CD8^+$ T-cell development.

Although the exact nature of the requirement for a specific peptide array in positive selection requires further study, evidence eludes to the necessity of presentation of both specific peptides for the selection of some TCR specificities, as well as peptides distinct from those facilitating negative selection in the medulla. However, what remains clear is that, via their unique expression of proteins involved in the processing and presentation of endogenous peptide antigen, cTEC are highly specialized to mediate quality control measures on developing thymocytes, producing a polyclonal pool of reactive, and functionally capable T-cells.

1.3.2. mTEC mirror antigen expression in peripheral tissues for negative selection

The medullary micro-environment is home to multiple populations of antigen presenting cells which play distinct roles in the establishment of central tolerance. In addition to mTEC, both medullary dendritic cells and B cells have been shown to be of great importance in the deletion of auto-reactive T-cells. Both haematopoietic cell types have been suggested to consist of cells formed within the thymus (Wu et al., 2001, Perera et al., 2013), as well as, in the case of dendritic cells, those that have homed to the thymus in response to chemokine receptor signalling (Lei et al., 2011). As a result of this, DCs are postulated to present a combination of endogenous and exogenous antigens within the medulla (Klein et al., 2014). Recent evidence also suggests that B-cells may have the capacity to mirror the role of mTEC in the production of tissue restricted antigens, and may hence also play a leading role in negative selection (Lu et al., 2015, Walters et al., 2014, Yamano et al., 2015). However, the contribution of mTEC to this process directly, as well as through mediation of the positioning of other medullary APCs, appears to be essential for the prevention of aberrant autoimmunity (Burkly et al., 1995).

Tissue restricted antigen expression

Central tolerance is achieved in the medulla through two main processes – the antigen-specific deletion of thymocytes with a high TCR affinity for self-antigen, and the generation of T-Reg (Millar and Ohashi, 2016). Both aspects require engagement with self-antigens to elicit high levels of TCR triggering in

single positive thymocytes (Moran et al., 2011, Stritesky et al., 2013), and hence mTEC are uniquely specialized in the production of peptide antigens for this purpose. To a degree, some of these specializations overlap with those observed in cTEC; ~10% of mTEC^{hi} have also been observed to have high constitutive levels of macroautophagy (Nedjic et al., 2008), and athymic mice grafted with *Atg5*$^{-/-}$ thymus present with a moderate autoimmune phenotype, suggested a breakdown in central tolerance mechanisms in the absence of autophagic processes (Aichinger et al., 2013). However, better characterized is the unique ability of mTEC to express an array of genes normally restricted to few tissues or cell types within the body – tissue restricted antigens (Anderson et al., 2002). Expression of TRAs occurs in a mosaic pattern, with individual mTEC expressing a limited combination of TRAs, allowing the population together to express and display a huge pool of antigens broadly representative of those available endogenously for presentation in the periphery (Brennecke et al., 2015, Rattay et al., 2016, Meredith et al., 2015). Recently, this has been explained to occur as the result of expression of small inter-chromosomal gene clusters in individual cells, and hence is likely regulated epigenetically (Brennecke et al., 2015, Meredith et al., 2015). TRA expression is regulated at multiple levels, but until recently only one transcription factor had been identified to have a major impact on TRA expression in mTEC – the product of the autoimmune regulator gene, Aire (Anderson et al., 2002), disturbance of which is responsible for the severe autoimmune pathology in patients with polyendocrinopathy-candidiasis-ectodermal dystrophy (APECED) (Nagamine et al., 1997). Expression of Aire is relatively distinct to the thymus in adult mice - although certain reporter models suggest rare bone marrow derived cells to express low levels of Aire in murine

thymus and peripheral tissues (Gardner et al., 2013; Yamano et al., 2015) – and Aire^{+} cells, which are restricted to the mTEC^{hi} compartment, form approximately 60% of this population in adult mice (Kawano et al., 2015). mTEC genetically deficient in Aire are estimated to have repression of an estimated 3,980 genes in mTEC, the vast majority of which are TRAs (Sansom et al., 2015). The first direct evidence for requirement for Aire in negative selection came from a model wherein the non-endogenouS HEL protein was expressed under the control of the rat insulin promoter – insulin being an Aire-dependent TRA (Liston et al., 2003). 3A9 TCR-transgenic T-cells, which are reactive to HEL-derived antigens, were negatively selected in *Aire*$^{+/+}$ RIP-HEL mice, but survived negative selection in RIP-HEL mice that were deficient for Aire, showing a direct reliance for Aire-dependent TRA expression for negative selection of autoreactive T-cell clones by mTEC (Liston et al., 2003). Although mTEC are the major source of TRAs within the thymic medulla, several interesting studies have suggested that DC play an equally important role in the negative selection of TRA-reactive thymocytes. Initially this effect was observed in TCR transgenic mice where expression of MHC-I was absent from mTEC, dendritic cells, or both populations. Negative selection of MHC-I-restricted T-cells was observed to a degree if MHC-I was absent from either population, but was lost when neither medullary APC type had class I expression (Gallegos and Bevan, 2004). This suggests the capacity for antigen transfer between mTEC and DCs in the medulla, which was later visualised directly through analysis of Foxn1:GFP mice (Koble and Kyewski, 2009). Here, GFP expression is restricted to thymic epithelium – however, CD11c^{+} DC with low levels of GFP can be found in the thymus, suggesting DC can rip antigen from mTEC directly (Koble and Kyewski, 2009). A recent study by Perry et al. presented a great insight into the

contribution of mTEC and DC to the negative selection of thymocytes with naturally occurring TCR specificities (Perry et al., 2014). In complicated models lacking MHC-II on either mTEC or DC, the contribution of either cell type to the deletion of various transgenic T-cells recognising Aire-dependent and Aire-independent TRAs was investigated (Perry et al., 2014). In fact, negative selection of T-cells recognizing both Aire-dependent and independent TRA were found to be deleted either by mTEC alone, DC alone, or both in combination, confirming the transfer of mTEC-derived antigens to DC has a direct necessity in shaping the TCR repertoire of T-cells output from the thymus (Perry et al., 2014).

In contrast to the development of conventional CD4 T-cells, T-Reg have been shown to have a fundamental requirement for interaction with the medulla for their thymic generation in a process also heavily dependent on TRA expression. A recent publication from our lab demonstrated a failure in the development of T-Reg from their $CD25^{+}$ precursor stage in kidney capsule grafted fetal thymic lobes lacking RelB, a transcription factor required for the development of mTEC (Cowan et al., 2013). By the same methods used to assess negative selection, the Perry paper showed the Aire-dependent and Aire-independent generation of T-Reg with an array of transgenic TCRs again to be a shared function of both mTEC and medullary DCs (Perry et al., 2014). This finding has been confirmed in less complex terms in vivo through the identification of a small proportion of endogenous prostate antigen-specific T-Regs baring the MJ23 TCR (Malchow et al., 2013). $MJ23^{+}$ T-Regs are implicated in limiting the T-cell response to murine models of prostate cancer, and have been shown to be absent from the thymus of $Aire^{-/-}$ mice, where their selecting antigen is not expressed (Malchow et al., 2013). Interestingly, despite having normal

numbers peripherally, T-Reg are significantly reduced in the thymus of *Aire*$^{-/-}$ mice, although this can in part be attributed to the loss of expression of XCL1 from Aire-deficient mTEC, a factor controlling the migration and positioning of conventional medullary DCs (Lei et al., 2011).

Many TRAs have known Aire-dependence, with the expression of most being almost entirely lost from *Aire*$^{-/-}$ mTEC (Anderson et al., 2002, Derbinski et al., 2005). Even a modest reduction in antigen expression is likely to impact on the generation antigen-specific T-Reg, as bone marrow chimera mice with increasingly dilute fractions of TCR transgenic T-cells have demonstrated a strict relationship between antigen availability and the efficiency of Foxp3 induction (Moran et al., 2011). Regardless, although many TRAs are lost, the expression of the majority has been found to persist in *Aire*$^{-/-}$ mTEC (Derbinski et al., 2005). This long suggested the existence of a secondary transcriptional regulator of thymic TRA expression that remained elusive for more than a decade, but in a recent landmark publication was identified to be the forebrain embryonic zinc finger-like protein Fezf2, which gene expression profiling determined to control the expression of ~490 genes (Takaba et al., 2015). These two transcription factors dictate the expression of largely non-overlapping groups of TRAs, and deficiency of either has been demonstrated to alter thymic selection, as demonstrated by differences in Vβ-chain usage by developing SP4 and SP8 thymocytes, as well as impact negatively on T-Reg development (Takaba et al., 2015). Tissue-specific autoimmune disease has been noted in *Aire*$^{-/-}$ mice, as well as mice with TEC deficient for Fezf2 to different severities; *Aire*$^{-/-}$ mice develop mild, non-fatal disease (Anderson et al., 2002, Hubert et al., 2008), whereas the consequences of Fezf2 deficiency are more severe, likely as a high proportion of

Fezf2-promoted TRAs are proteins expressed in the central nervous system (Takaba et al., 2015). That disease is comparatively mild in *Aire*$^{-/-}$ mice contrasts significantly with human APECED patients, perhaps for complex reasons, as Aire is known to play a role in murine TEC development (Anderson et al., 2002, Gray et al., 2007, Gillard et al., 2007), and control the expression of other factors required for T-cell development besides that of TRAs. It is also worth noting that, although mTEC act together with DC to present peptide antigen for T-Reg development, their role also encompasses the provision of an array of co-stimulatory molecules that, although largely redundant in the production of conventional thymocytes, are an essential axis for Foxp3 induction in the thymus. These have been discovered to include CD80/CD86 (Lio et al., 2010), CD70 (Coquet et al., 2013), OX40L and GITRL (Mahmud et al., 2014), the absence of each of which has a differential impact on the initial induction of T-Reg precursor populations, as well as subsequent up-regulation of Foxp3.

1.3.3. Development of thymic epithelial cells

Emergence of the cTEC and mTEC lineages

Although commencement of T-cell development begins embryonically, output of mature T-cells from the thymus is only detected post-natally in mice, coinciding with full functional maturation of stromal elements forming the thymic microenvironment. The thymic primordium emerges at E10 (Rodewald, 2008), and becomes invaded by haematopoietic precursor populations in a chemokine receptor dependent manner at E11.5 (Liu et al., 2006), which in turn acts to trigger progressive differentiation and maturation of the epithelium until

competence to foster thymocyte development is reached. As mature thymic epithelium is made up of two distinct cellular lineages in cTEC and mTEC, early experiments sought to determine the nature of the emergence of these populations in the embryonic thymus (models of fetal and adult TEC development are summarized in Figures 1.3 and 1.4). Through the isolation and spiking of individual fluorescently tagged cells into fetal thymus, it was determined that the cTEC and mTEC lineages can emerge from a bipotent progenitor, as yellow fluorescent protein^{+} (YFP^{+}) cTEC and mTEC were observed to develop from a single progenitor (Rossi et al., 2006, Bleul et al., 2006). More recent schools of thought have utilised reporter models tracing cells expressing the functional cTEC marker β5t. β5t expression is apparent in the E12 embryo (Ripen et al., 2011), before the emergence of the mTEC lineage from E13 onwards, and initial fate mapping of β5t expressing cells yielded a surprise result – β5t expressing cells were found to go on to form not only the cTEC lineage, but also a substantial proportion of mTEC (Ohigashi et al., 2013). Interestingly, subsequent studies using inducible reporters have demonstrated the majority of mTEC to emerge from β5t^{+} cTEC progenitors in the embryonic thymus, but to a far lesser extent in the adult, even on recovery after substantial thymic damage (Ohigashi et al., 2015, Mayer et al., 2016), suggesting the majority of mTEC in the adult thymus to originate from a unipotent progenitor population. Indeed, TEC expressing claudins 3 & 4 (Cld3,4) have been found to have the capacity to reconstitute the medulla on introduction into mTEC-deficient *aly*/*aly* fetal thymic lobes (Hamazaki et al., 2007), and have been recently traced to form phenotypically mature mTEC (Baik et al., 2016). Furthermore, a small subset of Cld3,4^{+}SSEA1^{+} cells has been shown to possess unique self-renewal capacity,

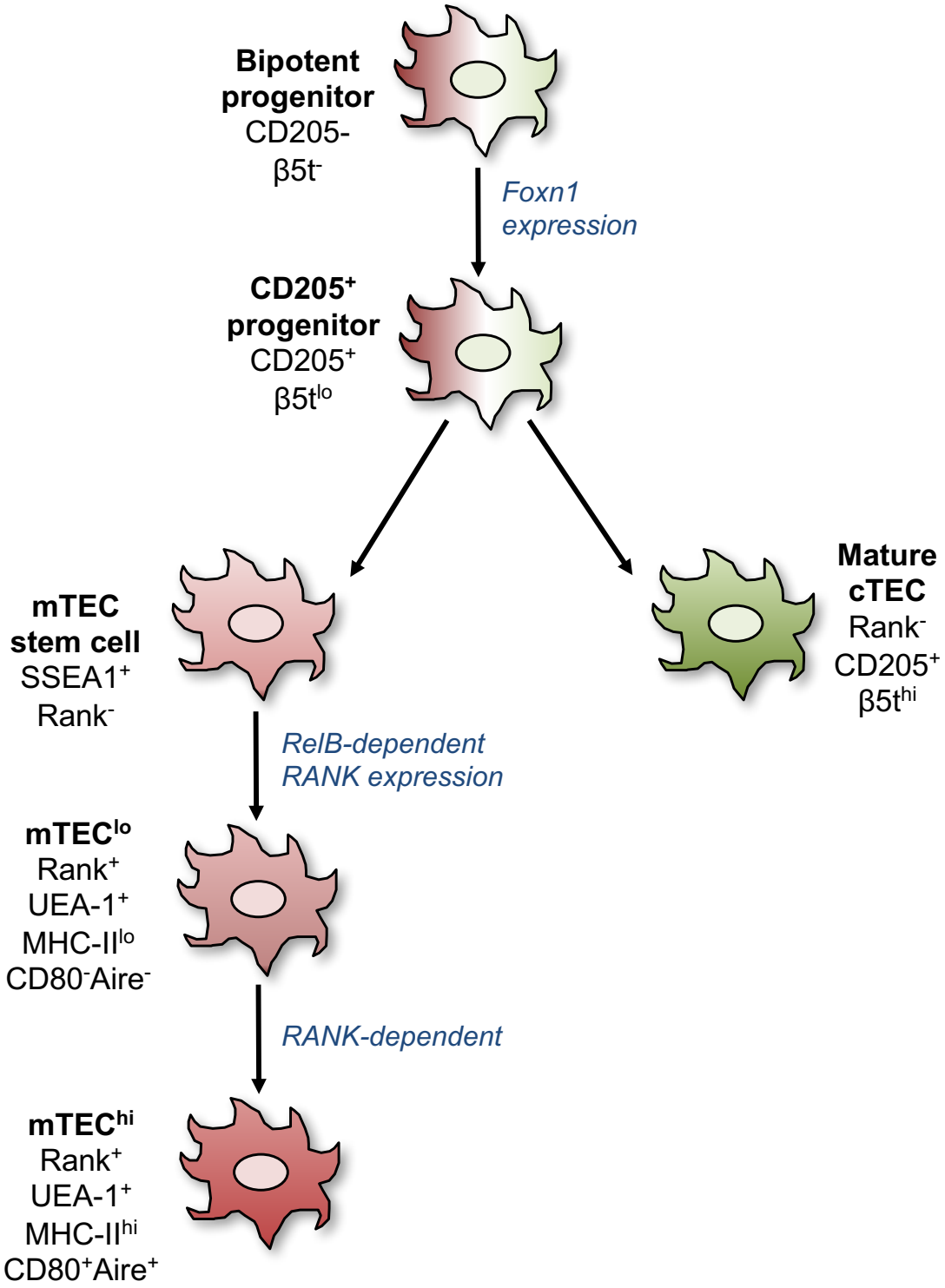
Bipotent progenitor
CD205-
β5t-
Foxn1 expression
CD205+ progenitor
CD205+
β5tlo
mTEC stem cell
SSEA1+
Rank-
Mature cTEC
Rank-
CD205+
β5thi
RelB-dependent RANK expression
mTEClo
Rank+
UEA-1+
MHC-IIlo
CD80-Aire-
RANK-dependent
mTEChi
Rank+
UEA-1+
MHC-IIhi
CD80+Aire+

Figure 1.3: Fetal TEC development

Sequential development and maturation of cTEC and mTEC lineages is known to be initiated from a bipotent progenitor population, which gives rise to subsequent progenitors of a cTEC phenotype.

A Committed progenitor model

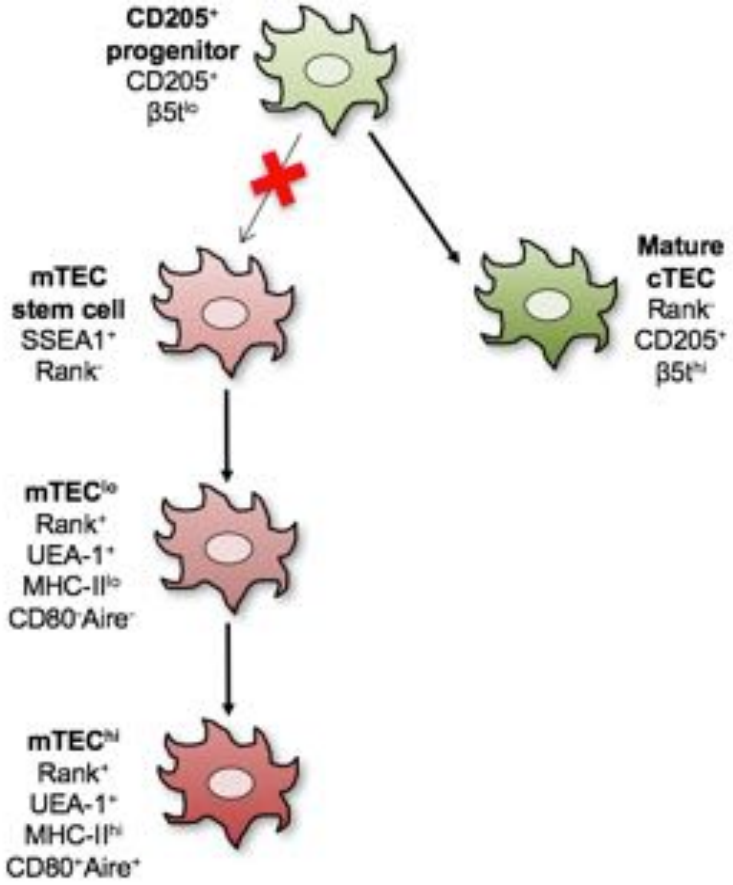

B Bipotent progenitor model

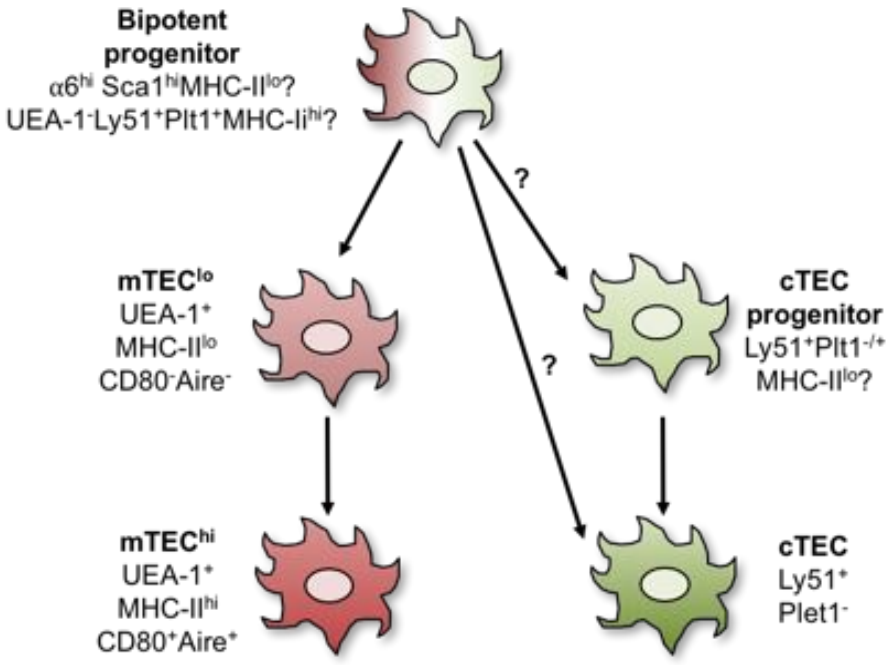

Figure 1.4: Models of adult TEC development

Development of cTEC and mTEC in adult mice likely occurs through one of two mechanisms; one involving committed cTEC and mTEC progenitor populations (top), and the other involving a bipotent progenitor population (bottom) with self-renewing capacity which gives rise to both committed cTEC progenitors and immature mTEC.

suggesting these to represent a population of mTEC stem cells (Hamazaki et al., 2007, Sekai et al., 2014). Although likely to be of limited contribution to mTEC in the adult, potential multilineage TEC stem cell populations have been identified through their capacity to form spheroid structures through self-renewal in culture, and by such means have been suggested to exist among TEC subsets identifiable as UEA-1^{-}MHC-II^{lo}Sca1^{hi} (Wong et al., 2014), Ly51^{+}Plet1^{+}MHC-II^{hi} (Ulyanchenko et al., 2016) or alternatively Foxn1^{-} (Ucar et al., 2014). The study by Ulyanchenko et al. isolated not only Ly51^{+}Plet1^{+}MHC-II^{hi} cells from adult thymus capable of contributing to both mTEC and cTEC populations in thymic re-aggregations, but also Ly51^{+}Plet1^{-}MHC-II^{lo} populations that could sustainably give rise to cortical regions, suggesting this to be a possible commited cTEC progenitor population downstream of multipotent Plet1^{+} cells (Ulyanchenko et al., 2016).

Although the transcription factor Foxn1 is an absolute requirement for TEC development, the early emergence of both lineages has now been shown to occur independently of Foxn1 expression (Ucar et al., 2014, Baik et al., 2016). Instead, Foxn1 has been found to regulate the developmental progression of both cTEC and mTEC after their earliest progenitor stages, controlling the pool size of SSEA1^{+} mTEC progenitors (Baik et al., 2016), as well as regulating the functional maturation of cTEC, including their acquisition of expression of Dll4 and cathepsin-L (Nowell et al., 2011). Fittingly, a recent reporter model has shown Foxn1 expression to be serially down-regulated in TEC with age, where Foxn1$^{lo/neg}$ TEC accumulate, associated with a reduction in cTEC function, but up-regulated in the recovery stages of models of thymic damage (Rode et al., 2015). Epithelial lineage commitment for the formation of cortical and medullary

structures capable of supporting thymocyte development hence occurs in multiple stages, with the contribution of bipotent and unipotent progenitors of differential importance in the fetal and adult thymus.

Functional maturation of mTEC in response to haematopoietic cross-talk

The formation of the mTEC lineage has long been known to critically depend on the transcription factor RelB, a member of the NF κB family (Burkly et al., 1995), whereas functional maturation is tailored through signalling by various members of the tumour necrosis factor receptor superfamily (TNFRSF) . Medullary regions are absent from *Relb*$^{-/-}$ thymus, as well as models lacking functional variants of Traf6 and NIK, proteins respectively required to enable transcription and activation of Relb (Akiyama et al., 2005, Kajiura et al., 2004). Interestingly, a recent study Baik et al. has demonstrated the mTEC lineage to emerge in RelB-deficient thymus, as SSEA1^{+} mTEC stem cells persist; however, *Relb*$^{-/-}$ mTEC fail to up-regulate expression of the receptor activator of NF κB (Rank), a TNFRSF member observed to critically regulate functional maturation of mTEC (Baik et al., 2016).

Rank is one of a trifecta of TNFRSF members known to play an important role in mTEC development at both the embryonic and adult stages – the others being CD40, and the lymphotoxin-β receptor (Ltbr). The discovery of this axis of TNFR signalling has yielded interesting research into cross-talk between distinct waves of haematopoietic cells and epithelium, which appears to drive the maturation of the mTEC compartment, and the formation of the medulla (Rossi et al., 2005, Desanti et al., 2012). The initial appearance of Aire^{+} mTEC, evident from E16 in wildtype thymus, has been shown to be severely delayed in the

absence of Rank (Akiyama et al., 2008). Equally, treatment of fetal thymic organ cultures (FTOC) with 2-deoxyguanosine (dGuo) - which is selectively toxic to rapidly dividing haematopoietic cells – effectively blocks the development of Aire^{+} mTEC *in vitro* (Rossi et al., 2007), suggesting the cellular source of Rank ligand (RankL) to be haematopoietic in origin. Subsequent analyses of haematopoietic cells present in the early stages of fetal thymic development demonstrated the presence of lymphoid tissue inducer cells (LTi) and innate-like Vγ5^{+} dendritic epidermal T-cells (DETC) expressing RankL (Rossi et al., 2007, Roberts et al., 2012). Introduction of sorted populations of LTi or DETC into dGuo FTOC was found to induce the formation of Aire^{+} mTEC from Aire^{-} precursors in a Rank-dependent manner (Rossi et al., 2007, Roberts et al., 2012). Analysis of fetal thymi deficient for RORγt, a transcription factor required for LTi development, showed Aire^{+} cells to be lacking in the late stages of embryonic development (Rossi et al., 2007, White et al., 2008), together suggesting the maturation of the mTEC compartment to be controlled by cross-talk with innate immune cells at the fetal stage. Interestingly, although greatly reduced, *Rank*$^{-/-}$ mTEC do form a small fraction of Aire^{+} cells post-natally (Hikosaka et al., 2008). This coincides with the appearance of mature SP thymocytes in the medulla, which have been shown to express a combination of RankL and CD40L on their cell surface. Like Rank stimulation, introduction of CD40L into dGuo FTOC has been shown to induce the formation of Aire^{+} cells, albeit to a lesser extent (Akiyama et al., 2008). This finding is likely to play out *in vivo*, as double deficiency for Rank and CD40 in adult mTEC compounds the defect seen in the formation of mature Aire^{+} cells (Mouri et al., 2011). These findings suggested fetal and adult mTEC maturation to be regulated by differential mechanisms; a

finding which was supported by studies involving *Zap70*$^{-/-}$ mice, which fail to develop mature T-cells due to blockade in the TCR signalling pathway (Chan et al., 1992). *Zap70*$^{-/-}$ mice have approximately a 50% reduction in the number of Aire^{+} mTEC^{hi}, which can be restored by re-introduction of SP thymocytes, as shown by the re-emergence of Aire^{+} cells in mice in which the *Zap70* gene is inducible on administration of the antibiotic doxycycline (White et al., 2010). This nicely demonstrates the reliance of adult epithelium on adaptive immune cells for conditioning and maturation. In addition to regulating maturation directly, interplay between the three receptors has been observed. Treatment of dGuo FTOC cultures with a stimulatory antibody against the Rank receptor triggers up-regulation of CD40 by mTEC, expression of which is reduced in mTEC^{hi} in adult *Rank*$^{-/-}$ mice (Desanti et al., 2012). Hence, given the recent identification of Rank^{+} mTEC precursors, it appears likely that Rank acts to both facilitate the commencement of the mTEC differentiation programme from the embryonic stage, as well as maintaining CD40L-receptiveness for the formation of Aire^{+} cells in the adult mTEC.

Early research into the role of Ltbr in mTEC development was conflicting, however a consensus has now been reached that Ltbr signalling, provided by at least two identified ligands in lymphotoxin-α and LIGHT, controls the expression of a range of functional genes in adult mTEC in a manner independent of Aire (Seach et al., 2008, Zhu et al., 2007). Anti-Ltbr stimulation *in vitro* does compound the induction of Aire^{+} cells by RankL (but not alone), although this has been shown to occur via the Ltbr-dependent up-regulation of expression of the Rank receptor (Mouri et al., 2011). Indeed, gene expression analyses have shown the genes controlled by the Ltbr axis to be almost entirely non-

overlapping by those lost in Aire-deficiency (Seach et al., 2008). However, both regulators have been demonstrated to be required for expression of the chemokine receptor ligand CCL21 (Lkhagvasuren et al., 2013), which plays an important role in the cortex-medulla trafficking of SP thymocytes (Zhu et al., 2007). Regardless, the issue of largely non-overlapping control of mTEC gene expression by Ltbr signalling was another issue addressed by the discovery of Fezf2. Fezf2 protein is largely undetectable by flow cytometry and confocal microscopy in *Ltbr*$^{-/-}$ tissues, accompanied by loss of expression of a host of Fezf2-dependent TRAs (Takaba et al., 2015). In addition, *Ltbr*$^{-/-}$ mice have long been reported to possess an autoimmune phenotype, albeit comparatively mild compared to that observed on deletion of Fezf2 – likely explainable by persisting low-level expression of Fezf2 in *Ltbr*$^{-/-}$ TEC (Takaba et al., 2015). As a relatively recent discovery, the cellular regulators of Fezf2 expression throughout development have yet to be addressed, although they are likely to be separate from those controlling Aire expression, as Fezf2 is unaffected by the absence of the Rank receptor, and Aire itself (Takaba et al., 2015). However, what appears clear is that an amalgamation of TNFRSF member signals regulates different aspects of the functional maturation of mTEC, inclusive of the expression of TRAs, for negative selection of SP thymocytes.

1.4. GENERAL AIMS

The epithelial cells of the thymic medulla play an essential role in inducing tolerance in αβ T-cells, and are involved in the production of important non-conventional T-cell subsets with immunomodulatory properties. Recent findings suggest mTEC to be greatly heterogeneous, and inclusive of multiple subsets of cells functionally specialised for the production of chemokine receptor ligands and tissue restricted antigens. Moreover, these distinct subsets have been found to have differential requirements for their functional maturation, involving alternative pathways of stimulation via TNFRSF members. Our recently produced microarray data identified further genes corresponding to functional molecules differentially expressed by mTEC subsets; namely *Tnfrsf11b* and *Nos2*, which respectively code for osteoprotegerin (OPG) and inducible nitrix oxide synthase (iNOS). We therefore aimed to address the following questions through analysis of *Tnfrsf11b*$^{-/-}$ and *Nos2*$^{-/-}$ mice;

1) What are the conditions for expression of OPG and iNOS by mTEC, and how does expression effect medullary homeostasis; specifically, the development, functional maturation and survival of medullary stromal subsets, including mTEC?

2) How do OPG and iNOS directly or indirectly impact on thymocyte development and maturation, negative selection in the medulla, and the generation of non-conventional T-cell subsets?

2. MATERIALS AND METHODS

2.1. Mice

The mice used in this study were housed in accordance with Home Office regulations in the [redacted] at [redacted]. Non-genetically manipulated (wildtype) C57BL/6 mice were used to characterise the development of T-cells and thymic epithelial cells under steady state conditions. All wildtype mice used were C57BL/6 unless stated, and all knockout mouse strains were bred onto the C57BL/6 background. Knockout mouse strains (listed in Table 2.1) were obtained either from the [redacted], as a kind gift from collaborating research groups, or from a commercial supplier. Mice in experiments comparing wildtype and knockout strains were matched for age and sex, and adult mice were defined as those between 8-12 weeks of age. Mice were genotyped in PCR assays by obtaining ear/tail tissues by Transnetyx. Timed matings were derived from co-habitation of 1 male and 2 female mice, wherein the number of days of embryonic development were calculated as the number of days which had elapsed from first detection of a vaginal plug. For the collection of tissues, mice were culled by cervical dislocation in accordance with Schedule 1 of the Animals (Scientific Procedures) Act.

Table 2.1 - Table of mouse strains

Mouse strain	Phenotype	Source
C57BL/6	Wildtype	
Balb/c	Wildtype	
BoyJ	Wildtype	
Plt/plt	A spontaneously occurring deletion of the Ccl19/21 loci on chromosome 4 leads to lack of expression of the Ccr7 ligands Ccl19/21 in secondary lymphoid tissues (Mory et al., The Journal of Experimental Medicine, 2001)	
Tnfrsf11b$^{-/-}$	Mice lack expression o f osteoprotegerin (OPG), an inhibitory false receptor capable of binding free ligand for the Rank receptor (Mizuno, Biochemical and Biophysical Research Communications, 1998).	
Rag-2p-GFP	Transgenic mice carrying a bacterial artificial chromosome (BAC) carrying green fluorescent protein (GFP) under control of the locus for the Rag2 gene (Yu et al., 1999).	
Tnfrsf11b$^{-/-}$ x Rag-2p-GFP	Mice lack expression of OPG, in addition to expressing GFP under the control of the Rag2 gene.	Crossing of *Tnfrsf11b*$^{-/-}$ and Rag-2p-GFP mice at
Rank-Venus	Transgenic mice carrying a BAC carrying the fluorescent protein Venus under control of regulatory elements for the Tnfrsf11a gene (McCarthy et al, 2015).	Created by
Aire$^{-/-}$	Mice lack expression of the transcription factor product of the autoimmune regulator gene, leading to self antigen expression by mTEC (Ramsey, Human Molecular Genetics, 2002).	
Aire$^{-/-}$ x Rag-2p-GFP	Mice lack expression of Aire, in addition to expressing GFP under the control of the Rag2 gene.	Crossing of *Aire*$^{-/-}$ and Rag-2p-GFP mice at
Nos2$^{-/-}$	Mice are deficient for expression of the inducible isoform of nitric oxide synthase (iNOS), an enzyme catalysing the formation of the free radical nitric oxide (NO) from L-arginine.	
Aire$^{-/-}$ x *Nos2*$^{-/-}$	Mice lack expression of Aire, in addition to iNOS.	Crossing of *Aire*$^{-/-}$ and *Nos2*$^{-/-}$ mice at
Ifng$^{-/-}$	Mice lack expression of the inflammatory cytokine interferon gamma (IFNY).	
Tnfr1/2$^{-/-}$	Cells lack responsiveness to the inflammatory cytokine tumor necrosis factor alpha (TNFα).	

2.2. Media and tissue culture reagents

For short-term storage, isolated cells were incubated in RF10 media (ingredients listed in Table 2.2, top). For cell and organ culture experiments, cells were instead incubated in DMEM (ingredients listed in Table 2.2, bottom).

Table 2.2 - Table of media and tissue culture reagents

Medium and Additives	Volume	Final concentration in solution
RPMI-1640 + 20mM Hepes, with L-glutamine, without bicarbonate (Sigma)	10mls	-
200nM L-glutamine	100ul	2mM
5000 IU/ml Penicillin and Streptomycin	200ul	100IU/ml
Heat-inactivated fetal calf serum (FCS)	1ml	10%

Medium and Additives	Volume	Final concentration in solution
Dulbecco's Medium with 3.7g/l bicarbonate, without glutamine (Sigma)	20ml	
100x non-essential amino acids (Concentrations in mg/ml; 8.9 L-Alanine, 15.0 L-Asparagine, 13.0 L-Aspartic acid, 7.5 Glycine, 14.2 L-Glutamic acid, 11.5 L-Proline, 10.5 L-Serine)	200ul	1x
1 m Hepes	200ul	10mM
5X103 M2 Mercaptoethanol	200ul	
200mM L-Glutamine	400ul	4mM
5000 IU/ml Penicillin and Streptomycin	400ul	100 IU/ml
Heat-inactivated FCS	2ml	10%

2.3. Isolation of specific cell populations

Isolation of lymphocytes

Desired lymphoid organs were dissected from culled mice, and carefully cleaned of excess fat and connective tissues in RF10 under a light microscope. Isolated tissues were kept on ice before dissociation into cell suspensions. Lymphocyte isolates were obtained by manually teasing organs into single cell

suspensions between the frosted ends of two microscope slides, after which cells were filtered by passage through fine mesh, and re-suspended in a known volume for counting of total organ cellularity. Values for total cellularity were obtained by diluting cells in a suspension containing $5x10^3$ counting beads, and running them through the flow cytometer. Total cellularity was calculated as cells per bead x $5x10^3$ x (sample volume counted ÷ total sample volume).

Isolation of stromal cells from adult tissues

The isolation of stromal cell populations required enzymatic digestion using 20ng/ml DNAse I isolated from bovine pancreas (Sigma), together with 2.5mg/ml collagenase dispase (TEC) or collagenase D (dendritic cells, both Roche), depending on the cell population desired (both Roche). Cells were digested in 1ml RF10 for periods of 40 and 20 minutes in FACS tubes gently vortexed by a Thermomixer block at 37°c, before supernatant containing digested cells was removed. The cells were then supplemented with 0.5M EDTA to a final concentration of 0.5mM, and incubated on ice for 20 minutes to neutralise digestive enzymes.

Following their isolation through digestion, stromal cells were then subsequently enriched for the purposes of staining through the depletion of $CD45^+$ cells using the MACS approach. Cells were re-suspended in 800ul MACS buffer (PBS without Calcium and Magnesium plus 2.5ml FCS, 2ml 0.5M EDTA) supplemented with 25ul anti-CD45 microbeads (Miltenyi) for 20 minutes on ice. Following incubation, a further 2ml MACS buffer was added to suspension, and cells were passaged through magnet-bound LS columns (Miltenyi), and the

filtered suspension collected. CD45-depleted cells were then counted, and stained for the purposes of flow cytometry or cell sorting.

Isolation of stromal cells from fetal tissues

For the isolation of TEC from fetal thymic lobes, fresh or cultured tissues were first washed x3 in PBS w/o calcium and magnesium, before re-suspension in 600ul 1:10 trypsin in 0.5mM EDTA (Sigma) for 10 minutes at 37°c. Lobes were gently agitated using a 1ml pipette to aid disaggregation before trypsin was neutralised through addition of an equal volume of RF-10. Cells were centrifuged, and supernatant removed prior to re-suspension in 1ml RF-10 for accurate cell counting.

2.4. Immuno-labelling and flow cytometry

For the purposes of analysis of isolated cell populations by flow cytometry, cells were labelled with fluorochrome-conjugated antibodies. Depending on the size of the sample obtained, typically either $5x10^6$ cells, or the total sample (if less than this number) were stained in volumes of 100ul of antibodies in solution with 'FACS buffer', consisting of PBS with Calcium and Magnesium, with 3% FCS. Cells were incubated on ice in antibody solution for 30 minutes, and subsequently washed with the addition of a further 1ml volume of FACS buffer, wherein cells were centrifuged at 1400rpm for 4 minutes. Surface stained cells were then re-suspended in 200ul FACS buffer, and filtered into 12.5ml polystyrene FACS tubes (Becton), ready for their acquisition by the LSR

Fortessa (BD Bioscience) flow cytometer, and together with BD FACSDiva software.

Intracellular staining of antibodies was achieved by one of two methods. Typically for the intracellular staining of transcription and nuclear factors (Aire, Foxp3, Ki67), chemokines (CCL21) and other secreted factors (OPG, iNOS), cells were fixed with the Foxp3/transcription factor staining buffer kit (eBioscience) according to the manufacturer's instructions. Briefly, surface-stained cells were re-suspended in 'Fix/Perm' buffer (1 concentrate: 3 diluent) for 40 minutes at 4°c. Cells were then permeabilised by washing in 1ml 'Perm/wash' buffer, and re-suspended in 100ul antibody mixes made up in 'Perm/Wash' buffer (1 'Perm/wash' 10x: 9 dH_2O) for 30 minutes on ice. Cells were washed a final time in 1ml 'Perm/Wash,' filtered and acquired on the flow cytometer as above. Certain cytokines (TNFα, IL-17) and intracellular markers (cleaved Caspase 3, RORγt) required fixation with the Cytofix/cytoperm kit (BD Bioscience). Alternatively, this kit was used for the intracellular staining of established markers (Aire, CCL21, OPG, iNOS, Foxp3) while allowing the preservation of fluorescent proteins such as GFP or Venus in reporter models. In these instances, surface-stained cells were fixed in 200ul 'Cytofix/cytoperm' buffer for 40 minutes at 4°c, and subsequently washed in 1ml 'BD Perm/wash' buffer (1 'BD Perm/wash' 10x: 9 dH_2O). Fixed and permeabilised cells were then subsequently stained in 100ul antibody mix made in 'BD Perm/wash buffer' for 30 minutes on ice, and lastly washed in 1ml 'BD Perm/wash' buffer prior to being acquired by the flow cytometer. Antibodies used for the staining of cell surface markers, and intracellular staining via the eBioscience or BD fixation methods for the

identification of lymphocyte, TEC and dendritic cell populations are listed in Tables 2.3, 2.4 and 2.5 respectively.

Table 2.3 - List of antibodies for the staining of lymphocytes

Antigen	Fluorochrome	Clone / Manufacturer	Intra/Extrace-llular (fix kit)	Working dilution
CD4	PE Cy7 V510 Brilliant violet 711	GK1.5 (eBio) RM4/5 (BioLegend)	EC	1/200 1/1000 1/50-200
CD8α	Brilliant violet 786 Brolliant violet 510	53-6.7 (BioLegend)	EC	1/200 1/200
TCRβ	APC Cy7	H57-597 (eBio)	EC	1/200
B220	Pacific blue	RA3-6B2 (eBio)	EC	1/50
CD19	APC PE	MB19-1 (eBio)	EC	1/200 1/200
CD25	APC A700 PE	PC61.5 (eBio)	EC	1/500 1/200 1/400
CD44	A700 FITC	IM7 (eBio)	EC	1/100 1/600
CD69	PerCP Cy5.5 FITC	H1.2F3 (eBio)	EC	1/200 1/200
Foxp3	FITC Pacific blue PE	FJK-16s (eBio)	IC (eBio)	1/100 1/100 1/100
CD43	PE	eBioR2/60 (eBio)	EC	1/100
BrdU	APC	MoBU-1 (Molecular probes)	IC (BD)	1/50
TCRγδ	PerCP Cy5.5	GL3 (BioLegend)	EC	1/200
RORγt	PE	AFKJS-9 (eBio)	IC (BD)	1/50
IL-17	Brilliant violet 605	TC11-18H10.1 (BioLegend)	IC (BD)	1/200
Nitrotyrosine	FITC	1A6 (Millipore)	IC (BD)	1/10
Annexin V	APC	(eBio)	EC	1/10
Qa2	Biotin APC	695H1-9-9 (BioLegend)	EC	1/200 1/200
CD45.1	Pacific blue	A20 (eBio)	EC	1/200
CD45.2	A700	104 (eBioscience)	EC	1/200
$H2K^d$	Biotin	AF6-88.5 (BD Pharmingen)	EC	1/200
$H2K^b$	Pacific blue	28-14-8 (eBio)	EC	1/50
CCR7	PE	4B12 (eBio)	EC	1/50
TNFα	PE	MP6-XT22 (eBio)	IC (BD)	1/50
IFNAR-1	Biotin	MAR1-5A3 (BioLegend)	EC	1/100
CD62L	Brilliant violet 510 APC	MEL-14 (BioLegend)	EC	1/200 1/3000
PBS57 tetramer	Pacific blue APC	NIH Tetramer Facility	EC	1/200 1/200
HSA (CD24)	PerCP Cy5.5 PE	M1/69 (eBio)	EC	1/1000 1/100

Table 2.4 - List of antibodies for the staining of TEC

Antigen	Fluorochrome	Clone / Manufacturer	Intra/Extrace-llular (fix kit)	Working dilution
CD45	APC Cy7	30-F11 (eBio)	EC	1/800
EpCAM1	PerCP Cy5.5	G8.8 (BioLegend)	EC	1/300-1000
Ly51	PE APC	6C3 (eBio)	EC	1/1000 1/600
IA/IE	Pacific blue	M5/114.15.2 (eBio)	EC	1/3000
CD80	Brilliant violet 605	16-10-A1 (BioLegend)	EC	1/400
CCL21	Polyclonal rabbit + Goat anti-rabbit 647	(Life Sciences) (Molecular probes)	IC (eBio)	1/100 1/200
Aire	FITC Alexa fluor 660	5H12 (eBio)	IC (eBio)	1/1000 1/500
OPG	Polyclonal goat biotin	(R&D)	IC (eBio)	1/100
Ki67	PE Cy7	SolA15 (eBio)	IC (eBio)	1/600
Cleaved Caspase 3	FITC	D175 (Cell Signaling Tech)	IC (eBio)	1/50
iNOS	PE FITC	CXNFT (eBio)	IC (eBio)	1/10,000 1/1000
UEA-1	Biotin	(Vector Labs)	EC	1/6,000

Table 2.5 - List of antibodies for the staining of dendritic cells

Antigen	Fluorochrome	Clone / Manufacturer	Intra/Extrace-llular (fix kit)	Working dilution
CD11c	PE Cy7 FITC	N418 (eBio)	EC	1/200 1/200
B220	Pacific blue APC	RA3-6B2 (eBio)	EC	1/50 1/500
CD8α	APC APC Cy7 BV510	53-6.7 (eBio)	EC	1/800 1/200 1/200
CD11b	PE	M1/70 (eBio)	EC	1/200
IA/IE (MHC-II)	A700	M5/114.15.2 (eBio)	EC	1/200
CD80	Brilliant violet 605	16-10-A1 (BioLegend)	EC	1/400
CD86	APC	GL1 (eBio)	EC	1/100

2.5. Cell preparation for fluorescence activated cell sorting (FACS)

Sorting TEC subsets

For the comparison of gene expression between TEC subsets from wildtype and knockout mouse models, thymic stroma was isolated by digestion, and purified through the depletion of $CD45^+$ cells by the MACS method, as described above. Cells were then stained with antibodies against surface-expressed markers (antibodies and concentrations listed in Table 2.6), and filtered through 30um pre-separation filters (Miltenyi) for before sorting individual populations on the MoFlo XDP cell sorter (Beckman). Populations

were collected in 1.5ml sterile eppendorfs with 200ul MACS buffer, and re-suspended in 1ml RF-10, and a small sample taken to assess the purity, and record an accurate cell count through acquisition on the flow cytometer. At this point cells were spun down, and supernatant removed before snap-freezing on dry ice.

Table 2.6 - List of antibodies for sorting TEC

Antigen (Fluorochrome)	Clone / Manufacturer	Working dilution
CD45 APC Cy780	30-F11 (eBio)	1/400
EpCAM APC	G8.8 (eBio)	1/400
Ly51 PE	6C3 (eBio)	1/300
IA/IE biotin (SA PE Cy7)	2G9 (BD Pharmingen)	1/4000 (1:2000)
CD80 FITC	1610A1 (eBio)	1/100

As an alternative approach to sorting, fetal TEC from wildtype and *Aire*$^{-/-}$ embryos were obtained by culturing whole fetal thymic lobes in 2-deoxyguanosine to selectively induce apoptosis of haematopoietic cells (see Figure 2.10 for details), before disaggregation, and incubation in anti-CD45 Dynabeads (Thermofisher) in an eppendorf. Dynabead labelling was confirmed by viewing a small aliquot of cells under a light microscope, before eppendorfs containing labelled cells were placed on a magnetic column, and the CD45-depleted supernatant removed. Lastly, CD45-depleted cells were centrifuged, and supernatant completely removed before snap-freezing of cell pellet on dry ice.

Sorting thymocyte subsets

Isolation of immature and mature thymocyte subsets for culture was also achieved by cell sorting of desired populations. Thymocytes were isolated by teasing fresh thymic tissue between glass slides as described above. Cell suspensions were then depleted of $CD8^+$ cells via the MACS method. Whole thymus was stained with anti-CD8 PE in a volume of 350ul per $5x10^7$ cells for 30 minutes on ice, before being washed in 3mls of MACS buffer. At this point, a small aliquot of cells was taken to ensure correct PE labelling of $CD8^+$ thymocytes. Cells were then re-suspended in 80ul MACS buffer plus 20ul anti-PE Microbeads (Miltenyi) per 10^7 cells for 20 minutes on ice. A further 2mls of MACS were then added, and cells were passaged through magnetic LD columns (Miltenyi), and the supernatant collected. A small aliquot of cells was then taken to count the $CD8^-$ depleted fraction, and ensure the complete depletion of $CD8^+$ thymocytes (typically >99% depletion). Cells were then surface stained for the remaining markers (as listed in Tables 2.7-8) in a volume of 100ul MACS buffer on ice for 30 minutes, and excess antibodies washed off in 1ml MACS buffer prior to filtration of sort samples by passage through 30um pre-separation filters (Miltenyi) in a volume of 600ul. Cells were finally sorted on the XDP MoFlo sorter (Beckman), and collected in sterile 1.5ml eppendorfs with 200ul MACS buffer, and collected populations re-suspended in 1ml RF-10 prior to a small sample being taken for counting and checking sort purities on the flow cytometer.

Table 2.7 - List of antibodies for sorting SP subsets (Qa2)

Antigen (Fluorochrome)	Clone / Manufacturer	Working dilution
CD4 PerCP Cy5.5	RM4-5 (eBio)	1/200
CD8 PE	53-6.7 (eBio)	1/200
TCRβ APC CY7	H57-597 (eBio)	1/100
Qa2 biotin (SA PE Cy7)	695H1-9-9 (BioLegend)	1/100 (1/500)
CD69 FITC	H1.2F3 (eBio)	1/50

Table 2.8 - List of antibodies for sorting SP subsets (MHC-I)

Antigen (Fluorochrome)	Clone / Manufacturer	Working dilution
CD4 PerCP Cy5.5	RM4-5 (eBio)	1/100
CD8 PE	53-6.7 (eBio)	1/200
TCRβ APC CY7	H57-597 (eBio)	1/100
$H2K^b$ biotin (SA PE Cy7)	AF6-88.5 (BD Pharmingen) (eBio)	1/100 (1/1000)
CD69 APC	6C3 (eBio)	1/50
CD44 PE	IM7 (BD)	1/400
CD25 PE	PC61.5 (eBio)	1/400

2.6. Preparation of samples for gene expression analysis

Snap-freezing of isolated cell populations

Cells isolated by MoFlo sorting or CD45 bead depletion were transferred to 1.5ml RNAse free eppendorfs (Camlab) and spun at 1000rpm for 10 minutes before supernatant was removed. Cells were then spun briefly in a MicroCentaur micro-centrifuge to displace the cell pellet to the side of the tube, and any remaining supernatant removed prior to snap-freezing of cells on dry ice. Cells were stored at -80°c until needed.

mRNA extraction and DNA synthesis

mRNA was extrancted from snap-frozen cell populations using the μMACSTM one-step mRNA isolation and reverse transcription kit (Miltenyi Biotech). Cells were re-suspended in 1ml room temperature lysis/binding buffer and vortexed for 3-5 minutes to ensure complete lysis. Cell lysates were then centrifuged at 13,000g for 3 minutes in LysateClear columns. 50μls of μMACS oligo deoxy-thymidine microbeads was added and gently mixed to encourage hybridisation of mRNA polyA tails to the oligo-beads. Samples were then loaded into primed MACSm columns within a magnetic MACS Separator. Columns were then washed twice (200μl wash buffer) to remaining protein and DNA, and a further four times (100μl wash buffer) to remove rRNA. Complementary DNA (cDNA) was then synthesized from RNA retained within the columns directly. 100μl equilibration buffer was twice added to each column, before reverse transcription mastermix solution (power dissolved in 20μls re-suspension buffer) was added, followed by 1ml sealing solution, to prevent sample evaporation. Columns were then incubated for an hour on the thermo-block at 42°c for reverse transcription to occur. Following this period, columns were washed twice in 100μl equilibration buffer, then 20μl release solution was added to each sample for 30 additional minutes at 42°c. cDNAs were then eluted from the columns by adding 50μls elution buffer, and collected in eppendorfs.

Real-time quantitative polymerase chain reaction (qPCR)

Real-time qPCR was performed using a RotorGene RG-3000 PCR machine (Corbett Research) using the SYBR green method. Details of the primers for each

gene of interest (GOI) are summarized in Table 2.9, but β-actin was used as a housekeeping gene for the purposes of normalizing the expression of a gene across separately isolated cDNAs according to the Pfaffl method (Pfaffl, 2001). Oligonucleotide primers were synthesized by Sigma-Genosys, and qPCR reactions were performed in 15µl reaction buffer, consisting of 7.5µl qPCR 2x Sensimix NoRox SybrGreen mastermix (Bioline), 6.2µl DNAse-free/RNAse-free PCR grade free water (Sigma), forward and reverse primers ([0.2µM]) and sample 1µl cDNA. β-actin primers were designed and synthesised by Qiagen (QuantiTect Mm Actb 1SG Primer Assay, QT00095242), and used according to the manufacturer's instructions. PCR amplification programme was as follows; 95°c for 10 minutes, followed by cycling at 95°c for 15 seconds, 58-62°c for 20 seconds (temperature dependent on primer pair), and 72°c for 15 seconds for 39 cycle periods. The reaction efficiency and Ct values were determined by the Rotor Gene 6.0 software (Corbett Research) using standard curves generated as standard from mouse Biochain cDNA. Where qPCR products were run on agarose gel, reactions were run for 40 cycles.

Table 2.9 - List of PCR primers

Gene Name (Protein)	Forward primer sequence	Reverse primer sequence	Product length
Tnrfsf11a (Rank)	GCTGGCTACCACTGGAACTC	GTGCAGTTGGTCCAAGGTTT	182
Nos1 (nNOS)	CTGGTGAAGGAACGGGTCAG	CCGATCATTGACGGCGAGAAT	120
Nos2 (iNOS)	GTTCTCAGCCCAACAATACAAGA	GTGGACGGGTCGATGTCAC	127
Nos3 (eNOS)	TGTGACCCTCACCGCTACAA	GCACAATCCAGGCCCAATC	247
Ddit3 (CHOP)	CTGGAAGCCTGGTATGAGGAT	CAGGGTCAAGAGTAGTGAAGGT	121
Xbp1s	CTGAGTCCGCAGCAGGTG	GGCAACAGTGTCAGAGTCCA	74
Xbp1s – exon 2	CCTGAGCCCGGAGGAGAA	CTCGAGCAGTCTGCGCTG	70
Ifnb1 (IFNβ)	CTGAATGGAAAGATCAACCTCAC	TACCTTTGCACCCTCCAGTAATA	311

2.7. Fetal thymic organ cultures (FTOC)

As summarized pictorially (Figure 2.10), mouse embryos were isolated from the mother at the desired stage of development by removal of the uterus, and subsequent disassociation from the womb and egg sac within a laminar flow hood, allowing maintenance of sterile conditions prior to culture. Embryos were stored transiently in a 1:1 mixture of RF10 and PBS before dissection of thymic lobes. Under a light microscope, embryos were decapitated, and cut down the length of the breastbone, exposing the thoracic tree, and allowing direct dissection of fetal thymic lobes. Dissected lobes were stored in RF10 prior to their transfer to organ culture conditions as described previously (Jenkinson and Anderson, 1994). Briefly, thymic lobes were placed on top of a sterile isopore membrane filter (0.8um ATTP, Millipore) and a 1cm^2 sterile antiwrap sponge

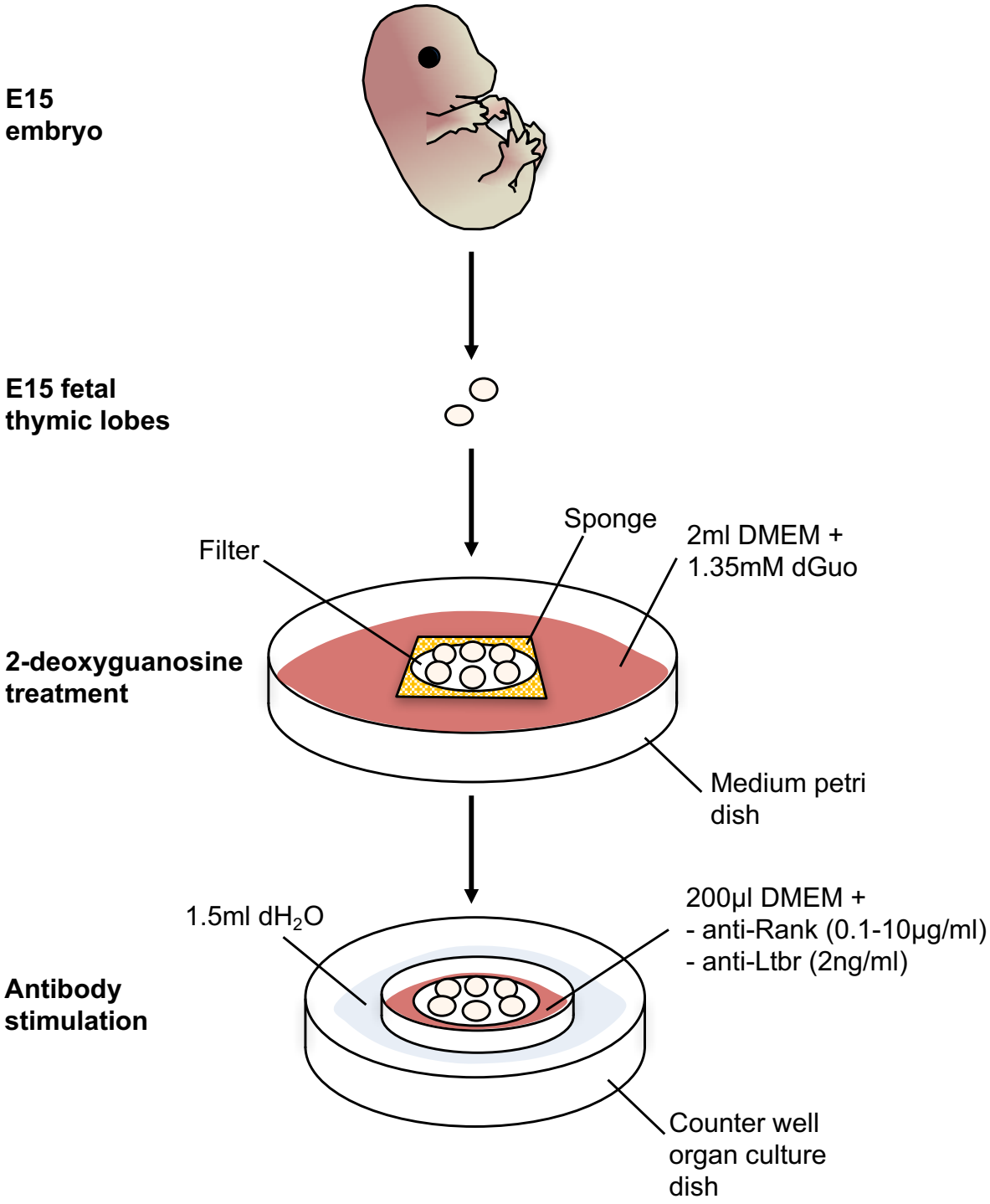
E15
embryo
E15 fetal
thymic lobes
Sponge
2ml DMEM +
1.35mM dGuo
Filter
2-deoxyguanosine
treatment
Medium petri
dish
1.5ml dH2O
200µl DMEM +
- anti-Rank (0.1-10µg/ml)
- anti-Ltbr (2ng/ml)
Antibody
stimulation
Counter well
organ culture
dish

Figure 2.10: Fetal thymic organ culture

Dissected E15 fetal thymic lobes are placed onto filters and sponges steeped in DMEM +/- 1.35mM 2-deoxyguanosine for a period up to 7 days. Filters are then removed, and transferred to a counter well organ culture dish, in which lobes are incubated in stimulatory antibody solutions in DMEM for up to a further 7 days as required.

(Medipost) in a large petri dish with 2mls RF10. For the ablation of haematopoietic cells from FTOC, DMEM was supplemented with 2-deoxguanosine (final concentration 1.35mM) for 7 days. Subsequent experiments involving stimulation of fetal stromal cells required the transfer of the filter-bound thymic lobes to a counter-well organ culture dish (Falcon) filled with 200ul DMEM containing 0.1-10ug/ml anti-Rank (R&D), or 2ng/ml anti-Ltbr (a kind gift from Jorge Camaano).

2.8. T-cell cultures and stimulations

PMA/ionomycin stimulation for IL-17 induction

For the induction of IL-17 expression, and the subsequent detection of Th17 cells, $7x10^6$ thymocytes were incubated in wells of a 24 well plate containing 1.5ml DMEM together with 50ng/ml PMA and 1.5uM ionomycin for 1.5 hours at 37°c, 5% CO_2. At this point BFA was added at a concentration of 10ug/ml to inhibit IL-17 secretion, before a further 2.5 hours of culture. Cells were stained for IL-17 using the eBioscience Foxp3/transcription factor staining buffer set according to the manufacturer's instructions.

Anti-CD3/28 stimulation

To investigate the responses of thymocyte populations to TCR-triggering in terms of proliferation, apoptosis and cytokine production, cells were stimulated with plate-bound anti-CD3 and/or CD28. For this purpose, anti-CD3e (eBioscience, clone 145-2C11) and/or anti-CD28 (eBioscience, 37.51) were added to PBS at 10ug/ml or 20ug/ml respectively. Antibody solution was added

to wells, and incubated at 4°c overnight, wherein excess antibody was removed by washing in PBS. 200ul antibody solution was used to coat 24 well plates, whereas 100ul was sufficient to coat the wells of 96 well plates.

TNFα production as proof of cytokine licensing

$5x10^6$ whole thymocytes were cultured on a 24 well plate coated with anti-CD3/28 as above for 6 hours (37°c, 5% CO_2) in 1ml DMEM plus 0.7ul GolgiPlug (BD Bioscience). Post-stimulation, cells were surface stained, and fixed for 40 minutes at 4°c using the Cytofix/cytoperm fixation and permeabilisation kit (BD) according to the manufacturer's instructions. Cells were then stained with anti-mouse TNFα for 40 minutes on ice to assess their capacity to produce cytokines on stimulation.

Apoptosis induction in thymocytes by TCR triggering and nitric oxide exposure

For the assessment of the apoptotic effects of TCR triggering and nitric oxide in thymocyte populations, either $1x10^6$ whole thymocytes were cultured on dishes coated with anti-CD3 and/or anti-CD28 as described above, with or without the presence of the nitric oxide donor S-nitroso-N-acetly-DL-penacillamine (SNAP, Sigma), which spontaneously releases nitric oxide in culture. SNAP was used at 100uM as a standard concentration, but between 20uM-1mM for dose:response experiments.

Apoptosis of cultured cells was assessed by either of two methods. Firstly, through fixation/permeabilization with the Cytofix/cytoperm kit as described, followed by intracellular staining with anti-cleaved Caspase 3 Alexa Fluor 488

(clone Asp175, Cell Signalling) at a concentration of 1:50. As an alternative approach, apoptotic thymocytes were measured via detection of flipped phosphatidyl serine residues on the cell surface via labelling with APC-conjugated Annexin V using the 'Annexin V apoptosis detection kit' (eBioscience) according to the manufacturer's instructions. Briefly, surface-stained cells were washed in 1ml 'Annexin V staining buffer', and re-suspended in 50ul Annexin V APC diluted 1:10 in 'Annexin V staining buffer' for 20 minutes at room temperature, and a further 15 minutes on ice. Post-incubation, cells were washed with 1ml 'Annexin V staining buffer', and re-suspended in the same solution for acquisition on the flow cytometer. 2 minutes before acquisition, cell suspensions were supplemented with 6ul 'Propidium iodide staining solution' (for the identification of lysed, late-stage apoptotic cells) and vortexed well.

Membrane dye labelling for the assessment of proliferation

To determine the capacity of mature and immature thymocyte subsets to undergo TCR-induced proliferation, sorted populations of SM, M1 and M2 thymocytes were isolated by cell sorting, and loaded with cell-trace violet (CTV) for the assessment of proliferation in culture. Sorted cells were re-suspended in 1ml PBS containing 1:1000 CTV for 20 minutes at 37°c, and washed twice upon the addition of 500ul RF10. After labelling, cells cultured for 2-3 days in round-bottom 96 well culture plates coated with 100ul anti-CD3/28 as described above, wherein 10-20k cells were cultured in 200ul DMEM at 37°c, 5% CO_2. Harvested cells were stained with 5ul propidium iodide staining solution (eBioscience) prior to analysis on the flow cytometer. Proliferation was

measured using the average number of cell divisions of live cells over 2-3 days in culture, inclusive of non-dividing cells (the division index).

2.9. Fluorescence microscopy

For the analysis of thymic tissues by immunofluorescence, individual thymic lobes were isolated and carefully cleaned of excess fat and connective tissues, before being frozen flat on a square of tin foil over dry ice. Lobes were then transferred to a cryostat, affixed to the cryostat chuck by fixing in OCT compound (Tissue Tek), and cut into whole thymus sections to a thickness of 7um. Tissue sections were then transferred to multispot microscope slides (Hendley-Essex) fixed for 40 minutes by immersion in acetone (Sigma) and air dried completely prior to long-term storage at -20°c.

Tissue sections were stained with fluorescent antibodies for confocal microscopy in the following manner. Sections were defrosted and air-dried for 30 minutes prior to staining. Individual tissue sections (1 per spot) were stained in a volume of 75ul antibody mix, made up in PBS with 0.1% powdered bovine serum albumin (BSA). Spots were stained in a dark humidified section staining tray for 30 minutes per incubation step, after which droplets of antibody were flicked off, and slides were washed in a bath of PBS (Sigma, P4417-100TAB) for 10 minutes. This process was repeated for the staining of primary/secondary/tertiary antibodies on individual sections, the details of which are listed in Table 2.11. After the final staining step, sections were stained for 4',6-diamidino-2-phenylindole (DAPI) nuclear dye by immersion in a DAPI solution for 30 seconds, followed by serial transfer to 3 tubes of PBS, and

transfer into the PBS bath for a final 10 minutes. At this stage, being careful not to disturb the tissue sections, slides were dried with a paper towel, and fixed to a 22mm x 64mm glass coverslip (Menzel-Glaser) coated with DABCO solution (1,4 diazabicyclooctane) at pH 7 for the preservation of fluorochromes. The edges of the coverslip were then sealed to the glass slide using clear nail varnish. When dried, the tissue sections were imaged using the Zeiss 780 Live Confocal microscope, together with Zen 2010 software.

2.10. Kidney capsule grafting

To assess the capacity of peripheral T-cells to re-circulate to the thymus, fresh E16-18 BoyJ ($CD45.1^+$) fetal thymic lobes were grafted under the kidney capsule of $CD45.2^+$ host mice. Grafts were then left in place for 6 weeks before the mice were culled, and T-cell populations were assessed in the grafts, as well as the spleen and thymus of the host. Re-circulation of graft-derived peripheral T-cells to the host thymus was assessed by staining for the congenic marker CD45.1, which was absent from host-derived cells.

2.11. Intraperitoneal injections for assessment of cell cycle status

To assess the cell cycle status of thymic epithelial and T-cell populations, mice were injected intraperitoneally (i.p.) with 200mg BrdU re-suspended in PBS without calcium and magnesium. Mouse tissues were harvested 18 hours after the injection, and processed for detection of BrdU using the BD BrdU flow kit according to the manufacturer's instructions. Direct detection of BrdU was

achieved using the anti-BrdU (MoBU-1) Alexa Fluor 647 antibody (Thermofisher Scientific). For co-detection of BrdU and Foxp3, cells were fixed with the eBioscience Foxp3/Transcription factor staining buffer set after surface marker staining, stained for Foxp3 PE as above for 1hr, and subsequently stained for BrdU using the BD BrdU flow kit.

2.12. Statistical analyses and data presentation

Analysis of flow cytometry plots was achieved using FlowJo version 8.8.6 (Treestar). Data analysis and graphical representation was performed using Prism 6 (Graphpad) – bars represent the mean average, and error bars SEM unless stated, and p values were obtained by performing either unpaired or paired two-tailed student's t-tests as stated. P values are represented throughout as follows; ns = non-significant, * < 0.05, ** < 0.01, *** < 0.001, and **** < 0.0001.

3. RESULTS CHAPTER 1: OPG-MEDIATED REGULATION OF MEDULLARY HOMEOSTASIS

3.1. Introduction

The induction of T-cell tolerance in the thymic medulla is known to occur through two interlinked mechanisms; namely, the deletion of cells possessing auto-reactive T-cell receptors (negative selection), and the induction of $Foxp3^{+}$ regulatory T-cells. These processes are martialled by the heterogeneous compartment of antigen presenting cells present in the medulla, consisting of mTEC, dendritic cells and B-cells. The fate of SP thymocytes is dictated by their antigen-dependent interaction with these cell types, and hence requires their effective co-localisation with medullary APCs following positive selection in the cortex (Cowan et al., 2014, Ueno et al., 2004), in addition to the specific expression and presentation of tissue-specific antigens within the medulla itself. To this end, functionally distinct populations of mTEC influence negative selection through the expression of the chemokine receptor ligand CCL21 (Lkhagvasuren et al., 2013), which induces cortex to medulla migration of $CCR7^{+}$ SP thymocytes (Ueno et al., 2004), in addition to the transcription factor Aire (Zuklys et al., 2000), which induces the expression of TSAs in mature mTEC populations (Anderson et al., 2002). Formation of functionally mature mTEC populations is influenced by external factors, requiring the expression of TNFR ligands on the surface of haematopoietic cells (Sun et al., 2014). The formation of MHC-$II^{hi}CD80^{+}$ mTEC expressing Aire is dictated by signalling through the Rank receptor (Rossi et al., 2007), whereas recent evidence suggests CCL21 expression

to occur largely within a separate compartment of MHC-II^{lo}CD80^{-} cells in response to Ltbr triggering (Lkhagvasuren et al., 2013).

In addition to cross-talk with haematopoietic cells, mTEC homeostasis is in part self-governed through the expression of Aire and OPG. As well as losing expression of certain TSAs, Aire-deficient mTEC have a reduction in the proportion of cells expressing CCL21 (Laan et al., 2009, Lkhagvasuren et al., 2013), and are thought to fail to reach their terminal stage of differentiation (Yano et al., 2008). Emerging evidence suggests OPG, a negative regulator of Rank signalling, to play an active role in maintaining medullary homeostasis by limiting the population size of the mTEC compartment (Hikosaka et al., 2008, Akiyama et al., 2014). Although both molecules are important mTEC regulators, the causes and consequences of mTEC dis-regulation in their absence are unclear, and in particular the impact of OPG expression on tolerance induction is poorly understood. Studies on mTEC-deficient *Relb*$^{-/-}$ thymic tissues have demonstrated interaction with mTEC to be an absolute requirement for the induction of Foxp3^{+} T-Reg within the thymus (Cowan et al., 2013). The idea that T-Reg production is strictly regulated by the pool size of mTEC is supported by an array of publications. The induction of Foxp3^{+} cells in TCR transgenic models has been found to be limited by the availability of antigen in the medulla, as the generation of mixed bone marrow chimeras with increasingly dilute fractions of G113 TCR-transgenic T-cells resulted in an increase in the regulatory T-cell fraction (Moran et al., 2011). Similarly, thymic T-Reg are greatly reduced in the thymus of mice lacking mTEC expression of the transcription factors Aire (Lei et al., 2011) and Fezf2 (Takaba et al., 2015), which control the expression of non-overlapping arrays of TSAs. These findings suggest the expression of a full array

of TSAs by mTEC to be a critical factor in Foxp3-induction. Similarly, limiting the size of the mTEC compartment has been suggested to impede the formation of regulatory T-cells, in addition to allowing the escape of autoreactive T-cells to the periphery (Cowan et al., 2013). *Cd40*$^{-/-}$ mice, which have a reduced number of mTEC relative to their wildtype counterparts (Williams et al., 2014), have a corresponding drop in the number of thymic T-Reg (Cuss and Green, 2012). Treatment of mice with blocking antibodies against RankL for a 2 week period was shown to transiently reduce the size of the mTEC pool, with a substantial impact on the maintenance of Aire^{+} mTEC (Khan et al., 2014). This was not only sufficient to reduce thymic T-Reg production, but also increased tumor clearance in mice inoculated with B16 melanoma (Khan et al., 2014).

Given the recent characterisation of *Tnfrsf11b*$^{-/-}$ mice, which lack expression of OPG, the purpose of this chapter was to use this model to assess the consequences of unrestrained Rank signalling on the thymus. Rank is a key regulator of the homeostasis of mTEC (Rossi et al., 2007), which have critical importance in central tolerance mechanisms through their induction of regulatory T-cells. Hence, our investigations aimed firstly to assess the impact of OPG-deficiency directly on the homeostasis of functionally distinct compartments of thymic epithelium. In addition, we utilised *Tnfrsf11b*$^{-/-}$ mice to investigate the relationship of the mTEC pool size with the capacity for induction of Foxp3^{+} regulatory T-cells within the medulla.

3.2. Results

3.2.1. Mapping the expression of functional molecules to the mTEC compartment

To define the TEC (EpCAM-1^{+}CD45^{-}) compartment utilising previously described functional molecules, we developed a gating strategy for the analysis of cTEC (Ly51^{+}), mTEC^{hi} (Ly51^{-}MHC-II^{hi}CD80^{+}) and mTEC^{lo} (Ly51^{-}MHC-II^{lo}CD80^{-}) in thymus samples digested with collagenase dispase, and depleted of CD45^{+} haematopoietic cells (Figure 3.1A). Stromal cells were fixed and permeabilised to facilitate antibody staining of intracellular antigens, in which case sub-populations of TEC were found to express the transcription factor Aire, and the chemokine receptor ligand CCL21. Aire was expression was unique to cells of the mTEC^{hi} lineage, wherein ~65% were Aire^{+} relative to the levels of staining observed in *Aire*$^{-/-}$ control stroma (Figure 3.1B). Expression of CCL21 was controlled for by staining of *plt*/*plt* mutant mice (Mori et al., 2001), in which expression of CCL21 is absent from lymphoid organs (Figure 3.1C). Positive CCL21 staining was apparent in all subsets, however CCL21^{+} cells represented only minor fractions of cTEC and mTEC^{hi}, whereas the majority of mTEC^{lo} strongly expressed CCL21 (Figure 3.1C). These findings suggest that the expression of Aire and CCL21 defines functional subsets mTEC^{hi} and mTEC^{lo} respectively.

It was recently reported that osteoprotegerin (OPG) - a soluble decoy receptor structurally similar to Rank - is expressed by thymic epithelial cells (Hikosaka et al., 2008). To map the exact cellular source of OPG in our defined populations, we applied our technique for staining intracellular antigens to

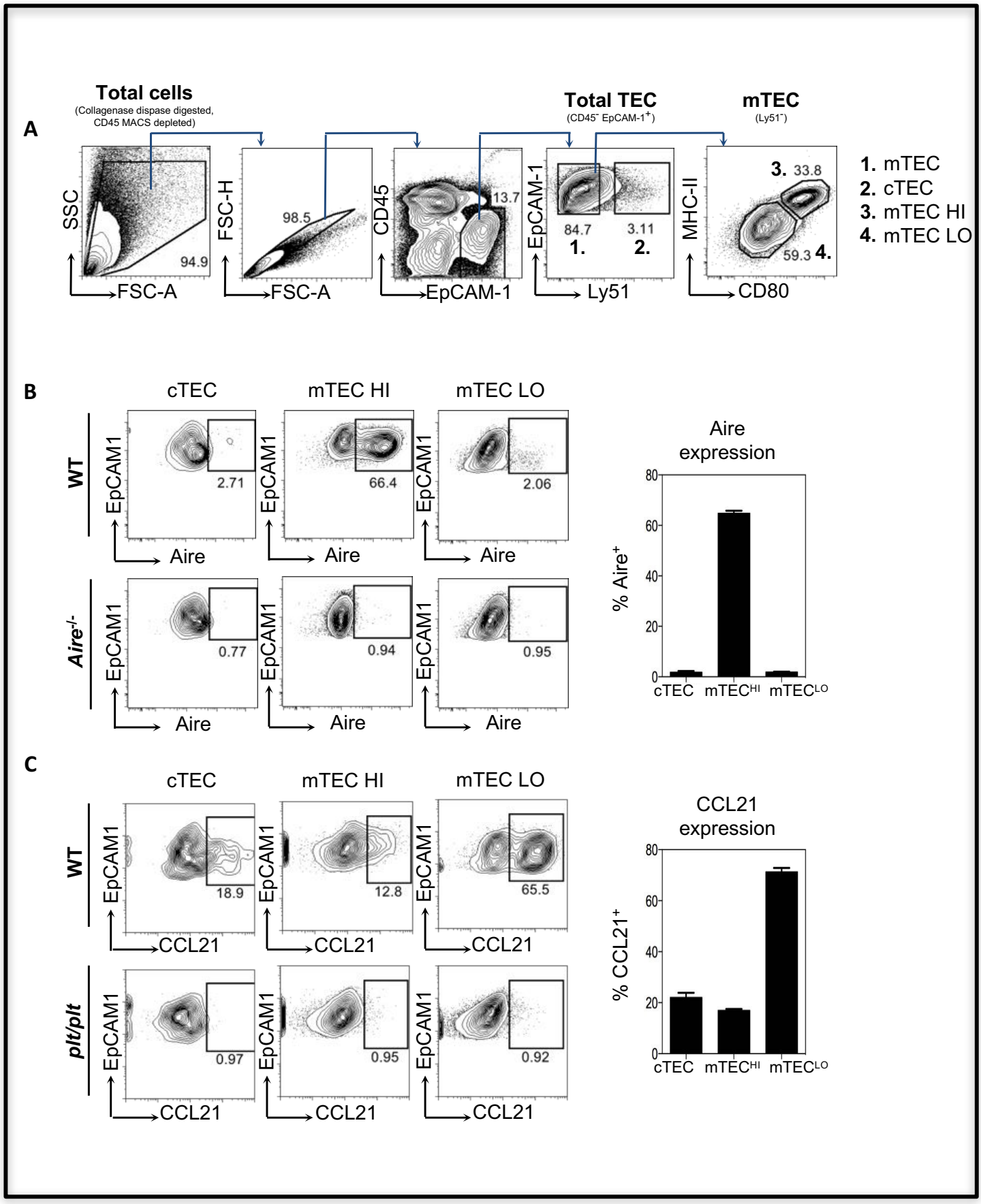
A
Total cells
(Collagenase dispase digested, CD45 MACS depleted)
Total TEC
(CD45⁻ EpCAM-1⁺)
mTEC
(Ly51⁻)
SSC
FSC-A
94.9
FSC-H
FSC-A
98.5
CD45
EpCAM-1
13.7
EpCAM-1
Ly51
84.7
1.
3.11
2.
MHC-II
CD80
3.
33.8
59.3
4.
1. mTEC
2. cTEC
3. mTEC HI
4. mTEC LO
B
cTEC
mTEC HI
mTEC LO
WT
Aire-/-
EpCAM1
Aire
2.71
66.4
2.06
0.77
0.94
0.95
Aire expression
% Aire+
80
60
40
20
0
cTEC
mTECHI
mTECLO
C
cTEC
mTEC HI
mTEC LO
WT
plt/plt
EpCAM1
CCL21
18.9
12.8
65.5
0.97
0.95
0.92
CCL21 expression
% CCL21+
80
60
40
20
0
cTEC
mTECHI
mTECLO

Figure 3.1: Gating strategy for the analysis of functionally heterogeneous mTEC

(A) Isolated thymic epithelial cells were stained for analysis of functional markers relevant to negative selection by FACS. CD45^{-} EpCAM-1^{+} TEC were gated into Ly51^{+} cTEC, Ly51^{-}CD80^{-}MHC-II^{lo} mTEC^{lo} and Ly51^{-}CD80^{+}MHC-II^{hi} mTEC^{hi} fractions.

(B-C) cTEC, mTEC^{lo} and mTEC^{hi} were analysed for their expression of Aire (B) and CCL21 (C) by intracellular antibody staining after fixation/permeabilisation. Staining was controlled for by co-staining of TEC from *Aire*$^{-/-}$ and CCL21-deficient *Plt/Plt* mice

stromal and haematopoietic populations from the thymus of wildtype and OPG-deficient *Tnfrsf11b*$^{-/-}$ mice (Figure 3.2). With this approach, expression of OPG protein was not detected in haematopoietic cells, including B- and T-lymphocytes, and either conventional or plasmocytoid dendritic cell lineages (Figure 3.2A, C-D). EpCAM-1^{-} non-epithelial stromal cells were similarly OPG^{-}, however we found ~12% of EpCAM-1^{+} TEC to express OPG (Figure 3.2B, C, E). OPG^{+} cells were found to be almost uniformly mTEC^{hi}, the majority (~80%) of which were Aire^{+} (Figure 3.3A-B). OPG^{+} mTEC were detected among the first emerging cohort of mTEC^{hi} at embryonic day 16 (E16), and represented a substantial portion of the Aire^{+} mTEC pool at E16, postnatal day 2 (P2), as well as in adult mice (Figure 3.3C). Although Aire- mTEC^{hi} were also seen to express OPG, the proportion of OPG^{+} cells co-expressing Aire was seen to be consistently between 75-80% throughout development (Figure 3.3D). To determine the location of OPG-expressing cells within the thymus, frozen tissue sections from wildtype and *Tnfrsf11b*$^{-/-}$ thymuses were stained with antibodies against ER-TR5 – a marker of medullary epithelium – and Aire together with OPG (Figure 3.4). OPG expression was restricted to the medulla (M), as defined by the presence of ER-TR5^{+} cells, with globular OPG staining largely associating with ER-TR5^{+} mTEC (Figure 3.4, left panel). As expected, no positive staining was detected on the *Tnfrsf11b*$^{-/-}$ tissue sections (Figure 3.4, right panel).

Having mapped medullary OPG expression to a sub-population of mTEC^{hi}, we next investigated the possible mechanisms regulating expression. Induction of Aire and CCL21 expression by mTEC is known to depend on crosstalk with thymocytes mediated by tumor necrosis factor receptor superfamily (TNFRSF) members, respectively Rank (Rossi et al., 2007) and Ltbr

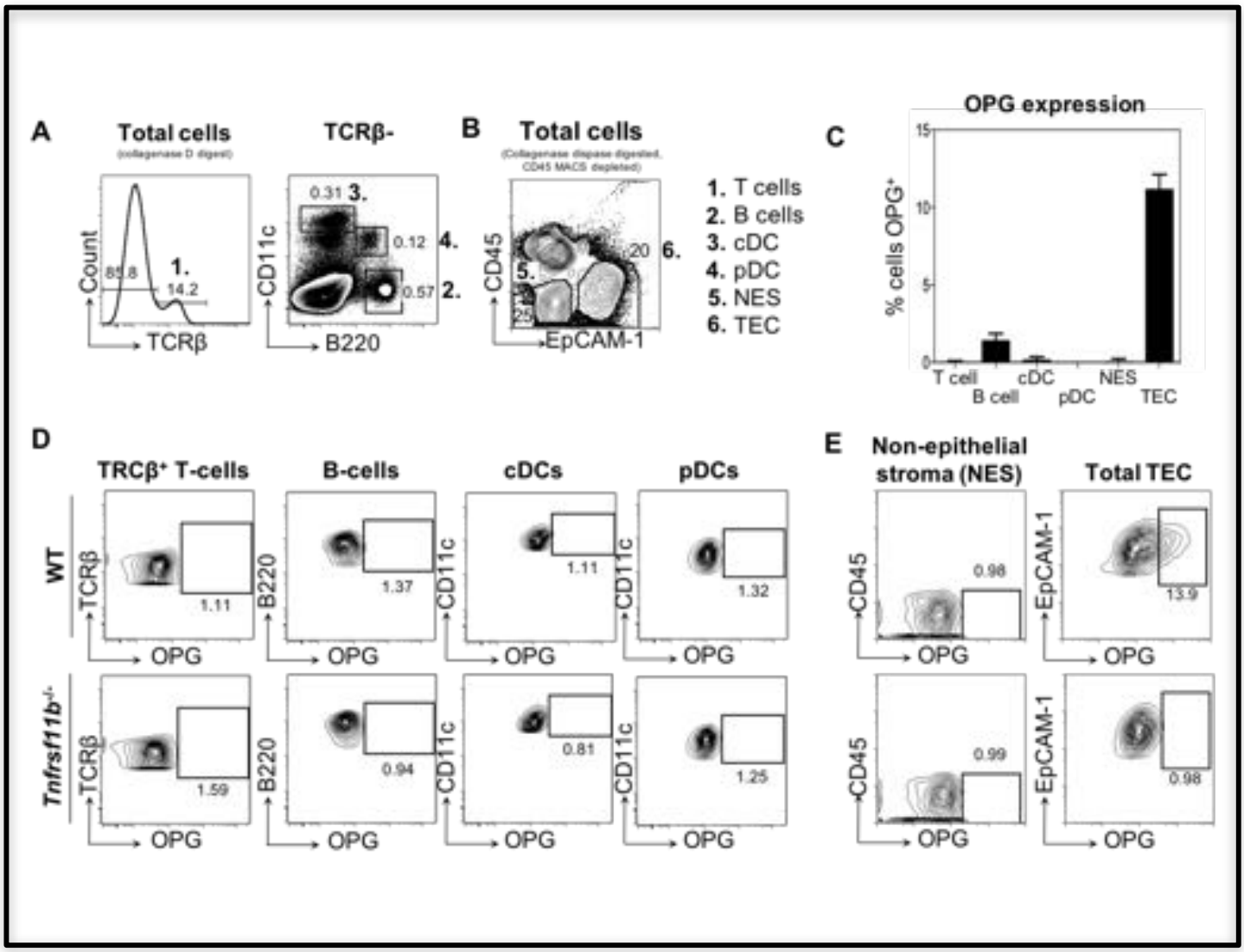
A
Total cells
(collagenase D digest)
TCRβ-
Count
85.8
1.
14.2
TCRβ
0.31
3.
0.12
4.
0.57
2.
CD11c
B220
B
Total cells
(Collagenase dispase digested, CD45 MACS depleted)
CD45
5.
20
6.
EpCAM-1
1. T cells
2. B cells
3. cDC
4. pDC
5. NES
6. TEC
C
OPG expression
% cells OPG+
15
10
5
0
T cell
B cell
cDC
pDC
NES
TEC
D
TRCβ+ T-cells
B-cells
cDCs
pDCs
WT
Tnfrsf11b-/-
TCRβ
B220
CD11c
OPG
1.11
1.37
1.11
1.32
1.59
0.94
0.81
1.25
E
Non-epithelial stroma (NES)
Total TEC
CD45
EpCAM-1
OPG
0.98
13.9
0.99
0.98

Figure 3.2: Thymic osteoprotegerin expression is restricted to the TEC compartment

(A) Gating strategy for the analysis of B-/T-lymphocytes, conventional dendritic cells and plasmocytoid dendritic cells, and additionally (B) thymic epithelial cells and non-epithelial thymic stroma.

(C-D) Analysis of expression of OPG protein in thymic cell populations via intracellular antibody staining versus an OPG-deficient *Tnfrsf11b*$^{-/-}$ control. No positive staining was observed in (C) lymphocyte and dendritic cell populations, or (D) non-epithelial stroma (NES), but was apparent in TEC. Analysis of OPG expression is representative of 3 mice.

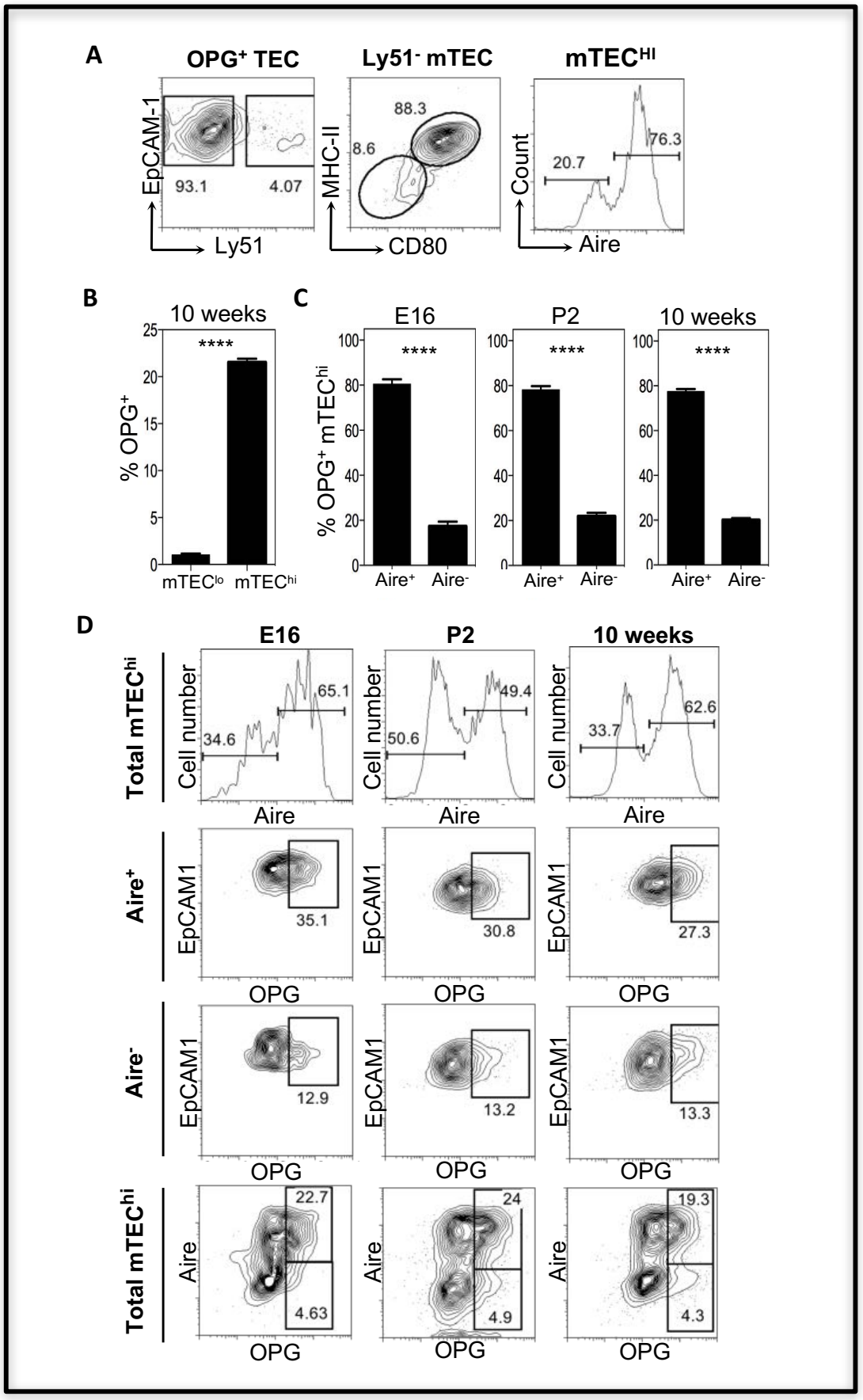
A
OPG+ TEC
Ly51- mTEC
mTECHI
EpCAM-1
93.1
4.07
Ly51
MHC-II
88.3
8.6
CD80
Count
20.7
76.3
Aire
B
10 weeks
% OPG+
****
mTEClo
mTEChi
C
E16
P2
10 weeks
% OPG+ mTEChi
****
Aire+
Aire-
D
E16
P2
10 weeks
Total mTEChi
Cell number
34.6
65.1
50.6
49.4
33.7
62.6
Aire
Aire+
EpCAM1
35.1
30.8
27.3
OPG
Aire-
12.9
13.2
13.3
22.7
4.63
24
4.9
19.3
4.3

Figure 3.3: A sub-population of Aire^{+} mTEC produce OPG throughout development

(A) Phenotype of OPG+ TEC; OPG+ cells are almost uniformly Ly51^{-}CD80^{+}MHC-II^{hi} mTEC^{hi}.

(B) Proportion of adult mTEC^{lo}/^{hi} expressing OPG as determined by FACS.

(C-D) Quantitation (C) and representative FACS plots (D) of OPG^{+} mTEC^{hi} expressing Aire throughout development; at embryonic day 16 (E16), post-natal day 2 (P2) and in 10 week adult mice.

Statistical analysis was performed using unpaired student's t-tests, where **** denotes a p value <0.0001. Data representative of at least 3 mice, from at least 2 separate experiments.

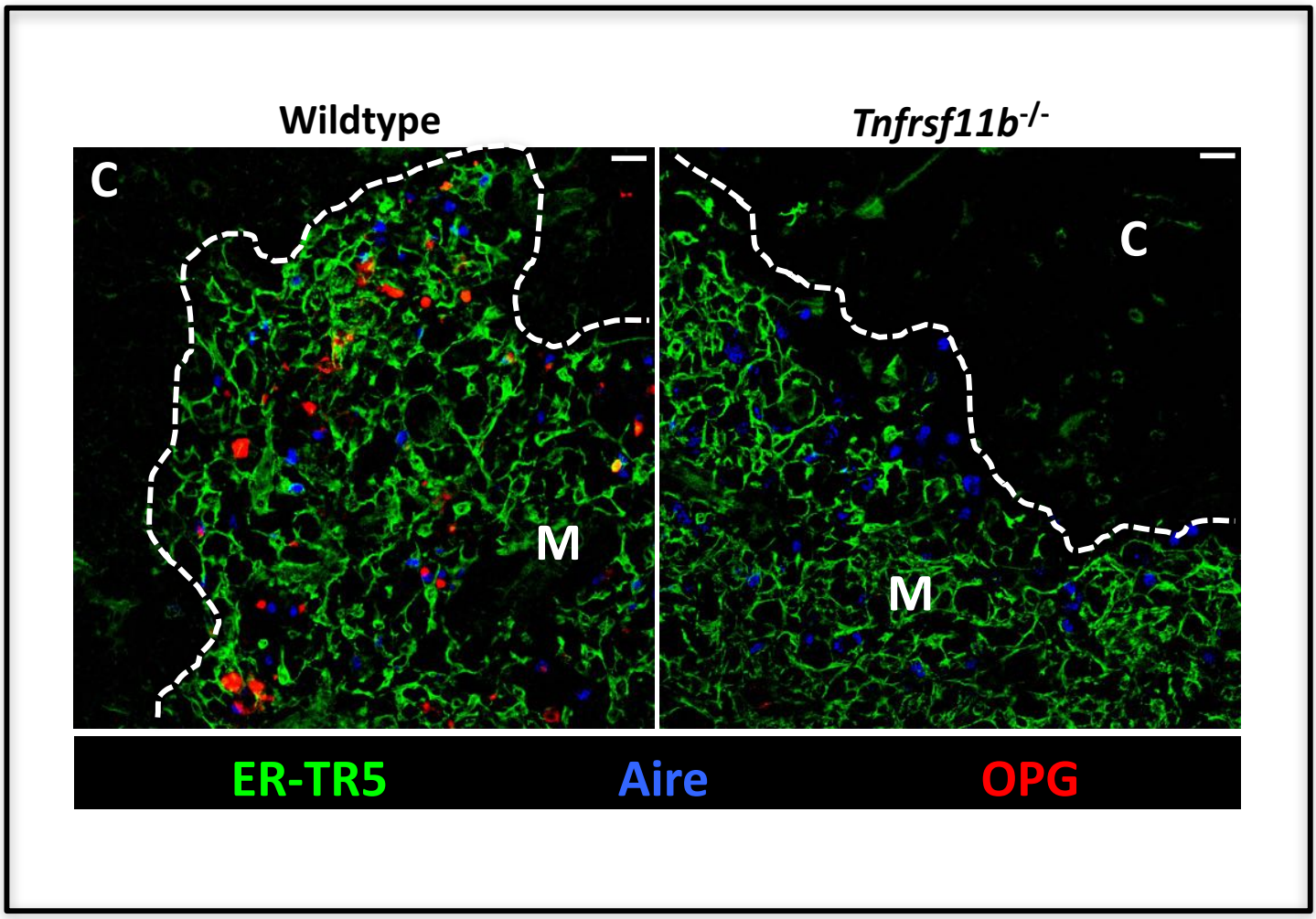
Wildtype
Tnfrsf11b-/-
C
M
C
M
ER-TR5
Aire
OPG

Figure 3.4: OPG-expressing TEC are distributed throughout the medulla

Confocal immunofluorescence analysis of sections of wildtype (left) and *Tnfrsf11b*$^{-/-}$ (right) thymus. Sections were stained for antibodies against Aire, OPG and ER-TR5, the latter of which was used to determine the boundaries of cortical (ER-TR5^{-}) and medullary (ER-TR5^{+}) areas. Scale bar = 20um.

(Laan et al., 2009, Lkhagvasuren et al., 2013). Treatment of fetal thymic organ cultures (FTOC) with 2-deoxyguanosine (dGuo) triggers selective loss of haematopoietic cells (Jenkinson and Anderson, 1994), eliminating cross-talk with TEC. By stimulating dGuo treated FTOC with stimulatory antibodies raised against the Rank and Ltbr receptors, we investigated the effect of TNFRSF member signalling on immature TEC populations. mTEC derived from un-stimulated dGuo FTOC were MHC-II^{lo}CD80^{-} mTEC^{lo}, and negative for expression of CCL21 and Aire (Figure 3.5A, 3.6). The addition of anti-Rank, but not anti-Ltbr was sufficient to induce the formation of MHC-II^{hi}CD80^{+} mTEC^{hi}, inclusive of Aire^{+} cells (Figure 3.5B-C, 3.6). This effect was enhanced when FTOC were stimulated with both anti-Rank and anti-Ltbr in combination (Figure 3.5D, 3.6). Expression of CCL21 by mTEC^{lo} was triggered upon stimulation with either anti-Ltbr and/or anti-Rank, although anti-Ltbr in isolation was marginally more effective (Figure 3.5B-D, 3.6). In addition to the formation of Aire^{+} cells, anti-Rank stimulation (but not addition of anti-Ltbr) was similarly efficient at inducing the expression of OPG in newly formed mTEC^{hi} (Figure 3.5B, 3.6). In fetal, newborn and adult mice, expression of OPG largely overlaps with Aire, although substantial populations of Aire^{+}OPG^{-} and Aire^{-}OPG^{+} cells are apparent (Figure 3.3D). To determine whether this expression profile is mirrored *in vitro*, a time-course of anti-Rank stimulation was performed (Figure 3.7). Few mTEC^{hi} were detectable after day 2 (d2), with an increasing proportion and number of these cells present over time until d7 (d12 was also analysed, however the viability of organ culture was severely reduced) (Figure 3.7A-B). Co-staining of Aire and OPG revealed mTEC^{hi} at d2 to be largely Aire^{-}OPG^{-}, with small separate populations of Aire^{+} and OPG^{+} cells, however at later time-points, the majority

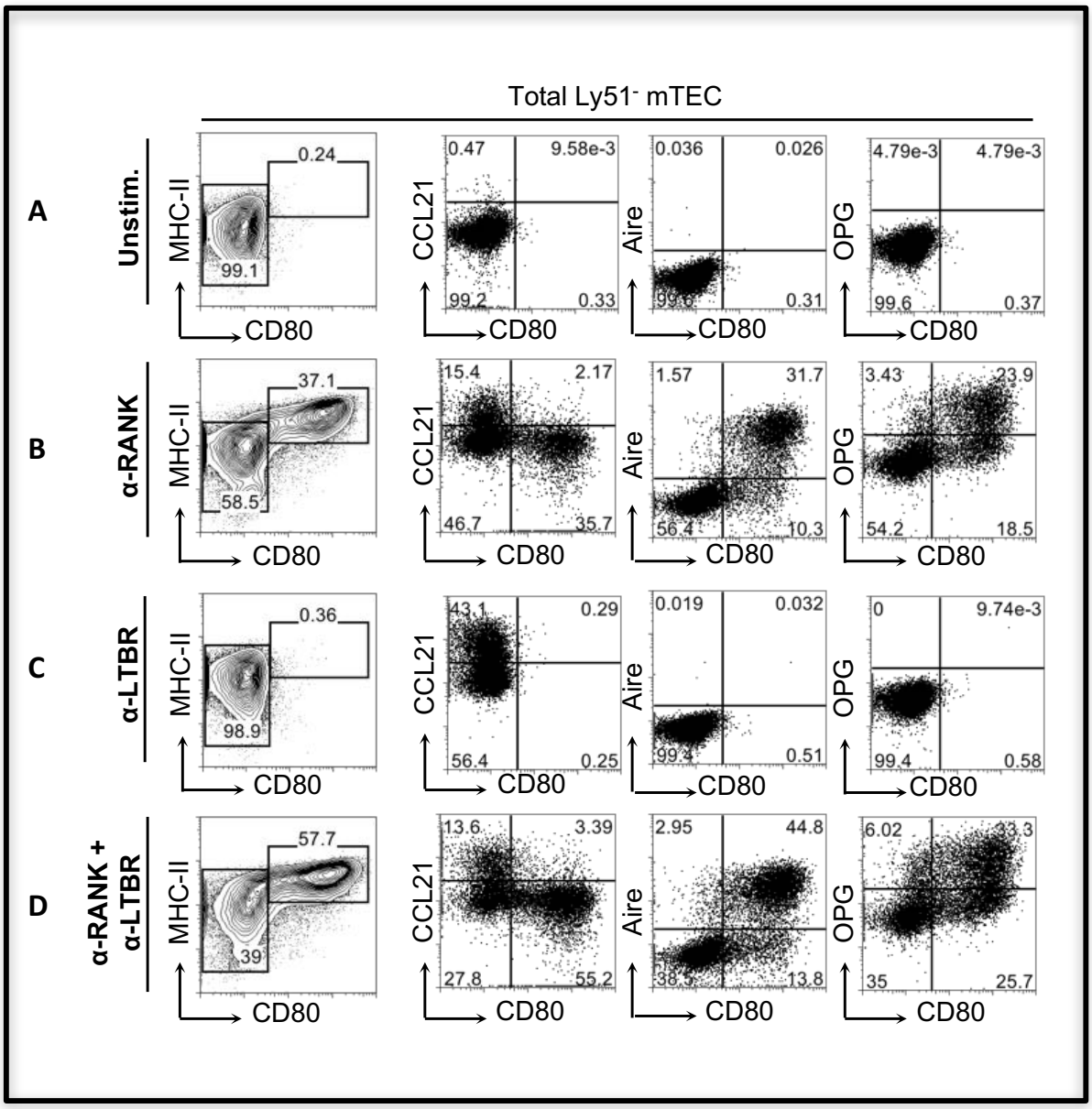
Total Ly51- mTEC
A
Unstim.
B
α-RANK
C
α-LTBR
D
α-RANK + α-LTBR
MHC-II
CD80
CCL21
Aire
OPG
0.24
99.1
0.47
9.58e-3
99.2
0.33
0.036
0.026
0.31
4.79e-3
4.79e-3
99.6
0.37
37.1
58.5
15.4
2.17
46.7
35.7
1.57
31.7
56.4
10.3
3.43
23.9
54.2
18.5
0.36
98.9
43.1
0.29
56.4
0.25
0.019
0.032
99.4
0.51
0
9.74e-3
99.4
0.58
57.7
39
13.6
3.39
27.8
55.2
2.95
44.8
38.3
13.8
6.02
33.3
35
25.7

Figure 3.5: Expression of Aire, CCL21 and OPG is inducible in vitro by TNFRSF signaling

Representative FACS plots of cultures of E15 Balb/c fetal thymic lobes treated with dGuo for 7 days, then left either un-stimulated (A), or stimulated for 7 days with (B) anti-Rank, (C) anti-Ltbr or (D) both. FACS plots are representative of a minimum of 3 separate experiments, and pre-gated on $CD45^{-}$ $EpCAM\text{-}1^{+}Ly51^{-}$ mTEC.

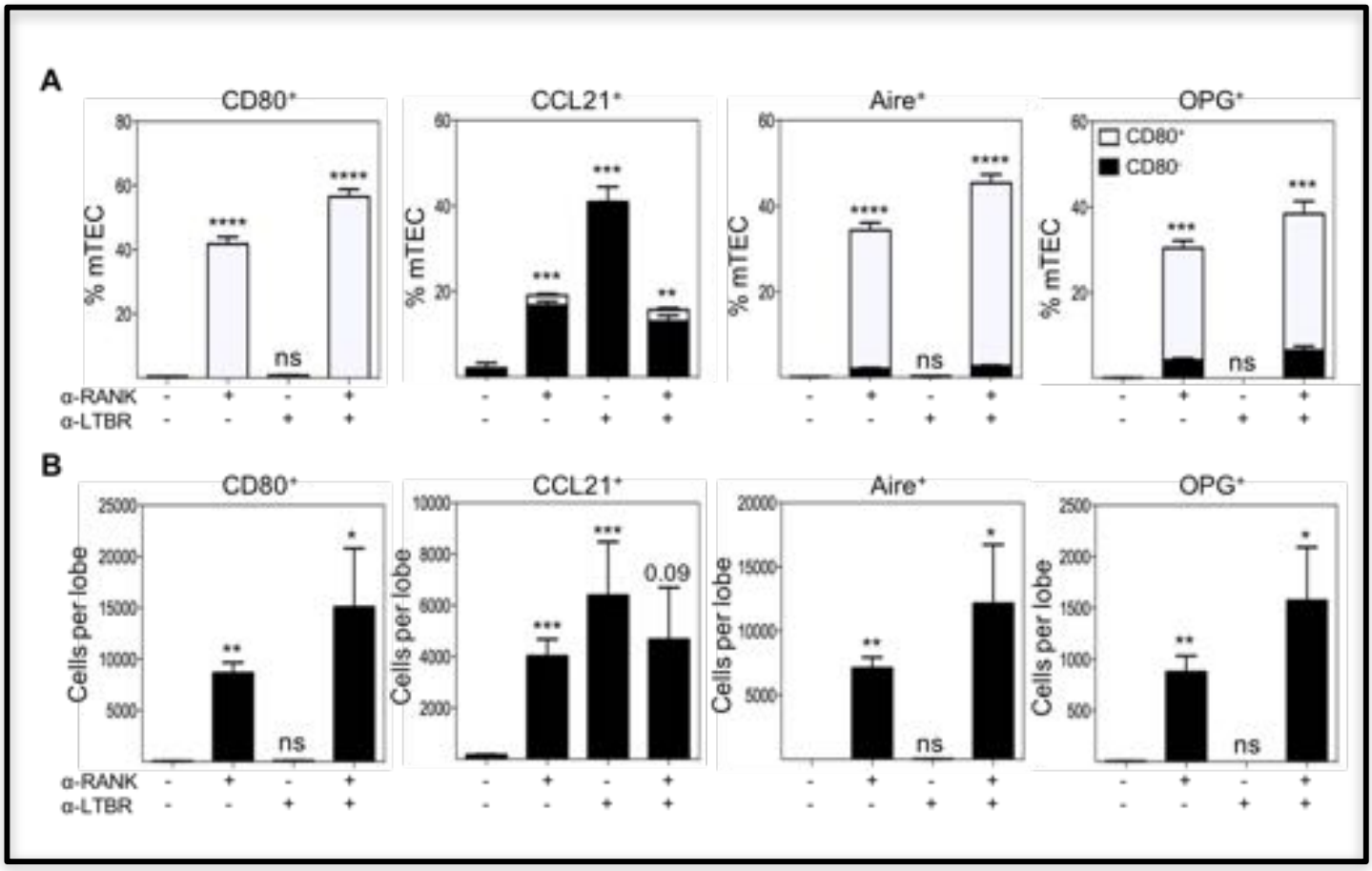
A
CD80+
CCL21+
Aire+
OPG+
% mTEC
CD80+
CD80-
ns
α-RANK
α-LTBR
B
Cells per lobe
0.09

Figure 3.6: Expression of Aire, CCL21 and OPG is inducible in vitro by TNFRSF signaling

Quantitation of FACS staining of 7 day anti-Rank/Ltbr stimulated dGuo lobes expressing CD80, Aire, CCL21, and OPG (figure 3.5) in terms of the proportion of total mTEC (A) and absolute cell numbers per lobe (B). In part A, black bars represent $CD80^-$ mTEC, and white bars $CD80^+$ cells.

Data are representative of at least 3 cultures from at least 2 independent experiments. Statistical analysis was performed using paired student's t-tests, where * = $p<0.05$, ** = $p< 0.01$, *** = $p< 0.001$, **** = $p<0.0001$.

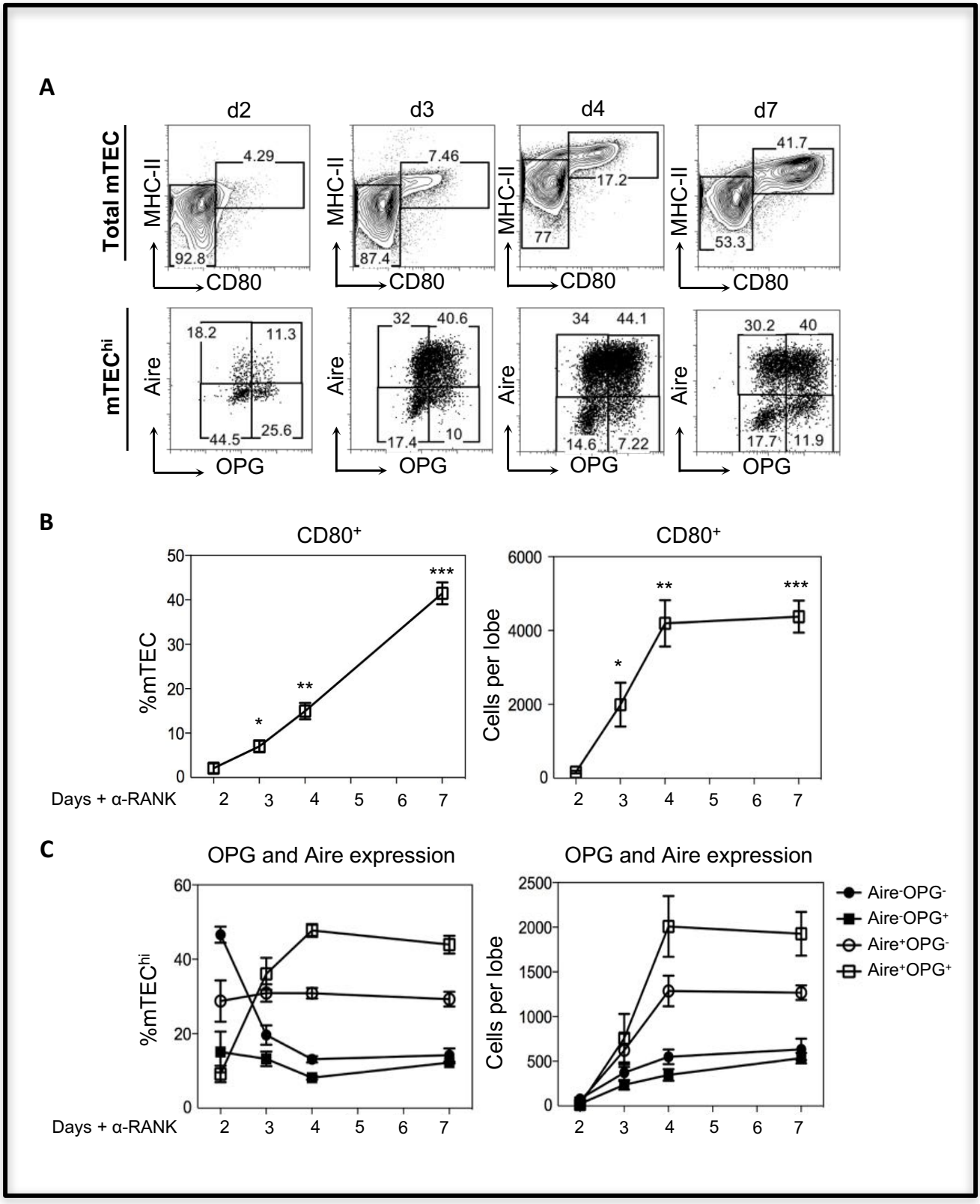
A
d2
d3
d4
d7
Total mTEC
MHC-II
CD80
4.29
92.8
7.46
87.4
17.2
77
41.7
53.3
mTEC^hi
Aire
OPG
18.2
11.3
44.5
25.6
32
40.6
17.4
10
34
44.1
14.6
7.22
30.2
40
17.7
11.9
B
CD80+
%mTEC
Cells per lobe
Days + α-RANK
C
OPG and Aire expression
%mTEC^hi
Aire-OPG-
Aire-OPG+
Aire+OPG-
Aire+OPG+

Figure 3.7: RANK-dependent induction of OPG in FTOC mirrors the expression profile in adult TEC

(A) Representative FACS plots of CD80 and MHC-II expression in total mTEC, and intracellular expression of OPG and Aire in $mTEC^{hi}$ in dGuo cultures stimulated for 2, 3, 4 and 7 days with 10ug/ml anti-Rank.

(B) Quantitation of CD80 induction during anti-Rank time-course.

(C) Quantitation of co-expression of Aire and OPG among $mTEC^{hi}$ during anti-Rank time-course; closed circles $Aire^{-}OPG^{-}$, closed squares $Aire^{-}OPG^{+}$, open circles $Aire^{+}OPG^{-}$, open squares $Aire^{+}OPG^{+}$.

Data are representative of at least 3 cultures from at least 2 independent experiments. Statistical analysis was performed using paired student's t-tests, where * = $p<0.05$, ** = $p< 0.01$, *** = $p< 0.001$.

(~70%) of mTEC^{hi} were Aire^{+}, with the largest population Aire^{+}OPG^{+} (Figure 3.7A, C). These findings may suggest mTEC^{hi} to become double-positive for Aire and OPG in a stepwise manner, initiated by the formation of Aire^{+}OPG^{-} or Aire^{-}OPG^{+} cells.

Given their distinct pattern of co-expression in mTEC^{hi}, we utilised *Aire*$^{-/-}$ mice to investigate the requirement for Aire in the formation of OPG^{+} mTEC. FACS analysis demonstrated OPG expression to be maintained in *Aire*$^{-/-}$ mTEC (Figure 3.8). OPG^{+} cells were still restricted to the mTEC^{hi} compartment, where the proportion of cells expressing OPG was increased in Aire-deficiency (Figure 3.8A-B). Given the mTEC^{hi} compartment is expanded in *Aire*$^{-/-}$ thymus, this culminated in greater than a 3-fold increase in the total number of OPG^{+} mTEC (Figure 3.8B). These findings were supported by confocal analysis of wildtype and *Aire*$^{-/-}$ thymus sections. Here, partial overlap in the expression of Aire and OPG was observed in wildtype mTEC, consistent with our FACS observations, and the frequency of OPG^{+} cells was greatly increased in the medulla of *Aire*$^{-/-}$ mice (Figure 3.8C). Although the defects in homeostasis of the mTEC compartment failed to be recapitulated when *Aire*$^{-/-}$ dGuo FTOC were stimulated with anti-Rank, this resulted in induction of OPG^{+} mTEC^{hi} that was at least equivalent to that seen in wildtype FTOC (Figure 3.8D). These findings suggest that, although OPG expression is largely restricted to Aire^{+} mTEC, this occurs in an Aire-independent manner.

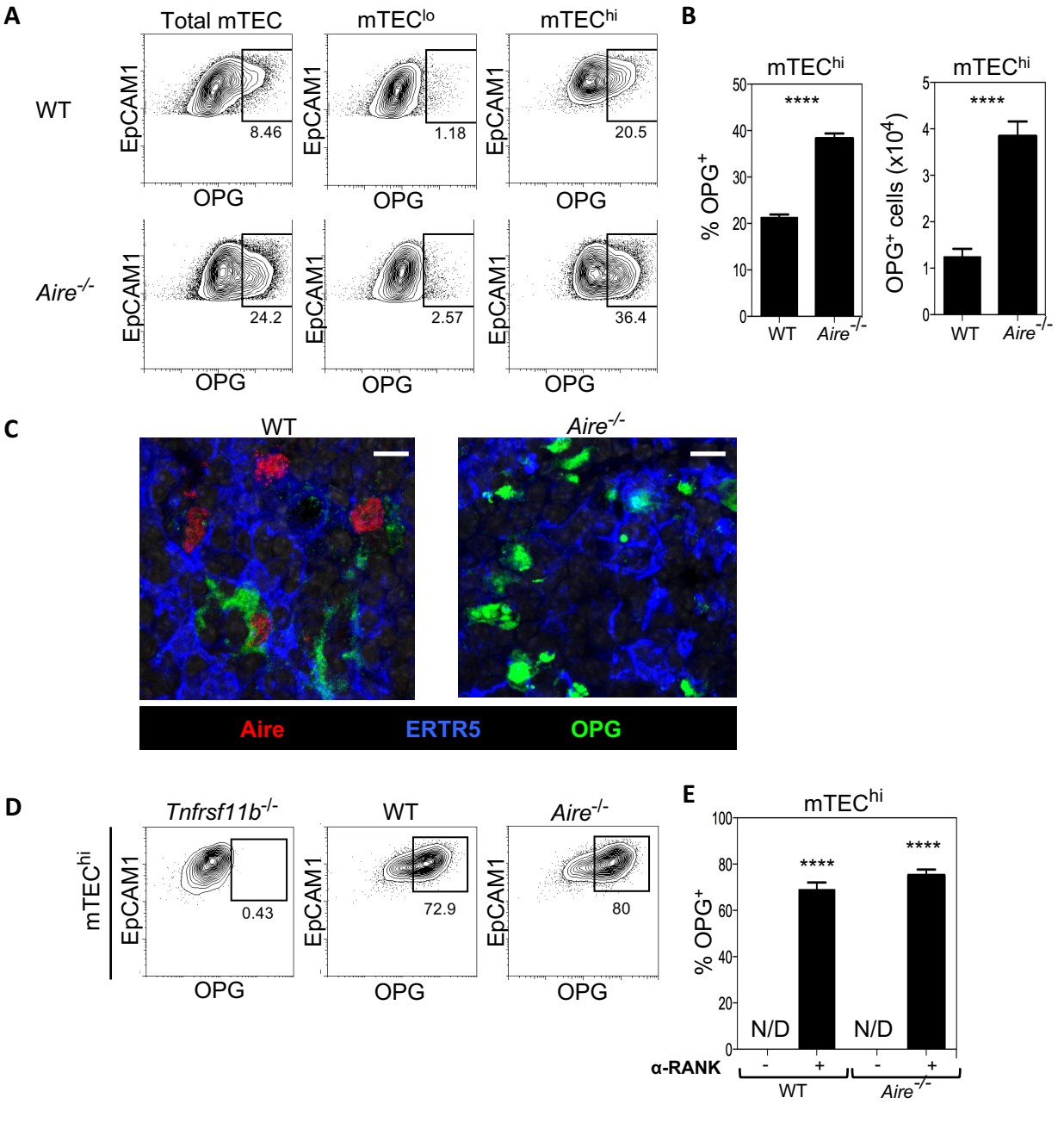
A
Total mTEC
mTEC^lo
mTEC^hi
WT
Aire-/-
EpCAM1
OPG
8.46
1.18
20.5
24.2
2.57
36.4
B
mTEC^hi
% OPG+
OPG+ cells (x10^4)
****
WT
Aire-/-
C
WT
Aire-/-
Aire
ERTR5
OPG
D
Tnfrsf11b-/-
WT
Aire-/-
mTEC^hi
0.43
72.9
80
E
mTEC^hi
% OPG+
N/D
α-RANK
WT
Aire-/-

Figure 3.8: Aire negatively regulates expression of OPG

(A) FACS plots and (B) quantitation showing expression of OPG in mTEC sub-populations from wildtype and *Aire*$^{-/-}$ mice. n= 7 wildtype, 9 *Aire*$^{-/-}$ mice.

(C) Confocal images of the medulla of thymic tissue sections from wildtype and *Aire*$^{-/-}$ mice stained for expression of Aire (red), OPG (green) and ER-TR5 (blue). Scale bars, 10uM.

(D) Representative FACS plots and (E) quantitation of OPG-expressing cells among mTEC^{hi} induced by culturing C57BL/6 wildtype, *Aire*$^{-/-}$ or *Tnfrsf11b*$^{-/-}$ (negative control) dGuo FTOC lobes with anti-Rank for 7 days. N/D = not determined. Data are representative of at least 3 cultures from at least 2 independent experiments.

Statistical analysis was performed using unpaired (B) or paired (E) student's t-tests, where **** = p< 0.0001.

3.2.2. Aire and OPG differentially regulate mTEC homeostasis

To assess potential targets for regulation by OPG, we utilised recently generated Rank-Venus reporter mice - BAC transgenic mice wherein the fluorescent protein Venus is expressed under control of regulatory elements for the *Tnfrsf11a* gene (McCarthy et al., 2015). Analysis of TEC populations from these mice showed Rank expression in 68% of mTEC (Figure 3.9A). The fidelity of this model was tested by cell sorting Venus^{+} and Venus^{-} TEC populations, and analysing Rank expression via PCR, which determined Venus to be a faithful reporter for Rank gene expression, as Rank mRNA was detected only in Venus^{+} cells (Figure 3.9B). Next, the previously defined mTEC sub-populations were analysed for Rank expression. Rank^{+} cells were found to form the majority of both mTEC^{hi} (69%) and mTEC^{lo} (60%) (Figure 3.9C). In addition, distinct heterogeneity of expression of Rank, as well as Aire in mTEC^{hi}, and CCL21 in mTEC^{lo} was observed, including Rank$^{+/-}$Aire^{+}, Rank$^{+/-}$Aire^{-}, Rank$^{+/-}$CCL21^{+} and Rank$^{+/-}$CCL21^{-} populations (Figure 3.9C). When broken down further, Rank^{+} cells were seen to form the majority of both Aire^{+} and Aire^{-} mTEC^{hi} subsets, as well as CCL21^{+} mTEC^{lo}, however only 42% of CCL21^{-} mTEC^{lo} expressed Rank (Figure 3.9D-E). Separate analysis also showed heterogeneity of Rank expression among OPG^{+} and OPG^{-} subsets of mTEC^{hi}, wherein ~50-55% of each subset was Rank^{+} (Figure 3.9D-E).

Given the multitude of potential mTEC targets of OPG regulation, we next sought to examine the effect of OPG-deficiency on the homeostasis of the mTEC compartment. Confocal analysis of *Tnfrsf11b*$^{-/-}$ thymus revealed an increase in

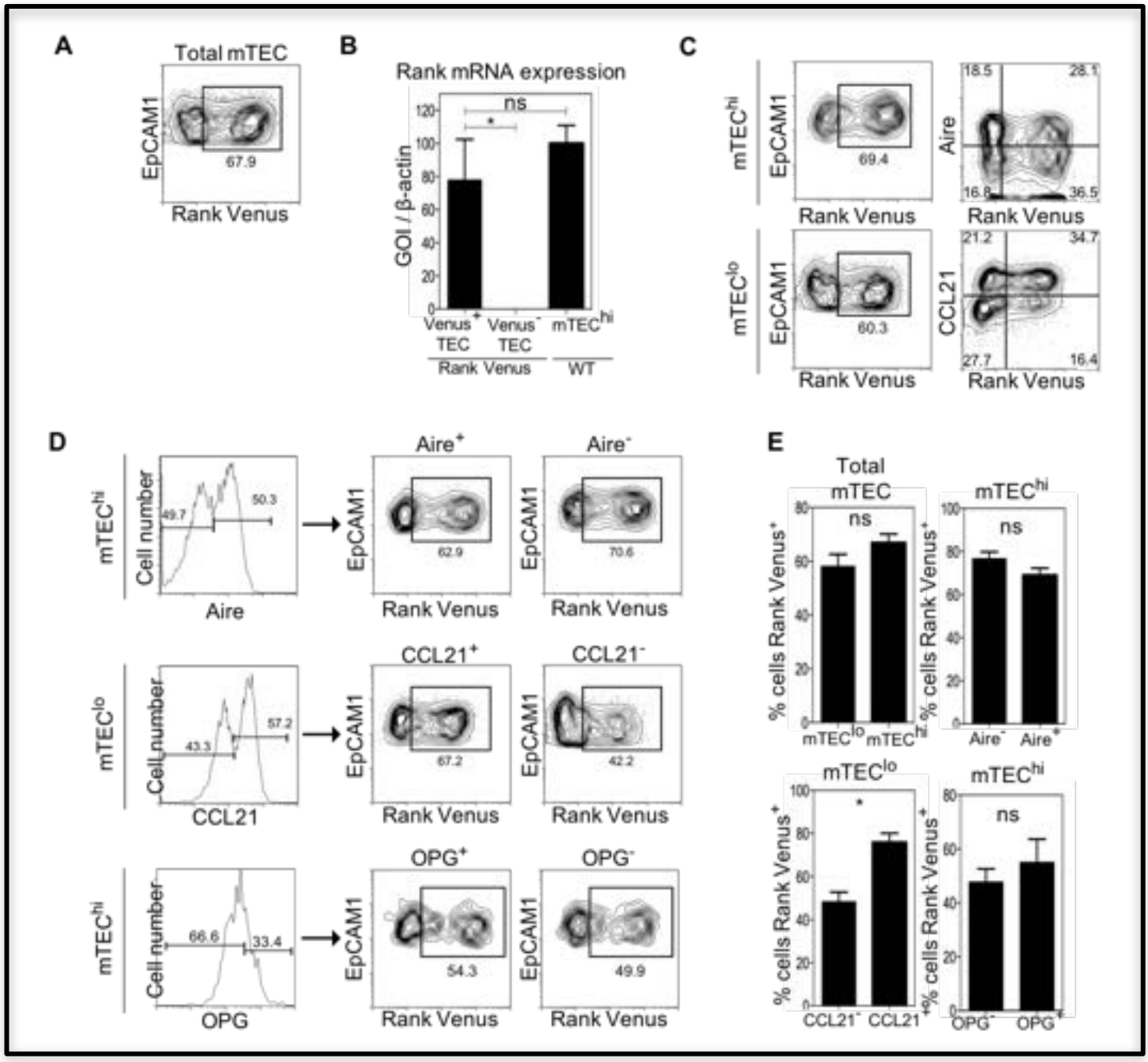
A
Total mTEC
EpCAM1
67.9
Rank Venus
B
Rank mRNA expression
ns
*
GOI / β-actin
120
100
80
60
40
20
0
Venus+ TEC
Venus- TEC
mTEChi
Rank Venus
WT
C
mTEChi
EpCAM1
69.4
Rank Venus
Aire
18.5
28.1
16.8
36.5
Rank Venus
mTEClo
EpCAM1
60.3
Rank Venus
CCL21
21.2
34.7
27.7
16.4
Rank Venus
D
mTEChi
Cell number
49.7
50.3
Aire
Aire+
EpCAM1
62.9
Rank Venus
Aire-
EpCAM1
70.6
Rank Venus
mTEClo
Cell number
43.3
57.2
CCL21
CCL21+
EpCAM1
67.2
Rank Venus
CCL21-
EpCAM1
42.2
Rank Venus
mTEChi
Cell number
66.6
33.4
OPG
OPG+
EpCAM1
54.3
Rank Venus
OPG-
EpCAM1
49.9
Rank Venus
E
Total mTEC
ns
% cells Rank Venus+
80
60
40
20
0
mTEClo
mTEChi
mTEChi
ns
% cells Rank Venus+
100
80
60
40
20
0
Aire-
Aire+
mTEClo
*
% cells Rank Venus+
100
80
60
40
20
0
CCL21-
CCL21+
mTEChi
ns
% cells Rank Venus+
80
60
40
20
0
OPG-
OPG+

Figure 3.9: The Rank receptor is expressed by heterogeneous populations of mTEC

(A) FACS plot of mTEC from Rank-Venus reporter mice (FVB background), where the negative is set against the equivalent population in wildtype FVB cells.

(B) Rank gene expression via PCR in sorted total wildtype TEC, in addition to $Venus^{+}$ and $Venus^{-}$ TEC from Rank-Venus reporter mice. Rank expression is normalised to the housekeeping gene β-actin.

(C) Representative plots of Rank expression in reporter cells among mTEChi and mTEClo (left) in addition to co-expression of Rank with Aire (top right) and CCL21 (bottom right).

(D) Representative FACS plots and (E) quantitation of Rank-expressing cells in $Aire^{+/-}$ $mTEC^{hi}$, $CCL21^{+/-}$ $mTEC^{lo}$ and $OPG^{+/-}$ $mTEC^{hi}$.

Statistical analysis was performed using unpaired student's t-tests, where * = $p< 0.05$.

medullary area - as defined by expression of ER-TR5 (Figure 3.10, top panels), and the presence of CD4 and CD8 SP thymocytes (Figure 3.10, bottom panels) - relative to wildtype thymus. In addition, the *Tnfrsf11b*$^{-/-}$ thymus contained a large central medulla, rather than the smaller, scattered medullary areas of the wildtype, with higher intensity staining for ER-TR5 (Figure 3.10, top panels). As the transgenic absence of OPG resulted in expansion of the medulla, we next attempted to assess whether this correlated to an increase in specific populations of TEC. Flow cytometric analysis showed a 3-fold increase in total EpCAM-1^{+} cells in *Tnfrsf11b*$^{-/-}$ thymus as a result of specific expansion of the mTEC compartment (cTEC were unaffected, Figure 3.12A-B). Although both mTEC^{hi} and mTEC^{lo} subsets were increased, there was a preferential increase in mTEC^{hi}, resulting in skewing of the mTEC^{hi}:mTEC^{lo} ratio relative to that of the wildtype thymus, where mTEC^{lo} are the majority population (Figure 3.11A-B). Equally, the increase in mTEC was not restricted to a particular functional subpopulation of mTEC – both Aire$^{+/-}$ mTEC^{hi}, and CCL21$^{+/-}$ mTEC^{lo} were increased by number, with no alteration in the proportion of Aire^{+} or CCL21^{+} cells in their respective compartments (Figure 3.12A-B). The mTEC^{hi} subset has also been shown to be expanded in *Aire*$^{-/-}$ mice; however, we observed no increase in the total number of mTEC in the thymus of *Aire*$^{-/-}$ mice (Figure 3.11C-D). Although the mTEC^{hi}:mTEC^{lo} ratio was skewed similarly to the effect observed in the *Tnfrsf11b*$^{-/-}$, and mTEC^{hi} were increased in number in Aire-deficiency, this was accompanied by an equivalent reduction in the number of mTEC^{lo} – specifically the sub-population expressing CCL21 (Figure 3.12C-D). These results suggest that, although expression is overlapping, OPG and Aire regulate mTEC homeostasis by independent mechanisms.

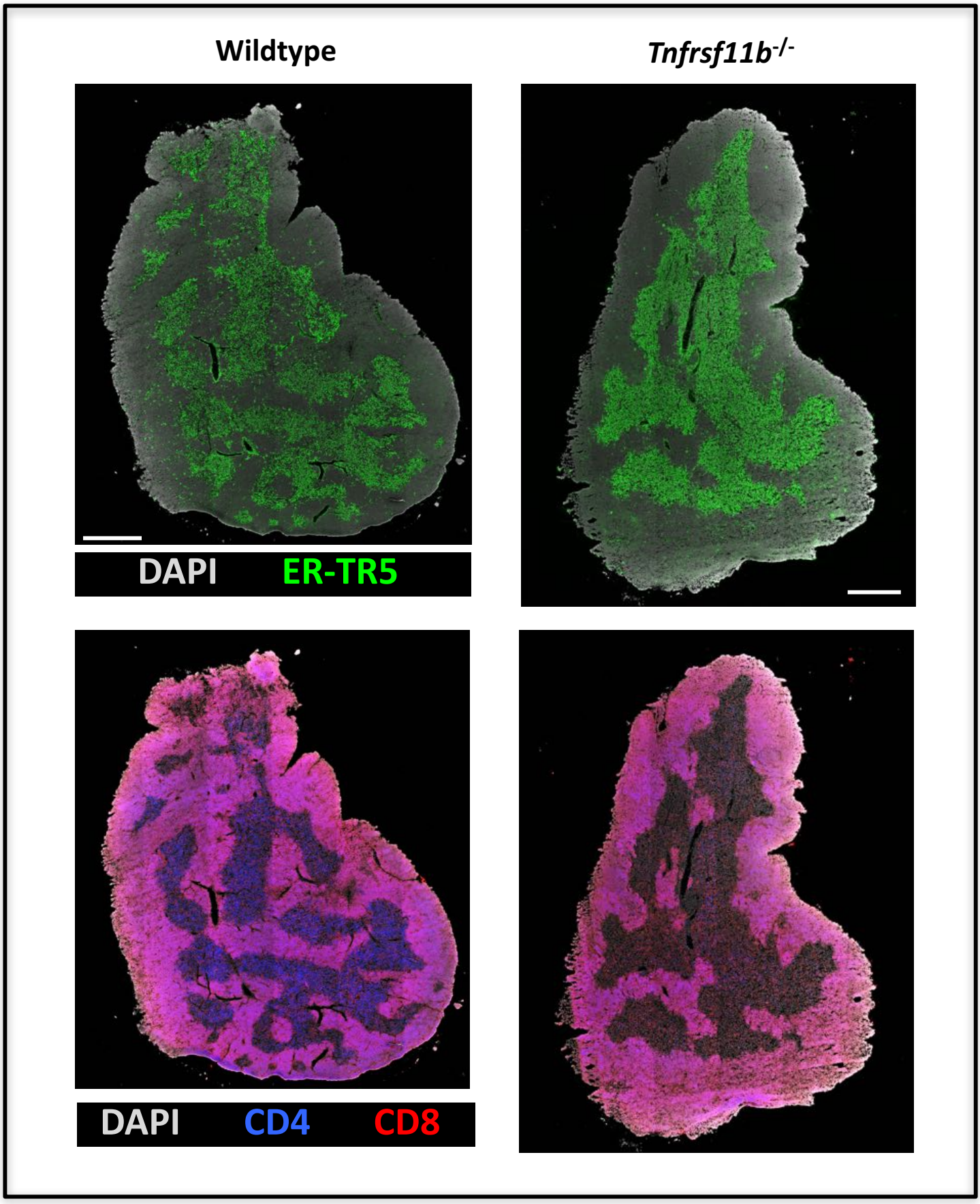
Wildtype
Tnfrsf11b-/-
DAPI ER-TR5
DAPI CD4 CD8

Figure 3.10: The medulla is expanded in OPG-deficient mice

Confocal immunofluorescence analysis of sections of wildtype (left) and *Tnfrsf11b*$^{-/-}$ (right) thymus. Sections were stained for antibodies against ER-TR5 (green), CD4 (blue) and CD8 (red), as well as a DAPI nuclear stain (grey) before tile scan images were obtained. Scale bar = 1mm.

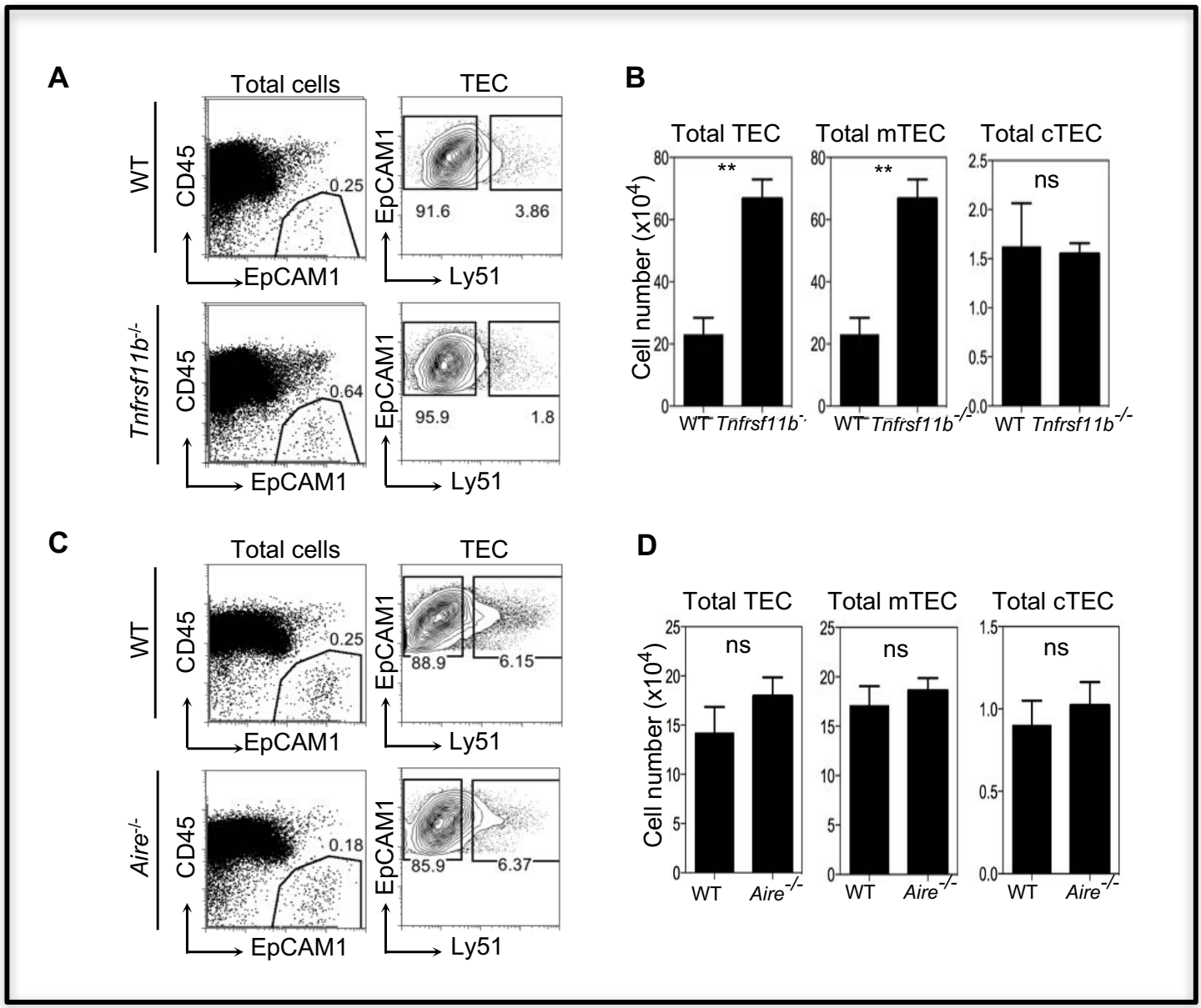
A
Total cells
TEC
WT
CD45
EpCAM1
0.25
91.6
3.86
Ly51
Tnfrsf11b-/-
0.64
95.9
1.8
B
Total TEC
Total mTEC
Total cTEC
Cell number (x10^4)
**
**
ns
WT
Tnfrsf11b-/-
C
Aire-/-
0.18
88.9
6.15
85.9
6.37
D
ns

Figure 3.11: OPG and Aire differentially impact TEC homeostasis

(A, C) Comparative FACS plots and (B, D) quantitation of total CD45^{-}EpCAM-1^{+} TEC, Ly51^{+} cTEC and Ly51^{-} mTEC from wildtype and *Aire*$^{-/-}$ mice (A-B), and wildtype and *Tnfrsf11b*$^{-/-}$ mice (C-D).

Statistical analysis was performed using unpaired student's t-tests, where ** = $p < 0.01$.

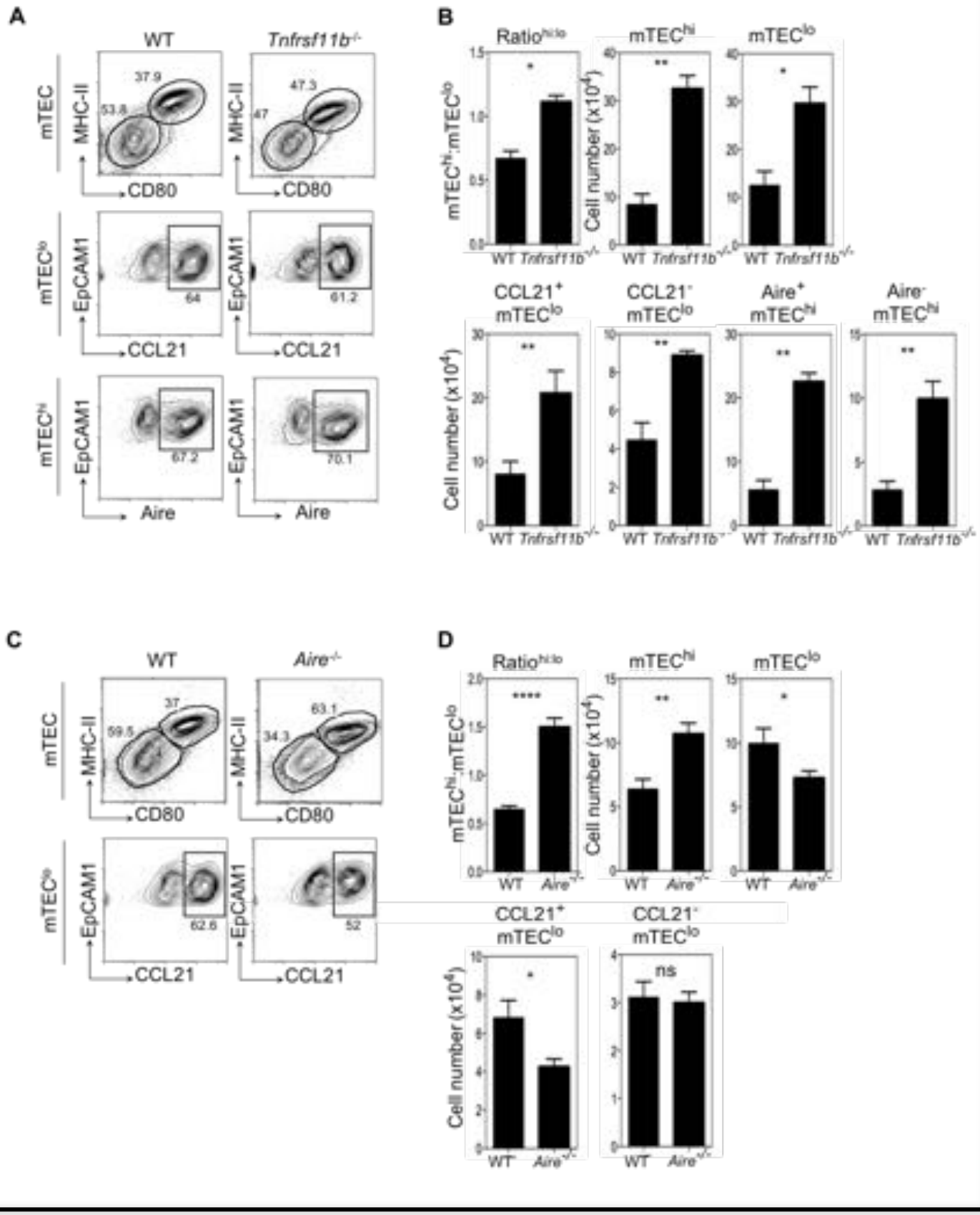
A
WT
Tnfrsf11b-/-
mTEC
MHC-II
37.9
53.8
CD80
47.3
47
CD80
mTEChi
EpCAM1
64
CCL21
61.2
CCL21
mTEClo
EpCAM1
67.2
Aire
70.1
Aire
B
Ratiohi:lo
mTEChi:mTEClo
mTEChi
Cell number (x10-4)
mTEClo
Cell number (x10-4)
WT Tnfrsf11b-/-
CCL21+ mTEClo
CCL21- mTEClo
Aire+ mTEChi
Aire- mTEChi
Cell number (x10-4)
WT Tnfrsf11b-/-
C
WT
Aire-/-
mTEC
MHC-II
37
59.5
CD80
63.1
34.3
CD80
mTEClo
EpCAM1
62.6
CCL21
52
CCL21
D
Ratiohi:lo
mTEChi:mTEClo
mTEChi
Cell number (x10-4)
mTEClo
Cell number (x10-4)
WT Aire-/-
CCL21+ mTEClo
CCL21- mTEClo
Cell number (x10-4)
ns
WT Aire-/-

Figure 3.12: OPG and Aire differentially impact TEC homeostasis

(A) Representative FACS plots of $mTEC^{hi/lo}$, and expression of Aire and CCL21 in mTEC sub-populations in wildtype and *Tnfrsf11b*$^{-/-}$ mice.

(B) Ratio of $mTEC^{hi}$:$mTEC^{lo}$, and quantification of $mTEC^{hi/lo}$, $CCL21^{+/-}$ $mTEC^{lo}$ and $Aire^{+/-}$ $mTEC^{hi}$ from *Tnfrsf11b*$^{-/-}$ mice.

(C) Representative FACS plots of $mTEC^{hi/lo}$, and expression of CCL21 in $mTEC^{lo}$ in wildtype and *Aire*$^{-/-}$ mice.

(D) Ratio of $mTEC^{hi}$:$mTEC^{lo}$, and quantification of $mTEC^{hi/lo}$ and $CCL21^{+/-}$ $mTEC^{lo}$ from *Aire*$^{-/-}$ mice.

Statistical analysis was performed using unpaired student's t-tests, where * = $p< 0.05$, ** = $p<0.01$ and **** = $p<0.0001$.

Next we sought to clarify the mechanism by which OPG-deficiency causes expansion of the mTEC compartment. Cleavage of cytoplasmic caspase 3 has been proven to be a precise marker for cellular apoptosis. Through intracellular FACS staining with an antibody specific for cleaved caspase 3, we found the highest proportion of cells undergoing apoptosis in the $mTEC^{lo}$ compartment (Figure 3.13A-B). However, there was no difference in the proportion of $mTEC^{hi}$ or $mTEC^{lo}$ undergoing apoptosis between wildtype and *Tnfrsf11b*$^{-/-}$ mice (Figure 3.13A-B). In fact, the number of apoptotic mTEC was greatly increased as a result of the global increase in mTEC numbers (Figure 3.13B), suggesting the accumulation of these cells is not as a result of their prolonged survival. Similarly, using Ki67 as a marker for proliferation, we saw no difference in the proportion of proliferating $mTEC^{lo}$ or $mTEC^{hi}$ in *Tnfrsf11b*$^{-/-}$ mTEC (Figure 3.13C-D). Finally, we attempted to address whether mTEC maturation could be accelerated in OPG-deficiency. Firstly, we assessed the expression of Rank in embryonic Rank Venus TEC, wherein we observed 25% of EpCAM-1^{+} cells to be positive for Rank gene expression at E15, increasing to ~32% at E16, suggesting TEC to include OPG target subsets prenatally, as well as in the adult stage (Figure 14A-B). Next, we assessed the effect of Rank receptor triggering on Rank expression by TEC. E15 dGuo treated FTOC were stimulated for 4 days with 10ug/ml anti-Rank, leading to up-regulation of Rank expression in terms of both the proportion of $Rank^{+}$ cells, and the levels of Rank expression (Figure 14C-D). To determine whether TEC from OPG-deficient embryos may have an increase in Rank expression and hence receptivity at this early stage, dGuo FTOC derived from wildtype and *Tnfrsf11b*$^{-/-}$ foetuses were stimulated with increasing doses of anti-Rank. Induction of $mTEC^{hi}$ was observed to an extent at doses as low as

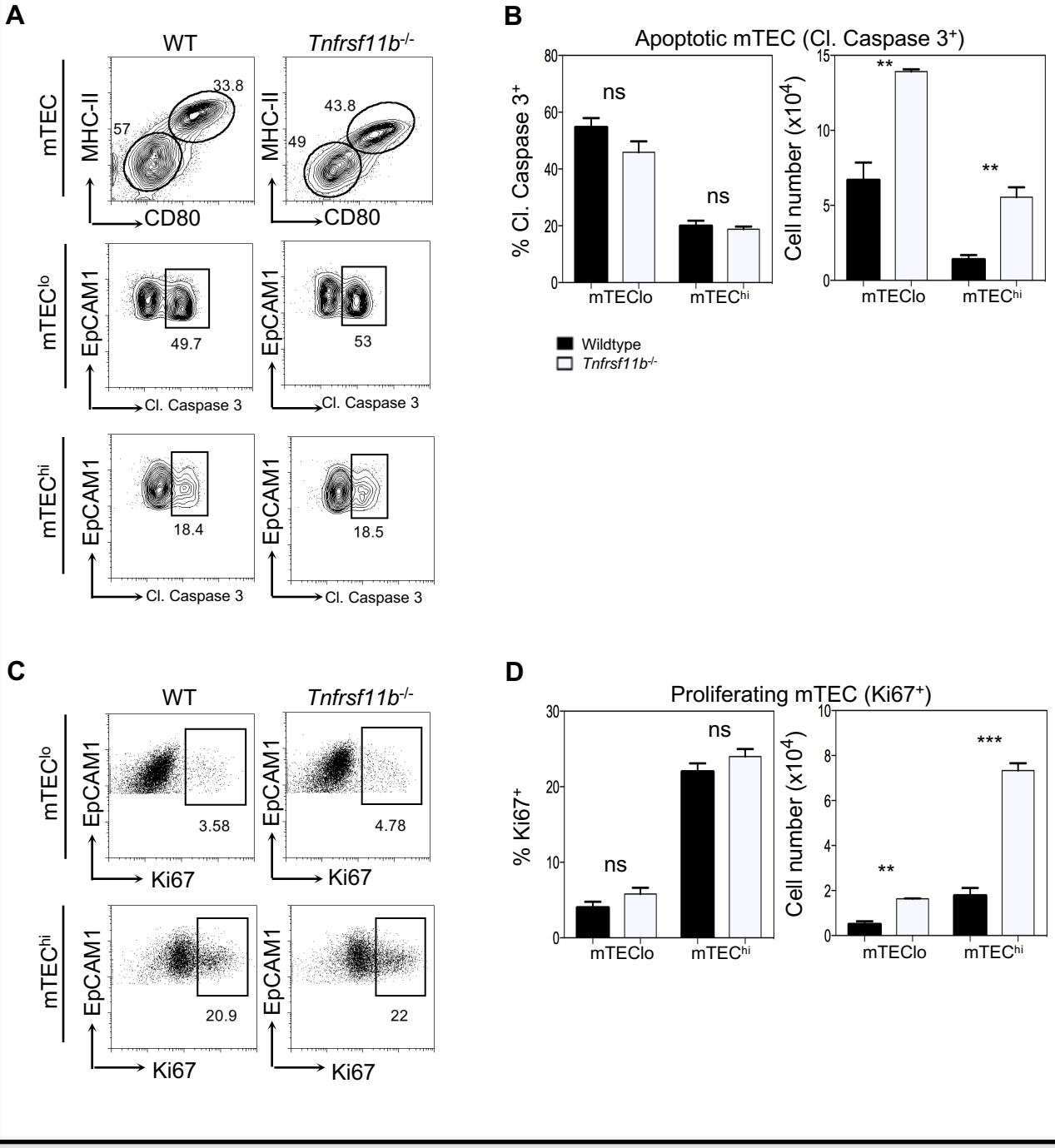
A
WT
Tnfrsf11b-/-
mTEC
MHC-II
CD80
33.8
57
43.8
49
mTEClo
EpCAM1
Cl. Caspase 3
49.7
53
mTEChi
18.4
18.5
B
Apoptotic mTEC (Cl. Caspase 3+)
% Cl. Caspase 3+
ns
Cell number (x10^4)
**
mTEClo
mTEChi
Wildtype
Tnfrsf11b-/-
C
Ki67
3.58
4.78
20.9
22
D
Proliferating mTEC (Ki67+)
% Ki67+
***

Figure 3.13: OPG has no impact on apoptosis or proliferation of adult TEC

(A) Intracellular antibody staining for activated (cleaved) caspase 3 as a marker for apoptotic mTEC in wildtype and *Tnfrsf11b*$^{-/-}$ mice , as quantitated in (B).

(C) Staining for Ki67 in mTEC^{hi}/^{lo} from wildtype and *Tnfrsf11b*$^{-/-}$ mice as a surrogate marker for proliferation – quantified in terms of proportions and cell numbers in (D).

Statistical analysis was performed using unpaired student's t-tests, where * = $p< 0.05$, ** = $p<0.01$ and **** = $p<0.0001$. Representative of n= 3 wildtype mice, and n= 3 *Tnfrsf11b*$^{-/-}$ mice from 2 independent experiments.

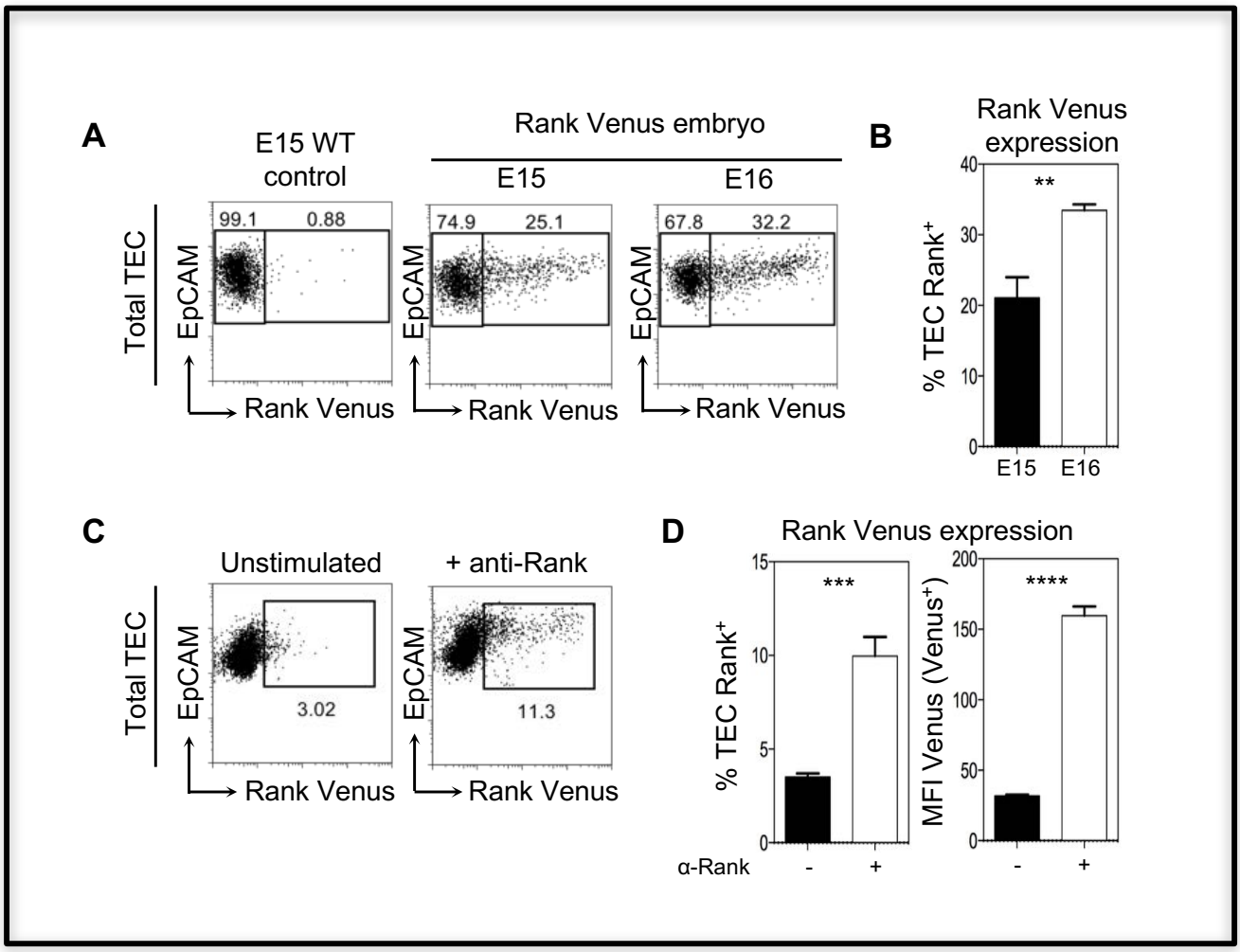
A
E15 WT control
Rank Venus embryo
E15
E16
Total TEC
EpCAM
Rank Venus
99.1
0.88
74.9
25.1
67.8
32.2
B
Rank Venus expression
% TEC Rank+
**
E15
E16
C
Unstimulated
+ anti-Rank
3.02
11.3
D
Rank Venus expression
% TEC Rank+
***
MFI Venus (Venus+)
****
α-Rank
-
+

Figure 3.14: Rank up-regulation occurs in embryonic TEC at the emergence of mTEC^{hi}, and is Rank inducible

(A) Representative FACS plots and (B) proportional analysis of Rank expression in total EpCAM-1^{+} TEC from E15 and E16 Rank Venus embryos.

(C) FACS plots showing Rank expression in E15 Rank Venus embryonic thymus after dGuo treatment, and +/- stimulation with 10ug/ml anti-Rank.

(D) Proportion of total cultured EpCAM-1+ TEC expressing Rank.

(E) MFI of Venus in Rank Venus+ cells in cultures +/- anti-Rank.

Statistical analysis was performed using unpaired student's t-tests, where ** = $p<0.01$, *** = $p<0.001$, **** = $p<0.0001$.

0.5ug/ml anti-Rank, but increased proportionally to the anti-Rank concentration (Figure 3.15B). At all concentrations, the induction of Aire^{+} mTEC^{hi} was greater in *Tnfrsf11b*$^{-/-}$ FTOC than wildtype FTOC, however the proportion and number of Aire^{+} mTEC^{hi} was only significantly greater at 5ug/ml (Figure 3.15A-C). Staining with Ki67 suggested that this increase in mTEC^{hi} was not the result of an increase in the proliferation of this subset (although almost all mTEC^{hi} were found to be Ki67^{+} in culture), as the proportion of proliferating mTEC^{hi} was actually slightly lower in *Tnfrsf11b*$^{-/-}$ lobes (Figure 3.15D-E). OPG-expression by embryonic TEC hence appears to impact on the expression of Rank, and receptivity to Rank triggering of maturational processes.

3.2.3. The size of the mTEC niche doesn't limit production of conventional and regulatory T-cells

The expansion of the mTEC compartment in *Tnfrsf11b*$^{-/-}$ thymus provided us with an interesting model to investigate the consequences of the relative limitation of the size of the mTEC niche in the wildtype thymus. Despite the large expansion of mTEC numbers, we observed no difference in the weight or total cellularity of the thymus in OPG-deficient mice (perhaps unsurprisingly, as TEC account for ~0.2% of total cells) (Figure 3.16A). FACS analysis revealed little alteration in gross thymocyte development, with no significant differences in the total numbers of thymocytes at DN stages 1-4 (the proportion of DN1 cells was increased, but this is attributable to an increase in numbers of thymic B cells, Figure 3.21), nor in the numbers of pre- and post-selection DP thymocytes, or SP8s (Figure 3.16B-D). The proportion of SP4 thymocytes was slightly but

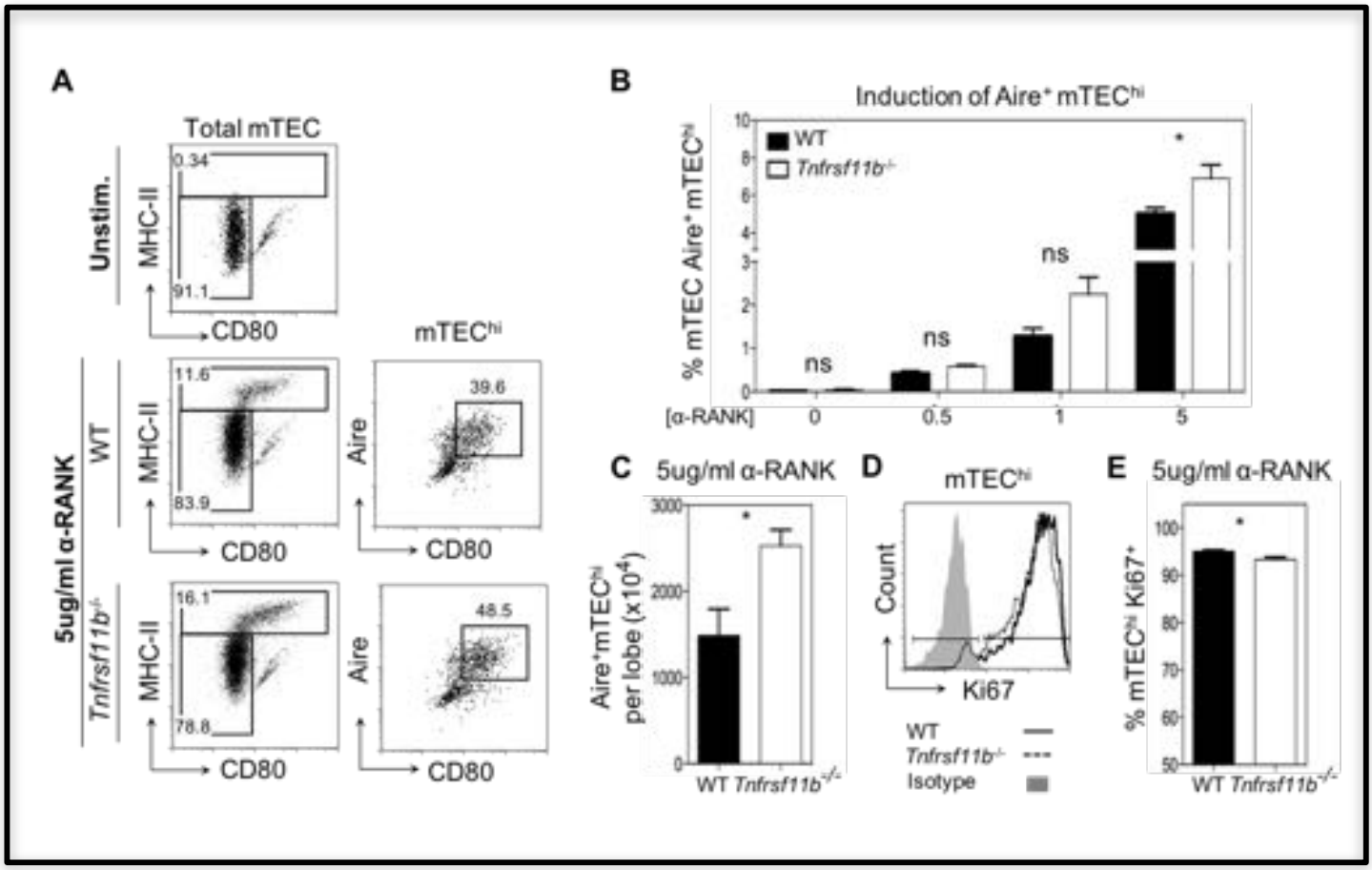
A
Total mTEC
Unstim.
MHC-II
CD80
0.34
91.1
5ug/ml α-RANK
WT
Tnfrsf11b-/-
11.6
83.9
16.1
78.8
mTEChi
Aire
39.6
48.5
B
Induction of Aire+ mTEChi
% mTEC Aire+ mTEChi
WT
Tnfrsf11b-/-
ns
*
[α-RANK]
0
0.5
1
5
C
5ug/ml α-RANK
Aire+mTEChi per lobe (x10^4)
WT Tnfrsf11b-/-
D
mTEChi
Count
Ki67
WT
Tnfrsf11b-/-
Isotype
E
5ug/ml α-RANK
% mTEChi Ki67+
WT Tnfrsf11b-/-

Figure 3.15: OPG controls the transition of mTEC to their mature Aire^{+} phenotype

(A) Representative FACS plots for mTEC^{lo}/^{hi} populations, and Aire induction in wildtype and *Tnfrsf11b*$^{-/-}$ dGuo FTOC left un-stimulated, or stimulated with 5ug/ml anti-Rank for 4 days.

(B) Dose:response assay using induction of Aire+ mTEC^{hi} as a readout of responsiveness to increasing concentrations (0, 0.5, 1, 5ug/ml) of stimulatory anti-Rank for 4 days of culture.

(C) Total numbers of Aire+ mTEChi per lobe after 5ug/ml anti-Rank for 4 days.

(D) Representative FACS histogram and quantification (E) of proliferation (Ki67 expression) by wildtype and *Tnfrsf11b*$^{-/-}$ mTEC^{hi} after anti-Rank stimulation at 5ug/ml.

Statistical analysis was performed using unpaired student's t-tests, where * = $p<0.05$.

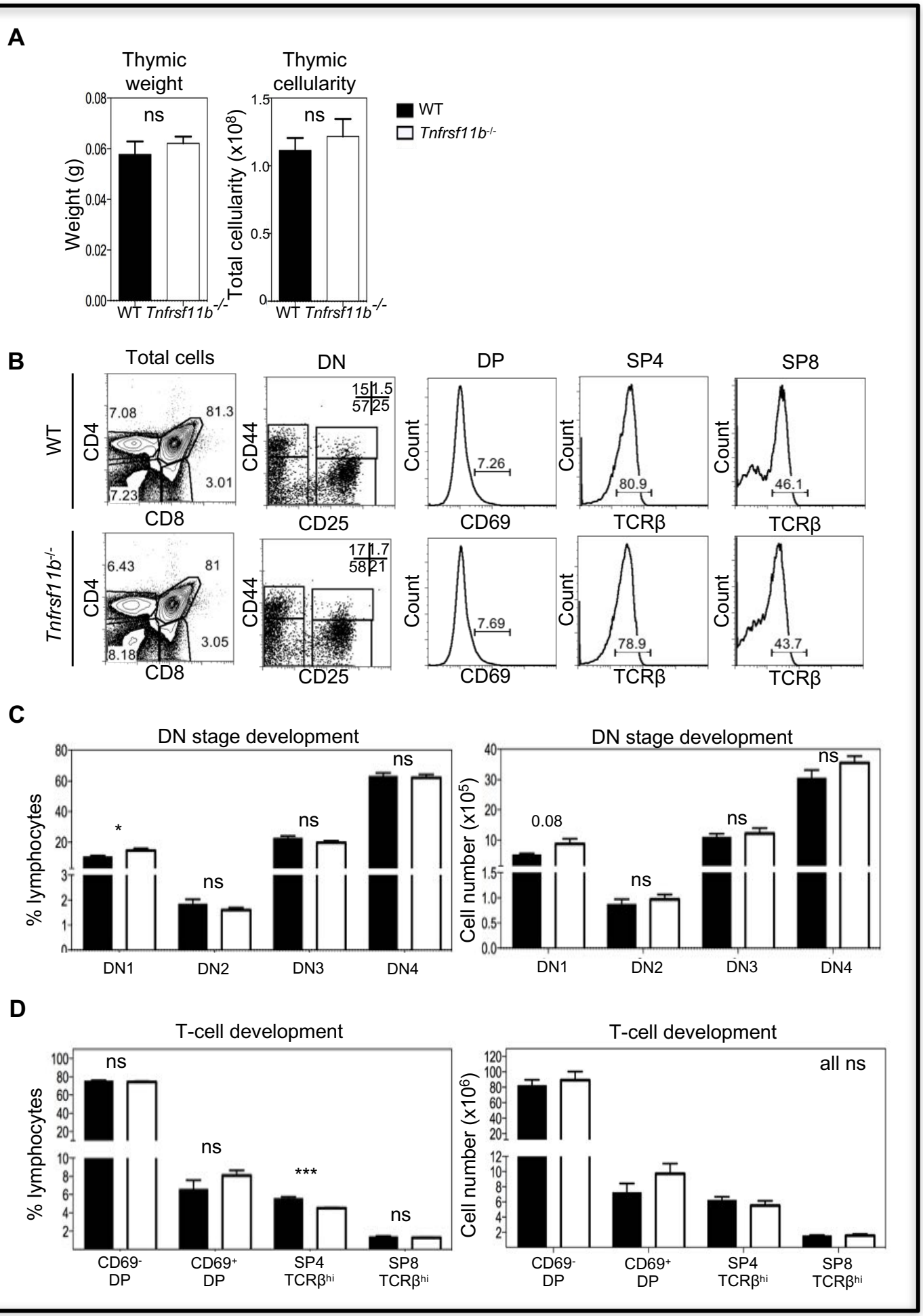
A
Thymic weight
Thymic cellularity
ns
ns
Weight (g)
Total cellularity (x10^8)
WT
Tnfrsf11b-/-
WT Tnfrsf11b-/-
WT Tnfrsf11b-/-
B
Total cells
DN
DP
SP4
SP8
WT
Tnfrsf11b-/-
CD4
CD8
CD44
CD25
Count
CD69
TCRβ
7.08
81.3
3.01
7.23
15
1.5
57
25
7.26
80.9
46.1
6.43
81
3.05
8.18
17
1.7
58
21
7.69
78.9
43.7
C
DN stage development
DN stage development
% lymphocytes
Cell number (x10^5)
0.08
*
ns
DN1
DN2
DN3
DN4
D
T-cell development
T-cell development
% lymphocytes
Cell number (x10^6)
all ns
***
CD69- DP
CD69+ DP
SP4 TCRβhi
SP8 TCRβhi

Figure 3.16: T-cell development is grossly normal in OPG-deficient thymus

(A) Weight and total cellularity of teased thymi from wildtype and *Tnfrsf11b*$^{-/-}$ mice.

(B) T-cell development, including DN, DP and SP stages in wildtype and *Tnfrsf11b*$^{-/-}$ mice.

(C) Quantitation of DN developmental subsets ($CD44^{+}CD25^{-}$ DN1, $CD44^{+}CD25^{+}$ DN2, $CD44^{-}CD25^{+}$ DN3 and $CD44^{-}CD25^{-}$ DN4) in wildtype and *Tnfrsf11b*$^{-/-}$ mice.

(D) Quantitation of DP-SP thymocyte development in wildtype and *Tnfrsf11b*$^{-/-}$ mice, including pre-selection DPs ($CD69^{-}CD4^{+}8^{+}$), post-selection DPs ($CD69^{+}CD4^{+}8^{+}$), as well as SP4 ($CD4^{+}8^{-}$ $TCR\beta^{hi}$) and SP8 ($CD4^{-}8^{+}$ $TCR\beta^{hi}$) thymocytes.

Data representative of 8 wildtype and 5 *Tnfrsf11b*$^{-/-}$ mice, and at least 3 independent experiments. Statistical testing was performed using unpaired student's t-tests, where * = $p<0.05$ and *** = $p<0.001$.

significantly reduced, however this did not equate to a significant difference in the absolute number of SP4 thymocytes (Figure 3.16B, D).

Regulatory T-cells have a known dependence on mTEC for their generation in the thymus (Cowan et al., 2013). To address the issue of whether T-Reg production is enhanced when mTEC numbers are increased, SP4 thymocytes were stained for CD25 and Foxp3, known markers of the T-Reg lineage (Figure 3.17A-B). T-Reg are possess a $CD25^{+}Foxp3^{+}$ phenotype, however distinct populations of T-Reg precursor cells have been identified to have the following phenotypes; $CD25^{+}Foxp3^{-}$ ($CD25^{+}$ precursors) and $CD25^{-}Foxp3^{+}$ ($Foxp3^{+}$ precursors). The proportion and number of thymic T-Reg was indeed increased in *Tnfrsf11b*$^{-/-}$ mice, however no significant increase in the numbers of either precursor population was observed (Figure 3.17A-B), and the proportion of $Ki67^{+}$ T-Reg was unchanged, suggesting the increase not to be the result of T-Reg proliferation intrathymically (3.17C-D). This effect however appeared limited to the thymus, as no alteration in the proportions or numbers of T-Reg, or indeed conventional CD4 T-cells, was observed in the spleen or inguinal lymph nodes of *Tnfrsf11b*$^{-/-}$ animals (Figure 3.18A-D). Enumeration of GFP^{+} cells in transgenic Rag-2p-GFP reporter mice has been demonstrated as an accurate measure of *de novo* production of T-cells (Monroe et al., 1999), and acts as an important differential, as a substantial proportion of thymic T-Reg is known to consist of mature cells that have re-circulated from the periphery (Thiault et al., 2015, Weist et al., 2015). Hence, we crossed *Tnfrsf11b*$^{-/-}$ mice onto the Rag-2p-GFP background. We saw no increase in the absolute numbers of GFP^{+} conventional (T-Conv) SP4s, T-Reg, or T-Reg precursors in the thymus of *Tnfrsf11b*$^{-/-}$ Rag-2p-GFP mice compared to their wildtype Rag-2p-GFP controls

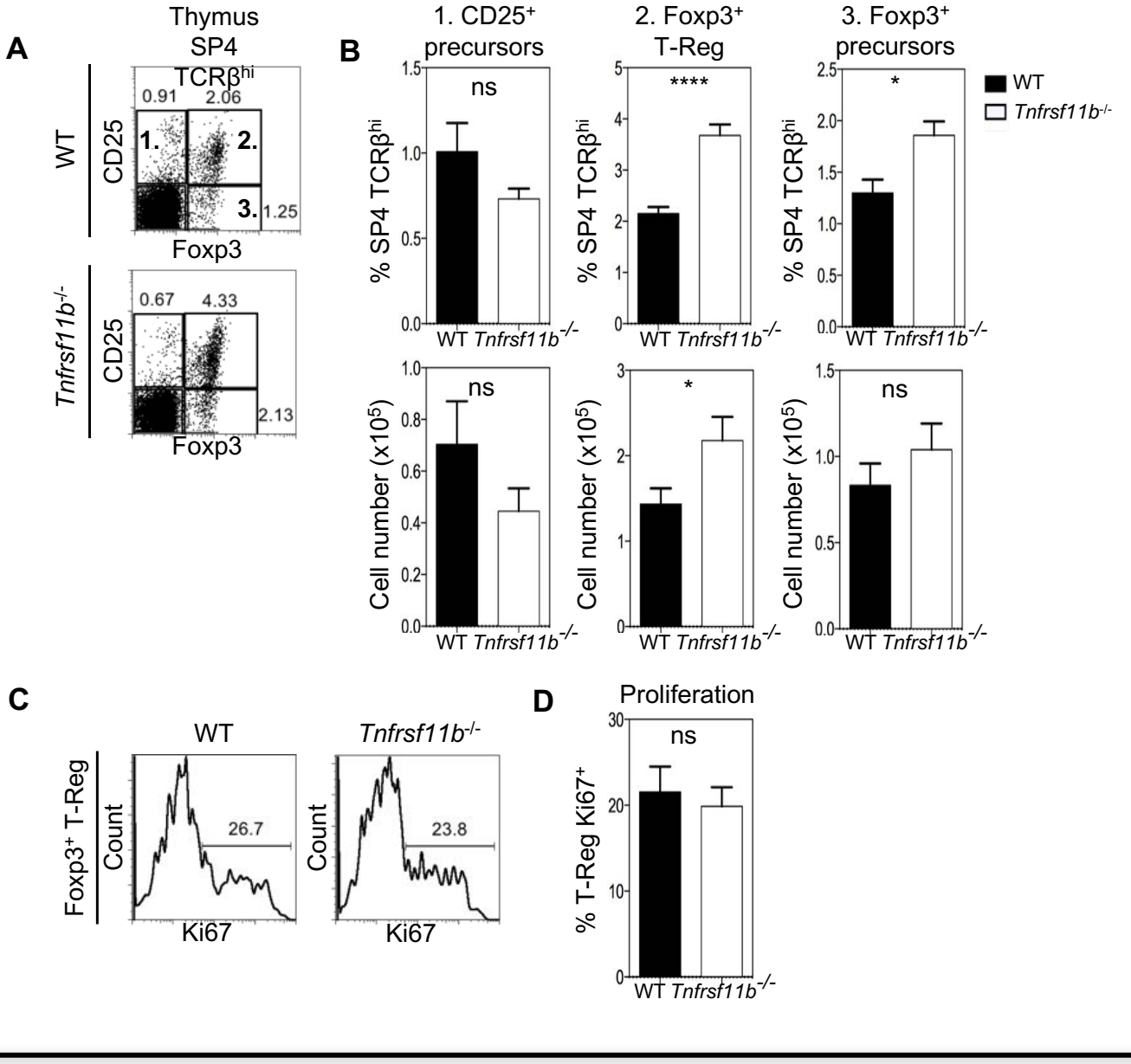
A
Thymus
SP4
TCRβhi
WT
CD25
0.91
2.06
1.
2.
3.
1.25
Foxp3
Tnfrsf11b-/-
0.67
4.33
2.13
B
1. CD25+ precursors
2. Foxp3+ T-Reg
3. Foxp3+ precursors
WT
Tnfrsf11b-/-
% SP4 TCRβhi
ns
****
*
Cell number (x10^5)
C
WT
Tnfrsf11b-/-
Foxp3+ T-Reg
Count
26.7
23.8
Ki67
D
Proliferation
% T-Reg Ki67+

Figure 3.17: Expansion of the medulla enhances thymic generation of regulatory T-cells

(A) T-Reg development in wildtype and *Tnfrsf11b*$^{-/-}$ mice, in which CD25^{+}Foxp3^{+} (1) and CD25^{-}Foxp3^{+} (3) populations represent T-Reg precursor populations, and T-Reg are defined as CD25^{+}Foxp3^{+} (2).

(B) Quantitation of stages in the development of T-Reg (and conventional CD4 T-cells) in the thymus of wildtype and *Tnfrsf11b*$^{-/-}$ mice.

(C-D) Representative FACS plots and graphs showing the proportion of thymic T-Reg proliferating in wildtype and *Tnfrsf11b*$^{-/-}$ mice, as determined through staining with the marker Ki67.

Plots are representative of (A-B) 8 wildtype and 10 *Tnfrsf11b*$^{-/-}$ mice, or (C-D) 4 wildtype, and 3 *Tnfrsf11b*$^{-/-}$ mice across at least 3 independent experiments. Statistical testing was performed using unpaired student's t-tests, wherein * = $p<0.05$, **** = $p<0.0001$.

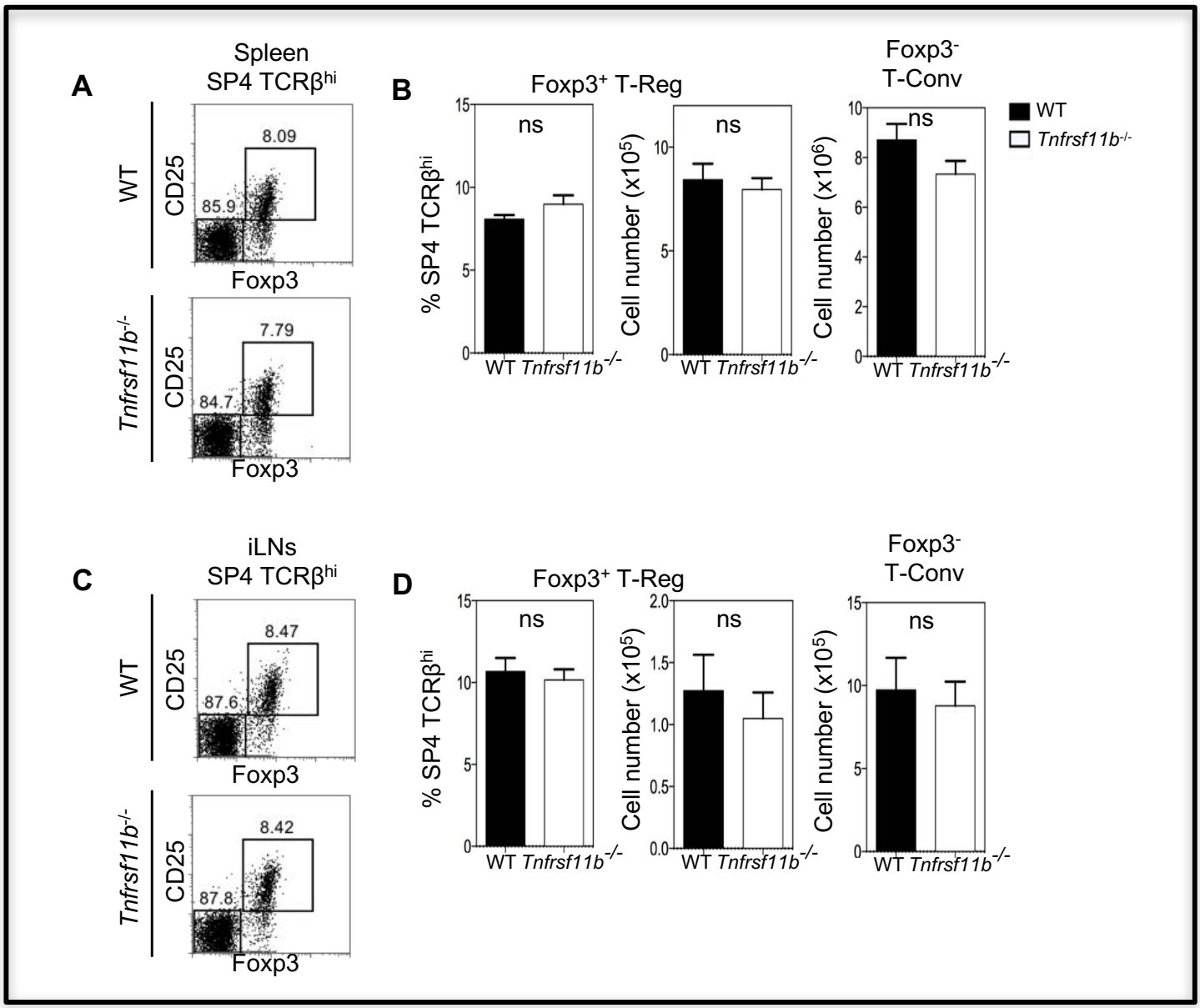
A
Spleen
SP4 TCRβhi
WT
CD25
8.09
85.9
Foxp3
Tnfrsf11b-/-
CD25
7.79
84.7
Foxp3
B
Foxp3+ T-Reg
% SP4 TCRβhi
ns
WT Tnfrsf11b-/-
Cell number (x10^5)
ns
WT Tnfrsf11b-/-
Foxp3-
T-Conv
Cell number (x10^6)
ns
WT Tnfrsf11b-/-
WT
Tnfrsf11b-/-
C
iLNs
SP4 TCRβhi
WT
CD25
8.47
87.6
Foxp3
Tnfrsf11b-/-
CD25
8.42
87.8
Foxp3
D
Foxp3+ T-Reg
% SP4 TCRβhi
ns
WT Tnfrsf11b-/-
Cell number (x10^5)
ns
WT Tnfrsf11b-/-
Foxp3-
T-Conv
Cell number (x10^5)
ns
WT Tnfrsf11b-/-

Figure 3.18: Enhanced thymic generation of regulatory T-cells fails to impact on peripheral populations

(A) Representative FACS plots of Foxp3 expression, and (B) quantification of $CD25^{+}Foxp3^{+}$ T-Reg in the spleen of wildtype and *Tnfrsf11b*$^{-/-}$ mice.

(C) Representative FACS plots of Foxp3 expression, and (D) quantification of $CD25^{+}Foxp3^{+}$ T-Reg in the inguinal lymph nodes (iLNs) of wildtype and *Tnfrsf11b*$^{-/-}$ mice.

Plots are representative of 7 wildtype and 5 *Tnfrsf11b*$^{-/-}$ mice across at least 3 independent experiments. Statistical testing was performed using unpaired student's t-tests..

(in fact, the number of GFP$^+$ CD25$^+$ precursors was significantly reduced, Figure 3.19). Instead, in each population there was an increase in the proportion of GFP- cells (Figure 3.19). In each instance, this was reflected as an increase in absolute numbers of the GFP$^-$ fraction, which in the case of T-Reg accounted for the entirety of their increase in absolute number in the thymus of *Tnfrsf11b*$^{-/-}$ mice (Figure 3.19D-E). These findings are consistent with the restriction of the size of the mTEC niche by OPG limiting the re-circulation of peripheral T-cells to the thymus, rather than effecting the production of either conventional or regulatory T-cells. GFP$^+$ T-cells in the periphery of Rag-2p-GFP mice represent recent thymic emmigrants (RTE). We observed no differences in the proportion of GFP$^+$ T-Conv or T-Reg in the spleen of *Tnfrsf11b*$^{-/-}$ mice relative to their wildtype controls, suggesting that the output of thymic T-cells is similarly unaltered (Figure 3.20). Lastly, we performed analysis on P2 newborn mice to test whether the production of CD4 T-cells is accelerated by expansion of the mTEC compartment. TEC analysis showed phenotypic similarity between adult and postnatal *Tnfrsf11b*$^{-/-}$ mice, as mTEC^{hi} were increased in number at P2, and the ratio of mTEC^{hi}:mTEC^{lo} greatly skewed in favour of the mature cells (Figure 3.21A-B). However, we observed no difference in the numbers of thymic SP4 at this stage, and although the fraction of regulatory T-cells present was minimal compared to later stages of development, there was no increase in the proportion or number of these cells present in the thymus (Figure 3.21C-D). In addition, the number of splenic CD4$^+$ T-cells was unchanged between newborn wildtype and *Tnfrsf11b*$^{-/-}$ mice, and T-Reg were essentially absent in the spleen at this stage (no Foxp3 expression in 2/3 wildtype and 3/3 *Tnfrsf11b*$^{-/-}$ mice, Figure 3.21). Combined, these data suggest the increase in mTEC availability in

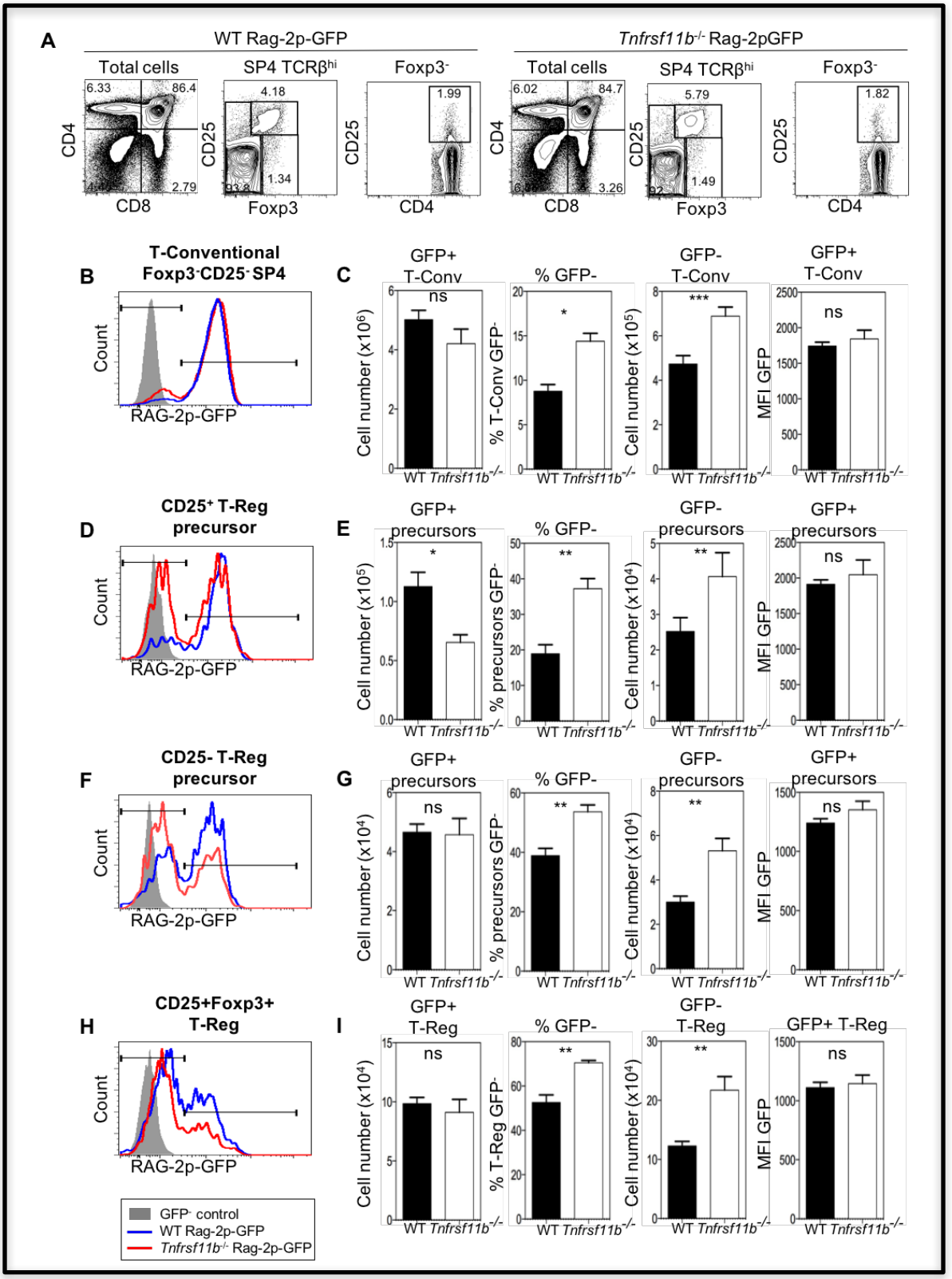
A
WT Rag-2p-GFP
Tnfrsf11b-/- Rag-2pGFP
Total cells
SP4 TCRβhi
Foxp3-
6.33
86.4
2.79
4.18
1.34
1.99
6.02
84.7
3.26
5.79
1.49
1.82
CD4
CD8
CD25
Foxp3
B
T-Conventional Foxp3-CD25- SP4
Count
RAG-2p-GFP
C
GFP+ T-Conv
% GFP-
GFP- T-Conv
GFP+ T-Conv
Cell number (x10^6)
% T-Conv GFP-
Cell number (x10^5)
MFI GFP
ns
*
***
WT
Tnfrsf11b-/-
D
CD25+ T-Reg precursor
E
GFP+ precursors
% GFP-
GFP- precursors
GFP+ precursors
Cell number (x10^5)
% precursors GFP-
Cell number (x10^4)
MFI GFP
F
CD25- T-Reg precursor
G
H
CD25+Foxp3+ T-Reg
I
GFP+ T-Reg
% GFP-
GFP- T-Reg
GFP+ T-Reg
% T-Reg GFP-
GFP- control
WT Rag-2p-GFP
Tnfrsf11b-/- Rag-2p-GFP

Figure 3.19: Recirculation of peripheral T-cells to the thymus is enhanced in the absence of OPG

(A) T-Reg development in wildtype and OPG-deficient mice bred onto the Rag-2pGFP background.

(B-I) Histogram overlays (left) representing expression of Rag-2p-GFP in thymocyte populations from wildtype and *Tnfrsf11b*$^{-/-}$ Rag-2p-GFP mice, together with quantitation of the absolute number of GFP^{+} and GFP^{-} cells (right). Histograms and graphs show conventional SP4s (B-C), CD25^{+}Foxp3^{-} T-Reg precursors (D-E), CD25^{-}Foxp3^{+} T-Reg precursors (F-G) and CD25^{+}Foxp3^{+} T-Reg (H-I) Blue histograms are the GFP profile of wildtype cells, and red histograms representative of their *Tnfrsf11b*$^{-/-}$ counterparts. Gates are set on shaded grey histograms (wildtype mice negative for the GFP transgene).

Plots are representative of 8 wildtype Rag-2p-GFP and 5 *Tnfrsf11b*$^{-/-}$ Rag-2p-GFP mice from at least 3 independent experiments. Statistical testing was performed using unpaired student's t-tests, where * = $p<0.05$, ** = $p<0.01$ and *** = $p<0.001$.

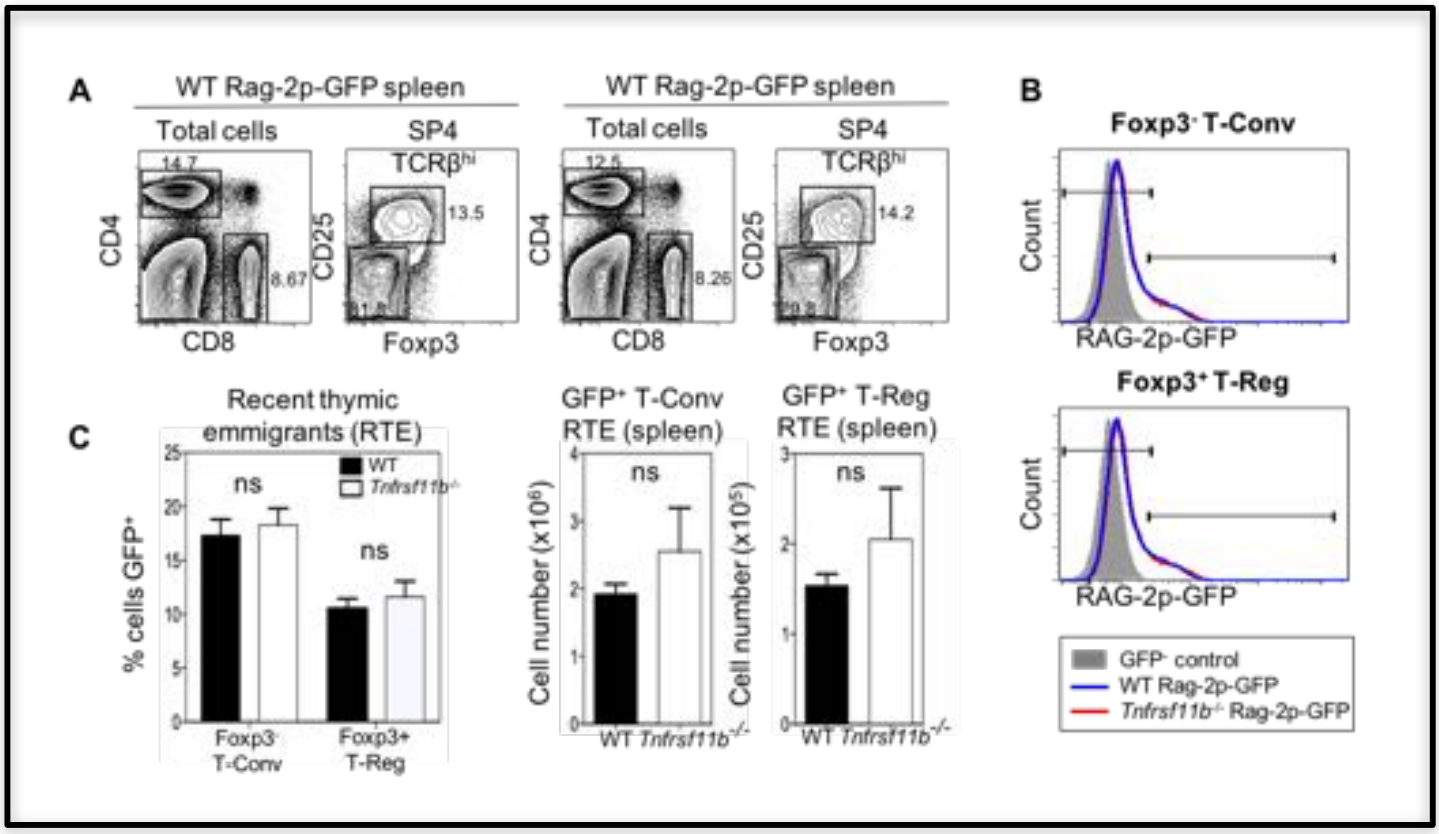
A
WT Rag-2p-GFP spleen
Total cells
SP4
CD4
CD25
CD8
Foxp3
TCRβhi
14.7
8.67
13.5
12.6
8.26
14.2
WT Rag-2p-GFP spleen
B
Foxp3- T-Conv
Count
RAG-2p-GFP
Foxp3+ T-Reg
GFP- control
WT Rag-2p-GFP
Tnfrsf11b-/- Rag-2p-GFP
C
Recent thymic emmigrants (RTE)
% cells GFP+
WT
Tnfrsf11b-/-
ns
Foxp3- T-Conv
Foxp3+ T-Reg
GFP+ T-Conv RTE (spleen)
Cell number (x10^6)
GFP+ T-Reg RTE (spleen)
Cell number (x10^5)
WT Tnfrsf11b-/-

Figure 3.20: Thymic output is unaltered by expansion of the medulla

(A) Gating strategy for the analysis of conventional CD4 ($CD25^{-}$ $Foxp3^{-}$) and T-Reg ($CD25^{+}Foxp3^{+}$) recent thymic emigrants (RTE).

(B) Histograms of Rag-2p-GFP expression among conventional and regulatory CD4 T-cell subsets in the spleen of wildtype and *Tnfrsf11b*$^{-/-}$ Rag-2p-GFP mice. Blue histograms represent wildtype Rag-2p-GFP cells, red histograms *Tnfrsf11b*$^{-/-}$ Rag-2p-GFP cells, and closed grey histograms GFP negative control mice, against which the gates were set to measure RTE.

(C) Quantification of splenic RTE.

Plots are representative of 8 wildtype Rag-2p-GFP and 5 *Tnfrsf11b*$^{-/-}$ Rag-2p-GFP mice from at least 3 independent experiments. Statistical testing was performed using unpaired student's t-tests.

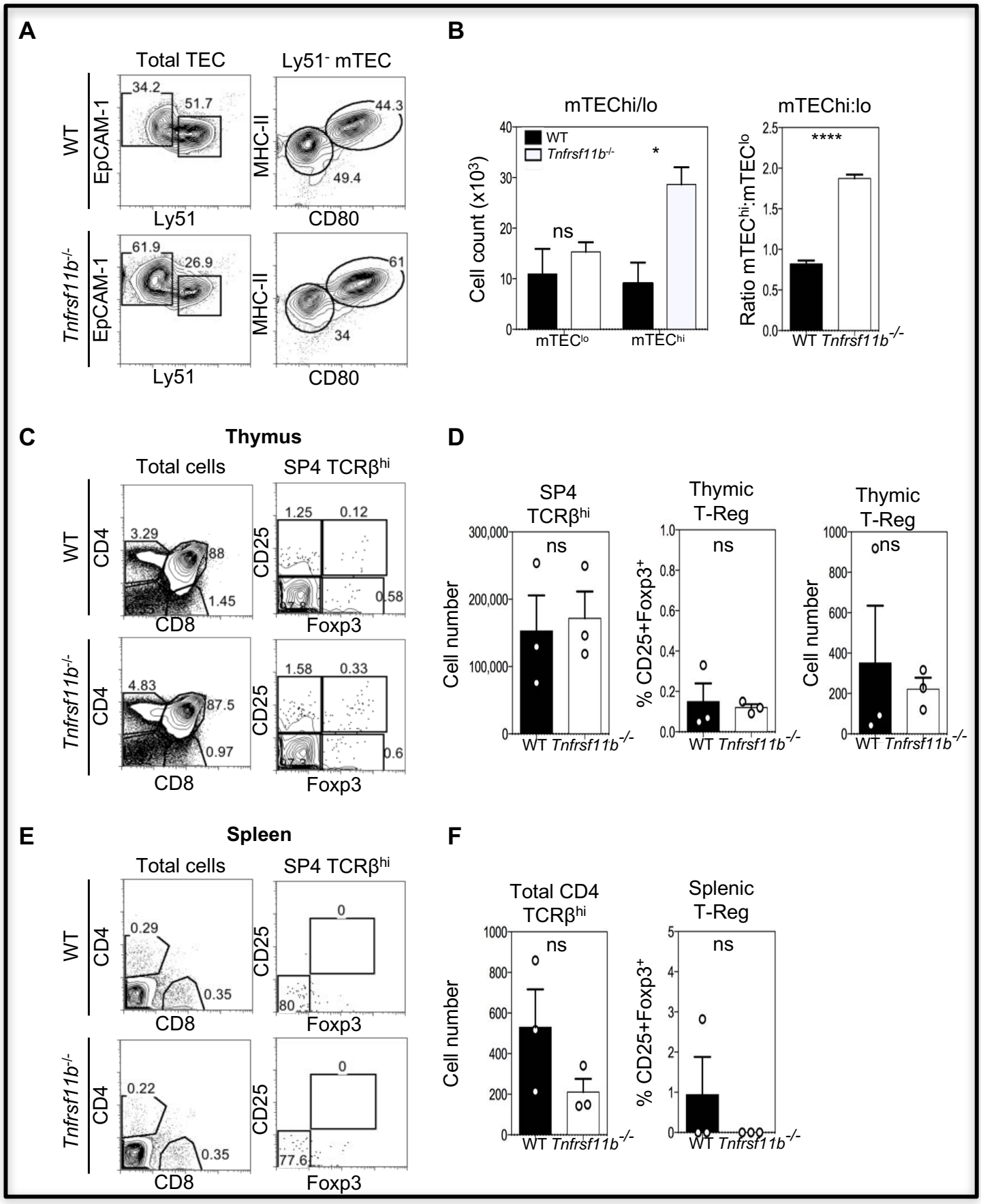
A
Total TEC
Ly51- mTEC
WT
Tnfrsf11b-/-
EpCAM-1
MHC-II
Ly51
CD80
34.2
51.7
44.3
49.4
61.9
26.9
61
34
B
mTEChi/lo
mTEChi:lo
WT
Tnfrsf11b-/-
Cell count (x10^3)
ns
*
****
mTEClo
mTEChi
Ratio mTEChi:mTEClo
WT Tnfrsf11b-/-
C
Thymus
Total cells
SP4 TCRβhi
CD4
CD8
CD25
Foxp3
3.29
88
1.45
1.25
0.12
0.58
4.83
87.5
0.97
1.58
0.33
0.6
D
SP4 TCRβhi
Thymic T-Reg
Cell number
% CD25+Foxp3+
ns
WT Tnfrsf11b-/-
E
Spleen
0.29
0.35
0.22
0
80
77.6
F
Total CD4 TCRβhi
Splenic T-Reg

Figure 3.21: Postnatal expansion of the mTEC compartment is insufficient to hasten the production and output of regulatory T-cells

(A-B) Representative FACS plots and quantitation showing thymic epithelial cells from wildtype and *Tnfrsf11b*$^{-/-}$ 2 day old newborn mice.

(C-D) T-cell development in 2 day old newborn mice, including the development of CD25+Foxp3+ regulatory T-cells.

(E-F) The makeup of peripheral T-cells in wildtype and Tnfrsf11b$^{-/-}$ 2 day old newborn mice.

Plots are representative of 3 wildtype and 3 *Tnfrsf11b*$^{-/-}$ littermates from 2 independent experiments. Statistical testing was performed using unpaired student's t-tests, where * = $p<0.05$, **** = $p<0.0001$.

Tnfrsf11b$^{-/-}$ mice to be insufficient to impact on the efficiency or volume of production of conventional or regulatory T-cells.

In addition to mTEC, the occupation of the medulla by dendritic cells and B-cells is thought to contribute to negative selection, and the selection of regulatory T-cells. However, the factors controlling the homeostasis of these populations are less well understood. Our initial analysis of lymphocyte populations in *Tnfrsf11b*$^{-/-}$ mice showed a substantial increase in the proportion and number of CD19^{+}B220^{+} B-cells in the thymus, with normal numbers present in the spleen (Figure 3.22A-D). Thymic B-cells have been shown to be a phenotypically distinct population largely derived from immature precursors within the thymus, but with minimal contribution from the recirculating B-cell pool (Perera et al., 2013). We matched the findings of Perera et al. that in Rag-2p-GFP mice, thymic B-cells up-regulate CD19 and MHC-II during maturation from the pro-B cell equivalent B220^{lo}GFP^{+} stage to the intermediate (B220^{hi}GFP^{+}) and late (B220^{hi}GFP^{-}) stages of development, as well as losing expression of CD43 (Figure 3.22E-F). Analysis of these populations in *Tnfrsf11b*$^{-/-}$ Rag-2p-GFP mice showed no alteration in the number of B220^{lo}GFP^{+} cells, but substantial increases in the proportion and number of cells at the later B220^{hi}GFP^{+} and B220^{hi}GFP^{-} stages (Figure 3.22E, G). Unlike their T-cell counterparts, peripheral B-cells are predominantly GFP^{+} in adult mice, and hence as the thymic pro-B-cell stage is unaffected by OPG-deficiency, it appears likely that the increase in both GFP$^{+/-}$ B220^{hi} B-cell subsets in *Tnfrsf11b*$^{-/-}$ mice is representative of an increase in re-circulating B-cells. Finally, we analysed the presence of thymic dendritic cells in *Tnfrsf11b*$^{-/-}$ mice. In contrast to B- and T-lymphocytes, which were uniformly Rank negative, thymic dendritic cells in

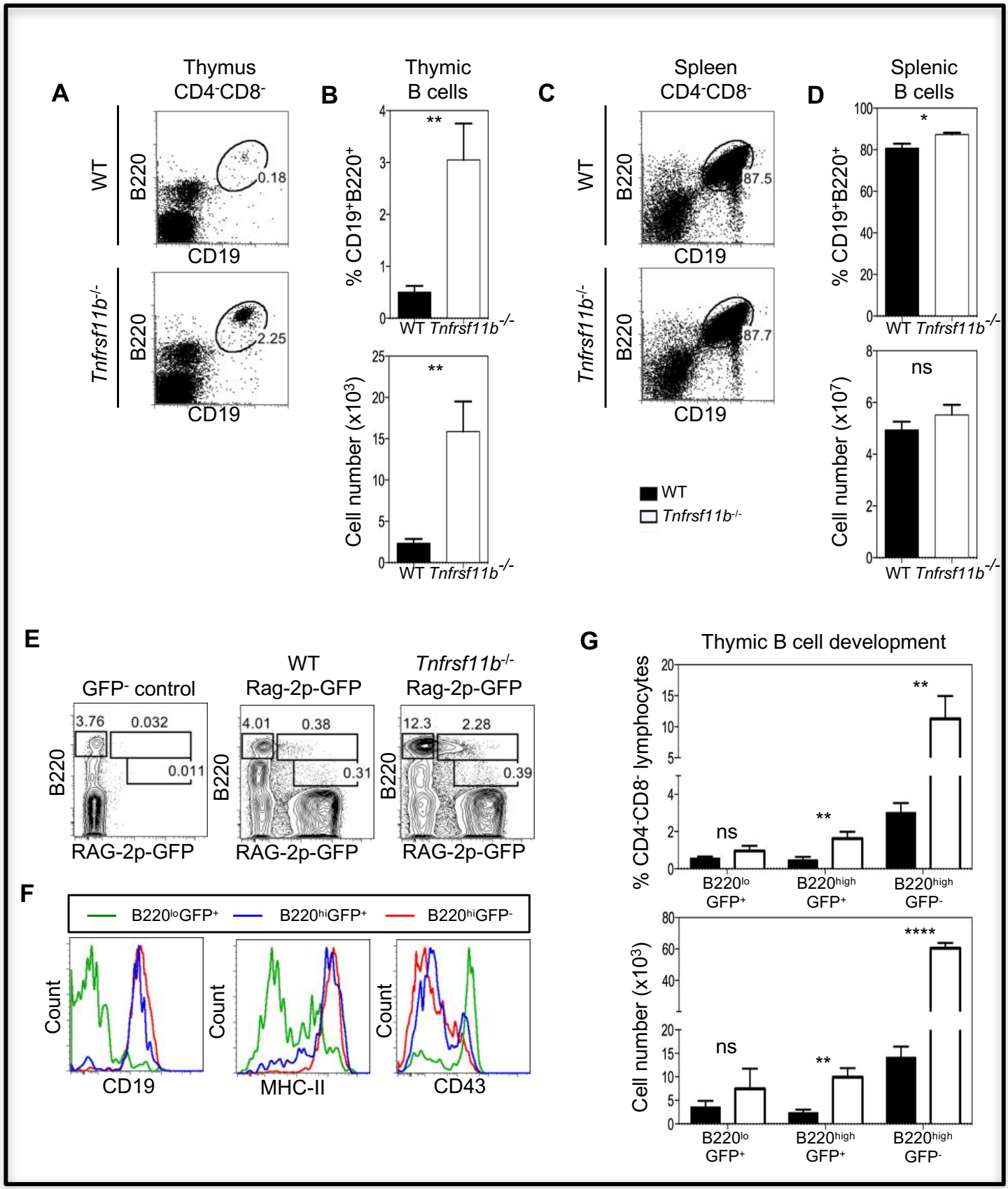
A
Thymus
CD4-CD8-
WT
B220
0.18
CD19
Tnfrsf11b-/-
B220
2.25
CD19
B
Thymic
B cells
% CD19+B220+
**
WT Tnfrsf11b-/-
Cell number (x10^3)
**
WT Tnfrsf11b-/-
C
Spleen
CD4-CD8-
WT
B220
87.5
CD19
Tnfrsf11b-/-
B220
87.7
CD19
WT
Tnfrsf11b-/-
D
Splenic
B cells
% CD19+B220+
*
WT Tnfrsf11b-/-
Cell number (x10^7)
ns
WT Tnfrsf11b-/-
E
GFP- control
WT
Rag-2p-GFP
Tnfrsf11b-/-
Rag-2p-GFP
B220
3.76
0.032
0.011
RAG-2p-GFP
B220
4.01
0.38
0.31
RAG-2p-GFP
B220
12.3
2.28
0.39
RAG-2p-GFP
F
B220loGFP+
B220hiGFP+
B220hiGFP-
Count
CD19
Count
MHC-II
Count
CD43
G
Thymic B cell development
% CD4-CD8- lymphocytes
ns
**
**
B220lo GFP+
B220high GFP+
B220high GFP-
Cell number (x10^3)
ns
**
****
B220lo GFP+
B220high GFP+
B220high GFP-

Figure 3.22: The thymic B-cell population is expanded in *Tnfrsf11b*$^{-/-}$ mice

(A-B) Analysis of B220^{+}CD19^{+} thymic B-cells and (C-D) splenic B-cells from wildtype and *Tnfrsf11b*$^{-/-}$ mice (n=7 wildtype, and 5 *Tnfrsf11b*$^{-/-}$ mice). Plots are pre-gated on CD4^{-}8^{-} lymphocytes.

(E) Gating strategy for the analysis of thymic B-cell development in wildtype and *Tnfrsf11b*$^{-/-}$ Rag-2p-GFP mice; pro-B-cells are B220^{lo}GFP^{+}, immature cells B220^{hi}GFP^{+}, mature cells B220^{hi}GFP^{-} (gates are based on staining of wildtype GFP^{-} control).

(F) Phenotyping of B-cell developmental subsets in wildtype Rag-2p-GFP mice for CD43, MHC-II and CD19, where green histograms represent pro-, blue histograms immature, and red histograms mature B-cells.

(G) Quantitation of thymic B-cell developmental subsets in wildtype and *Tnfrsf11b*$^{-/-}$ Rag-2p-GFP thymus (n=7 wildtype and 3 *Tnfrsf11b*$^{-/-}$ Rag-2p-GFP mice from 3 independent experiments).

Statistical testing was performed using unpaired student's t-tests, where * = $p<0.05$, **** = $p<0.0001$.

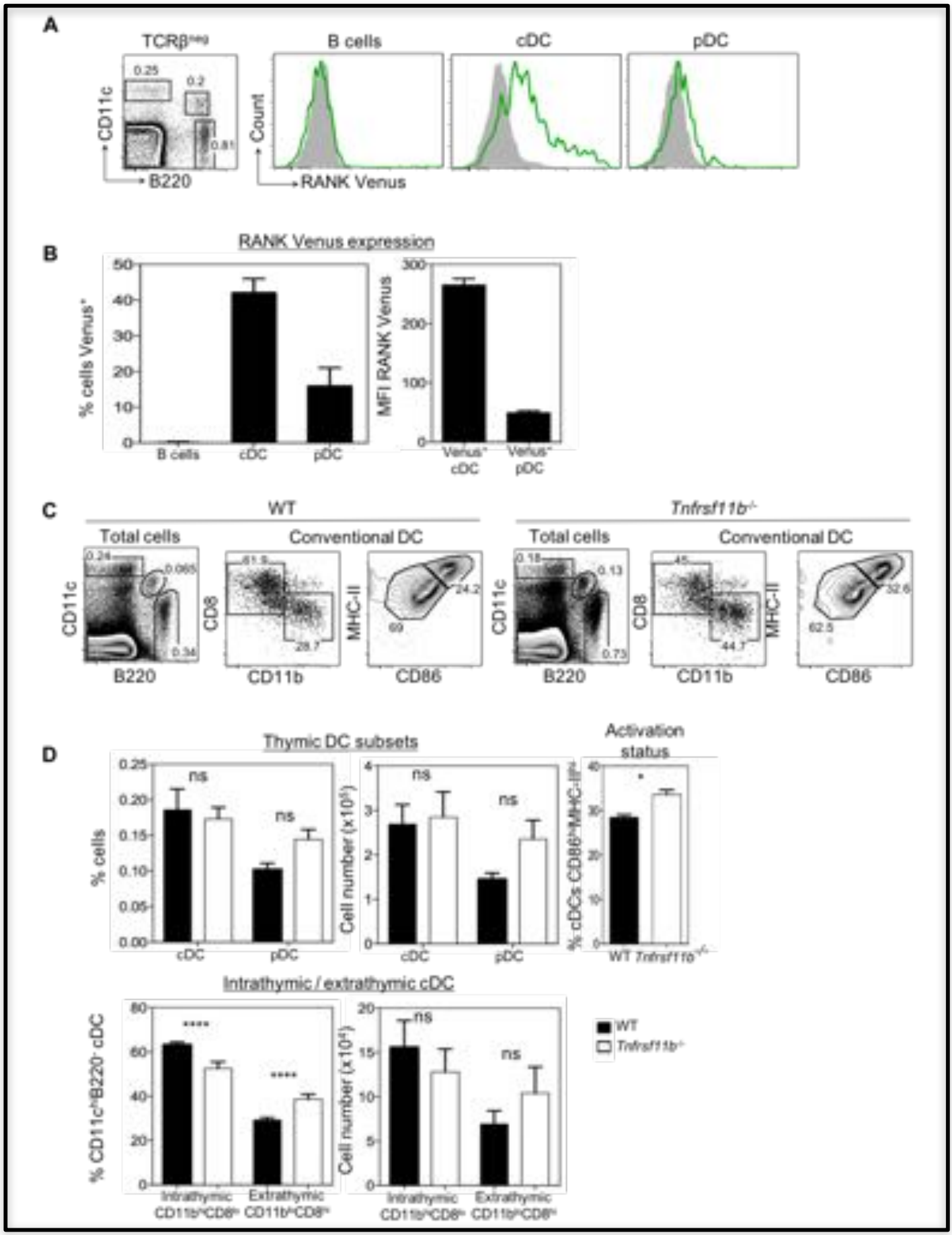
A
TCRβ neg
B cells
cDC
pDC
CD11c
B220
Count
RANK Venus
B
RANK Venus expression
% cells Venus+
MFI RANK Venus
B cells
cDC
pDC
Venus+ cDC
Venus+ pDC
C
WT
Tnfrsf11b-/-
Total cells
Conventional DC
CD11c
B220
CD8
CD11b
MHC-II
CD86
D
Thymic DC subsets
Activation status
% cells
Cell number (x10³)
% cDCs CD86hiMHC-IIhi
ns
*
WT
Tnfrsf11b-/-
Intrathymic / extrathymic cDC
% CD11chiB220- cDC
****
Intrathymic CD11bhiCD8lo
Extrathymic CD11bloCD8hi

Figure 3.23: OPG subtly impacts the makeup of the compartment of thymic dendritic cells

(A) Rank expression in thymic dendritic cell (and B-cell) subsets from Rank-Venus reporter mice (green histograms), where filled grey histogram represents a littermate control negative for the Venus transgene. B-cells are defined as $B220^{+}$, plasmocytoid DCs $B220^{+}CD11c^{+}$ and conventional DCs $B220^{-}CD11c^{+}$.

(B) Proportion of $Venus^{+}$ cells, and MFI of Venus (among $Venus^{+}$ cells only), n= 5 from 2 independent experiments.

(C-D) Analysis of thymic dendritic cell subsets from wildtype and *Tnfrsf11b*$^{-/-}$ mice. cDC subsets as defined above are further characterized based on their developmental origin and activation status. Cells were defined as of intrathymic/extrathymic origin as follows; intrathymic – $CD11b^{lo}CD8^{hi}$, extrathymic $CD11b^{hi}CD8^{lo}$ (n=7 wildtype, 7 *Tnfrsf11b*$^{-/-}$). Activated cells were defined as $CD80^{hi}$MHC-II^{hi} (n=6 wildtype, 6 *Tnfrsf11b*$^{-/-}$).

Statistical testing was performed using unpaired student's t-tests, where * = $p<0.05$, ** = $p<0.01$, **** = $p<0.0001$.

Rank Venus reporter mice were found to express the Rank receptor (Figure 3.23A). The proportion and MFI of Venus^{+} cells of the conventional DC lineage was greater than that of plasmocytoid dendritic cells, suggesting this population to be a potential target for direct regulation by OPG (Figure 3.23A-B). However, *Tnfrsf11b*$^{-/-}$ mice had no increase in total thymic numbers of the cDC or pDC populations, although the proportion of thymically-derived cDC was significantly reduced, with a slight but non-significant increase in the total numbers of extrathymic cDC (Figure 3.23C-D). Recent research within our lab (Emilie Cosway, unpublished) has shown a small subset of thymic cDC to up-regulate expression of MHC-II and B7 family members in steady state conditions. Activated cDCs were proportionally increased in *Tnfrsf11b*$^{-/-}$ thymus (Figure 3.23D, right), suggesting, although the total number of thymic dendritic cells is largely unchanged, the origin and activation status of these cells may be subtly modulated by the activity of OPG in wildtype thymus.

3.3. Discussion

Previous findings have identified crucial roles for signalling through TNFRSF members, including Ltbr (Mouri et al., 2011), Cd40 (Akiyama et al., 2008) and Rank (Rossi et al., 2007), in the homeostatic and maturational processes of medullary thymic epithelial cells. Our findings matched reports that OPG, a soluble decoy receptor capable of inhibiting Rank-RankL interactions, is constitutively expressed by a subset of mTEC that we identified as Aire^{+} mTEC^{hi}. The formation of Aire^{+}OPG^{+} mTEC^{hi} was inducible upon anti-Rank stimulation of dGuo FTOC, suggesting expression to occur intrinsically upon Rank-induced maturational events in a similar vein to that of Aire. Our analysis of *Tnfrsf11b*$^{-/-}$ TEC matched the findings of Khan et al. (2014), wherein mTEC populations were greatly expanded in the absence of OPG in a manner skewed towards mTEC^{hi}, and Aire^{+} cells, which have a known dependence on Rank signalling for their generation and maintenance. mTEC^{lo}, inclusive of the CCL21^{+} subset were again found to be expanded, albeit to a lesser extent, likely reflective of CCL21^{+} mTEC possessing distinct signalling requirements – namely, signalling through Ltbr, which we found to induce the expression of CCL21 *in vitro* at a greater efficiency than anti-Rank stimulation. However, although the total mTEC^{lo} population is known to be present in normal numbers (Desanti et al., 2012, Mouri et al., 2011), detailed phenotypic analysis of *Tnfrsf11a*$^{-/-}$ mice would be required to elucidate the degree of requirement for Rank signalling in the functional maturation of this population.

Due to the unavailability of suitable reagents, it has previously only been possible to identify Rank expression in TEC populations through PCR analysis.

Through use of a novel reporter model, we were able to identify Rank-expressing cells via flow cytometry through their expression of the fluorescent protein Venus. By this approach, we revealed great heterogeneity of expression of Rank in addition to other functional markers, including Aire, CCL21 and OPG, within the mTEC compartment. However, in adult mice we observed no difference in the proportion of $Rank^{+}$ mTEC among $mTEC^{hi}$ or $mTEC^{lo}$, suggesting restriction of expression not to be the cause of the disparity in expansion of these cell types in the *Tnfrsf11b*$^{-/-}$ thymus. However, our analysis was limited to adult mice. Indeed, we matched previous reports that the mTEC compartment is expanded from the early stages of postnatal development in the absence of OPG (Akiyama et al., 2014), at which point this effect mapped only to $mTEC^{hi}$. Hence it is possible that Rank expression predominates in $mTEC^{hi}$ in these early stages, causing preferential expansion of these cells that is not resolved in adulthood. Although not the focus of our research, previous analysis of fetal thymus from *Tnfrsf11b*$^{-/-}$ mice showed no alterations in the TEC compartment (Akiyama et al., 2014). Given the development of $RankL^{+}$ SP thymocytes is greatly enhanced post-partum (Rossi et al., 2007, Desanti et al., 2012), and expression of OPG protein was detectable from E16 it would be reasonable to suggest that the action of OPG is negligible in embryonic development as a result of the limited availability of the corresponding ligand. In addition, through their expression of high levels of MHC-II, $mTEC^{hi}$ may be in a unique position to sequester Rank-RankL interactions, as the expression of RankL is much greater on $CD4^{+}8^{-}$ MHC-II restricted cells than their $CD4^{+}8^{-}$ counterparts (Desanti et al., 2012). Interestingly, we observed no difference in the proportion of $mTEC^{hi/lo}$ undergoing proliferation or apoptosis in adult *Tnfrsf11b*$^{-/-}$ mice. As measured by

activation of caspase 3, the level of apoptosis was found to be highest among mTEC^{lo}, wherein approximately 50% of cells were dying. This proportion was likely inflated as a result of the digestion procedure for the isolation of TEC, and hence although no differences were found, we cannot rule out differences that are masked by enhanced rates of apoptosis in TEC isolates. Elucidation of the exact mechanism by which unimpeded Rank signalling triggers expansion of the mTEC compartment would hence likely require careful analysis of Rank expression throughout development, or analysis of responsiveness of *Tnfrsf11b*$^{-/-}$ mTEC to RankL in isolation.

A wealth of data exists to suggest an intrinsic link between mTEC and the development of T-Reg within the medulla (Leavy, 2013). This process is known to depend on the unique capacity for mTEC to express TSAs (Lei et al., 2011, Takaba et al., 2015) and co-stimulatory molecules (Mahmud et al., 2014) that provide distinct signals for induction of Foxp3 expression among SP4 thymocytes. In addition to the complete abrogation of T-Reg development in mTEC-deficient thymuses (Cowan et al., 2013), reduced numbers of T-Reg are observed in the thymus of mice lacking expression of the full repertoire of TSAs, as triggered through deficiency of the transcription factors Aire (Lei et al., 2011) and Fezf2 (Takaba et al., 2015). This finding is explainable by the requirement for high-affinity TCR-ligation for the formation of CD25^{+} T-Reg precursors, as determined by analysis of Nur-77 reporter mice (Moran et al., 2011). A recent study involved the treatment of mice with blocking anti-RankL antibodies to trigger the transient ablation of mTEC (Khan et al., 2014). Reduction in the size of the mTEC compartment was sufficient to limit thymic T-Reg generation, and allow for the escape of auto-reactive T-cells from negative selection, resulting in

enhancement of anti-tumor immunity and tumor clearance (Khan et al., 2014). Given these findings, the mechanisms underlying mTEC homeostasis are an attractive proposition for therapies aiming to alter the balance of production of pro- and anti-inflammatory T-cells, with the aim of boosting immune responses against malignancies and infections, or instead controlling autoimmunity. For this reason, the *Tnfrsf11b*$^{-/-}$ model provided a useful opportunity to assess the viability of enhancing the generation of T-Reg via expansion of the mTEC pool.

Three previous publications have attempted to address this issue using models in which mTEC are expanded through the deletion of mTEC regulatory elements, including TGFβ receptor 2 (Hauri-Hohl et al., 2014), or OPG itself (Akiyama et al., 2014, Lin et al., 2016). In both models, artificially increasing the size of the mTEC compartment was shown to result in an increase in the number of thymic T-Reg. By grafting wildtype or *Tnfrsf11b*$^{-/-}$ fetal thymus into tumor-recipient mice, Akiyama et al. (2014) mapped the apparent increase in T-Reg production to poorer anti-tumor responses. In common with these studies, we found Foxp3^{+} T-Reg to be expanded in number in the thymus in the presence of an expanded mTEC pool – although the number of peripheral T-Reg was unaltered in *Tnfrsf11b*$^{-/-}$ mice. However, the development of the Rag-2p-GFP reporter model, in which newly produced T-cells (GFP^{+}) can be distinguished from older mature populations (GFP^{-}) through their GFP status, has facilitated the surprising finding that thymic T-Reg are a heterogeneous population, consisting of a substantial fraction of GFP^{-} cells (Cuss and Green, 2012). In addition, a recent publication by Cowan et al. (Cowan et al., 2016) has revealed contamination of the Foxp3^{+} and CD25^{+} T-Reg precursor subsets by memory-phenotype peripheral T-cells. These points were not factored into the analyses of

the previous publications; however, by crossing *Tnfrsf11b*$^{-/-}$ mice to the Rag-2p-GFP background, we were able to identify bona fide newly produced populations of Foxp3^{+} T-Reg, in addition to the CD25^{+} and Foxp3^{+} precursor populations previously described. In this model, we saw no detectable increase in the thymic production of regulatory T-cells, as read by the presence of GFP^{+} T-Reg, and GFP^{+} precursors. Instead, an increase in the number of GFP^{-} thymocytes, the majority of which are though to represent thymic re-circulants in wildtype mice, was observed. The expanded GFP^{-} fraction within the *Tnfrsf11b*$^{-/-}$ thymus consisted of both T-Reg and conventional CD4s, including cells that would otherwise have been included among T-Reg precursor populations. This phenotype largely mirrors that of *Ccr7*$^{-/-}$ mice, wherein memory-phenotype peripheral T-cells are known to become mis-localised to the medulla as a result of their incapacity to undergo CCL19/21-mediated chemotaxis to the secondary lymphoid organs (Cowan et al., 2016). As we could report no defects in the make-up of splenic or lymph node CD4 T-cells, it appears likely that the increase in re-circulating T-cells within the thymus of *Tnfrsf11b*$^{-/-}$ mice is as a direct result of the increase in the size of the mTEC niche. An array of chemokine receptor ligands are known to be expressed by mTEC in a manner controlled through the expression of Aire (Laan et al., 2009), Rank (Hikosaka et al., 2008) and Ltbr (Zhu et al., 2007). However, further analysis would be required to determine whether alterations in the medullary expression of CCR ligands impacts on the recruitment of peripheral T-cells to the thymus in this model.

Although not shown, our preliminary attempts to measure recirculation of peripheral T-cells through the grafting of congenically marked fetal thymus into *Tnfrsf11b*$^{-/-}$ mice yielded no obvious difference from the levels of

recirculation to the wildtype thymus (not shown). However, it remains possible that after homing back to the medulla, peripheral T-cells reside there long term, and hence the larger niche of the OPG-deficient thymus is largely occupied from earlier stages in development. Similarly, parabiosis experiments have shown the contribution of peripheral B-cells to the thymic B-cell pool to be minimal in adult mice (Perera et al., 2013). That this population is grossly inflated in *Tnfrsf11b*$^{-/-}$ thymus, without any effect on the B220^{lo}GFP^{lo} precursor population from which they develop, would suggest the increase in their presence to arise either through recruitment or proliferation rather than an increase in their development intrathymically. Although not attempted for thymic B-cells, Ki67 staining in T-Reg determined the increased presence of Foxp3^{+} cells not to be the result of proliferation of this population intrathymically. Accumulation of thymic T-Reg in OPG-deficient thymi has previously been detected at post-natal day 18, but not in the first week post-partum, and hence the origin of GFP^{-} thymic T-Reg and B-cell populations in *Tnfrsf11b*$^{-/-}$ mice may be better addressed by looking at an earlier time-point in the mouse's development, prior to the niche for recirculating cells being filled. Recently developed reporter models allow for the permanent expression of GFP in a small cohort of DP thymocytes (Zhang, Venice Thymus Conference asbtract, 2015), which can then be traced. Unlike surgical grafting, this approach would be suitable to track GFP^{+} cells re-entering the thymus at a timepoint as early as PN18. In spite of the large accumulation of GFP^{-} T-Reg, we observed no increase in the number of newly produced GFP^{+} cells intrathymically. Consistent with this finding, GFP^{+} T-Reg precursors were present in normal numbers (in fact, CD25^{+} precursors were marginally reduced), and the number of splenic T-Reg RTE was unaltered, suggesting T-Reg

development to occur normally in light of the increase in the size of their selective niche.

4. RESULTS CHAPTER 2:
THE ROLE OF INDUCIBLE NITRIC OXIDE SYNTHASE IN THE THYMIC MEDULLA

4.1 Introduction

A second gene of interest found to be specifically expressed by mTEC^{hi} among our microarray subsets was *Nos2*. The product of the *Nos2* gene is inducible nitric oxide synthase (iNOS), one of a family of three enzymes capable of catalysing the production of the free radical nitric oxide (NO) from L-arginine (Moncada et al., 1989), and an important regulator of inflammation and immunity (Bogdan, 2001, Bogdan, 2015). Nitric oxide synthase has 3 isoforms; 2 largely constitutively expressed in specific tissues - neuronal (nNOS, *Nos1*) (Bredt et al., 1990) and endothelial (eNOS, *Nos3*) (Huang et al., 1995) – as well as iNOS, which is commonly inducible in immune cells in response to inflammatory stimuli (Xie et al., 1992). The effects on nitric oxide on cells are varied, and heavily context dependent. Rather than acting as a receptor ligand, NO mediates its effects through the direct nitrosylation of amino acid tyrosine residues, allowing for modulation of the function of multiple protein targets (Stamler et al., 1992). As these can include transcription factors (Jianjun et al., 2013, D'Autreaux et al., 2005) and cell signalling intermediates (Bredt and Snyder, 1989, Paolucci et al., 2003, Serafini et al., 2006), the effects of NO on a given cell type can be complex. Equally, NO is capable of crossing channels in plasma membranes (Figueroa et al., 2013), and hence in many circumstances potential targets extend to intracellular and extracellular proteins of both iNOS^{+} cells and their neighbours. Furthermore, the effects of NO are highly dose-dependent, and NO

diffuses readily, which is estimated to result in up to 1000-fold differences in concentrations across the length of a single cell (10uM) (Lancaster, 1994).

Through the production of nitric oxide, iNOS has hence been shown to control T-cell responses through multiple mechanisms. iNOS expression is inducible in lymph node fibroblastic reticular cells (FRC) on stimulation with the inflammatory cytokines IFNγ and TNFα, in which instance nitric oxide powerfully suppresses T-cell proliferation (Lukacs-Kornek et al., 2011, Siegert et al., 2011). Similarly, myeloid derived suppressor cells (MDSCs) have been described to suppress T-cell proliferation through iNOS-mediated depletion of arginine (De Santo et al., 2005), and induce apoptosis via transmission of nitric oxide when cell contacts are formed (Talmadge, 2007). In this instance, iNOS also acts as a key signalling intermediate for the accumulation of cyclic GMP, leading to activation of MDSCs, facilitating their suppressive interaction with T-cells (Serafini et al., 2006). iNOS has also been shown to mediate the phenotypic maturation of LPS-stimulated dendritic cells, and is required for the surface presentation of MHC-II molecules (Wong et al., 2004). Upon strong TCR triggering *in vitro*, CD4 T-cells have also been shown to express iNOS (Jianjun et al., 2013). In this instance, iNOS has been suggested to limit the formation of IL-17-producing Th17 cells by nitrosylating the lineage-defining transcription factor RORγt (Jianjun et al., 2013). Although T-cell derived iNOS has been reported to have little impact on the induction of $Foxp3^+$ T-Reg *in vitro* (Jianjun et al., 2013), the addition of exogenous nitric oxide donors limits the TGFβ-induced formation of T-Reg, and skews T-cells towards the Th1 lineage (Lee et al., 2011).

In addition to the regulation of proliferation and lineage commitment of T-cells, nitric oxide is known to play important roles in inducing nitrosative stress and cell death in immunity, and contributes heavily to the clearance of bacteria by activated macrophages and dendritic cells (Wei et al., 1995), as well as tissue and organ damage in autoimmune diseases. Hence, in mouse models of inflammatory diseases, iNOS has been shown to play protective roles, such as in experimental arthritis models (McCartney-Francis et al., 1993), as well as contributing to pathogenesis, as is the case in some models of toxic shock (MacMicking et al., 1995). The constitutive expression of iNOS in the thymus was first noted in mice (Tai et al., 1997), but iNOS$^+$ cells were subsequently identified in rats as MHC-II$^+$ stromal cell populations by crude cell adherence assays (Aiello et al., 2000). The addition of the nitric oxide donor SNAP to cultures of mouse thymocytes potently induces apoptosis of DP cells (Fehsel et al., 1995, Tai et al., 1997), and hence initially iNOS was suggested to play a role in negative selection of cells in the thymic cortex. In addition, iNOS was shown to be inducible in TEC cells lines when cultured with anti-CD3-activated thymocytes, and contributed to TEC-induced apoptosis in a manner seemingly dependent on interferon-γ (Tai et al., 1997, Cohen et al., 2009). Contrastingly, the constitutive expression of iNOS has been linked to pro-survival mechanisms in secretory cell types. In plasma cells, iNOS regulates the unfolded protein response (UPR) – a feedback loop whereby sensors of endoplasmic reticulum stress in the form of accumulating misfolded proteins act to induce the expression of UPR-related genes involved in clearance of misfolded proteins, and hence maintenance of cellular homeostasis (Saini et al., 2014). The transcription factor Xbp1s lies downstream of ER stress sensors, and directly induces expression of UPR regulated genes (Cao and

Kaufman, 2012). *Nos2*$^{-/-}$ plasma cells have a reduction in Xbp1s expression, and hence fail to overcome ER stress, triggering premature apoptosis (Saini et al., 2014) – iNOS hence acts as a major intermediate in the pathways regulating homeostasis in response to ER stress. Constitutive expression of iNOS has also been noted in other secretory cell types associated with tonic UPR activation, including colonic (Perner et al., 2002) and bronchial epithelia (Felley-Bosco et al., 1994).

Given the many important roles played by iNOS in regulating the proliferative, apoptotic and homeostatic responses of immune cells in secondary lymphoid tissues, the aim of this chapter was to characterise the expression of iNOS under steady state conditions in the thymus. Using iNOS-deficient *Nos2*$^{-/-}$ mice, we attempted to assess the requirements for iNOS expression in medullary homeostasis, both in terms of the make-up of antigen presenting cell subsets, and the production of conventional and unconventional T-cell subsets.

4.2. Results

4.2.1. Constitutive expression of inducible nitric oxide synthase defines a subset of mTEC

As previous papers have also reported constitutive expression of iNOS in the antigen presenting cells of the thymus (Aiello et al., 2000), we first set out to characterize iNOS^{+} thymic APC. Confocal analysis of iNOS expression revealed that like Aire, iNOS-expressing cells were present in the medulla among the ER-TR5^{+} mTEC population, but could not be found in the thymic cortex, where no positive staining was observed (Figure 4.1). Next, we used flow cytometry to further define the expression of iNOS in medullary cell populations. Intracellular staining for iNOS in cells isolated from wildtype and *Nos2*$^{-/-}$ thymus revealed no detectable levels of expression in haematopoietic subsets, including T-cells, B-cells, cDC and pDC (Figure 4.2A, D). Similarly, non-epithelial stromal populations, which have been demonstrated to express iNOS in inflammatory conditions in the periphery, were iNOS^{-} (Figure 4.2B, D). However, very strong positive staining was detected in ~25% of thymic epithelium (Figure 4.2B). Further characterization revealed iNOS expression to be restricted to the mTEC^{hi} subset, as cTEC and mTEC^{lo} cells were uniformly iNOS negative (Figure 4.2C, D). Expression of iNOS was detectable from the emergence of mTEC^{hi} at E16 (Figure 4.3A), and iNOS^{+} cells increased as a proportion of mTEC^{hi} at P2, and the adult stages of development (Figure 4.3A-B). iNOS expression by fibroblastic reticular cells requires inflammatory cytokine signalling (Lukacs-Kornek et al., 2011). To determine whether iNOS^{+} mTEC have similar signalling requirements, we stained for iNOS in mTEC^{hi} isolated from mice deficient for TNF receptors 1 and

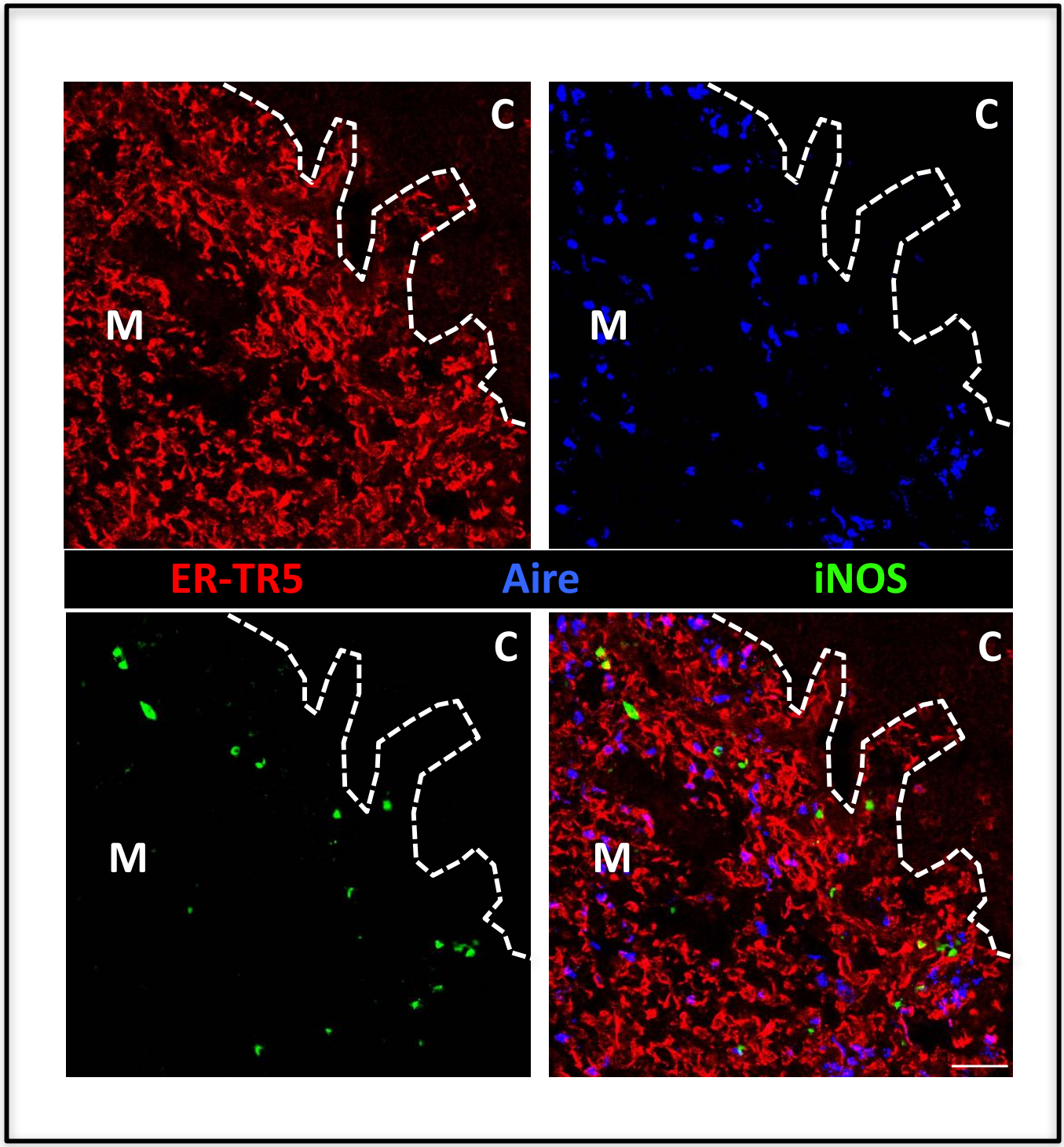
C
M
C
M
ER-TR5
Aire
iNOS
C
M
C
M

Figure 4.1: iNOS-expressing TEC are distributed throughout the medulla

Confocal staining of adult thymus sections showing restriction of expression of iNOS and Aire to the medulla (M), as defined by the mTEC marker ER-TR5. No positive staining for iNOS or Aire was observed in ER-TR5$^-$ cortical (C) areas. Scale bar = 40uM.

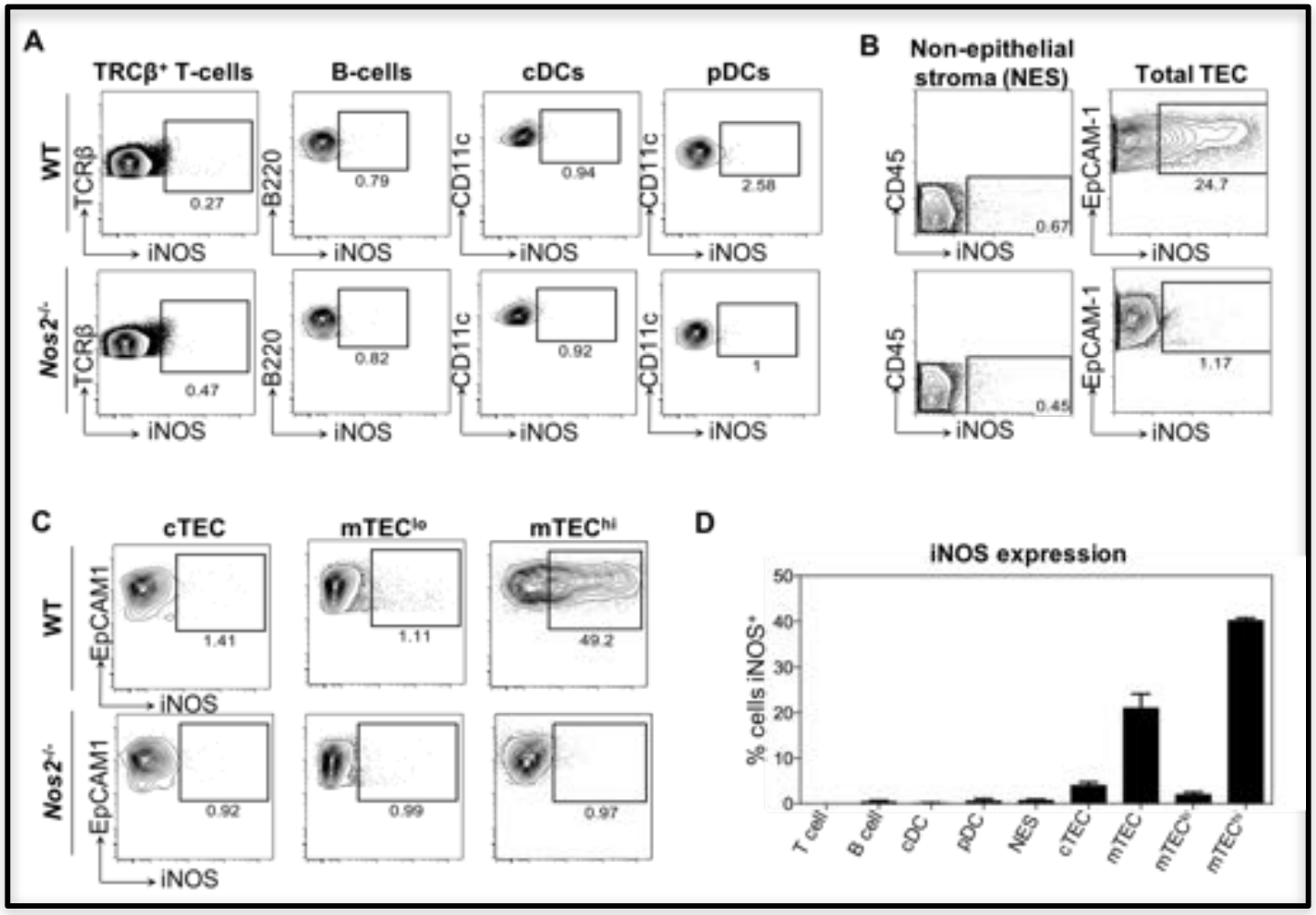
A
TRCβ⁺ T-cells
B-cells
cDCs
pDCs
WT
Nos2-/-
TCRβ
B220
CD11c
iNOS
0.27
0.79
0.94
2.58
0.47
0.82
0.92
1
B
Non-epithelial stroma (NES)
Total TEC
CD45
EpCAM-1
0.67
24.7
0.45
1.17
C
cTEC
mTEClo
mTEChi
EpCAM1
1.41
1.11
49.2
0.92
0.99
0.97
D
iNOS expression
% cells iNOS+
50
40
30
20
10
0
T cell
B cell
cDC
pDC
NES
cTEC
mTEC
mTEClo
mTEChi

Figure 4.2: Thymic inducible nitric oxide expression is restricted to the TEC compartment

(A) FACS data gated as in figure 3.2 showing intracellular staining for iNOS in T- and B-lymphocytes, conventional and plasmocytoid dendritic cells, and (B) non-epithelial stroma and TEC. Positive staining is determined as staining levels over those in the equivalent population isolated from *Nos2*$^{-/-}$ mice (bottom row).

(C) Representative FACS plots showing iNOS expression in cTEC, mTEC^{lo} and mTEC^{hi} populations.

(D) The proportion of iNOS^{+} cells in the populations identified in A-C. Data are representative of n=3 mice (n=6 in the instance of TEC populations), from a minimum of 2 independent experiments.

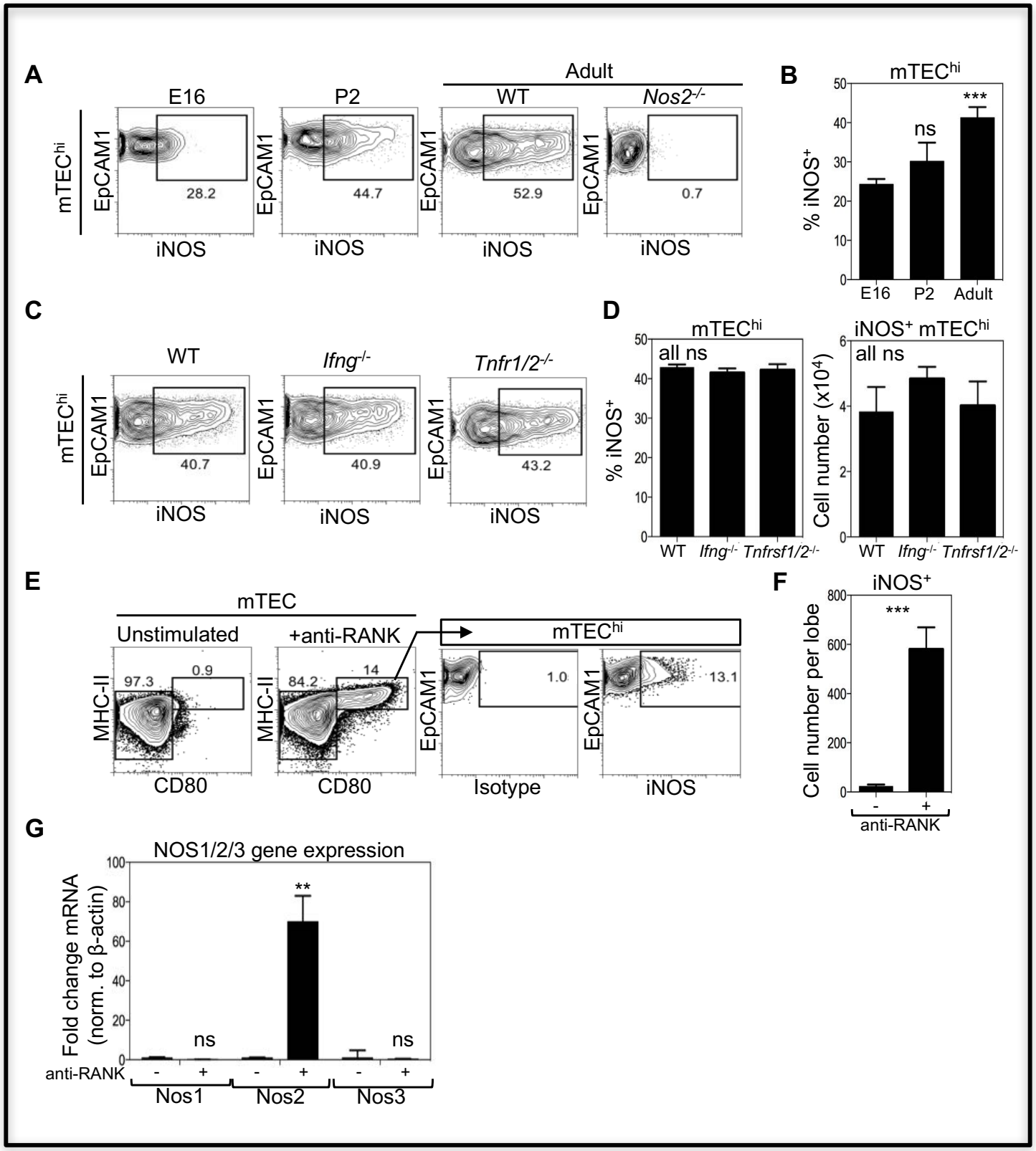
A
E16
P2
Adult
WT
Nos2-/-
mTEChi
EpCAM1
iNOS
28.2
44.7
52.9
0.7
B
mTEChi
% iNOS+
ns
***
E16
P2
Adult
C
WT
Ifng-/-
Tnfr1/2-/-
40.7
40.9
43.2
D
mTEChi
iNOS+ mTEChi
% iNOS+
Cell number (x10^4)
all ns
WT
Ifng-/-
Tnfrsf1/2-/-
E
mTEC
Unstimulated
+anti-RANK
mTEChi
MHC-II
CD80
97.3
0.9
84.2
14
Isotype
1.0
13.1
F
iNOS+
Cell number per lobe
anti-RANK
G
NOS1/2/3 gene expression
Fold change mRNA (norm. to β-actin)
**
Nos1
Nos2
Nos3

Figure 4.3: iNOS expression requires Rank signaling, and occurs independently of inflammatory stimuli

(A) FACS plots and (B) quantitation of iNOS+ cells as a proportion of mTEChi throughout during murine development, including the embryonic day 16 (E16), post-natal day 2 (P2) and the adult stage (8-12 weeks).

(C) Flow cytometric analysis of iNOS expression in $mTEC^{hi}$ from wildtype (n=6), *Ifng*$^{-/-}$ (n=4) and *Tnfr1/2*$^{-/-}$ (n=3) mice.

(D) Proportion and number of $iNOS^{+}$ $mTEC^{hi}$ in mice deficient for signaling by inflammatory cytokines.

(E-F) Induction of iNOS expression through 7 day anti-Rank stimulation of dGuo-treated fetal thymic organ cultures.

(G) Gene expression analysis of anti-Rank stimulated dGuo FTOC, showing expression of nitric oxide synthase isoforms Nos1, Nos2 and Nos3 with and without anti-Rank treatment.

Statistics were obtained using unpaired students t-tests, where *=$p<0.05$ and ****=$p<0.0001$.

2, or IFNγ. However, normal proportions and numbers of iNOS^{+} mTEC^{hi} were present in both *Tnfr1/2*$^{-/-}$ and *Ifng*$^{-/-}$ strains (Figure 4.3C-D). Next, we attempted to address the question whether, like Aire and OPG, iNOS was inducible by Rank signalling. dGuo treated FTOC lobes were stimulated for 7 days with stimulatory anti-Rank antibody, and stained intracellularly for iNOS. Anti-Rank treatment was sufficient to induce the formation of mTEC^{hi}, including a fraction of iNOS^{+} cells, which were not detected in unstimulated lobes (Figure 4.3E-F). This effect appeared specific to iNOS, as *Nos2* mRNA was increased 60-fold upon stimulation, whereas expression of the *Nos1* and *Nos3* isoforms was almost undetectable, and unaltered by the addition of anti-Rank (Figure 4.3G). This data would suggest iNOS expression to be induced in mTEC^{hi} by Rank signalling in the same manner as Aire and OPG. Stimulation of FTOC lobes with anti-Ltbr failed to induce iNOS^{+} mTEC, and anti-Ltbr in combination with anti-Rank had no additive effect in increasing iNOS induction (Figure 4.4A-B). Similarly, although reported to have a reduced number of mTEC^{hi}, *Ltbr*$^{-/-}$ mice had no reduction in the proportion of mTEC^{hi} expressing iNOS (although we did match previous findings (Lkhagvasuren et al., 2013) of a defect in CCL21 expression by mTEC^{lo} (Figure 4.4C-D)). Next, we analysed mTEC^{hi} from Rank-Venus reporter mice for expression of iNOS. Rank expression was apparent in ~50% of iNOS^{+} cells, and a similar proportion of iNOS^{-} cells (Figure 4.4E-F), suggesting that although iNOS and Rank expression do not fully overlap, a proportion of iNOS^{+} cells are direct targets for Rank signalling. These findings suggest signalling via the Rank receptor, but not Ltbr or inflammatory cytokine receptors, to be important for the induction of iNOS expression by mTEC.

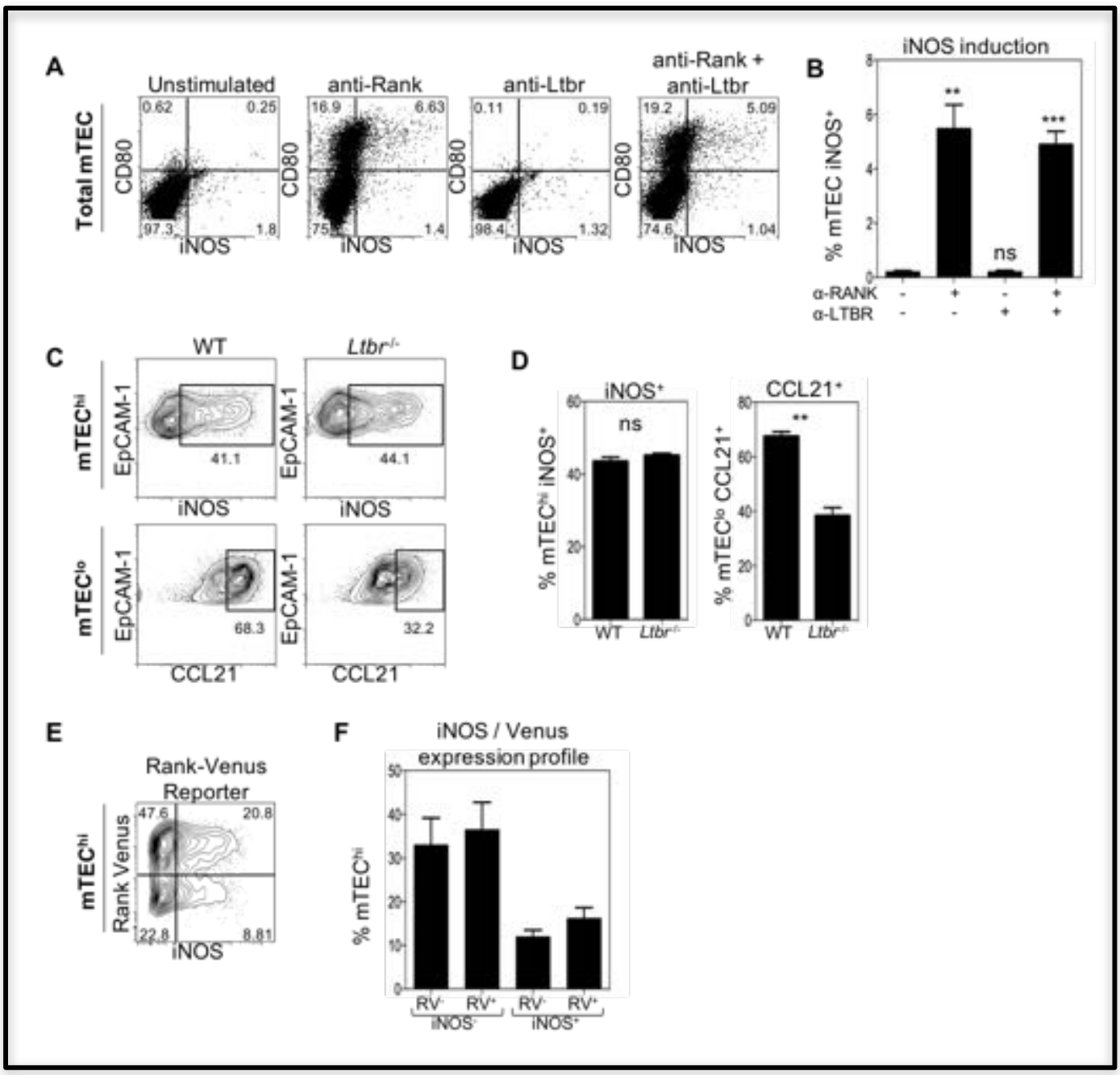
A
Unstimulated
anti-Rank
anti-Ltbr
anti-Rank + anti-Ltbr
Total mTEC
CD80
iNOS
0.62
0.25
97.3
1.8
16.9
6.63
75
1.4
0.11
0.19
98.4
1.32
19.2
5.09
74.6
1.04
B
iNOS induction
% mTEC iNOS+
**
***
ns
α-RANK
α-LTBR
C
WT
Ltbr-/-
mTEChi
mTEClo
EpCAM-1
iNOS
CCL21
41.1
44.1
68.3
32.2
D
iNOS+
CCL21+
% mTEChi iNOS+
% mTEClo CCL21+
ns
**
WT
Ltbr-/-
E
Rank-Venus Reporter
mTEChi
Rank Venus
iNOS
47.6
20.8
22.8
8.81
F
iNOS / Venus expression profile
% mTEChi
RV-
RV+
iNOS-
iNOS+

Figure 4.4: iNOS expression is controlled by Rank, but not Ltbr

(A) Representative FACS plots and (B) quantitation of iNOS induction in $CD80^+$ mTEC upon treatment of dGuo treated FTOC lobes with anti-Rank and/or anti-Ltbr for 7 days.

(C-D) Analysis of expression of iNOS and CCL21 in mTEC isolated from wildtype and *Ltbr*$^{-/-}$ mice (n=3 wildtype, and 3 *Ltbr*$^{-/-}$ mice).

(D-F) Expression pattern of Rank and iNOS as determined through intracellular staining for iNOS in TEC isolated from Rank-Venus reporter mice (n=3).

All data are representative of at least 2 independent experiments. Statistics were obtained using unpaired students t-tests, where **=$p<0.01$ and ***=$p<0.001$.

Lastly we sought to determine whether Aire and iNOS are co-expressed by mTEC. Co-staining of iNOS and Aire in mTEC^{hi} revealed the majority of iNOS^{+} cells to co-express Aire in the earliest stages of development at E16 (Figure 4.5A-B). However, from the postnatal to the adult stages an iNOS^{+}Aire^{-} subset emerges, meaning there are four distinct subsets of mTEC^{hi} according to expression of Aire and iNOS; Aire^{+}iNOS$^{+/-}$ and Aire^{-}iNOS$^{+/-}$, each of which increase in size throughout development (Figure 4.5A-B). The presence of Aire^{+}iNOS^{+} mTEC was also confirmed through confocal analysis (Figure 5E, arrow). As Aire and iNOS are both inducible by Rank stimulation, we repeated Aire and iNOS co-staining in anti-Rank stimulated dGuo FTOC (Figure 4.5C-D). The expression profile of Aire and iNOS in culture mirrored that of the embryo, where the majority of iNOS^{+} cells were Aire co-expressers (Figure 4.5C-D). Although the proportion of iNOS^{+} cells increased over the duration of anti-Rank stimulation, an iNOS^{+}Aire^{-} subset failed to emerge, possibly suggesting this to represent a population emerging late in the development of mTEC^{hi}, or possessive of unique signalling requirements.

4.2.2. The impact of iNOS on medullary homeostasis

Having mapped the constitutive expression of iNOS specifically to the mTEC^{hi} subset, we next attempted to determine the role of iNOS in the medulla. Confocal analysis revealed the architecture of *Nos2*$^{-/-}$ mice to be overtly normal, with distinct separation of cortical and medullary areas (Figure 4.6). Next we assessed the makeup of the mTEC compartment directly using functional markers. The total numbers of mTEC, including mTEC^{hi} and mTEC^{lo} were

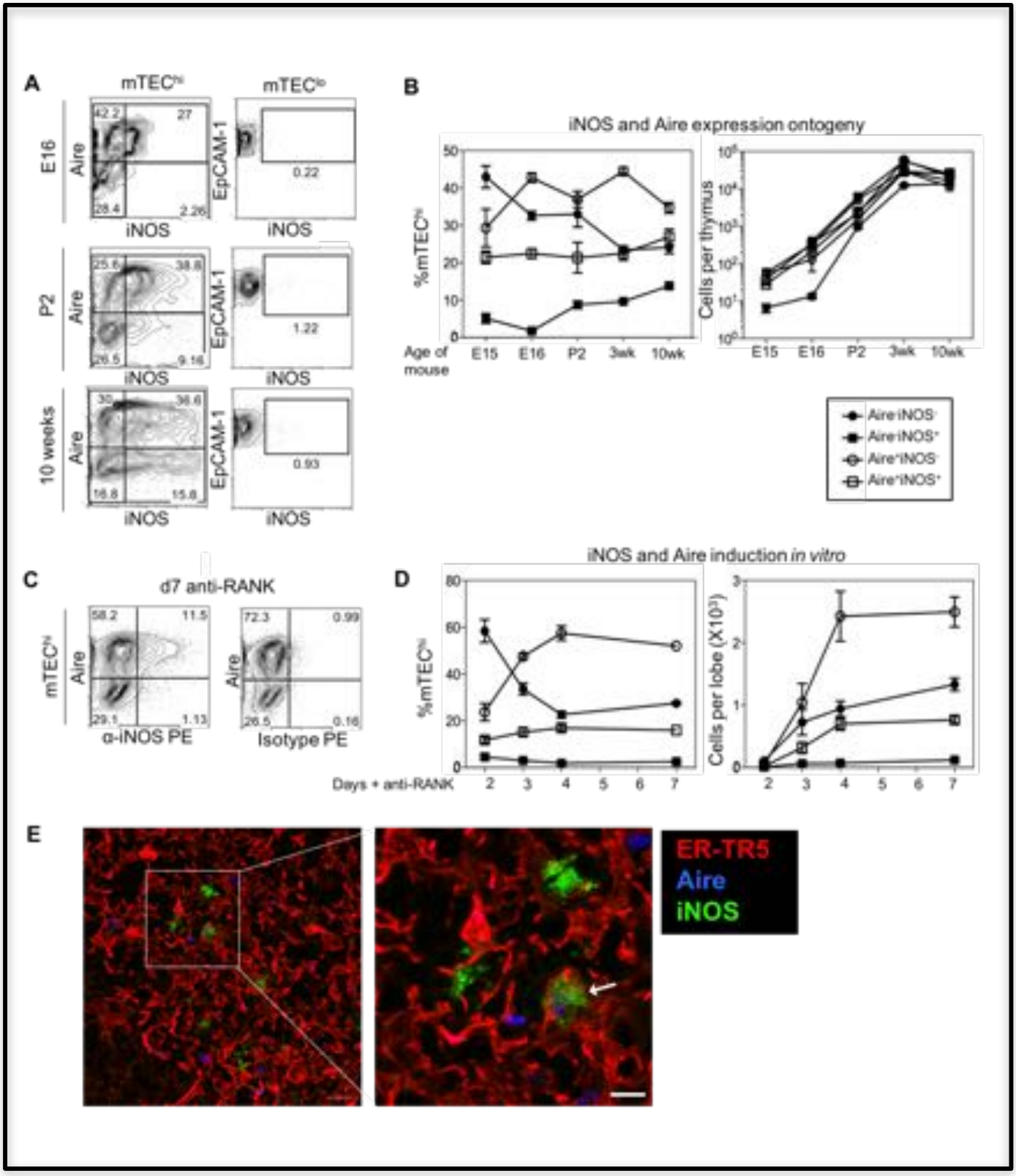
A
mTEC^hi
mTEC^lo
E16
P2
10 weeks
Aire
iNOS
EpCAM-1
42.2
27
28.4
2.26
0.22
25.6
38.8
26.5
9.16
1.22
30
36.6
16.8
15.8
0.93
B
iNOS and Aire expression ontogeny
%mTEC^hi
Cells per thymus
Age of mouse
E15
E16
P2
3wk
10wk
Aire-iNOS-
Aire-iNOS+
Aire+iNOS-
Aire+iNOS+
C
d7 anti-RANK
mTEC^hi
58.2
11.5
29.1
1.13
72.3
0.99
26.5
0.16
α-iNOS PE
Isotype PE
D
iNOS and Aire induction in vitro
%mTEC^hi
Cells per lobe (X10^3)
Days + anti-RANK
E
ER-TR5
Aire
iNOS

Figure 4.5: iNOS$^+$ mTEC are largely Aire$^+$ cells

(A) Flow cytometric analysis of TEC co-stained intracellularly for iNOS and the transcription factor Aire at the E16, P2 and adult (10 week) stages of development. Expression of Aire and iNOS is restricted to the mTEC^{hi} compartment, where both markers partially overlap in their expression patterns.

(B) Quantitation of Aire$^+$iNOS$^{+/-}$ and Aire$^-$iNOS$^{+/-}$ mTEC^{hi} subsets throughout development in terms of the proportion, and absolute number (note log scale) of cells. Each timepoint represents at least 3 mice, from at least 2 independent experiments.

(C-D) Timecourse analysis of Aire and iNOS co-expression in anti-Rank stimulated dGuo FTOC lobes, where FACS plots (C) represent mTEC^{hi} after 7 days of anti-Rank stimulation, and (D) quantification of the proportion of Aire$^+$iNOS$^{+/-}$ and Aire$^-$iNOS$^{+/-}$ mTEC^{hi} are 3 replicates obtained from at least 2 independent experiments.

(E) Confocal analysis showing the co-expression of Aire (blue) and iNOS (green) in mTEC (ER-TR5$^+$, red) in wildtype thymus sections; arrow shows an Aire$^+$iNOS$^+$ mTEC. Scale bar = 10uM.

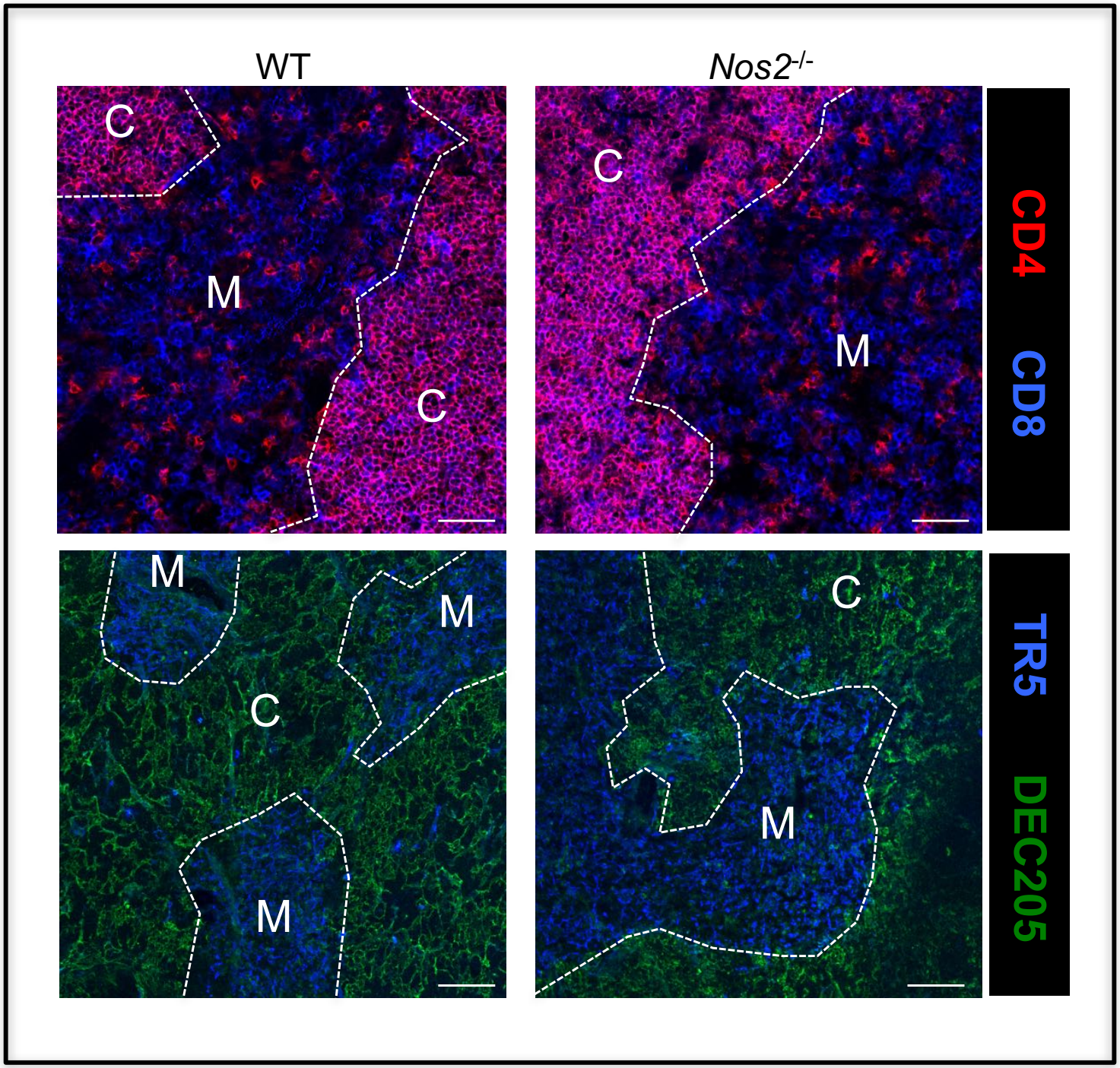
WT
Nos2-/-
C
M
C
C
M
CD4
CD8
M
M
C
M
C
M
TR5
DEC205

Figure 4.6: Thymic architecture is maintained in *Nos2*$^{-/-}$ mice

(A) Confocal analysis of thymic sections from wildtype and *Nos2*$^{-/-}$ mice. Architecture in terms of cortex (C) and medulla (M) was determined through co-staining of CD4 and CD8 (top row), wherein $CD4^{+}8^{-}$ (blue) and $CD8^{+}4^{-}$ (red) "SP" thymocytes are only detectable in the medulla, whereas $CD4^{+}8^{+}$ "DP" thymocytes (pink) occupy cortical areas. Alternatively, mTEC marker ER-TR5 (blue) and cTEC marker DEC205 (green) were used to determined the cortico-medullary boundaries (bottom row). Scale bars = 100um.

unchanged between wildtype and *Nos2*$^{-/-}$ mice, and the respective proportion and number of cells expressing Aire and CCL21 were normal in iNOS-deficiency (Figure 4.7A-B). As nitric oxide production by fibroblastic reticular cells is known to regulate the proliferation of peripheral T-cells (Lukacs-Kornek et al., 2011), we sought to identify the proliferative status of iNOS$^{+/-}$ mTEC^{hi} through staining with the proliferation marker Ki67, as well as by measuring BrdU incorporation by diving cells over 18 hours after i.p. administration of 1.5mg BrdU (Figure 4.7C-D). Strikingly, the population of iNOS^{+} mTEC^{hi} was distinctly non-overlapping with the proliferating contingent through either measure (Figure 4.7C-D). Only 19% of BrdU^{+}, and 26% of Ki67^{+} cells expressed iNOS, whereas consistently 50-60% of non-dividing cells were iNOS^{+} (Figure 4.7C-D). However, iNOS expression appeared to have little impact on the proliferative status of mTEC^{hi}. The proportion of Ki67^{+} *Nos2*$^{-/-}$ mTEC^{hi} was slightly higher than their wildtype counterparts, and mTEC^{lo} proliferated slightly less (Figure 4.7E-F), however these differences were too small to be realized in terms of absolute numbers, suggesting, although correlative with quiescence, iNOS does not substantially inhibit proliferation of mTEC^{hi}.

Constitutive expression of iNOS has been associated with the unfolded protein response (UPR) in the intestinal epithelium (Perner et al., 2002, Kaser et al., 2008), as well as plasma cells (Saini et al., 2014) (summarized in Figure 4.8A). iNOS acts as a positive regulator of expression of Xbp1s, the transcriptionally active product of the splice variant of the Xbp1 gene (Figure 4.8B), which controls the UPR in plasma cells (Njau and Jacob, 2014). Deletion of the *Nos2* gene reduces the activation of the UPR, and hence negatively impacts plasma cell survival (Saini et al., 2014). To determine whether the UPR is active in TEC,

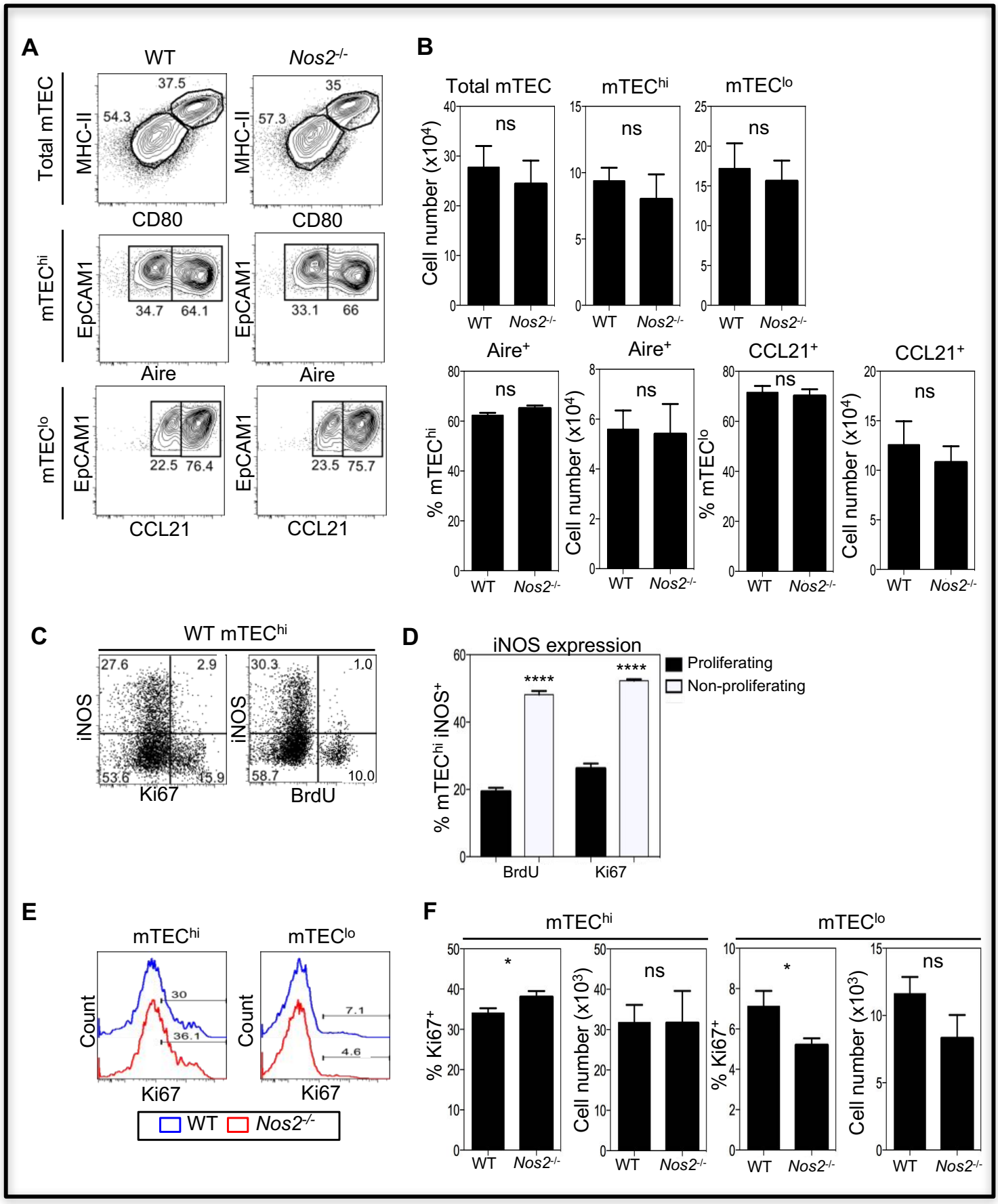
A
WT
Nos2-/-
Total mTEC
MHC-II
37.5
54.3
35
57.3
CD80
mTEChi
EpCAM1
34.7
64.1
33.1
66
Aire
mTEClo
22.5
76.4
23.5
75.7
CCL21
B
Total mTEC
mTEChi
mTEClo
Cell number (x10⁴)
ns
Aire+
CCL21+
% mTEChi
% mTEClo
C
WT mTEChi
iNOS
27.6
2.9
53.6
15.9
Ki67
30.3
1.0
58.7
10.0
BrdU
D
iNOS expression
% mTEChi iNOS+
****
Proliferating
Non-proliferating
E
mTEChi
mTEClo
Count
30
36.1
7.1
4.6
WT
Nos2-/-
F
% Ki67+
Cell number (x10³)
*

Figure 4.7: iNOS does not impact significantly on mTEC homeostasis

(A) Flow cytometric analysis and (B) quantitation of mTEC sub-types in wildtype and *Nos2*$^{-/-}$ thymus, including mTEChi and mTEC^{lo}, as well as Aire- and CCL21-expressing cells. n=5 wildtype and 5 *Nos2*$^{-/-}$ mice.

(C) Expression of iNOS in proliferating and non-proliferating mTEC^{hi}, as determined by the expression of the nuclear proliferation marker Ki67, and incorporation of BrdU 18 hours after i.p. injection with 1.5mg BrdU, as detected by nuclear staining with anti-BrdU Alexa Fluor 647.

(D) Quantitation of iNOS expression in proliferating and non-proliferating mTEC^{hi}, where iNOS is expressed by a far greater proportion of quiescent cells.

(E-F) Histograms representative of 5 wildtype and 5 *Nos2*$^{-/-}$ mice showing Ki67 expression in mTEC^{hi} and mTEC^{lo} from wildtype and *Nos2*$^{-/-}$ mice, as quantitated in part (F). All statistics were obtained using unpaired students t-tests, where *=$p<0.05$ and ****=$p<0.0001$.

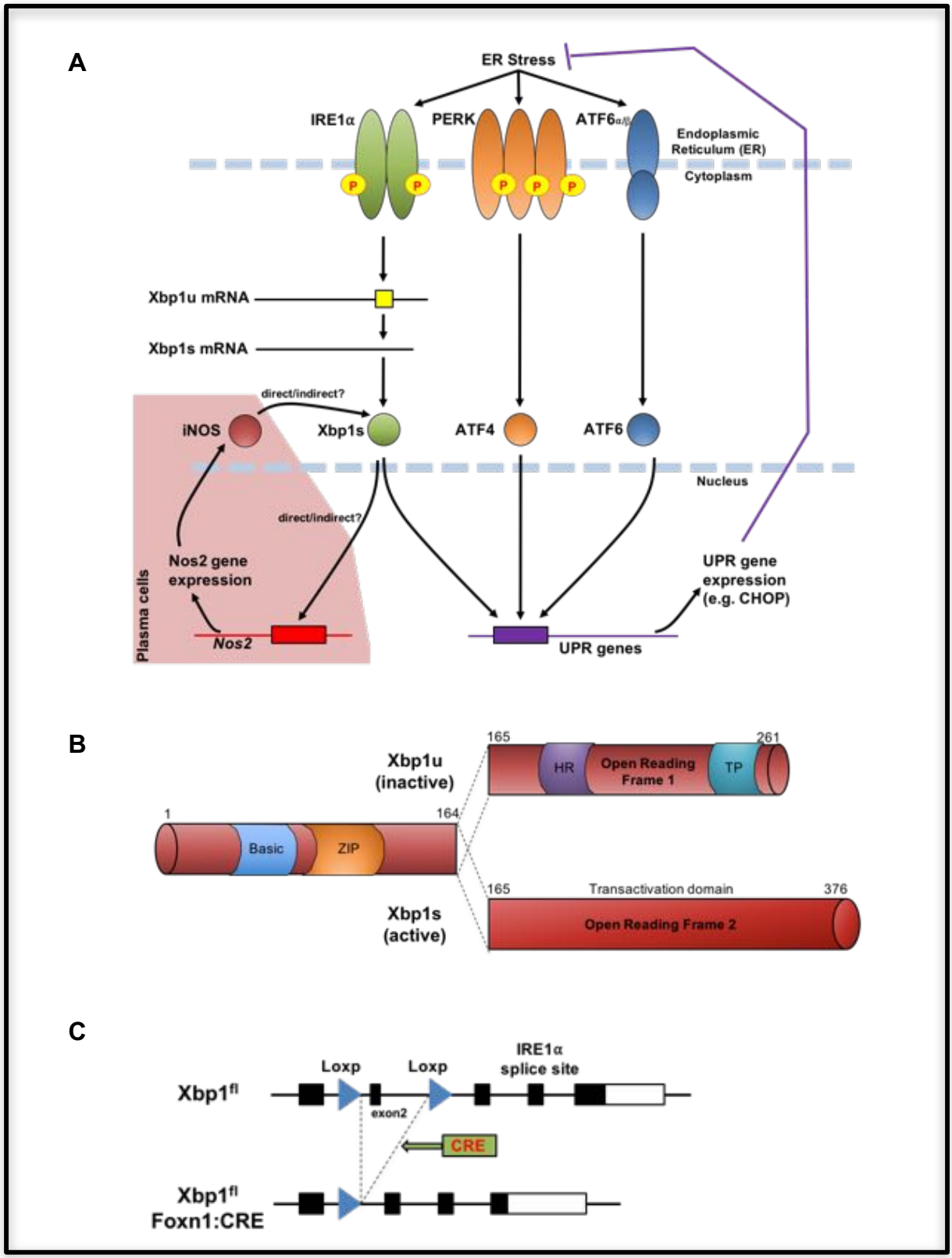
A
ER Stress
IRE1α
PERK
ATF6α/β
Endoplasmic Reticulum (ER)
Cytoplasm
P
Xbp1u mRNA
Xbp1s mRNA
direct/indirect?
iNOS
Xbp1s
ATF4
ATF6
Nucleus
direct/indirect?
Nos2 gene expression
Plasma cells
Nos2
UPR gene expression (e.g. CHOP)
UPR genes
B
Xbp1u (inactive)
165
261
HR
Open Reading Frame 1
TP
1
164
Basic
ZIP
165
Transactivation domain
376
Xbp1s (active)
Open Reading Frame 2
C
Loxp
Loxp
IRE1α splice site
Xbp1fl
exon2
CRE
Xbp1fl Foxn1:CRE

Figure 4.8: The unfolded protein response requires the active splice variant of the Xbp1 gene

(A) The unfolded protein response in mammals (UPR). Endoplasmic reticulum stress, and the accumulation of unfolded proteins triggers the activation of stress sensors, including IRE1α, PERK and ATF6α/β. Activation of these sensors triggers downstream signaling leading to the activation of the transcription factors Xbp1s, Atf4 and Atf6, which induce the expression of UPR genes, leading to an increase in clearance of unfolded proteins, and if unresolved the induction of pro-apoptotic pathways via CCAAT-enhancer-binding protein homologous protein (CHOP). IRE1α directly splices Xbp1u mRNA to produce the mRNA for the active form (Xbp1s). In plasma cells where the UPR is active, Xbp1s induces the expression of iNOS, which mediates pro-survival mechanisms, in addition to enhancing expression of Xbp1s itself.

(B) Alternative splicing of Xbp1 mRNA leads to a shift in the open reading frame, resulting in the formation of a transactivation domain in Xbp1s protein.

(C) Exon 2 of the Xbp1 gene is flanked by two LoxP sites in $Xbp1s^{fl}$ mice. When crossed to the Foxn1:CRE background CRE recombinase expression by TEC leads to the excision of the flanked region including exon 2, triggering a frame shift that leads to the formation of a stop codon after the IRE1α splice site. Hence, translation of Xbp1s mRNA is prematurely terminated, resulting in formation of a non-functional protein.

sorted TEC subsets were assessed for their expression of Xbp1s, as well as the CCAAT-enhancer-binding protein homologous protein (CHOP), a product of the PERK-mediated arm of the UPR, which acts as a readout for ER stress (Oyadomari and Mori, 2004). Expression of CHOP and Xbp1s was detected in cTEC, mTEC^{lo} and mTEC^{hi} – mTEC^{lo} had the greatest expression of both CHOP (Figure 4.9A) and Xbp1s (Figure 4.9B), suggesting they possess the highest level of ER stress in adult mice. However, the expression of neither gene was altered in *Nos2*$^{-/-}$ TEC populations (Figure 4.9A-B). Next, we used mice deficient in Xbp1s to determine the requirement for this transcription factor for iNOS expression, as well as TEC homeostasis. *Xbp1*$^{-/-}$ mice have a lethal embryonic defect (Reimold et al., 2001), and so it was necessary to generate conditional knockout mice utilising the CRE/loxP system. In this model CRE was expressed in TEC under the control of the Foxn1 promoter, resulting in deletion of exon 2 of the Xbp1 gene in TEC, and premature termination of translation through the introduction of a stop codon (Figure 4.8C). Foxn1:CRE x Xbp1s$^{fl/fl}$ mice had efficient deletion of exon 2, as confirmed by PCR (Figure 4.9C); however, the absence of Xbp1s expression had no effect on the expression of iNOS by mTEC^{hi} (Figure 4.9F-G). Similarly, Xbp1s appeared to be dispensable for TEC homeostasis, as total mTEC numbers were unaffected, and mTEC$^{hi/lo}$, as well as the functionally important Aire^{+} and CCL21^{+} subsets were present in normal numbers in Xbp1s-deficient TEC (Figure 4.9D-E).

Given the high degree of co-expression of Aire and iNOS, and previous observations of ours and others that Aire regulates the expression of functional markers such as CCL21 and OPG, we attempted to assess the requirement for

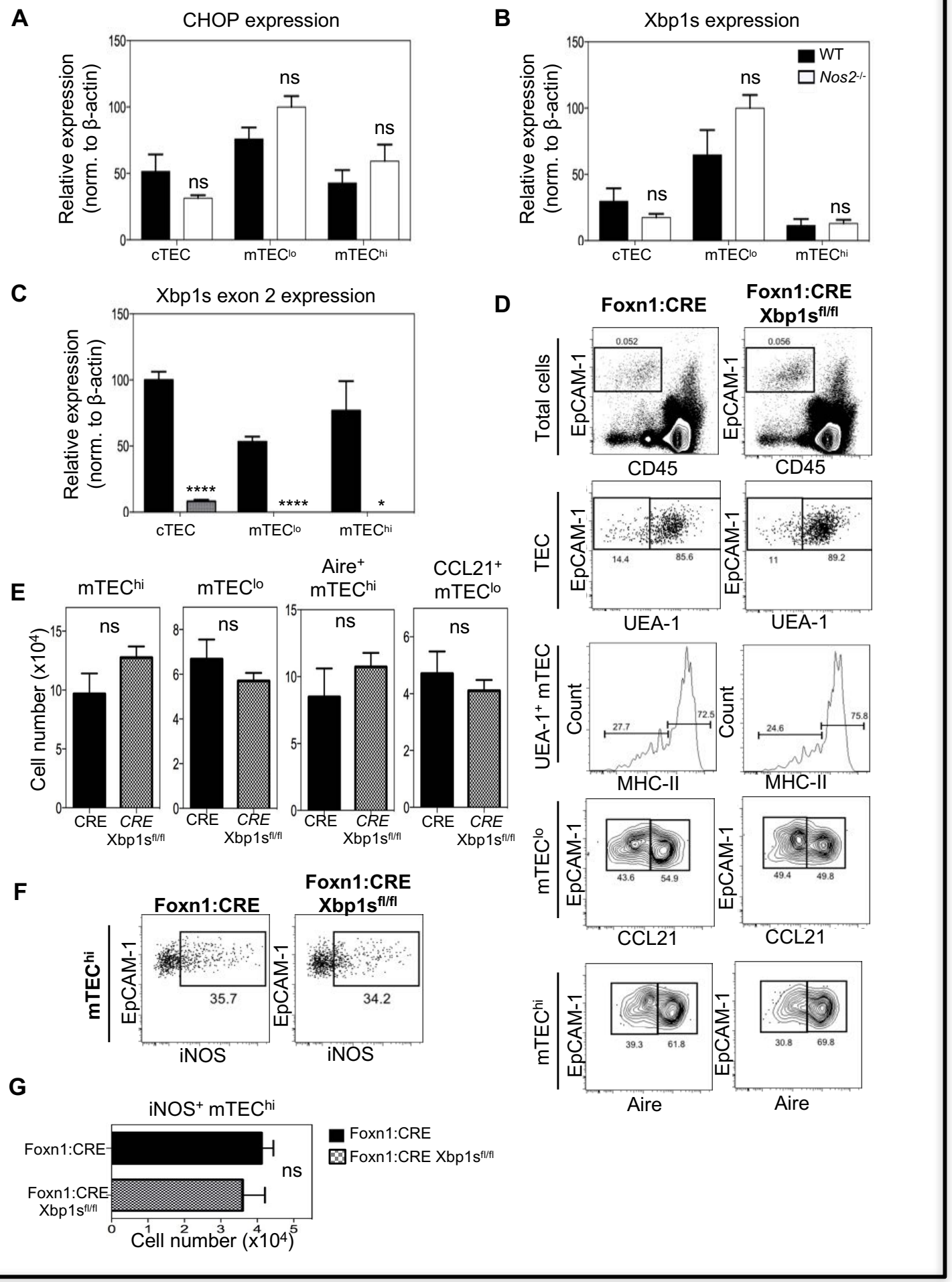
A
CHOP expression
Relative expression (norm. to β-actin)
ns
cTEC
mTEClo
mTEChi
B
Xbp1s expression
WT
Nos2-/-
C
Xbp1s exon 2 expression
****
*
D
Foxn1:CRE
Foxn1:CRE Xbp1sfl/fl
Total cells
EpCAM-1
CD45
TEC
UEA-1
UEA-1+ mTEC
Count
MHC-II
CCL21
Aire
E
mTEChi
mTEClo
Aire+ mTEChi
CCL21+ mTEClo
Cell number (x10^4)
CRE
CRE Xbp1sfl/fl
F
mTEChi
iNOS
G
iNOS+ mTEChi
Foxn1:CRE
Foxn1:CRE Xbp1sfl/fl

Figure 4.9: iNOS does not modulate the UPR in TEC

(A-B) Quantitative RT-PCR analysis of markers of the unfolded protein response pathway in sorted adult populations of cTEC (EpCAM-1^{+}Ly51^{+}), mTEC^{hi} (EpCAM-1^{+}Ly51^{-}CD80^{+}MHC-II^{hi}) and mTEC^{lo} (EpCAM-1^{+}Ly51^{-}CD80^{-}MHC-II^{lo}) from wildtype and *Nos2*$^{-/-}$ mice. Expression of CHOP (A) and the alternatively spliced, active variant of Xbp1 (Xbp1s, B) were analysed.

(C) q-RT-PCR confirmation of efficient Xbp1s deletion in CRE^{+} Xbp1s$^{fl/fl}$ thymic stroma.

(D-E) Intracellular staining for Aire and CCL21 in thymic epithelium isolated from Foxn1:CRE and Foxn1:CRE Xbp1s$^{fl/fl}$ mice (E), and quantitation (F) of mTEC sub-populations.

(F-G) Representative FACS plots (C) and quantitation (D) of iNOS expression in mTEC^{hi} from Foxn1:CRE and Foxn1:CRE x Xbp1s$^{fl/fl}$ mice, which lack expression of Xbp1s in Foxn1^{+} thymic epithelium.

Figures A-C are representative of at least 2 biological replicates, and in C-F, n= 7 CRE^{+} control mice, 7 Xbp1s$^{fl/fl}$ mice. Statistics were obtained using unpaired students t-tests, where *=$p<0.05$ and ****=$p<0.0001$.

Aire for the establishment of iNOS^{+} mTEC. Through FACS analysis of *Aire*$^{-/-}$ TEC, we observed an increase in the proportion of iNOS^{+} mTEC^{hi} in *Aire*$^{-/-}$ mice (Figure 4.10A-B). Given this population is greatly expanded in Aire-deficiency, this translated to more than a three-fold increase in the absolute number of iNOS^{+} mTEC^{hi} (Figure 4.10B). Interestingly, iNOS^{-} mTEC^{hi} were present in normal numbers (Figure 4.10B), suggesting a specific expansion of iNOS^{+} cells within the mTEC^{hi} subset. In addition, the level of iNOS protein in iNOS^{+} mTEC^{hi} was higher in *Aire*$^{-/-}$ mTEC, as shown by the greater MFI for iNOS staining (Figure 4.10C-D). To further confirm the Aire-independent nature of iNOS expression, wildtype and *Aire*$^{-/-}$ dGuo treated FTOC lobes were stimulated for 7 days with anti-Rank, and CD45^{-} cells isolated for PCR or FACS analysis of iNOS expression (Figure 10E-G). As expected, iNOS protein (Figure 4.10E-F) and gene (Figure 4.10G) expression was induced to an equal extent upon anti-Rank stimulation of both wildtype and *Aire*$^{-/-}$ TEC. Lastly, thymic sections from wildtype and *Aire*$^{-/-}$ mice were stained for ER-TR5 and iNOS (Figure 4.10G). A vastly greater number of iNOS^{+} cells were detected in the medulla of *Aire*$^{-/-}$ mice, confirming the over-representation of iNOS^{+} mTEC^{hi} among *Aire*$^{-/-}$ TEC (Figure 4.10G). Previously we have identified multiple defects in mTEC homeostasis in *Aire*$^{-/-}$ mice, and hence we next attempted to assess whether the over-expression of iNOS is causative of this instance. By crossing *Nos2*$^{-/-}$ and *Aire*$^{-/-}$ mice, we were able to generate *Aire*$^{-/-}$ x *Nos2*$^{-/-}$ "double knockout" (DKO) offspring, which were compared phenotypically to *Aire*$^{-/-}$ mice. We observed no alteration in the makeup of the mTEC compartment in DKO mice relative to single knockout controls – mTEC^{hi} were still expanded relative to the wildtype, and the deficiency in CCL21^{+} mTEC^{lo} was still maintained (Figure 4.11A-B). Interestingly, the proportion of Ki67^{+}

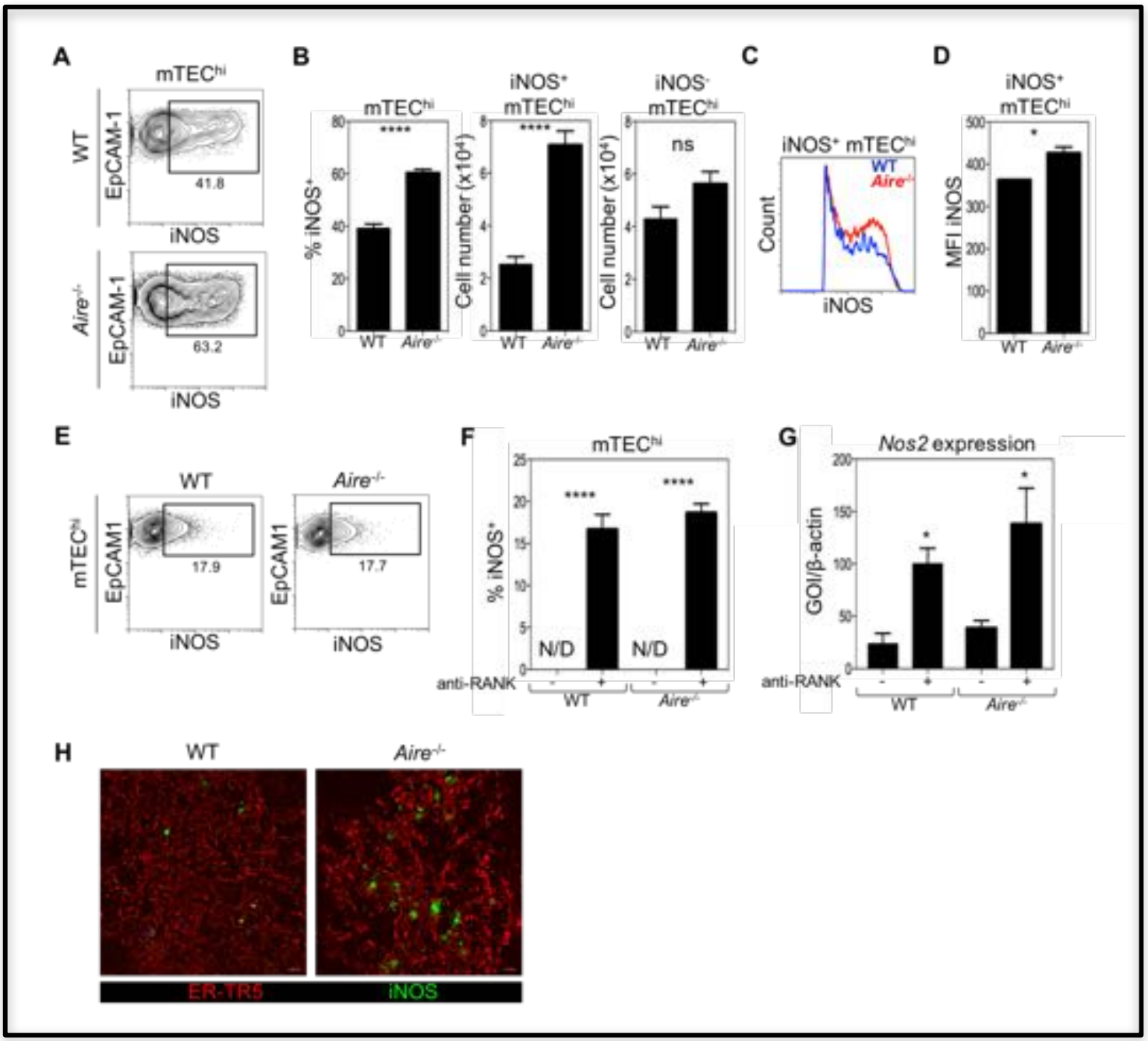
A
mTEC^hi
WT
EpCAM-1
41.8
iNOS
Aire-/-
EpCAM-1
63.2
iNOS
B
mTEC^hi
% iNOS+
****
WT
Aire-/-
iNOS+ mTEC^hi
Cell number (x10^4)
****
WT
Aire-/-
iNOS- mTEC^hi
Cell number (x10^4)
ns
WT
Aire-/-
C
iNOS+ mTEC^hi
WT
Aire-/-
Count
iNOS
D
iNOS+ mTEC^hi
MFI iNOS
*
WT
Aire-/-
E
WT
Aire-/-
mTEC^hi
EpCAM1
17.9
iNOS
EpCAM1
17.7
iNOS
F
mTEC^hi
% iNOS+
****
****
N/D
N/D
anti-RANK
WT
Aire-/-
G
Nos2 expression
GOI/β-actin
*
*
anti-RANK
WT
Aire-/-
H
WT
Aire-/-
ER-TR5
iNOS

Figure 4.10: iNOS expression is Aire-independent, and iNOS^{+} mTEC are expanded in Aire$^{-/-}$ mice

(A-B) Representative plots of iNOS expression in mTEC^{hi} isolated from wildtype and *Aire*$^{-/-}$ mice, together with quantitation of iNOS^{+} and iNOS^{-} mTEC^{hi} (n=7 wildtype, 6 *Aire*$^{-/-}$ mice).

(C-D) Histogram showing staining intensity for iNOS in wildtype and *Aire*$^{-/-}$ iNOS^{+} cells (C), and MFI for iNOS (D) representative of 3 wildtype and 3 *Aire*$^{-/-}$ mice.

(E-G) FACS (E-F) and Quantitative RT-PCR analysis (G) of iNOS induction in CD45-depleted cells from dGuo-treated wildtype and *Aire*$^{-/-}$ fetal thymic organ cultures in the presence or absence of stimulatory anti-Rank antibody. Representative of 2 independent biological replicates.

(H) Confocal analysis of iNOS (green) expression in the ER-TR5^{+} (red) medullas of wildtype and *Aire*$^{-/-}$ mice. Scale bars = 10uM.

Statistics were obtained using unpaired students t-tests, where *=$p<0.05$ and ****=$p<0.0001$.

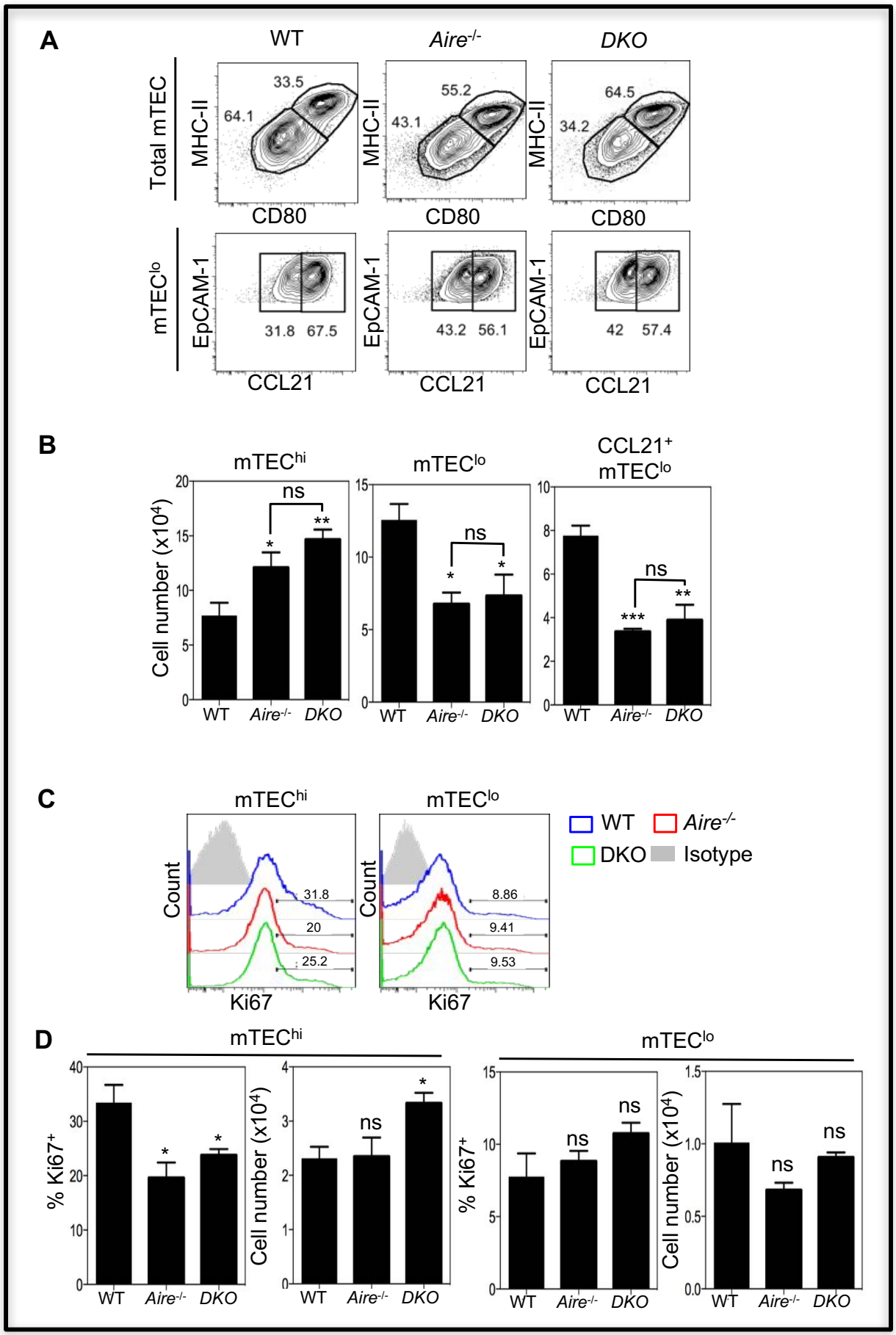
A
WT
Aire-/-
DKO
Total mTEC
MHC-II
CD80
33.5
64.1
55.2
43.1
64.5
34.2
mTEClo
EpCAM-1
CCL21
31.8 67.5
43.2 56.1
42 57.4
B
mTEChi
mTEClo
CCL21+ mTEClo
Cell number (x10⁴)
ns
*
**
***
WT
Aire-/-
DKO
C
mTEChi
mTEClo
Count
Ki67
31.8
20
25.2
8.86
9.41
9.53
WT
Aire-/-
DKO
Isotype
D
mTEChi
mTEClo
% Ki67+
Cell number (x10⁴)
ns
*
WT
Aire-/-
DKO

Figure 4.11: iNOS over-expression is not responsible for defective homeostasis in *Aire*$^{-/-}$ mice

(A) FACS plots and quantitation (B) demonstrating the distribution of mTEC between mTEC^{lo} and mTEC^{hi} subtypes, and CCL21 expression in the mTEC^{lo} compartment of wildtype, *Aire*$^{-/-}$ and *Aire*$^{-/-}$ x *Nos2*$^{-/-}$ (DKO) mice.

(C) Histograms showing the frequency of Ki67^{+} dividing cells among mTEC^{lo} and mTEC^{hi} in wildtype, *Aire*$^{-/-}$ and DKO mice, together with quanititation of dividing cells in terms of their proportion and number.

Statistics were obtained using unpaired students t-tests, where *=p<0.05, **=p<0.01 and ***=p<0.001, and data are representative of n=5 wildtype, 5 *Aire*$^{-/-}$ and 5 DKO mice.

mTEC^{hi} was reduced in *Aire*$^{-/-}$ mice, although the absolute number of proliferating cells was unchanged (Figure 4.11C-D). This observation was also evident in the DKO mice, however there was a slight increase in the absolute number of proliferating mTEC^{hi} (Figure 4.11C-D). No differences in the proliferative status of mTEC^{lo} were detected in either of the knockout models (Figure 4.11C-D). These findings suggest that, although iNOS^{+} mTEC^{hi} are specifically expanded in *Aire*$^{-/-}$ mice, and the fraction of proliferating cells lowered, iNOS over-expression does not significantly impact on the defects in mTEC homeostasis, nor cell cycle status.

4.2.3. The impact of iNOS on the development of conventional and unconventional T-cell lineages

To address whether iNOS expression by mTEC instead plays an important role in regulating T-cell development, we assessed thymocyte development in gross terms in *Nos2*$^{-/-}$ mice, wherein we observed no difference in the proportions or absolute numbers of DP, SP4 or SP8 thymocytes, nor Foxp3^{+} regulatory T-cells (Figure 4.12A-B). In the spleen of *Nos2*$^{-/-}$ mice, although both CD4 and CD8 T-cells were present, the number of CD4^{+} T-cells was consistently reduced by ~25% in *Nos2*$^{-/-}$ mice; however this wasn't specific to either the conventional or T-Reg lineage, as the proportion of Foxp3^{+} cells was maintained (Figure 4.12C-D). As thymic development of conventional T-cells appeared to be grossly normal, we next assessed the production of non-conventional T-cell lineages in the thymus of *Nos2*$^{-/-}$ mice. Nitric oxide is known to directly regulate the function of the transcription factor RORγt (Jianjun et al., 2013), and hence we

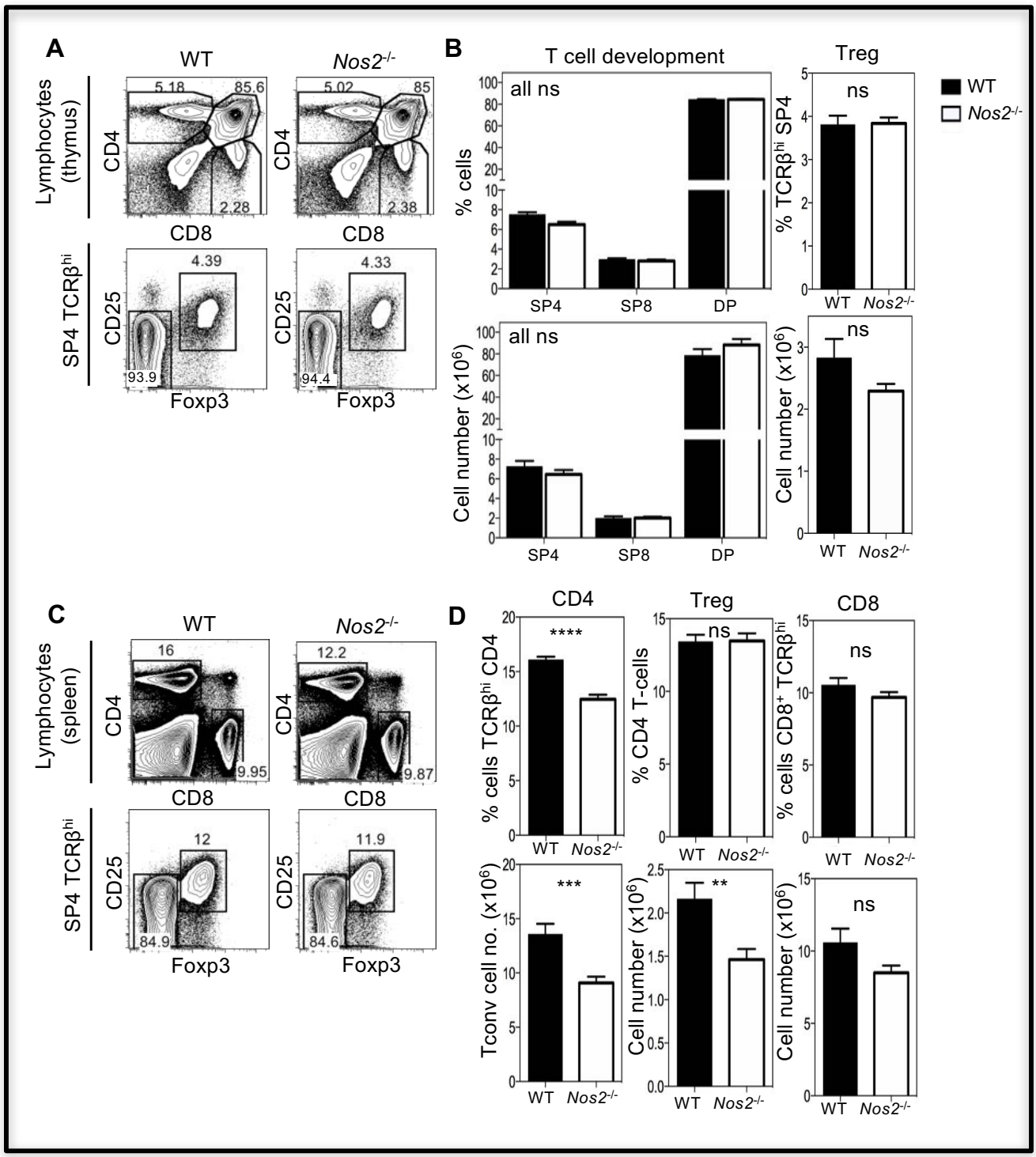
A
WT
Nos2-/-
Lymphocytes (thymus)
CD4
CD8
5.18
85.6
2.28
5.02
85
2.38
SP4 TCRβhi
CD25
Foxp3
4.39
93.9
4.33
94.4
B
T cell development
Treg
WT
Nos2-/-
all ns
% cells
SP4
SP8
DP
% TCRβhi SP4
ns
Cell number (x10^6)
C
Lymphocytes (spleen)
16
9.95
12.2
9.87
12
84.9
11.9
84.6
D
CD4
Treg
CD8
% cells TCRβhi CD4
****
% CD4 T-cells
% cells CD8+ TCRβhi
Tconv cell no. (x10^6)
***
**

Figure 4.12: Development of conventional and regulatory T-cells occurs normally in *Nos2*$^{-/-}$ mice

(A) FACS plots and (B) graphical representation of T-cell development in *Nos2*$^{-/-}$ thymus, including the development of DP, and conventional ($CD25^{-}Foxp3^{-}$) SP thymocytes, as well as $Foxp3^{+}CD25^{+}$ regulatory T-cells.

(C) FACS plots and (D) graphical representation of splenic T-cells in *Nos2*$^{-/-}$ mice, including CD4 and CD8 T-cells, as well as $Foxp3^{+}$ T-Reg.

Statistics were obtained using unpaired students t-tests, where **=$p<0.01$ and ***=$p<0.001$, and data are representative of n=11 wildtype, and 10 *Nos2*$^{-/-}$ mice.

decided to focus on thymic iNKT, γδ T-cells and natural Th17 cells, subsets of which express RORγt within the thymus. The proportion and number of total and RORγt^{+} iNKT and γδ T-cells were unchanged between wildtype and *Nos2*$^{-/-}$ mice (Figure 4.13A-D). Interestingly, the induction of RORγt^{+} Th17 cells in vitro has been shown to be limited by T-cell intrinsic expression of iNOS (Jianjun et al., 2013); however, we again saw no increase in the proportion or number of IL-17-producing SP4s in the thymus of *Nos2*$^{-/-}$ mice (Figure 4.13E-F). Finally, over-expression of either Nos2 or Nos3, or treatment with the nitric oxide donor has been shown to inhibit the caspase-dependent cleavage of MHC-II and a host of co-stimulatory molecules during dendritic cell development (Wong et al., 2004, Huang et al., 2008). A subset of thymic cDC are known to have a strongly activated phenotype, expressing high levels of MHC-II, CD80 and CD86; however, we observed no difference in the makeup of cDC or pDC in the thymus of *Nos2*$^{-/-}$ mice (Figure 4.13G-H), and similarly saw no alterations in the levels of expression of MHC-II, or B7 class molecules on the surface of cDC (Figure 4.13G, I).

Given our findings that gross conventional T-cell development is unperturbed in *Nos2*$^{-/-}$ mice, we conducted a more thorough analysis of SP4 development using the markers CD69 and Qa2. Immature SP4 thymocytes are defined as CD69^{+}Qa2^{lo}, and mature cells Qa2^{hi}CD69^{-} (summarized in Figure 4.14). Rather than acting as a ligand for a specific receptor, nitric oxide is able to exert effects on cells through the nitrosylation of tyrosine residues on surface and intracellular proteins, acting to modify their function. By staining SP4 thymocytes with an antibody specific for nitrotyrosine, we were able to detect a significant increase in tyrosine nitrosylation in intracellular proteins between

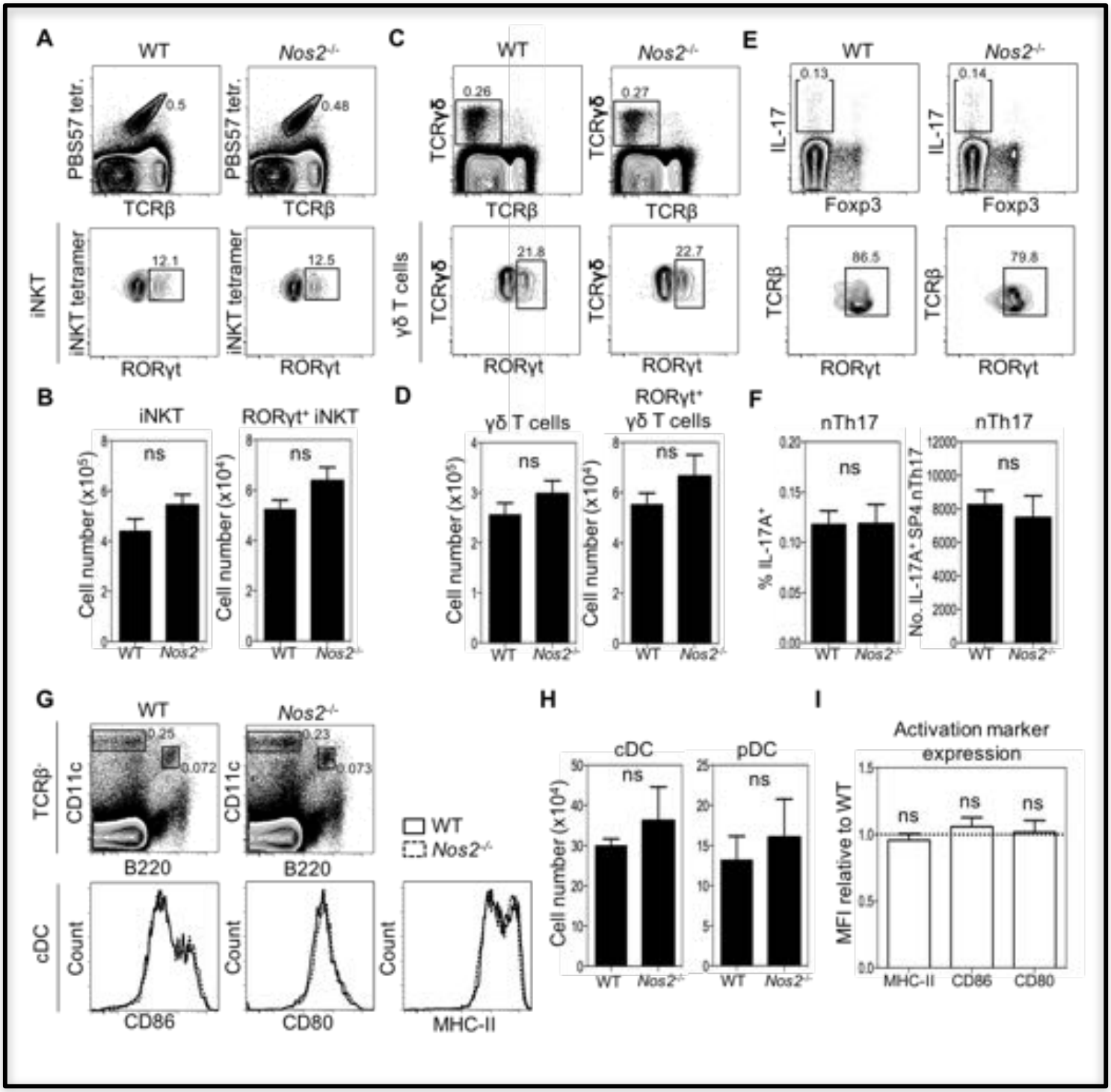
A
WT
Nos2-/-
PBS57 tetr.
0.5
0.48
TCRβ
iNKT
iNKT tetramer
12.1
12.5
RORγt
C
TCRγδ
0.26
0.27
γδ T cells
21.8
22.7
E
IL-17
0.13
0.14
Foxp3
TCRβ
86.5
79.8
B
iNKT
RORγt+ iNKT
Cell number (x10^5)
Cell number (x10^4)
ns
D
γδ T cells
RORγt+ γδ T cells
F
nTh17
% IL-17A+
No. IL-17A+ SP4 nTh17
G
TCRβ-
CD11c
0.25
0.072
0.23
0.073
B220
cDC
Count
CD86
CD80
MHC-II
H
cDC
pDC
I
Activation marker expression
MFI relative to WT

Figure 4.13: The production of unconventional T-cells, and the activation of thymic dendritic cells is unaffected by iNOS

(A-F) Analysis of unconventional T-cell subsets expressing the transcription factor RORγt in wildtype and *Nos2*$^{-/-}$ thymi, including iNKT cells (A-B), γδ T-cells (C-D) and natural IL-17 producing Th17 cells (E-F), where n=6 wildtype and 7 *Nos2*$^{-/-}$ mice.

(G) FACS plots representative of thymic dendritic cell subsets, including CD11c^{hi}B220^{-} cDC, and CD11c^{lo}B220^{+} pDC (top), and expression of MHC-II and co-stimulatory molecules CD86 and CD80 on the surface of thymic cDC (bottom).

(H-I) Quantitation of cDC and pDC subsets in wildtype and *Nos2*$^{-/-}$ mice (n=4 wildtype and 4 *Nos2*$^{-/-}$, H), and mean fluorescence intensity of activation markers expressed by *Nos2*$^{-/-}$ cDC relative to the corresponding wildtype population (I).

Statistics were obtained using unpaired students t-tests.

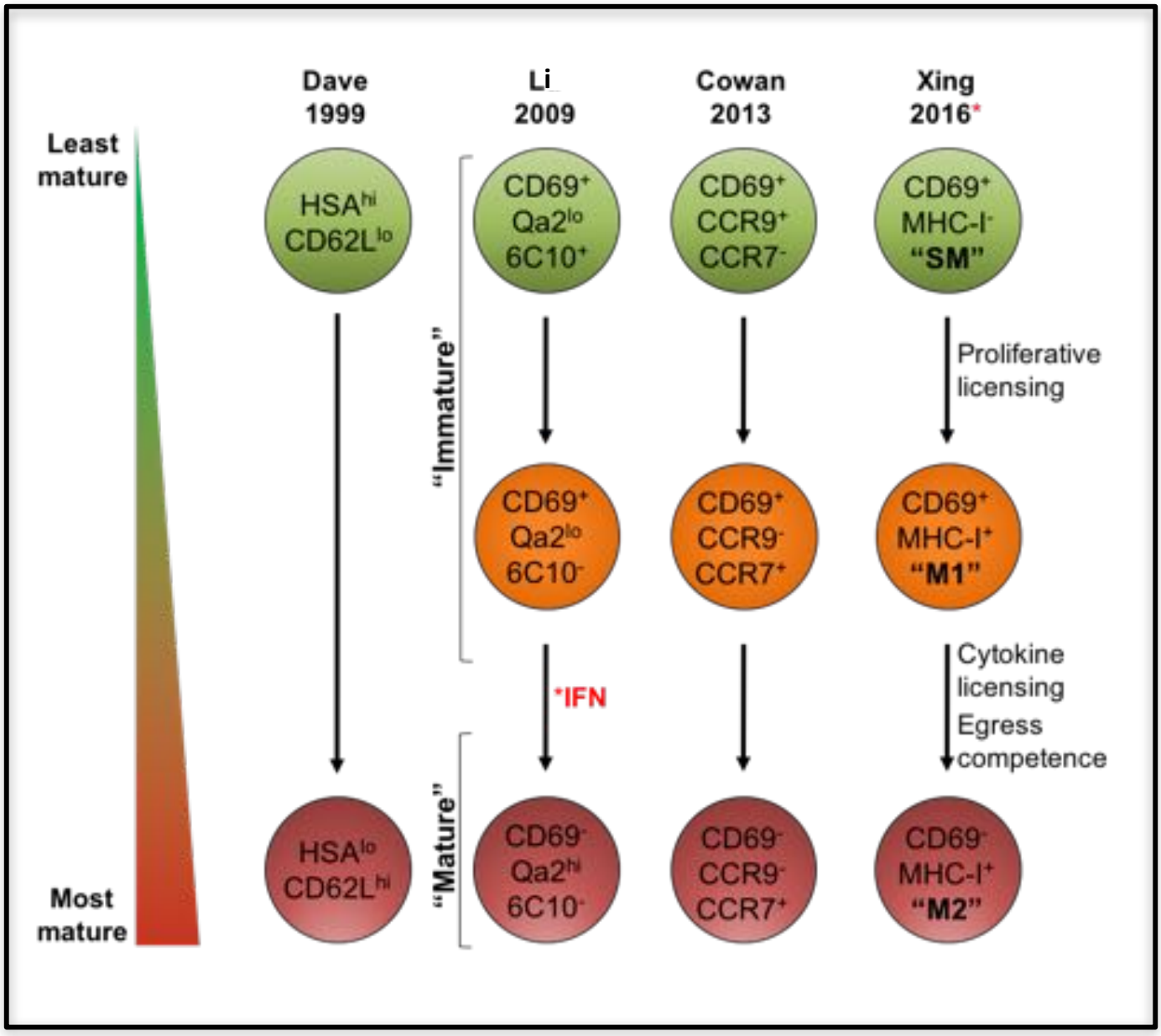
Dave
1999
Li
2009
Cowan
2013
Xing
2016*
Least
mature
Most
mature
HSA^hi
CD62L^lo
CD69+
Qa2^lo
6C10+
CD69+
CCR9+
CCR7-
CD69+
MHC-I-
"SM"
"Immature"
Proliferative
licensing
CD69+
Qa2^lo
6C10-
CD69+
CCR9-
CCR7+
CD69+
MHC-I+
"M1"
*IFN
Cytokine
licensing
Egress
competence
HSA^lo
CD62L^hi
"Mature"
CD69-
Qa2^hi
6C10-
CD69-
CCR9-
CCR7+
CD69-
MHC-I+
"M2"

Figure 4.14: Models of intrathymic maturation of SP thymocytes

Summary of phenotypic maturation of murine SP4 thymocytes, as identified using the markers HSA and CD62L (Dave et al., 1999), CD69, Qa2 and 6C10 (Li et al., 2009), CD69, CCR7 and CCR9 (Cowan et al., 2013) or CD69 and MHC-I (Xing et al., 2016).

the DP and immature SP4 stages of development (Figure 4.15A), suggesting Nos2-catalysed nitric oxide may exert effects on thymocytes at this stage. Interestingly, when we assessed the maturational profile of wildtype and *Nos2*$^{-/-}$ SP4 thymocytes, we saw an increase in the proportion of Qa2^{hi}CD69^{-} mature cells, although this actually represented a significant reduction in numbers of CD69^{+}Qa2^{lo} immature SP4s, and only a marginal and non-significant increase in their mature counterparts (Figure 4.15B). Regardless, the ratio of mature:immature cells was skewed in favour of the mature SP4 population (Figure 4.15C), possibly suggesting accelerated maturation of SP4 thymocytes in the absence of iNOS. Similarly, the MFI of Qa2 expressed by CD69^{-} SP4 thymocytes was significantly higher in *Nos2*$^{-/-}$ mice (Figure 4.15D).

Nitric oxide can potently induce apoptosis (Fehsel et al., 1995), or suppress proliferation of T-cell populations in an inflammatory environment (Lukacs-Kornek et al., 2011), although these effects are highly context dependent. To determine whether the alteration in SP4 maturity was the result of changes to the proliferation of mature/immature thymocytes, mice were injected with 1.5mg BrdU, and BrdU incorporation by SP thymocytes assessed after an 18-hour period. Mature Qa2^{hi}CD69^{-} SP4 thymocytes proliferated to a higher degree than their immature counterparts, however there was no difference in the proportion of BrdU^{+} cells among the mature/immature subsets between wildtype and *Nos2*$^{-/-}$ mice (Figure 4.15E). A previous report has demonstrated the capacity for the nitric oxide donor S-Nitroso-N-acetyl-DL-penicillamine (SNAP) to induce apoptosis of DP thymocytes (Tai et al., 1997). We replicated this experiment, by culturing whole thymocytes in 200uM SNAP for 8 hours, before assessing the levels of apoptosis using Annexin V staining. SNAP

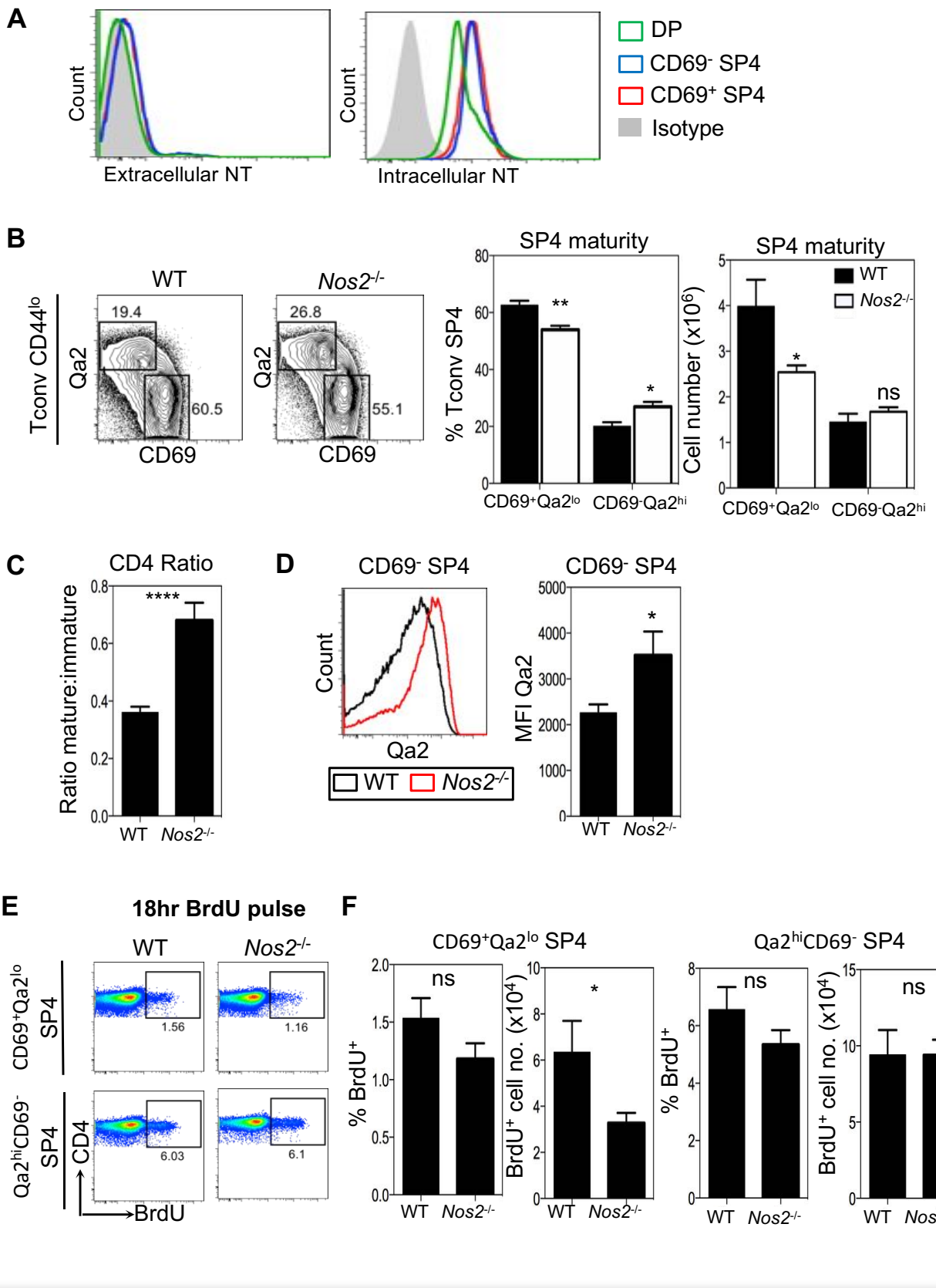
A
Count
Extracellular NT
Count
Intracellular NT
DP
CD69- SP4
CD69+ SP4
Isotype
B
WT
Nos2-/-
Tconv CD44lo
Qa2
19.4
60.5
CD69
26.8
55.1
CD69
SP4 maturity
% Tconv SP4
**
*
CD69+Qa2lo
CD69-Qa2hi
SP4 maturity
Cell number (x10^6)
WT
Nos2-/-
*
ns
CD69+Qa2lo
CD69-Qa2hi
C
CD4 Ratio
Ratio mature:immature
****
WT
Nos2-/-
D
CD69- SP4
Count
Qa2
WT
Nos2-/-
CD69- SP4
MFI Qa2
*
WT
Nos2-/-
E
18hr BrdU pulse
WT
Nos2-/-
CD69+Qa2lo SP4
1.56
1.16
Qa2hiCD69- SP4
CD4
6.03
6.1
BrdU
F
CD69+Qa2lo SP4
% BrdU+
ns
BrdU+ cell no. (x10^4)
*
WT
Nos2-/-
Qa2hiCD69- SP4
% BrdU+
ns
BrdU+ cell no. (x10^4)
ns
WT
Nos2-/-

Figure 4.15: Skewed maturational phenotype is not the result of uncontrolled proliferation in *Nos2*$^{-/-}$ thymus

(A) Histograms showing surface and intrcellular staining for nitrosylated tyrosine (NT) residues in DP, and immature/mature SP thymocyte populations in wildtype mice.

(B) FACS plots and quantitation showing maturational profile of SP thymocytes from wildtype and *Nos2*$^{-/-}$ thymus. Cells are classified based on their expression of the markers Qa2 and CD69, where immature SP4s are CD69+Qa2^{lo}, and mature cells Qa2^{hi}CD69^{-}.

(C) The ratio of mature:immature SP4 thymocytes in wildtype and *Nos2*$^{-/-}$ thymi.

(D) Histogram showing the expression levels of Qa2 expression by CD69- SP4 thymocytes from wildtype and *Nos2*$^{-/-}$ mice, as quantified by analysis of mean fluorescence intensity (right pane).

(E) BrdU staining in mature and immature SP thymocytes isolated 18 hours after i.p. injection of 1.5mg BrdU, and (F) quantitation of BrdU+ proliferating cells after the 18 hour pulse.

Statistics were obtained using unpaired students t-tests, where *=$p<0.05$ and **=$p<0.01$, and n=11 wildtype and 10 *Nos2*$^{-/-}$ mice.

was capable of inducing apoptosis in 18% of DP thymocytes within this short time frame (Figure 4.16A-B). In addition, although SNAP failed to trigger apoptosis of $CD44^{hi}$ SP4 T-cells, which are thought to represent a largely re-circulating population of cells (Boursalian et al., 2004), SNAP did induce cell death mildly in immature SP4s, and in ~9% of mature SP4s (Figure 4.16A-B). When thymocytes were incubated in multiple concentrations of SNAP, a strict dose:response relationship was observed only for DP and mature SP thymocytes, where the higher the concentration of SNAP, the greater the degree of apoptosis after 8 hours of treatment (Figure 4.16C). However, although SNAP can potently induce apoptosis of mature thymocytes, we saw no difference in the proportion of Annexin V^+ apoptotic cells among mature/immature thymocytes isolated from wildtype and *Nos2*$^{-/-}$ mice (Figure 4.16D-E), suggesting iNOS does not control thymocyte apoptosis *in vivo*.

In contrast to SP4 thymocytes in *Nos2*$^{-/-}$ mice, *Aire*$^{-/-}$ mice have been reported to lack mature $Qa2^{hi}$ SP4 thymocytes (Li et al., 2007). Given our observation that iNOS is greatly over-expressed by *Aire*$^{-/-}$ mTEC, we were interested to further investigate a possible link between iNOS and SP4 maturation. By staining *Aire*$^{-/-}$ thymocytes for Qa2 and CD69, we matched previous observations that, although the numbers of SP4 thymocytes are normal (Figure 4.17A-B), mature $Qa2^{hi}$ SP4s are almost completely absent from the thymus of *Aire*$^{-/-}$ mice (Figure 4.17A, C). Unexpectedly, when we compared these to SP4 thymocytes obtained from DKO mice, there was a partial restoration of the mature $Qa2^{hi}$ population in terms of both proportion and number (Figure 4.17A, C). In addition, the MFI readout of Qa2 expression again increased (Figure 4.17D), although not completely corrected. As we could again find no differences

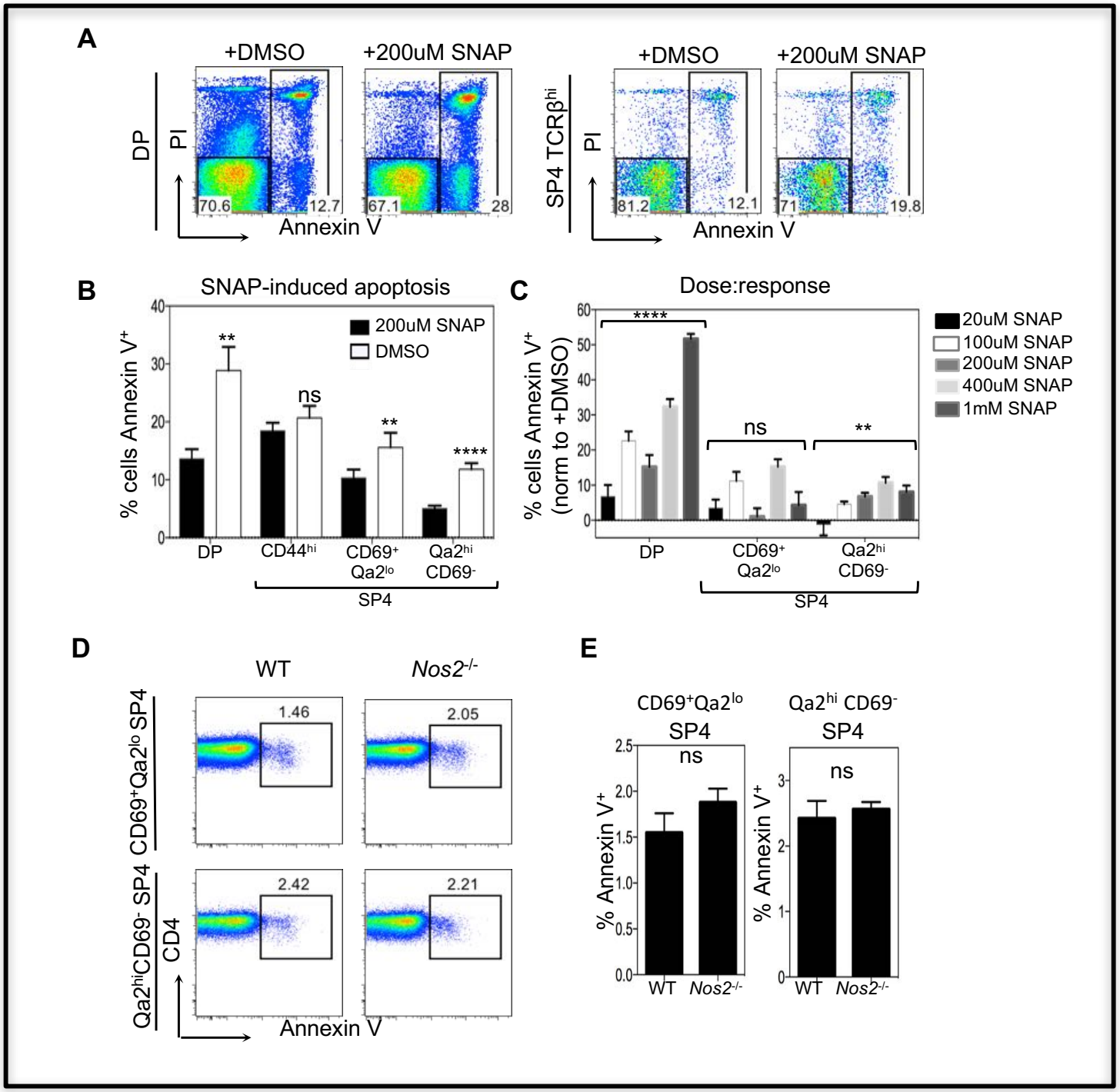
A
+DMSO
+200uM SNAP
DP
PI
70.6
12.7
67.1
28
Annexin V
SP4 TCRβhi
81.2
12.1
71
19.8
B
SNAP-induced apoptosis
200uM SNAP
DMSO
% cells Annexin V+
DP
CD44hi
CD69+ Qa2lo
Qa2hi CD69-
SP4
C
Dose:response
% cells Annexin V+ (norm to +DMSO)
20uM SNAP
100uM SNAP
200uM SNAP
400uM SNAP
1mM SNAP
D
WT
Nos2-/-
CD69+Qa2lo SP4
Qa2hiCD69- SP4
CD4
1.46
2.05
2.42
2.21
E
CD69+Qa2lo SP4
Qa2hi CD69- SP4
% Annexin V+
ns

Figure 4.16: Skewed maturational phenotype is not the result of uncontrolled apoptosis in *Nos2*$^{-/-}$ thymus

(A) Representative FACS plots of SNAP-induced apoptosis in DP (left) and SP4 (right) thymocytes, as determined by Annexin V staining.

(B) Quantitation of the absolute percentage of Annexin V^{+} cells in sub-gated populations from total thymocytes cultured in 200uM SNAP or vehicle (DMSO) for 8 hours.

(C) Quantitation of the percentage of Annexin V^{+} cells cultured for 8 hours in increasing concentrations of SNAP, normalized to levels of apoptosis induced by DMSO vehicle alone.

(D) Annexin V staining in ex vivo SP4 thymocytes isolated from wildtype and *Nos2*$^{-/-}$ mice, where n=6 wildtype, and 5 *Nos2*$^{-/-}$ mice.

(E) Quantification of rates of Annexin V^{+} apoptotic cells among mature and immature SP4 thymocytes.

Statistics were obtained using unpaired students t-tests (B, E) or linear regression analysis (C, where r^2 = 0.95 - DP thymocytes, 0.32 - CD69^{+} SP4, 0.82 - Qa2^{hi} SP4,), where **=p<0.01 and ****=p<0.0001. All data are representative of at least 3 independent experiments.

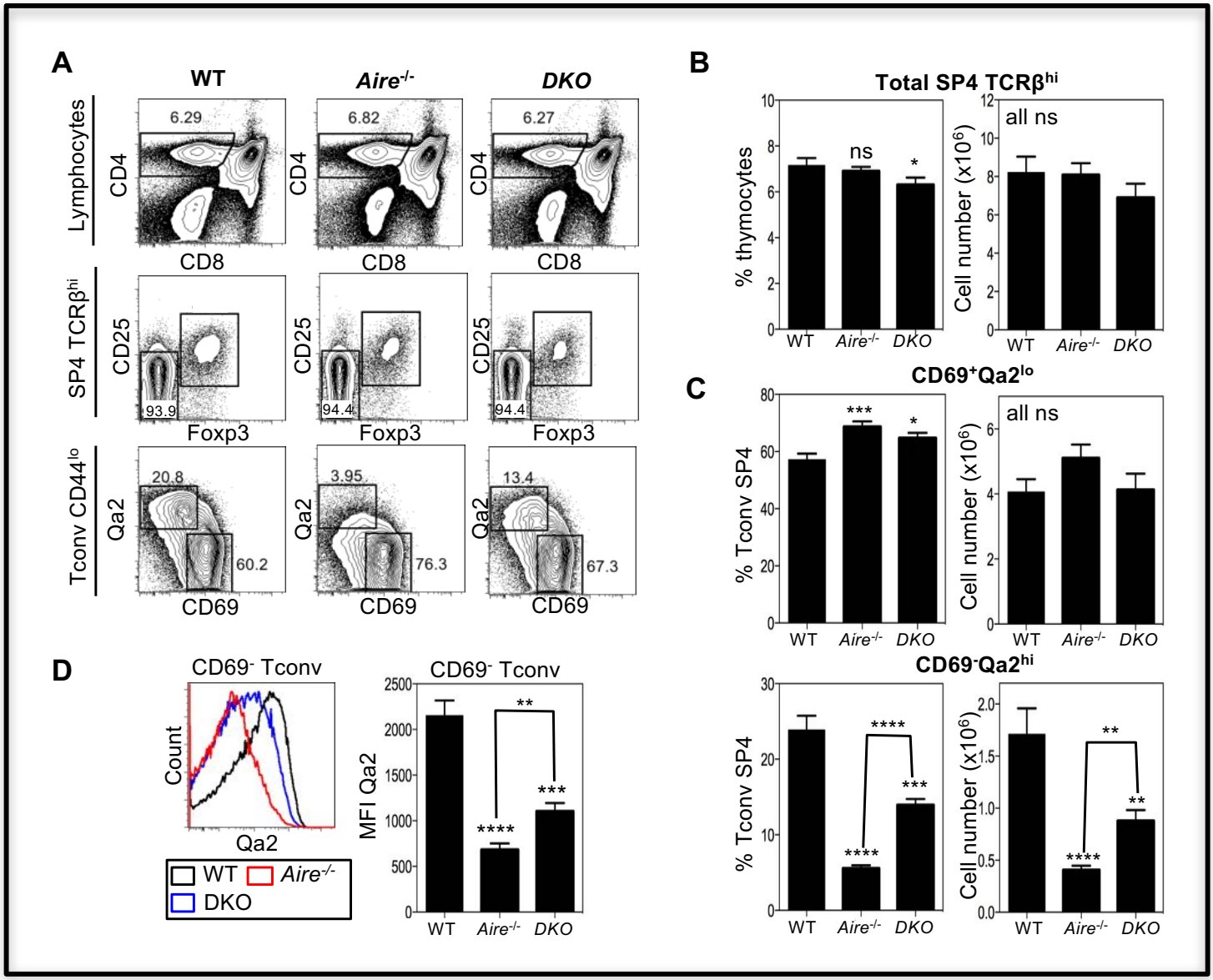
A
WT
Aire-/-
DKO
Lymphocytes
CD4
CD8
6.29
6.82
6.27
SP4 TCRβhi
CD25
Foxp3
93.9
94.4
94.4
Tconv CD44lo
Qa2
CD69
20.8
60.2
3.95
76.3
13.4
67.3
B
Total SP4 TCRβhi
% thymocytes
ns
*
Cell number (x10^6)
all ns
WT
Aire-/-
DKO
C
CD69+Qa2lo
% Tconv SP4
***
*
all ns
CD69-Qa2hi
****
**
D
CD69- Tconv
Count
Qa2
WT
Aire-/-
DKO
MFI Qa2

Figure 4.17: The absence of Qa2^{hi} cells in *Aire*$^{-/-}$ mice is partially iNOS dependent

(A) Representative FACS plots of thymocyte development in wildtype, *Aire*$^{-/-}$ and DKO mice.

(B) Quantitation of total SP4 thymocytes in Aire- and iNOS-deficient models, as well as (C) CD69^{+} immature and Qa2^{hi} mature subsets.

(D) Histogram representing Qa2 expression in CD69- thymocytes in wildtype, *Aire*$^{-/-}$ and DKO mice, with quantification of the mean fluorescence intensity (right).

Statistics were obtained using unpaired students t-tests, where * = $p<0.05$, ** = $p<0.01$, **=$p<0.01$ and ****=$p<0.0001$. n= 6 wildtype, 8 *Aire*$^{-/-}$ and 7 DKO mice.

in the proportion of proliferating or apoptotic cells (not shown), this would suggest that iNOS expression contributes towards blocking phenotypic maturation of SP4s intrathymically. Importantly, the levels of expression of Qa2 in the periphery were not significantly different between each Aire/iNOS-deficient strain (not shown), suggesting this effect is distinct to the thymus.

Our recent unpublished data (Jennifer Cowan, 2016) has shown using the Rag-2p-GFP mouse model that *Aire*$^{-/-}$ mice have a defect in re-circulation of peripheral T-cells - the majority of which are Foxp3^{+} T-Reg – to the thymus. In order to assess whether a) this defect is iNOS-dependent, and b) the re-circulation of mature Qa2^{hi} T-cells explains the alteration in the Qa2^{hi} SP4 subset, we investigated the capacity for peripheral T-cells to home to the thymus of *Nos2*$^{-/-}$, *Aire*$^{-/-}$ and DKO mice. We matched previous observations (Lei et al., 2011) that total Foxp3^{+} cell numbers are reduced in the *Aire*$^{-/-}$ thymus, and this defect was maintained in the DKO (Figure 18A-B). Next, we grafted lymphoid CD45.1^{+} BoyJ fetal thymic lobes under the kidney capsule of CD45.2^{+} host mice. In this model, graft-derived T-cells are detectable in the periphery, and the small fraction that re-circulates to the thymus is identifiable by expression of the congenic marker CD45.1 (Figure 4.19). The proportion of CD45.1^{+} cells in the spleen expressing Foxp3 is in line with host splenocytes (~15%); however, ~65% of CD45.1^{+} thymic re-circulants are Foxp3^{+}, suggesting targeted re-circulation of these cells to the thymus (Figure 4.18C). The proportion and number of re-circulating CD4 T-cells, and specifically Foxp3^{+} T-Reg thymic re-circulants was reduced in the thymus of *Aire*$^{-/-}$ hosts relative to the wildtype, but unchanged in

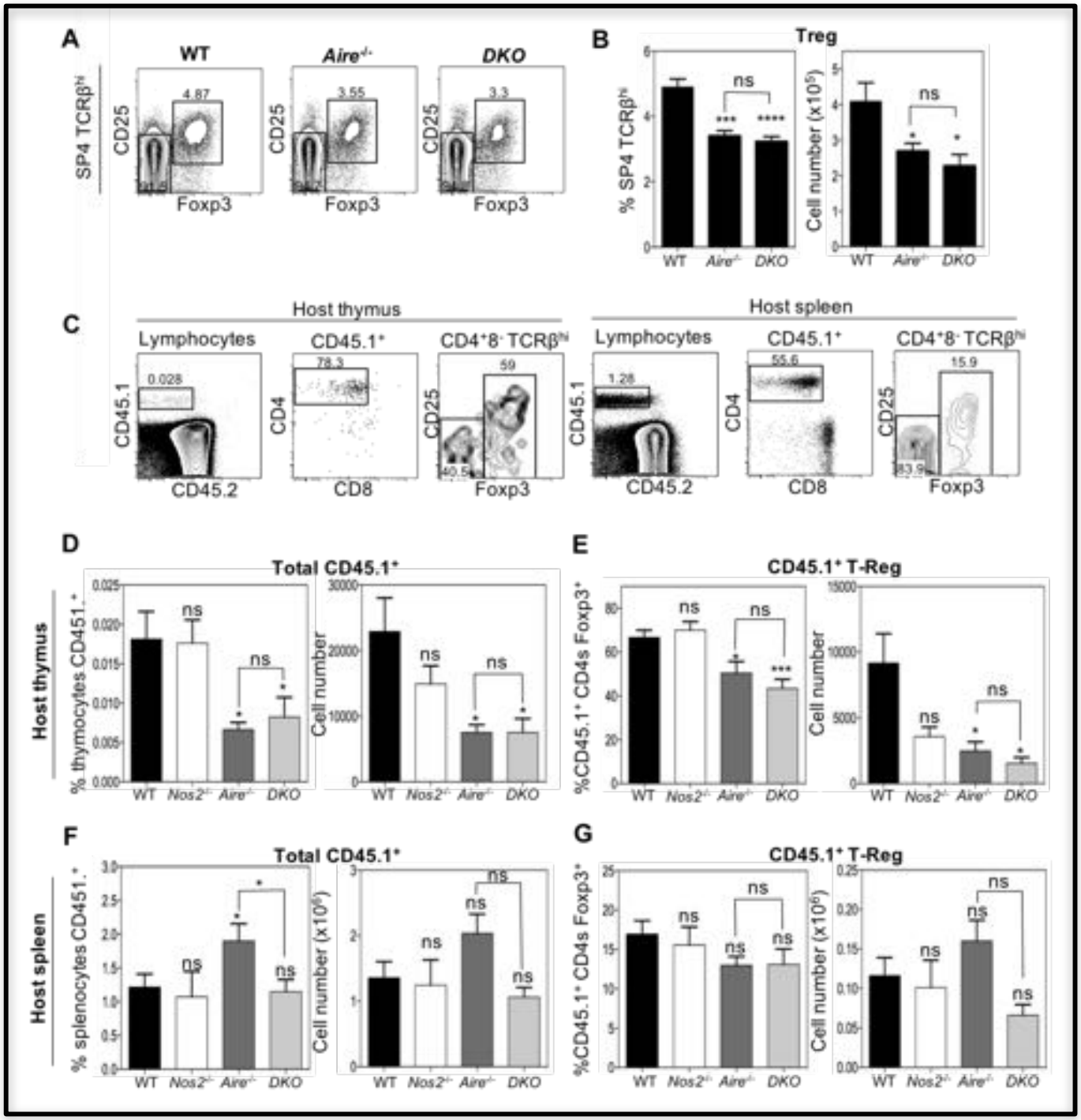
A
WT
Aire-/-
DKO
SP4 TCRβhi
CD25
Foxp3
4.87
3.55
3.3
B
Treg
% SP4 TCRβhi
Cell number (x10^5)
ns
***
****
*
WT
Aire-/-
DKO
C
Host thymus
Host spleen
Lymphocytes
CD45.1+
CD4+8- TCRβhi
CD45.1
CD45.2
CD4
CD8
CD25
Foxp3
0.028
78.3
59
40.5
1.28
55.6
15.9
83.9
D
Total CD45.1+
Host thymus
% thymocytes CD451.+
Cell number
ns
*
WT
Nos2-/-
Aire-/-
DKO
E
CD45.1+ T-Reg
%CD45.1+ CD4s Foxp3+
Cell number
F
Total CD45.1+
Host spleen
% splenocytes CD451.+
Cell number (x10^6)
G
CD45.1+ T-Reg
%CD45.1+ CD4s Foxp3+
Cell number (x10^6)

Figure 4.18: iNOS does not control the re-circulation of peripheral T-cells to the thymus

(A-B) Analysis of Foxp3^{+} T-Reg in the thymus of wildtype, *Aire*$^{-/-}$ and DKO mice, where n= 6 wildtype, 8 *Aire*$^{-/-}$ and 7 DKO mice.

(C) Gating strategy for the analysis of fetal thymic graft-derived peripheral T-cell re-circulating to the thymus and spleen of the host mouse. Re-circulating cells are CD45.1^{+}, and host T-cells CD45.2^{+}.

(D-E) Quantitation of graft-derived re-circulating total T-cells (D) and T-Reg (E) in the thymus of wildtype, *Nos2*$^{-/-}$, *Aire*$^{-/-}$ and DKO host mice. Representative of 14 wildtype, 7 *Nos2*$^{-/-}$, 7 *Aire*$^{-/-}$ and 7 DKO host mice.

(F-G) Quantitation of graft-derived re-circulating total T-cells (F) and T-Reg (G) in the spleen of wildtype, *Nos2*$^{-/-}$, *Aire*$^{-/-}$ and DKO host mice.

Statistics were obtained using unpaired students t-tests, where * = $p<0.05$, ** = $p<0.01$, ***=$p<0.01$ and ****=$p<0.0001$.

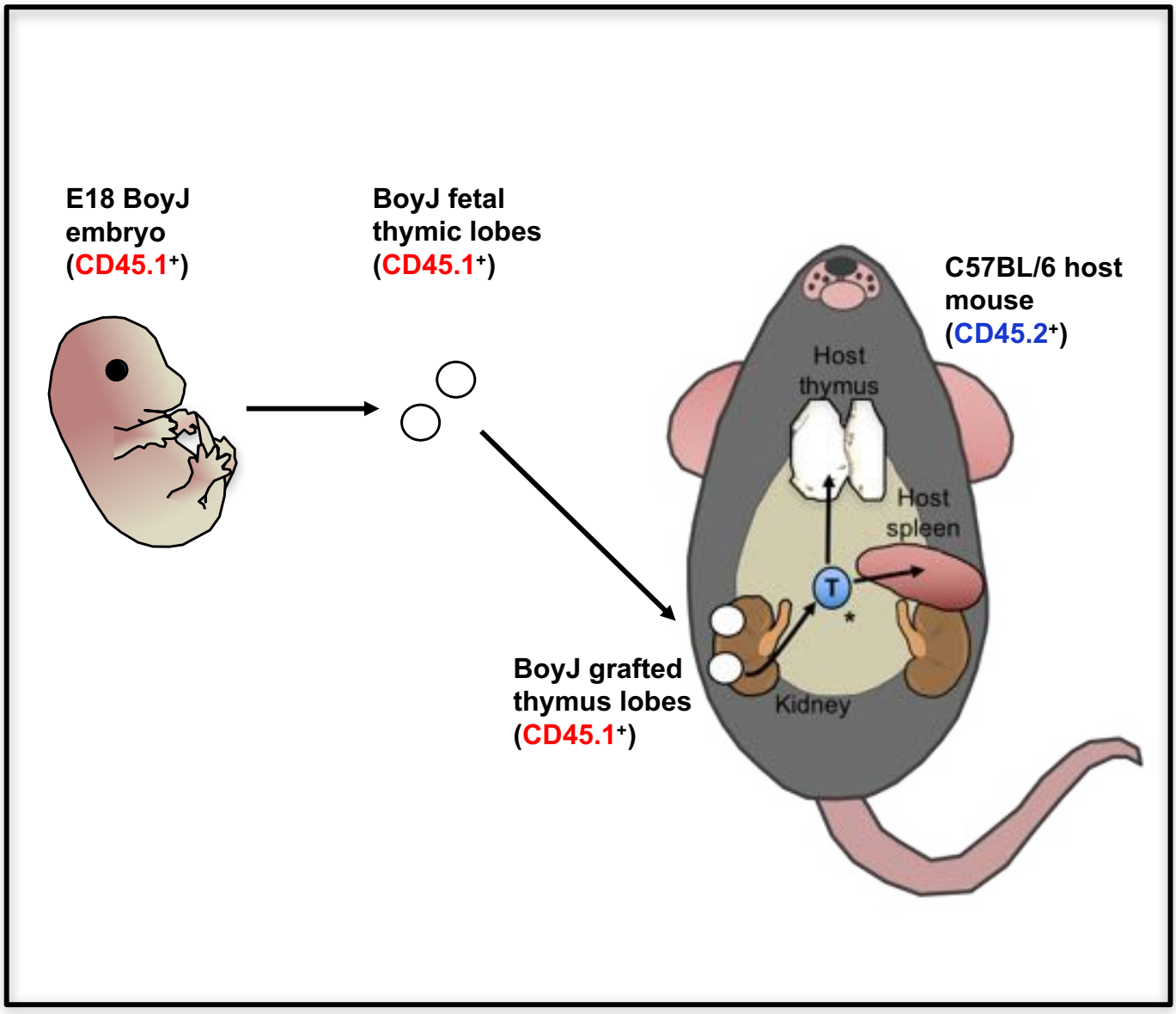
E18 BoyJ embryo (CD45.1+)
BoyJ fetal thymic lobes (CD45.1+)
C57BL/6 host mouse (CD45.2+)
Host thymus
Host spleen
T
Kidney
BoyJ grafted thymus lobes (CD45.1+)

Figure 4.19: A model to measure thymic recirculation

For the investigation of the capacity of peripheral T-cells to home to the thymus, thymic lobes were isolated from E18 BoyJ embryos ($CD45.1^+$), and surgically transplanted fresh under the kidney capsule of mice on the C57BL/6 background ($CD45.2^+$), including wildtype mice, as well as *Aire*$^{-/-}$, *Nos2*$^{-/-}$ and DKO strains. $CD45.1^+$ graft derived T-cells (*) emigrate from the graft, and are subsequently detectable in the thymus and spleen of host mice after a period of 6 weeks post-transplantation.

the thymus of *Nos2*$^{-/-}$ host mice (Figure 4.18D-E). Similarly, the proportion and number of re-circulating total and Foxp3^{+} CD4 T-cells was comparable between *Aire*$^{-/-}$ and DKO mice (Figure 4.18D-E). Importantly, the proportion and number of total and Foxp3^{+} CD45.1^{+} cells detected in the spleen of host mice was not significantly different between the various models (although the proportion of CD45.1^{+} cells was slightly raised in *Aire*$^{-/-}$ spleens, this did not correlate with a significant difference in absolute numbers, Figure 4.18F-G). Hence, we can conclude that re-circulation of peripheral T-cells is Aire-dependent, but occurs independently of iNOS expression, and hence the increase in Qa2^{hi} SP4 thymocytes we observe in *Nos2*$^{-/-}$ thymus is not the result of an influx of phenotypically mature peripheral T-cells.

A recent publication has shed new light on the nature of the intrathymic maturation of SP thymocytes. Rather than a firm guide of maturational status, Qa2 has been suggested to represent an interferon-dependent gene, up-regulated in response to signaling through the interferon alpha receptor (IFNAR) (Xing et al., 2016). *Ifnar*$^{-/-}$ mice have normal numbers of SP4 thymocytes, however they fail to up-regulate Qa2 (Xing et al., 2016). Hence, a new system for identifying maturational status has emerged (summarized in Figure 4.14), wherein SP thymocytes can be divided on the basis of expression of MHC-I and CD69 into the following subsets; semi-mature (SM, CD69^{+}MHC-I^{-}), mature 1 (M1, CD69^{+}MHC-I^{+}) and mature 2 (M2, CD69^{-}MHC-I^{+}) (Xing et al., 2016). Development by these parameters is un-perturbed by the absence of IFNAR signaling, and hence we were interested to apply this system to our Aire/iNOS deficient strains as a definitive analysis of maturation. By this method of analysis (gating strategy Figure 4.20A), we observed no differences in the proportion or number of the

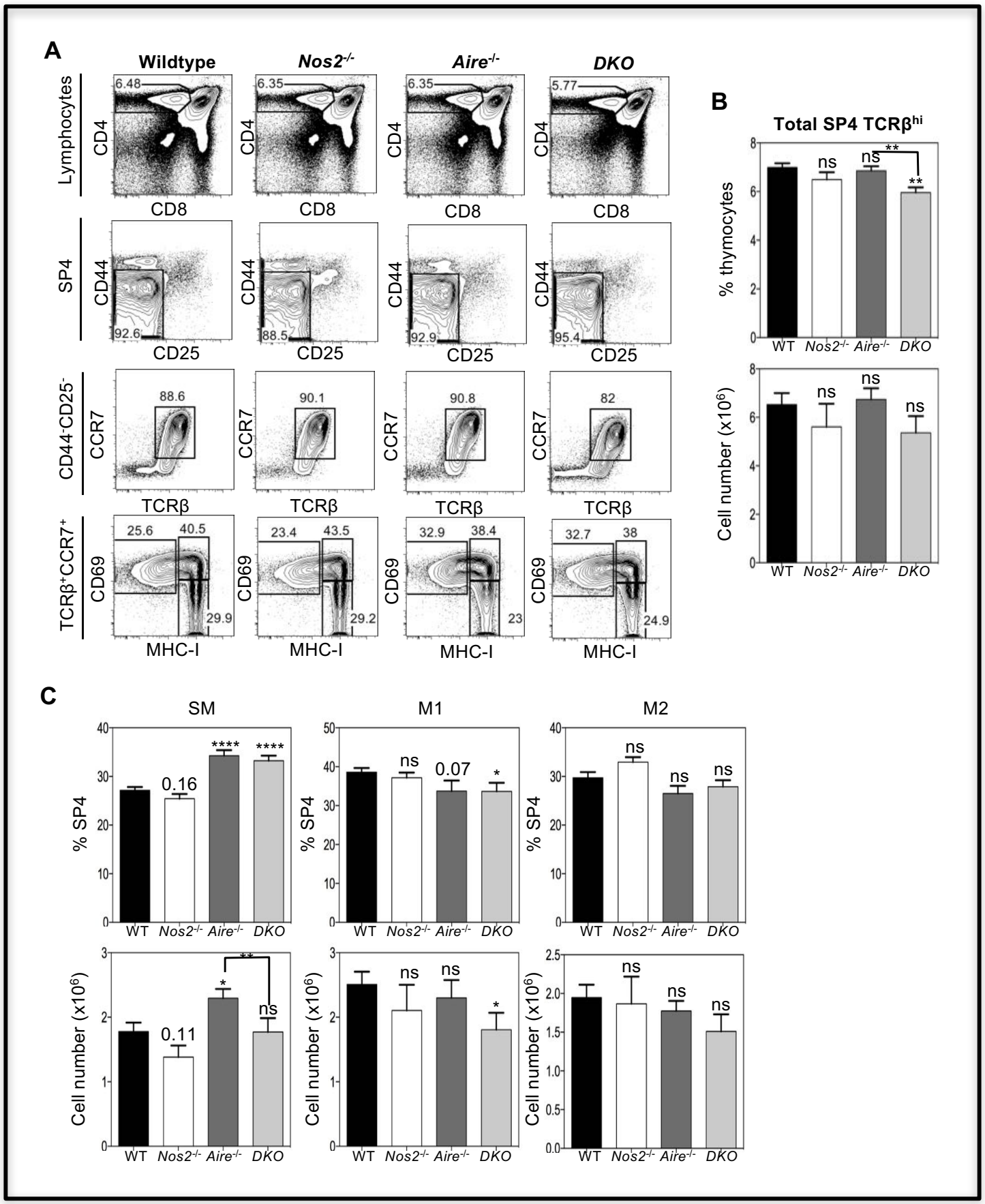
A
Wildtype
Nos2-/-
Aire-/-
DKO
Lymphocytes
CD4
CD8
6.48
6.35
6.35
5.77
SP4
CD44
CD25
92.6
88.5
92.9
95.4
CD44-CD25-
CCR7
TCRβ
88.6
90.1
90.8
82
TCRβ+CCR7+
CD69
MHC-I
25.6
40.5
29.9
23.4
43.5
29.2
32.9
38.4
23
32.7
38
24.9
B
Total SP4 TCRβhi
% thymocytes
Cell number (x10^6)
ns
**
WT
Nos2-/-
Aire-/-
DKO
C
SM
M1
M2
% SP4
Cell number (x10^6)
0.16
0.07
0.11
****
*
ns

Figure 4.20: Development of SM, M1 and M2 thymocytes not severely impacted by Aire and iNOS

(A) Gating strategy for the analysis of maturational subsets in non-GFP mice, where subsets were defined as semi-mature (SM, $CD69^{+}MHC\text{-}I^{-}$), mature 1 (M1, $CD69^{+}MHC\text{-}I^{+}$) and mature 2 (M2, $CD69^{-}MHC\text{-}I^{+}$).

(B) Quantitation of total SP4 thymocytes in wildtype, *Nos2*$^{-/-}$, *Aire*$^{-/-}$ and DKO mice (n=10 wildtype, 6 *Nos2*$^{-/-}$, 8 *Aire*$^{-/-}$ and 8 DKO mice).

(C) Quantitation of SM, M1 and M2 subsets.

Statistics were obtained using unpaired students t-tests, where * = $P<0.05$, ** = $p<0.01$.

most mature M2 subset in either *Nos2*$^{-/-}$ or *Aire*$^{-/-}$ mice (Figure 4.20A-C), suggesting Qa2 levels to be misleading in identifying terminally matured SP4 populations. We did, however, see a slight accumulation of SM SP4s in the thymus of *Aire*$^{-/-}$ mice, corresponding with a slight reduction in the percentage (but not number) of cells present at the M1 stage. In proportional terms, we saw no differences between *Aire*$^{-/-}$ and DKO mice; however, the number of SP4 was slightly but non-significantly reduced in DKO mice (Figure 4.20B). As a consequence, the number of SM cells was restored to an equivalent value to the wildtype, and the reduction in cells at the M1 stage was significant relative to the wildtype (Figure 4.20C), potentially suggesting either reversal of the slight block in the early stages of SP4 maturation seen in *Aire*$^{-/-}$ mice, or iNOS-dependent survival in the early stages. Regardless, as the total number of M2 cells was equal in each of the 4 strains (Figure 4.20C), our data would suggest no major perturbations in the generation of mature SP4 thymocytes in the absence of Aire and iNOS.

To further assess SP thymocyte maturation in *Aire*$^{-/-}$ and *Nos2*$^{-/-}$ mice, we crossed both strains to the Rag-2p-GFP background. As reported, GFP levels were reduced with increasing maturity (gating strategy Figure 4.21A), with SM cells possessing the highest, and M2 cells the lowest MFI for GFP (Figure 4.21B-C). This trend was matched in *Aire*$^{-/-}$ mice, and we noted no difference in the MFI of GFP at each maturational stage (Figure 21B), perhaps suggesting that the minor alterations in early development are not the result of a block. In fact, the only major difference between wildtype and *Aire*$^{-/-}$ SP4 detectable was the absence of Qa2 expression, which was significantly up-regulated from the M1 stage in wildtype, but not *Aire*$^{-/-}$ thymocytes (Figure 4.21C). Equally, the output

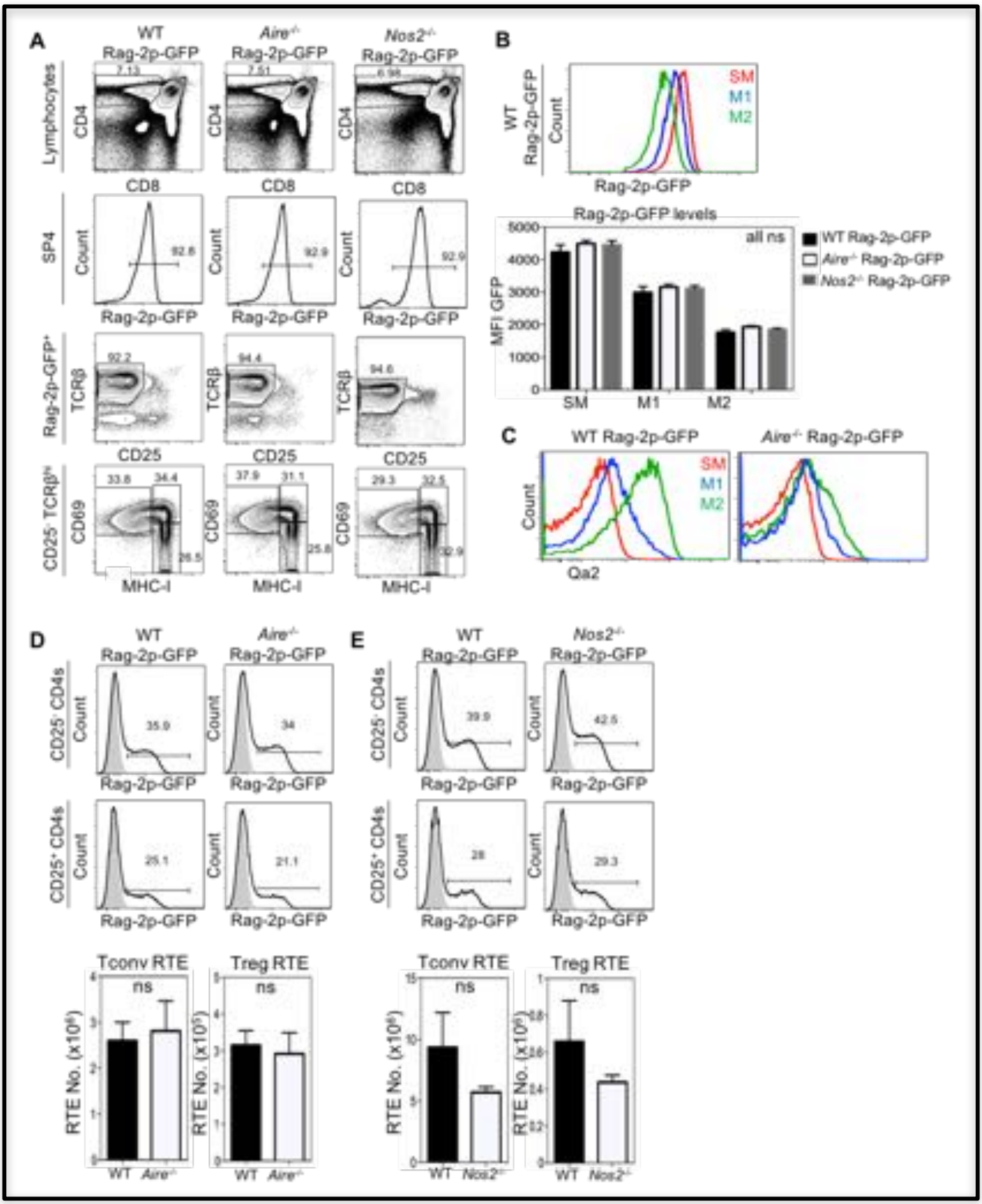
A
WT Rag-2p-GFP
Aire-/- Rag-2p-GFP
Nos2-/- Rag-2p-GFP
Lymphocytes
CD4
SP4
CD8
Count
Rag-2p-GFP
Rag-2p-GFP+
TCRβ
CD25- TCRβhi
CD69
CD25
MHC-I
B
WT Rag-2p-GFP
Count
SM
M1
M2
Rag-2p-GFP levels
all ns
MFI GFP
WT Rag-2p-GFP
Aire-/- Rag-2p-GFP
Nos2-/- Rag-2p-GFP
C
WT Rag-2p-GFP
Aire-/- Rag-2p-GFP
Qa2
D
CD25- CD4s
CD25+ CD4s
Tconv RTE
Treg RTE
RTE No. (x10^6)
RTE No. (x10^5)
ns
WT
Aire-/-
E
Nos2-/-
RTE No. (x10^6)

Figure 4.21: T-cell development in *Aire*$^{-/-}$ and *Nos2*$^{-/-}$ Rag-2p-GFP mice proceeds normally in quantitative terms

(A) Gating strategy for the analysis of maturational subsets in wildtype, *Aire*$^{-/-}$ and *Nos2*$^{-/-}$ Rag-2p-GFP mice. Subsets were defined as semi-mature (SM, CD69^{+}MHC-I^{-}), mature 1 (M1, CD69^{+}MHC-I^{+}) and mature 2 (M2, CD69^{-}MHC-I^{+})

(B) Mean fluorescence intensity (bottom) and histogram representation (top) of GFP levels in SM (red), M1 (blue) and M2 (green) developmental subsets in wildtype, *Nos2*$^{-/-}$ and *Aire*$^{-/-}$ Rag-2p-GFP mice.

(C) Histogram showing Qa2 expression in SM, M1 and M2 developmental subsets of wildtype and *Aire*$^{-/-}$ Rag-2p-GFP mice.

(D-E) Quantitation of conventional (CD25^{-}) and T-Reg (CD25^{+}) GFP^{+} CD4 RTE in the spleen of wildtype, as well as *Aire*$^{-/-}$ Rag-2p-GFP (D) and *Nos2*$^{-/-}$ Rag-2p-GFP (E) mice. Filled histograms represent GFP- control mice. Mice were aged between 8-12 weeks of age (D) or 6-8 weeks of age (E).

Statistics were obtained using unpaired students t-tests.

of T-cells from both conventional and T-Reg lineages – quantified as $CD25^-$ or $CD25^+$ GFP^+ RTE – was the same between wildtype and *Aire*$^{-/-}$ Rag-2p-GFP mice (Figure 4.21D). These findings were matched in *Nos2*$^{-/-}$ mice, in which again thymocytes had normal levels of GFP (Figure 4.21B), and normal numbers of RTE were present (Figure 4.21E). As it has recently been reported that intrathymic maturation plays an important role in modulating the responsiveness of T-cells to TCR stimulation (Xing et al., 2016), we were interested to assess this process in thymocytes from *Aire*$^{-/-}$ mice from a functional standpoint. By the M1 stage, thymocytes are able to proliferate in response to TCR triggering, whereas licensing to express inflammatory cytokines occurs at the M2 stage of development (Xing et al., 2016). To assess the functional capacity of *Aire*$^{-/-}$, *Nos2*$^{-/-}$ and DKO thymocytes, firstly total thymocytes were stimulated for 6 hours with anti-CD3/28 antibodies, and stained for TNFα. We report production of TNFα in wildtype thymocytes at both the M1 and M2 phases of development, but not SM cells (Figure 4.22A). In comparison, *Aire*$^{-/-}$ and *Nos2*$^{-/-}$ thymocytes were relatively poor at producing cytokines, with only ~50% as many $TNF\alpha^+$ cells at the M1 and M2 stages as was observed in the wildtype (Figure 4.22A-B). Combined deficiency of Aire and iNOS resulted compounded the defect in cytokine production, with only ~30% as high a proportion of M1/M2 cells positive for detectable TNFα production (Figure 4.22A-B). Next, we purified the SM, M1 and M2 populations (Figure 4.22C) from wildtype and *Aire*$^{-/-}$ mice, and stimulated cell-trace violet (CTV) labelled cells for 3 days in the presence of anti-CD3/28. In contrast to the findings by Xing et al., we observed substantial proliferation among the SM population in response to stimulation, albeit these cells had undergone fewer divisions than the more

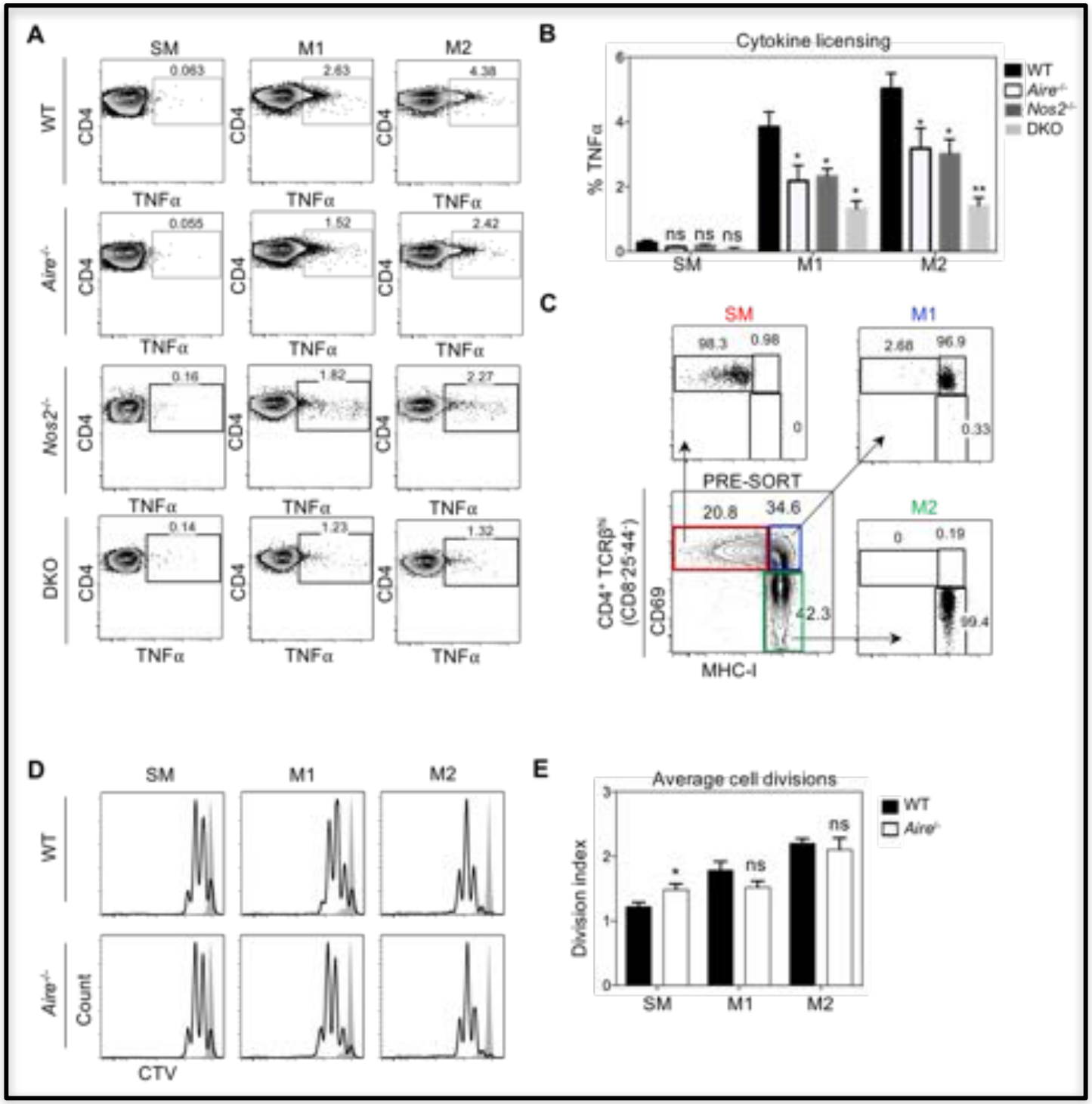
A
SM
M1
M2
WT
Aire-/-
Nos2-/-
DKO
CD4
TNFα
0.063
2.63
4.38
0.055
1.52
2.42
0.16
1.82
2.27
0.14
1.23
1.32
B
Cytokine licensing
% TNFα
WT
Aire-/-
Nos2-/-
DKO
ns
ns
ns
SM
M1
M2
C
SM
M1
M2
98.3
0.98
0
2.68
96.9
0.33
PRE-SORT
20.8
34.6
42.3
0
0.19
99.4
CD4+ TCRβhi (CD8-25-44-)
CD69
MHC-I
D
SM
M1
M2
WT
Aire-/-
Count
CTV
E
Average cell divisions
Division index
WT
Aire-/-
ns
ns
SM
M1
M2

Figure 4.22: Aire is required for full functional maturation of SP4 thymocytes

(A) Analysis of TNFα production by SM, M1 and M2 subsets of wildtype, *Aire*$^{-/-}$, *Nos2*$^{-/-}$ and DKO mice upon anti-CD3/28 stimulation of total thymocytes for 6 hours (n=13 WT, 8 *Aire*$^{-/-}$, 6 *Nos2*$^{-/-}$ and 3 DKO).

(B) Proportion of cells from SM, M1 and M2 subsets producing TNFα after 6 hours of stimulation.

(C) Purities of sorted populations of SM, M1 and M2 SP4 thymocytes,

(D) Proliferation of cell trace violet (CTV)-loaded isolated thymocytes after 3 days in culture with plate-bound anti-CD3 and anti-CD28 – plots represent live (PI negative cells).

(E) Average cell divisions per population, inclusive of non-divided cells (division index).

Statistics were obtained using unpaired students t-tests, where *=P<0.05, ** = p<0.01.

mature M1 and M2 thymocytes as determine by the division index (Figure 4.22D-E). We saw no major differences between the proliferative potentials of isolated wildtype and *Aire*$^{-/-}$ thymocytes; although *Aire*$^{-/-}$ SM cells had undergone slightly more divisions (Figure 4.22D-E), Aire appears to be un-important for the acquisition of the capacity to divide in response to TCR triggering.

As Qa2 expression has been linked to type 1 interferon signaling in the thymus, we investigated the possibility that Aire and iNOS may regulate this process. IFNAR expression was detectable on the majority of SP4 thymocytes, and was slightly up-regulated at the M1 phase of development where Qa2 up-regulation occurs (Figure 4.23A). Expression was also detected to an equal extent on *Aire*$^{-/-}$ SP4 thymocytes, suggesting *Aire*$^{-/-}$ thymocytes to be receptive to signaling by type 1 interferons (Figure 4.23A). Next, sorted TEC populations from wildtype, *Aire*$^{-/-}$ and *Nos2*$^{-/-}$ mice were assessed by fix-point PCR for expression of IFNβ. *Ifnb1* transcript was detectable in mTEC^{hi} from wildtype mice (but not cTEC or mTEC^{lo}); however, expression was lost in *Aire*$^{-/-}$ mTEC^{hi}, and appeared to be up-regulated in *Nos2*$^{-/-}$ mice, suggesting IFNβ expression to correlate with the expression of Qa2 by SP thymocytes (Figure 4.23B). To determine whether Qa2 is induced by IFNβ signaling, we cultured sorted SM, M1 and M2 cells in the presence of IFNβ for 3 days, before staining for Qa2 expression. We saw no induction of Qa2 in any of the populations assessed, suggesting IFNβ stimulation in isolation to be insufficient (Figure 4.23C). In addition to Qa2, the expression of MHC-I by CD69^{-} thymocytes was slightly reduced in *Aire*$^{-/-}$ mice, and again partially restored by the co-deletion of *Nos2* (Figure 4.23D). In contrast to Qa2, MHC-I was inducible by IFNβ stimulation in

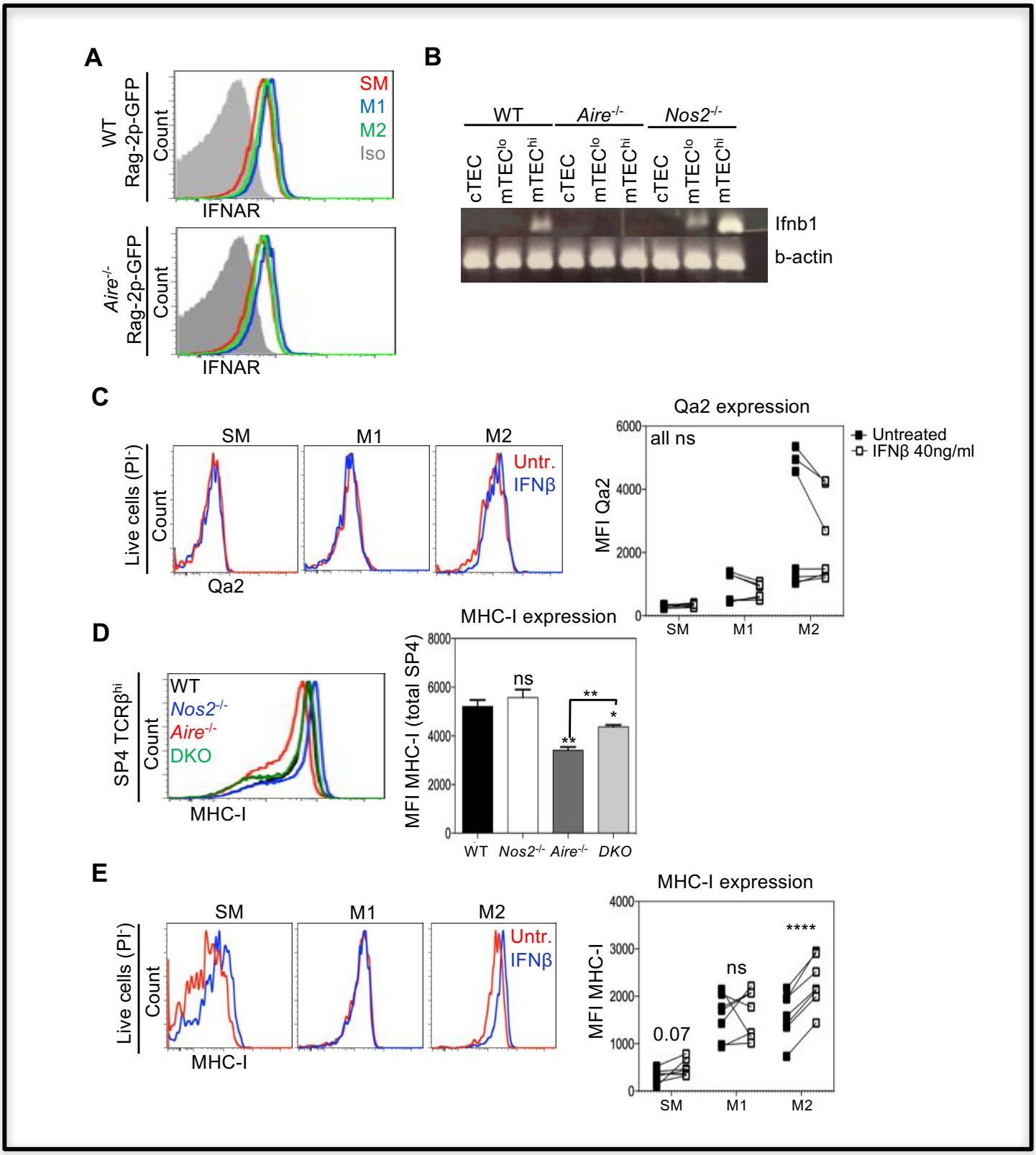
A
WT Rag-2p-GFP
Count
SM
M1
M2
Iso
IFNAR
Aire-/- Rag-2p-GFP
Count
IFNAR
B
WT
Aire-/-
Nos2-/-
cTEC
mTEClo
mTEChi
cTEC
mTEClo
mTEChi
cTEC
mTEClo
mTEChi
Ifnb1
b-actin
C
SM
M1
M2
Live cells (PI-)
Count
Untr.
IFNβ
Qa2
Qa2 expression
all ns
MFI Qa2
6000
4000
2000
0
SM
M1
M2
Untreated
IFNβ 40ng/ml
D
SP4 TCRβhi
Count
WT
Nos2-/-
Aire-/-
DKO
MHC-I
MHC-I expression
MFI MHC-I (total SP4)
8000
6000
4000
2000
0
ns
**
**
*
WT
Nos2-/-
Aire-/-
DKO
E
SM
M1
M2
Live cells (PI-)
Count
Untr.
IFNβ
MHC-I
MHC-I expression
MFI MHC-I
4000
3000
2000
1000
0
0.07
ns
****
SM
M1
M2

Figure 4.23: *Aire*$^{-/-}$ mice may have reduced IFNβ signaling as a result of reduced tonic expression by TEC

(A) IFNAR expression in thymocytes from wildtype and *Aire*$^{-/-}$ Rag-2p-GFP mice.

(B) Fix-point PCR analysis of Ifnb1 gene expression in sorted cTEC, mTEC^{hi} and mTEC^{lo} populations from wildtype, *Nos2*$^{-/-}$ and *Aire*$^{-/-}$ mice.

(C) Histograms showing Qa2 expression in sorted populations of SM, M1 and M2 cultured for 3 days in medium (red line) or in the presence of 40ng/ml recombinant IFNβ (blue line).

(D) Histogram and mean fluorescence intensity of MHC-I in CD69^{+} SP4 from wildtype, *Nos2*$^{-/-}$, *Aire*$^{-/-}$ and DKO mice.

(E) MHC-I expression in sorted populations of SM, M1 and M2 cultured for 3 days in medium or in the presence of 40ng/ml recombinant IFNβ.

Statistics were obtained using unpaired (D) or paired (C, E) students t-tests, where **** = $p<0.0001$.

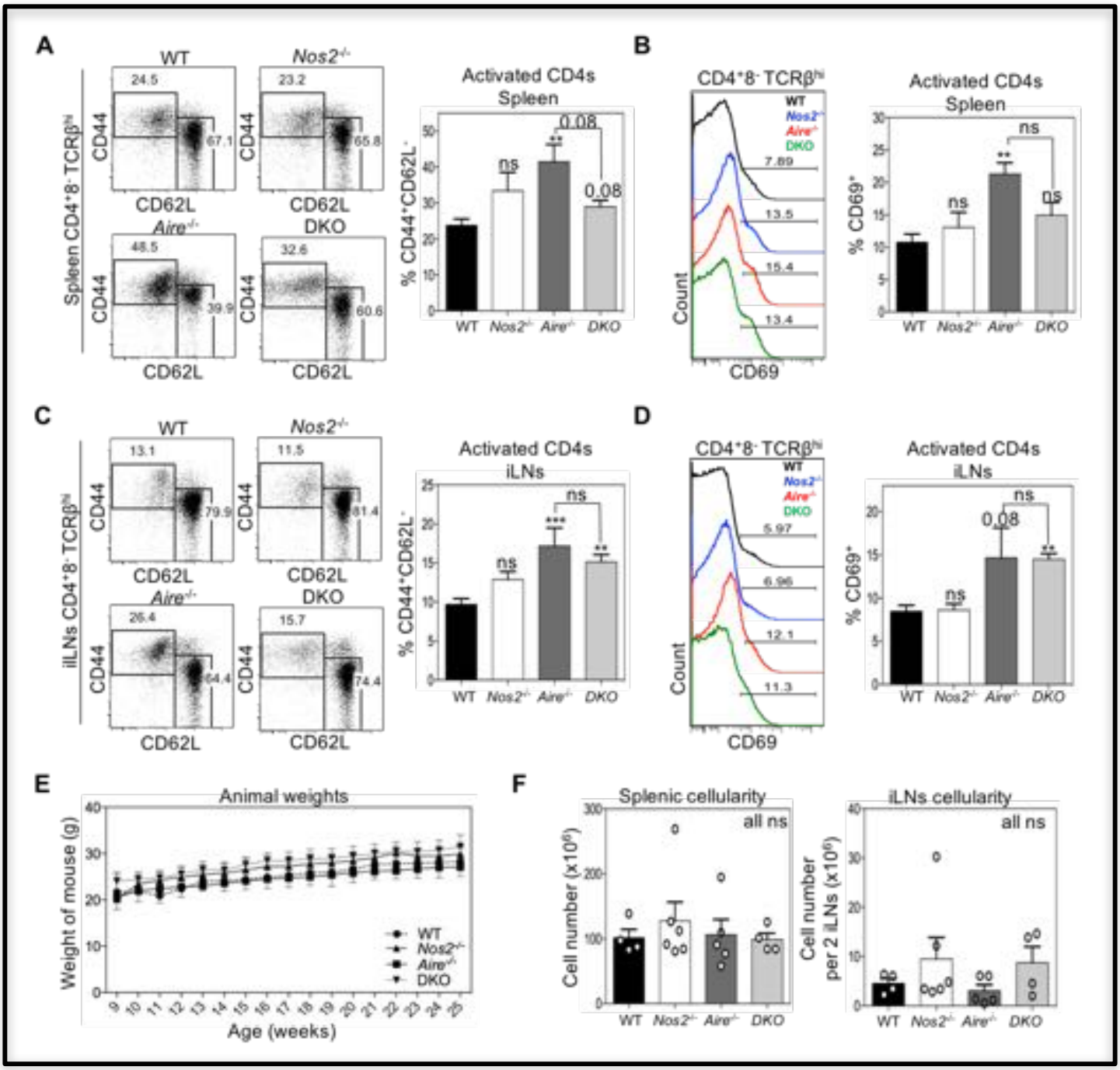
A
WT
Nos2-/-
Aire-/-
DKO
Spleen CD4+8- TCRβhi
CD44
CD62L
24.5
67.1
23.2
65.8
48.5
39.9
32.6
60.6
Activated CD4s
Spleen
% CD44+CD62L-
ns
0.08
0.08
B
CD4+8- TCRβhi
Count
CD69
7.89
13.5
15.4
13.4
Activated CD4s
Spleen
% CD69+
C
iILNs CD4+8- TCRβhi
13.1
79.9
11.5
81.4
26.4
64.4
15.7
74.4
Activated CD4s
iLNs
D
5.97
6.96
12.1
11.3
Activated CD4s
iLNs
0.08
E
Animal weights
Weight of mouse (g)
Age (weeks)
F
Splenic cellularity
all ns
Cell number (x10^6)
iLNs cellularity
all ns
Cell number per 2 iLNs (x10^6)

Figure 4.24: iNOS deficiency does not compound autoimmunity in *Aire*$^{-/-}$ mice

(A, C) Analysis of activated CD4^{+} (A) splenic and (C) inguinal lymph node T-cells from 6 month old wildtype, *Nos2*$^{-/-}$, *Aire*$^{-/-}$ and DKO mice, where activated cells are CD44^{+}CD62L^{-}.

(B, D) Expression of the activation marker CD69 by (B) splenic and (D) inguinal lymph node CD4^{+} T-cells.

(E) Weights of mice over time (g).

(F) Total cellularity of spleen and inguinal lymph nodes.

Statistics were obtained using unpaired students t-tests, where ** = $p<0.01$, *** = $p<0.001$. n= 4 wildtype, 6 *Nos2*$^{-/-}$, 5 *Aire*$^{-/-}$ and 4 DKO mice.

SM and M2 thymocytes (Figure 4.23E), suggesting the reduced MFI for MHC-I to be the direct result of the absence of IFNAR signaling.

Lastly, we aimed to address the consequences of *Nos2*-deficiency in terms of tolerance. C57BL/6 *Aire*$^{-/-}$ mice have a mild tissue-specific auto-immune phenotype which is detectable by 6 months of age (Anderson et al., 2002), and hence we aged wildtype, *Nos2*$^{-/-}$, *Aire*$^{-/-}$ and DKO animals in order to assess the development of auto-immunity. Splenic and inguinal lymph node (iLN) CD4 T-cells were stained for the activation markers CD44 and CD69 to assess the degree of auto-immunity in each mouse model. The proportion of activated T-cells defined as either CD44^{hi}CD62^{lo}, or CD69^{+} was increased in both the spleen and iLNs of *Aire*$^{-/-}$ mice relative to wildtype controls (Figure 4.24A-D). No T-cell activation above base-line was observed in *Nos2*$^{-/-}$ mice, suggesting iNOS expression by mTEC to be redundant in tolerance induction in CD4 T-cells (Figure 4.24A-D). Interestingly, the proportion of activated T-cells in the spleen of aged DKO mice was reduced relative to *Aire*$^{-/-}$ controls (Figure 4.24A-B), although activated T-cells were still detectable in the iLNs (Figure 4.24C-D). This may suggest a slightly milder auto-immune phenotype in DKO mice, however this is likely complicated by the fact iNOS is expressed by a variety of cell types under inflammatory conditions, and hence may not be a reflection of altered thymic selection. Regardless, all mice survived until 6 months of age with no severe auto-immunity as determined by loss of weight (Figure 4.24E). Although all spleens were comparable in size, enlargement of the iLNs was detected in 2/6 *Aire*$^{-/-}$ mice, and 2/4 DKO mice (Figure 4.24F), which was in all cases accompanied by mild alopecia. These data are consistent with a mild and

variable autoimmune phenotype in *Aire*$^{-/-}$ mice, which is not significantly impacted by iNOS-deficiency.

4.3. Discussion

We have observed for the first time the constitutive expression of inducible nitric oxide synthase in the thymus within a sub-population of mTEC^{hi} under steady state conditions. Previous studies have noted iNOS expression in thymic stroma through collection of adherent cells in culture (Aiello et al., 2000), or through PCR analysis of dGuo treated FTOC (Hager-Theodorides et al., 2009). In the former study, MHC-II^{hi} cells suggested to be thymic DC were shown to strongly express iNOS by FACS analysis; however, in cells stained *ex vivo* without culturing, we saw no constitutive expression of iNOS protein in any thymic DC sub-population, or thymic resident cells other than mTEC^{hi}. Hence, it seems likely that either the adherent cell populations collected were contaminated substantially with mTEC, or the DC isolated became activated by the repeated plastic adherence cultures involved in their isolation. In the latter study, *Nos2* expression in cultured stroma (in addition to expression of *Cxcl9* and *Rbp*) was determined to occur in a manner dependent on the Hedgehog responsive transcription factor Gli3 (Hager-Theodorides et al., 2009). However, we noted little expression of iNOS protein in mTEC isolated after dGuo treatment, where iNOS^{+} mTEC were shown to be inducible upon stimulation with anti-Rank antibody, but not anti-Ltbr; hence, it would appear unclear whether iNOS expression is Gli3 dependent in the adult state. Interestingly, suppression of the Hedgehog signalling pathway by neutralizing antibody resulted in a substantial Gli3-dependent increase in *Nos2* mRNA (Hager-Theodorides et al., 2009), suggesting this pathway to negatively regulate *Nos2* expression by mTEC. We have demonstrated iNOS to be similarly negatively regulated in adult mTEC by

the transcription factor Aire; however, it would seem likely the mechanisms are distinct, as Cxcl9 is an Aire-dependent chemokine receptor ligand (Anderson et al., 2005), and was shown to be similarly Gli3-dependent, but unaffected by inhibition of the Hedgehog pathway (Hager-Theodorides et al., 2009). Equally, mice deficient in the Hedgehog family member Sonic Hedgehog have been shown to have major defects in the development of both cTEC and mTEC, with Aire^{+} cells particularly effected (Saldana et al., 2016). Further research would be required to determine whether Aire directly regulates *Nos2* gene expression, or whether the increase in iNOS^{+} mTEC in *Aire*$^{-/-}$ mice is a secondary consequence. It is interesting also to note that the mechanisms controlling constitutive expression of iNOS in thymic stroma are completely distinct from those that induce expression in inflammatory conditions peripherally. Induction of iNOS expression in a variety of cell types, including FRCs (Lukacs-Kornek et al., 2011), dendritic cells (Serbina et al., 2003), MDSCs (Movahedi et al., 2008), macrophages (Karupiah et al., 1993) and astrocytes (Lee et al., 1993), has been shown to be completely abrogated in the absence of inflammatory cytokine signalling by IFNγ and TNFα. In stark contrast, iNOS^{+} mTEC are present in completely normal numbers in *Ifng*$^{-/-}$ mice, and mice deficient in Tnfr1/2. It hence seems likely that iNOS expression is part of the mTEC maturational programme as triggered by Rank signalling, rather than a product of inflammatory micro-environments within the medulla. iNOS expression is observed under similar conditions on the maturation of B-cells to antibody-secreting plasma cells. Here iNOS acts as a signalling mediator, which positively regulates the Xbp1s-dependent arm of the unfolded protein response, promoting plasma cell homeostasis and survival. However, although we noted UPR

activation in adult TEC, we both failed to establish a link between mTEC-derived iNOS and this pathway, and found no essential role for Xbp1s in mTEC homeostasis.

The second section of our study focussed on the direct effects of iNOS on the generation of T-cell subsets within the thymus. Interest in thymic iNOS expression had initially focussed on the capacity for NO to potently induce apoptosis of DP thymocytes in culture (Tai et al., 1997), however we could detect no increase in the numbers of DP thymocytes, nor changes in the rate of apoptosis in *Nos2*$^{-/-}$ mice. This is likely unsurprising, as iNOS expression appears to be restricted to the medulla, and although it is possible the effects of nitrosylated proteins could extend to the cortex, as NO readily dissipates (Lancaster, 1994), induction of apoptosis by nitrosative stress would require immediate vicinity to an iNOS^{+} cell type. Equally, we saw no changes in the total number of SP thymocytes, which again had normal rates of apoptosis. Proliferation of thymocytes was also unchanged in the absence of iNOS, suggesting unlike peripheral iNOS-expressing stroma, mTEC do not utilise this mechanism to restrain TCR-mediated expansion. The medulla is an important site for the generation of non-conventional T-cell subsets, including T-Reg, iNKT, Th17 and γδ T-cells (Cowan et al., 2015, Jenkinson et al., 2015), and T-cell derived iNOS expression has been shown to regulate the *in vitro* induction of T-Reg, Th17 and the activity of RORγt (Jianjun et al., 2013), but we saw no alterations in the development of these cells in *Nos2*$^{-/-}$ thymi. Hence, iNOS does not appear to play an important role in the thymus in terms of T-cell generation.

Multiple methods have been defined in order to characterise phenotypic maturation of SP thymocytes in the medulla. SP4s have been divided into

immature and mature subsets, as evidenced by GFP dilution in Rag-2p-GFP reporter mice, on the basis of expression of cell surface markers, such as CD69, Qa2, HSA, and CD62L and the chemokine receptors CCR7 and CCR9 (summarized in Figure 4.14). By these parameters, we were able to correlate iNOS expression by mTEC with the maturational status of SP4s, as Qa2 expression was not only up-regulated in mature thymocytes from *Nos2*$^{-/-}$ thymi, but also almost completely lost in thymocytes from *Aire*$^{-/-}$ mice, where iNOS is over-expressed. Co-deletion of iNOS in DKO mice lead to partial restoration of Qa2 expression, confirming this effect to be iNOS-dependent. However, a recent publication has cast doubt on the use of Qa2 as a marker of mature thymocytes (Xing et al., 2016). The latter stages of SP development are accompanied by the up-regulation of multiple interferon-dependent genes, including STAT1, Irf7 and Qa2 itself. *Ifnar*$^{-/-}$ mice, which are insensitive to signalling by type 1 interferons, have normal T-cell development, and normal numbers of peripheral T-cells, but SP thymocytes fail to up-regulate expression of Qa2 (Xing et al., 2016), suggesting maturation to be possible independent of Qa2 expression.

To circumvent this problem, the authors instead propose a new, definitive method for defining the maturational status of SP thymocytes using the surface marker MHC-I. By this method, SP thymocytes can be divided into semi-mature (SM, CD69^{+}MHC-I^{-}), 1st mature (M1, CD69^{+}MHC-I^{+}) and 2nd mature (M2, CD69^{-} MHC-I^{+}) populations, which correlate with the acquisition of proliferative competence in response to TCR stimulation (M1), and licensing for the production of cytokines, and the capacity for thymic egress (M2) (Xing et al., 2016). By this measure, T-cell development is completely normal in *Ifnar*$^{-/-}$ mice, and hence we were keen to use this knowledge to better define the impact of

Aire and iNOS on intrathymic maturation. Surprisingly, the development of M2 SP4 thymocytes was completely normal in *Aire*$^{-/-}$ and *Nos2*$^{-/-}$ mice, again supporting the notion that Qa2 is a poor marker of intrathymic maturation. Although the distribution of cells within the SM and M1 stages of development was altered slightly in the absence of Aire, this clearly had little impact on the development of mature thymocytes, nor the output of T-cells from the thymus, which was again normal. It is possible that the accumulation of cells at the SM stage is either the result of their requirement for TCR signalling for progression to the M1 stage, or alternatively defective negative selection of immature SP4 thymocytes in the absence of Aire-dependent TRAs. This could be investigated by analysing the consequences of deletion of other important regulators of TRA expression, such as Fezf2 on intrathymic maturation. It is instead possible that the fluctuation in Qa2 levels is controlled by Aire and iNOS at the level of IFNβ, which we found to be constitutively expressed by mTEC^{hi} in wildtype, but not *Aire*$^{-/-}$ mice, and increased in TEC in the absence of iNOS. However, TEC from DKO mice would need to be sorted to correlate the partial restoration of Qa2 expression with levels of mTEC-derived IFNβ. This hypothesis is supported by our findings that levels of expression of MHC-I are to a lesser extent affected by the absence of iNOS and/or Aire, and treatment of isolated SP4 populations with IFNβ in vitro is sufficient to induce the up-regulation of MHC-I by SM and M2 cells. IFNβ treatment alone did not induce Qa2 expression by sorted SP4 populations from wildtype, or *Aire*$^{-/-}$ mice (not shown), however it is possible a secondary signal, such as simultaneous TCR triggering is required for this to occur, which could be proven through further culture assays. If this is the case, we can propose a model whereby iNOS inhibits IFNβ expression by mTEC, and

hence negatively regulates signalling through the IFNAR on developing SP4 thymocytes, which is required for their up-regulation of IFN-dependent genes such as Qa2. Regardless of the factors controlling Qa2 expression in *Aire*$^{-/-}$ and *Nos2*$^{-/-}$ mice, it is likely that important questions regarding the requirement for interaction with the medulla need to be readdressed. Firstly, a developmental relationship between the SM, M1 and M2 subsets needs to be proven via ontogenetic analysis, and intrathymic injection of sorted populations to track whether their development is sequential in the adult thymus. Secondly, our lab has previously reported intrathymic development to occur normally in the absence of the medulla by using mice grafted with mTEC-deficient, *Relb*$^{-/-}$ thymi, however, it is unclear whether this holds up with regards to the new parameters of phenotypic and functional intrathymic development laid out by Xing et al. In this study, although we found that the production and maturation of thymocytes in *Nos2*$^{-/-}$ and *Aire*$^{-/-}$ mice was normal in numerical terms, cells at the M1 and M2 stages of development produced less TNFα in response to stimulation with plate-bound anti-CD3/28 than wildtype SP4. Despite only assessing *Aire*$^{-/-}$ SP4s for proliferative capacity, this was ostensibly normal in sorted SM, M1 and M2 subsets, and hence it is possible that only the very terminal stages of functional maturation may be perturbed in the absence of mTEC expression of Aire and iNOS.

5. DISCUSSION

5.1. Background and overall aims

The microenvironment provided to developing thymocytes by the antigen presenting cells of the thymic medulla has been shown to be of critical importance for the establishment of tolerance, and the prevention of T-cell mediated autoimmunity. SP thymocytes formed in the cortex migrate to the medulla (Ueno et al., 2004) where central tolerance is achieved through two major mechanisms; the deletion of auto-reactive T-cells from their ranks , and the generation of suppressive Foxp3^{+} T-Reg. In particular, mTEC are known to be central to the establishment of tolerance (Weih et al., 1995), and as such are highly specialized. Distinct mTEC subsets have been shown to express factors involved in the cortex:medulla trafficking of newly formed SP thymocytes (Lkhagvasuren et al., 2013), as well as negative selection itself. The latter subset possesses the unique capacity to, under the control of the transcription factors Aire (Zuklys et al., 2000) and Fezf2 (Takaba et al., 2015), generate an array of peptide antigens that mirrors those found in peripheral tissues in order to preferentially delete reactive, autoimmune T-cells from the thymocyte pool (Anderson et al., 2002). As mTEC play multiple important roles in tolerance induction, the signalling pathways mediating their homeostasis and functional maturation are of great interest. Multiple studies have shown the formation of mature mTEC to require signalling through the TNFR superfamily members Rank, Ltbr and CD40, the ligands for which are expressed by developing thymocytes (Rossi et al., 2007, Laan et al., 2009, Akiyama et al., 2008). However, the distinct requirements for each receptor, and the existence of negative

regulatory factors in the process of mTEC maturation have yet to be properly addressed. Our lab recently performed microarray analysis on isolated TEC sub-populations in an attempt to identify potential novel mediators of mTEC homeostasis, and in doing so revealed the distinct, high-level expression of two potentially functional genes by mature mTEC; namely *Tnfrsf11b*, the gene for osteoprotegerin, an inhibitor of Rank signalling in the thymus (Hikosaka et al., 2008), as well as *Nos2*, the product of which is the inducible isoform of nitric oxide synthase, an enzyme known to have powerful and varied immunomodulatory effects (Bogdan, 2001, Bogdan, 2015). Hence, the broad aim of this study was to examine the role of these two functional molecules for the maintenance of medullary homeostasis, and the thymic production of tolerant, and functionally mature T-cell populations.

5.2. The effect of OPG and iNOS on medullary homeostasis

Consistent with the known dependence of mTEC maturational processes on signalling through the Rank receptor (Rossi et al., 2007), we found OPG-deficient *Tnfrsf11b*$^{-/-}$ mice to have a great increase in the proportion and number of mTEC^{hi}, including the subset that expresses Aire. Previously, mTEC^{lo} - which express high levels of CCL21 for the migration of SP thymocytes into the medulla - were found to be Ltbr-dependent (Lkhagvasuren et al., 2013); however, this population was also expanded significantly in *Tnfrsf11b*$^{-/-}$ mice. As we found the mTEC^{lo} population to contain significant numbers of Rank^{+} cells, and observed the induction of CCL21 expression to occur upon Rank stimulation in isolation,

this finding would suggest OPG to directly regulate the size of the functionally heterogeneous mTEC compartment under steady state conditions (summarized in Figure 5.1, top). A recent study traced the expansion of the mTEC compartment in *Tnfrsf11b*$^{-/-}$ mice to a period post-partum, as mTEC were present in normal numbers throughout embryonic development (Akiyama et al., 2014). Although we found OPG to be expressed in a minor population of mTEC in the embryo, it seems likely that OPG plays a comparatively minor role prior to birth. Post-partum, however, OPG^{+} mTEC^{hi} are greatly expanded as the medulla matures, and form approximately 50% of mTEC present in the newborn thymus, although this proportion is reduced in adulthood. Consistent with previous findings, we found *Tnfrsf11b*$^{-/-}$ mice to have an increase in mTEC from day 2 of development, however this increase was selective to mTEC^{hi}, and hence differed to findings in adult mice. Although analysis of Rank-Venus mice yielded no differences in the proportion of Rank^{+} cells among mTEC^{hi} and mTEC^{lo} in the adult state, it is possible that the disparity of effect relates to preferential Rank expression by mTEC^{hi} immediately post-partum. Equally, although the requirements for high-level Rank expression appear to include triggering of both the Ltbr (Baik et al., 2013, Mouri et al., 2011), and the Rank receptor itself, it is unclear whether a reciprocal relationship exists, and hence Rank signalling may be a necessity at an early stage for the up-regulation of Ltbr expression by mTEC^{lo}, as required for their functional maturation. One alternative explanation would be that a proportion of mTEC^{lo} could consist of terminally differentiated cells that have progressed through the Rank-dependent mTEC^{hi} stage controlled by OPG. These possibilities could be addressed through more careful ontogenetic analysis of TEC development in wildtype and *Tnfrsf11b*$^{-/-}$ mice. In either instance,

Tnfrsf11b$^{-/-}$

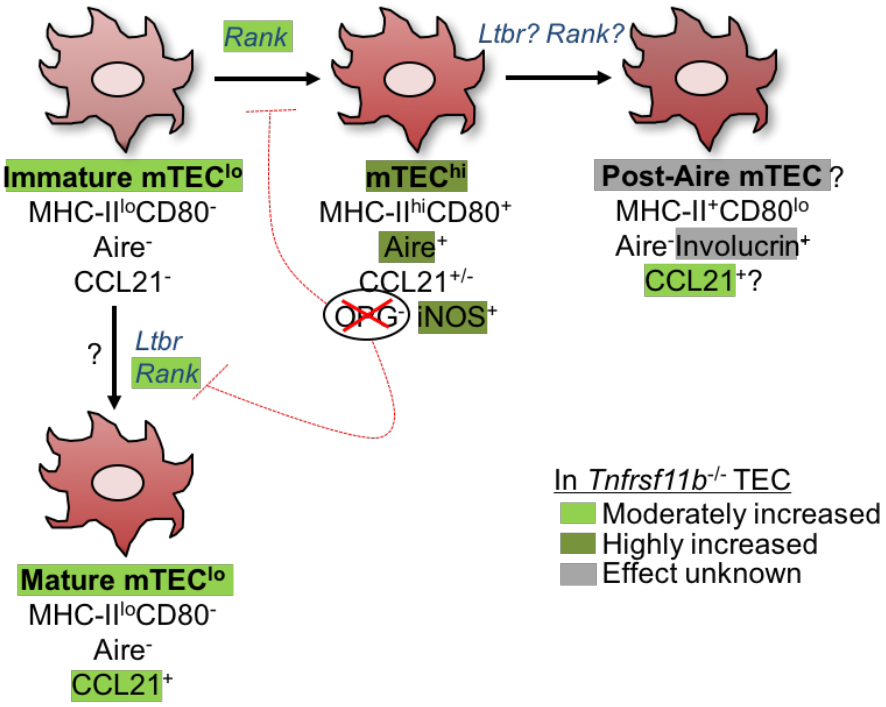

Aire$^{-/-}$

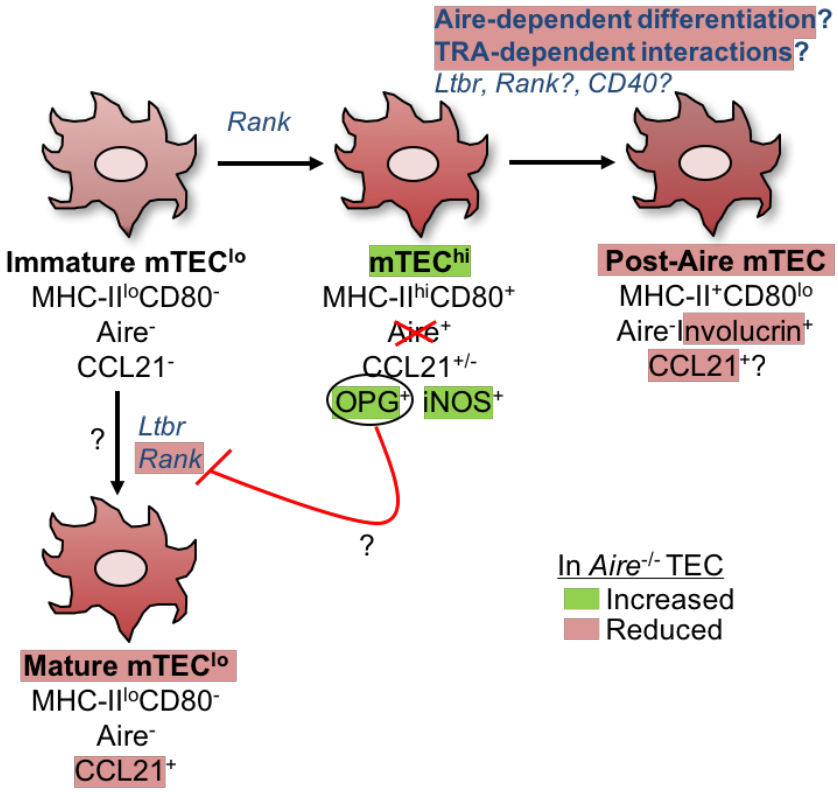

Figure 5.1: The impact of OPG and Aire on mTEC homeostasis

Top – The phenotype of mTEC in adult Tnfrsf11b-/- mice, where the absence of OPG-mediated negative regulation of Rank signaling leads to an increase in the TEC compartment as a whole, with a slight preferential increase in Aire^{+} mTEC^{hi}.

Bottom - The phenotype of mTEC in adult *Aire*$^{-/-}$ mice, in which functionally mature CCL21^{+} mTEC^{lo} are reduced in number (possibly as a result of OPG over-expression), as well as terminally mature involucrin^{+} mTEC, which may or may not form part of the same subset. mTEC^{hi} are preferentially expanded, most likely as a result of stalling in the mTEC developmental pathway in the absence of Aire.

it seems unlikely that the expansion of mTEC is simply the result of uncontrolled proliferation of this subset, as the proportion of Ki67^{+} cells among mTEC^{hi} and mTEC^{lo} was unaltered in *Tnfrsf11b*$^{-/-}$ TEC.

In line with our findings in OPG-deficient mice, *Aire*$^{-/-}$ mice have also been shown to have an expanded population of mTEC^{hi} (Yano et al., 2008). However, CCL21^{+} mTEC^{lo} are selectively reduced in *Aire*$^{-/-}$ TEC (Lkhagvasuren et al., 2013), suggesting Aire and OPG to regulate homeostasis via distinct mechanisms (summarized in Figure 5.1). Further experiments would be required to establish an understanding of the requirement for Aire in TEC development, as any precursor product relationship between Aire$^{+/-}$ mTEC^{hi} and CCL21$^{+/-}$ mTEC^{lo} is not well understood. It is certain that mTEC^{hi} can emerge from the mTEC^{lo} population both in vivo and in vitro, and CCL21^{+} mTEC^{lo} can be formed independently of mTEC^{hi} through Ltbr-triggering. It has also been determined through complex fate mapping models that loss of Aire expression defines a population of cells which are CD80^{lo} (Metzger et al., 2013, Wang et al., 2012), and positive for involucrin (Yano et al., 2008), a marker of terminal epithelial differentiation. The functional capacity of post-Aire mTEC is unknown, however if this population was found to contain a subset of CCL21^{+} cells, this would serve as an explanation for the Aire-dependent nature of CCL21 expression by mTEC^{lo}, which are uniformly Aire^{-}. This would also fit with separate findings that CCL21^{+} mTEC, and involucrin^{+} cells are reduced in numbers in *Ltbr*$^{-/-}$ mice (Lkhagvasuren et al., 2013, White et al., 2010). Similarly, mTEC^{hi} but not mTEC^{lo} were expanded in new-born *Tnfrsf11b*$^{-/-}$ mice, which may suggest that these cells are derived from the expanded pool of mTEC^{hi} at a later stage. Through both FACS and confocal analysis, we have also observed dysregulated expression of

OPG and iNOS in *Aire*$^{-/-}$ thymus, where both are expressed by a greater percentage and number of mTEC^{hi}. However, further research would be needed to determine whether Aire itself is capable of directly regulating expression of OPG and iNOS, particularly in light of the suggestion that *Aire*$^{-/-}$ TEC fail to reach the terminal stage of differentiation. Our findings imply expression of OPG and iNOS by mTEC^{hi} not to be directly inhibited by Aire at a transcriptional level, as we saw no significant difference in proportion of OPG^{+} or iNOS^{+} mTEC in anti-Rank treated dGuo lobes from wildtype and *Aire*$^{-/-}$ embryos. This would fit with observations that Aire influences the expression of TRAs by inducing chromatin opening (Org et al., 2009), and hence is mechanistically unlikely to directly suppress gene expression. Some evidence suggests mTEC differentiation in *Aire*$^{-/-}$ mice to stall as a consequence of loss of mTEC:SP thymocyte interactions which would normally be strengthened by the presentation of TRA peptides (Mouri et al., 2011, Gray et al., 2007). One study has attempted to address this issue by culturing whole thymi from 4-6 week old *Aire*$^{-/-}$ mice overnight in the presence of TNFR ligands, including Light, RankL and CD40L (Wang et al., 2012). Stimulation with either RankL or CD40L was sufficient to increase involucrin protein and mRNA to levels comparable to those seen in the wildtype thymus (Wang et al., 2012), and hence it seems plausible that the absence of cell:cell contacts with lymphotoxin-, RankL- and Cd40L-expressing SP thymocytes prevents terminal maturation of mTEC, causing accumulation of OPG^{+} and iNOS^{+} mTEC^{hi}. An alternative possibility is that the dysregulated expression of OPG, iNOS and CCL21 is not encompassed by one mechanism. Through the generation of *Aire*$^{-/-}$*Nos2*$^{-/-}$ mice, we were able to conclude that iNOS-overexpression is not the cause of the accumulation of mTEC^{hi}, and deletion of iNOS does not restore

the CCL21^{+} mTEC^{lo} population; however, we did not address whether the same is true for OPG. It may be possible that OPG over-expression selectively blocks terminal maturation of mTEC, or the induction of CCL21 in mTEC^{lo}, which can occur via Rank-stimulation in vitro. This possibility could be assessed by the generation of *Aire*$^{-/-}$*Tnfrsf11b*$^{-/-}$ mice.

Although iNOS expression appears to be the hallmark of a non-dividing population of mTEC^{hi}, we could find no indication that iNOS is required for homeostasis of mTEC in the steady state, as the makeup of mTEC was apparently normal in *Nos2*$^{-/-}$ mice, and no substantial changes in TEC cell cycle status were observed. Although not addressed here, preliminary experiments also suggested *Nos2*$^{-/-}$ mice to recover normally from irradiation and poly(I:C)-mediated damage, recovering to similar thymic cellularities as wildtype mice. Constitutive iNOS expression has been noted recently in secretory cell types in association with the unfolded protein response (UPR). In plasma cells in particular, iNOS acts as an essential signalling intermediate for the expression of the active variant of the transcription factor Xbp1 (Saini et al., 2014), a master regulator of one of the 3 arms of the UPR. In this instance, iNOS expression is Xbp1s-dependent, and iNOS acts to amplify UPR activity by increasing the formation of Xbp1s mRNA. Xbp1s mRNA requires alternative splicing by the ER stress sensor IRE1α (Calfon et al., 2002), and hence it is unclear whether iNOS regulates Xbp1s at a transcriptional level, or increases splicing efficiency. However, although we have found the UPR to be active in mTEC, the highest levels of mRNA for Xbp1s and CHOP (a downstream product of UPR activation) were found to be in mTEC^{lo}, which are iNOS^{-}. Equally, Xbp1s mRNA was present at normal levels in all TEC subsets isolated from *Nos2*$^{-/-}$ mice, and conditional deletion of active Xbp1s in

TEC failed to impact the expression of iNOS, or the homeostasis of mTEC in 4-6 week old mice. Xbp1s is essential for the survival of plasma cells, and upon conditional deletion, or deletion of the positive feedback mediated by iNOS, cells undergo accelerated apoptosis as a result of the accumulation of the pro-apoptotic mitochondrial regulator Bak (Saini et al., 2014). Conditional Xbp1s deletion in Paneth cells triggers their complete dysfunction, and leads to spontaneous development of severe intestinal inflammation in mice, with Xbp1s mutations being a proven risk factor in inflammatory colitis (Kaser et al., 2008). In these cell types, where the onus is on the production and export of proteins – immunoglobulin in the instance of plasma cells, and defensins and mucins for Paneth cells – loss of a single arm of the UPR results in catastrophic loss of cellular homeostasis. Although collectively mTEC are capable of expressing a large array of tissue restricted genes for the screening of auto-reactivity in developing T-cells, it has been shown that these genes are expressed in mosaic among the mTEC population (Derbinski et al., 2008); not all TRA genes are expressed by each individual mTEC. Hence, the burden on the endoplasmic reticulum caused by loss of one of the three arms of the UPR through Xbp1s deletion may be insufficient to effect mTEC biology. Xbp1s inactivation does not cause homeostatic defects in all cell types; $CD8^+$ dendritic cells also have constitutive activation of the UPR, however deletion of Xbp1s in these cells has no impact on their maintenance or survival (Osorio et al., 2014). Instead, Xbp1s appears to regulate the activity of some pathways involved in antigen uptake and surface presentation indirectly. By limiting ER stress, Xbp1s limits the activation of the ER stress sensor IRE1α; but when ER stress levels are high, active IRE1α degrades mRNAs through a process known as RIDD (regulated IRE1-dependent

decay), including mRNAs for proteins involved in MHC-I presentation (Osorio et al., 2014). mTEC are known to be comparatively inefficient in the uptake and cross-presentation of exogenous antigen (Eshel et al., 1990), however more investigation would be required to determine whether Xbp1s plays a similar role in fine-tuning antigen presentation in the medulla. Although further experiments are required, the development of conventional and regulatory T-cells appeared normal in conditional Xbp1s knockout mice (not shown), however it is still possible that activation of the UPR acts as a source of self-antigens within the medulla to screen against autoimmunity against secretory cell types. If this were the case, it would be expected that inflammatory responses would be triggered against cell types with constitutively active UPR pathways in $Xbp1s^{fl/fl}$ Fonx1:CRE mice.

5.3. The effect of OPG and iNOS on central tolerance induction

Having found a major role for OPG in limiting the size of the mTEC compartment, we were keen to assess the impact of having an expanded selective niche on the deletion of auto-reactive SP thymocytes, as well as the generation of regulatory T-cells. Previous studies have correlated the targeted deletion of suppressive mTEC regulatory elements to an increase in the presence of intrathymic T-Reg as a measure of the production of these cells in the medulla (Hauri-Hohl et al., 2014, Akiyama et al., 2014); however, by producing *Tnfrsf11b*$^{-/-}$ Rag-2p-GFP reporter mice, we were able to directly assess the presence of newly produced conventional and regulatory T-cells by their expression of GFP.

To our surprise, although T-Reg were indeed increased in numbers, there was no alteration in the rate of production of T-Conv or T-Reg SP4s in the thymus of *Tnfrsf11b*$^{-/-}$ mice, as gauged by both the presence of GFP^{+} cells in the thymus, as well as GFP^{+} RTE in the spleen. Instead, we observed an increase in the number of GFP^{-} SP4s, including both T-Conv and T-Reg subsets (summarised in Figure 5.2), the latter of which was enriched to a similar percentage found in secondary lymphoid organs. In addition, we saw an increase in the presence of GFP^{-} thymic B-cells, without expansion of the thymic pro-B-cell population. Both of these findings are strongly suggestive of OPG restraining the recirculation of peripheral T-cells to the thymus in wildtype mice, which may fit with recent findings in our lab that suggest this process to be defective in *Aire*$^{-/-}$ mice, possibly as a result of loss of chemokine receptor ligand expression, or antigen-dependent interactions.

That we saw no alteration in the numbers of GFP^{+} T-Reg would likely suggest to us one of two possibilities; that either the number of mTEC present in the wildtype thymus is optimal for the selection of T-Reg in a polyclonal setting, or instead that *Tnfrsf11b*$^{-/-}$ mTEC are enhanced in number, but not qualitatively in a way that benefits T-Reg selection. To assess the first point, it would be of use to replicate previous experiments, which have shown that increasing the fraction of TCR-transgenic bone marrow to wildtype bone marrow chimeras reduces the proportion of transgenic cells that become T-Reg in the thymus (Moran et al., 2011). By comparing wildtype and *Tnfrsf11b*$^{-/-}$ mice, it would be possible to assess whether T-Reg generation is more effective with higher numbers of monoclonal T-cells when the selective niche is expanded. Due to the complexity of signalling requirements for the development of T-Reg, there are many

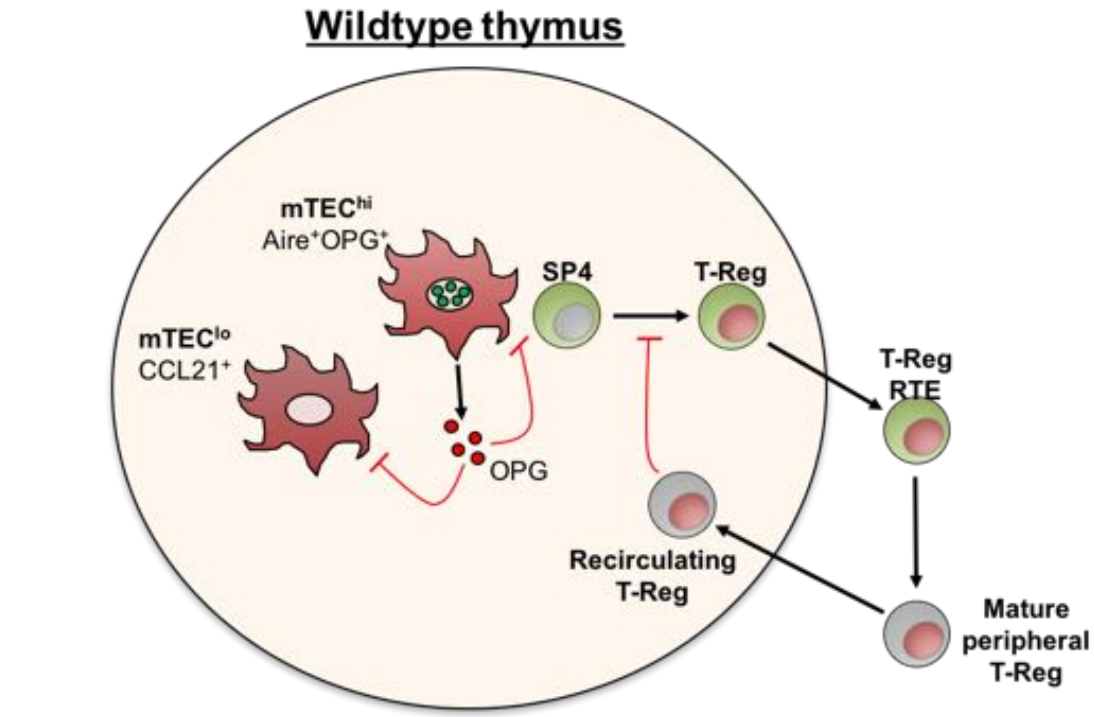
Wildtype thymus
mTEC^hi
Aire+OPG+
mTEC^lo
CCL21+
SP4
T-Reg
T-Reg
RTE
OPG
Recirculating
T-Reg
Mature
peripheral
T-Reg

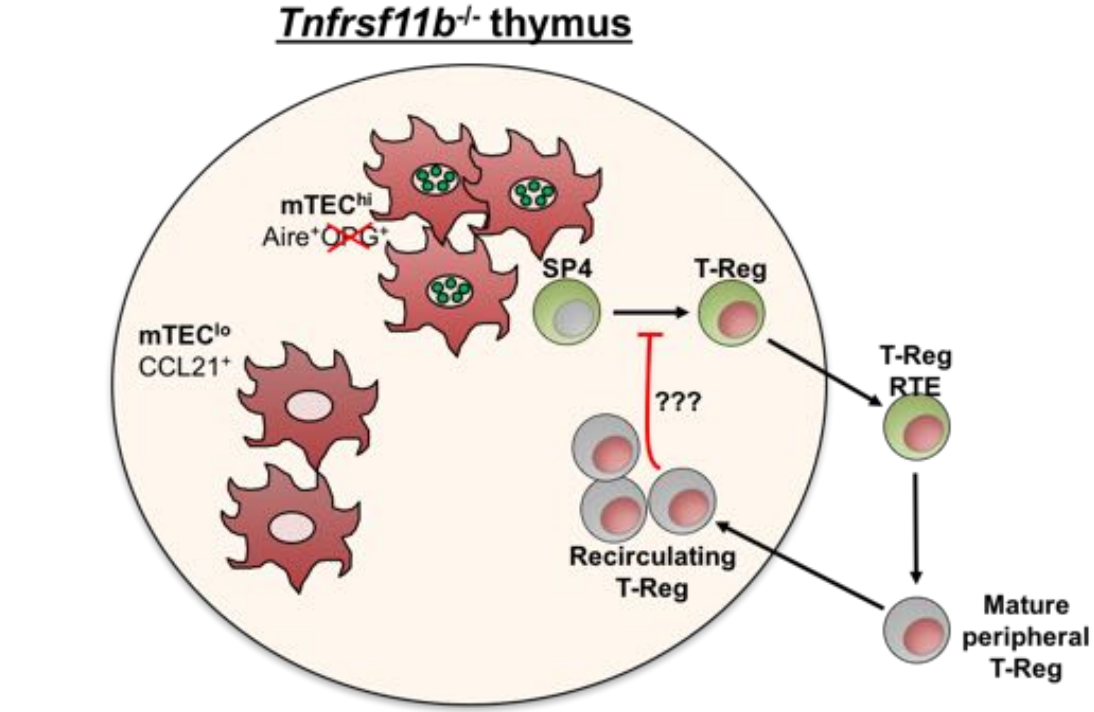
Tnfrsf11b-/- thymus
mTEC^hi
Aire+OPG+
mTEC^lo
CCL21+
SP4
T-Reg
T-Reg
RTE
???
Recirculating
T-Reg
Mature
peripheral
T-Reg

Figure 5.2: The effect of OPG on the generation and recirculation of regulatory T-cells

Top – in wildtype mice, OPG limits the size of the mTEC pool; however, $Foxp3^{+}$ (red nucleus) T-Reg are induced from conventional SP4 precursors. These cells leave the thymus, but a small fraction return, and impede the production of new $Foxp3^{+}$ cells by competing for DC-derived IL-2.

Bottom – OPG-deficient *Tnfrsf11b*$^{-/-}$ mice have an increase in the size of the medulla as a result of mTEC expansion in the absence of OPG-mediated negative regulation of Rank signalling. This has no effect on the production of new thymic T-Reg, but does dramatically increase the influx of $Foxp3^{+}$ thymic recirculants.

possible reasons the medulla of *Tnfrsf11b*$^{-/-}$ mice may be functionally insufficient to enhance T-Reg generation. A series of recent publications has shed light on the essential nature of co-stimulatory signals for both the induction of T-Reg precursors, and the up-regulation of Foxp3 expression. Although the proportion of mTEC expressing CD80 was increased in *Tnfrsf11b*$^{-/-}$ mice, this alone may be insufficient, and we did not address whether this finding extended to mTEC expressing CD86 (Cuss and Green, 2012), CD70 (Coquet et al., 2013), OX40L or GITRL (Mahmud et al., 2014), which are all known regulators of T-Reg development.

A pair of recent publications have also suggested mature T-Reg to play a role in limiting T-Reg generation in the thymus as part of a feedback loop (Thiault et al., 2015, Weist et al., 2015). It was shown that the presence of re-circulating peripheral T-Reg in the thymus was sufficient to limit the induction of new Foxp3^{+} cells through sequestering of IL-2 (Weist et al., 2015). The addition of high doses of IL-2 to thymic slices was insufficient to enhance T-Reg generation in cultures where peripheral T-Reg were introduced. Interestingly, in the absence of exogenous T-Reg, Foxp3 induction was seen to be dependent on IL-2 derived specifically from thymic dendritic cells (Weist et al., 2015). Hence, the expansion of the mTEC compartment in *Tnfrsf11b*$^{-/-}$ mice may be insufficient to trigger an increase in the rate of T-Reg production as re-circulating T-Reg compete for resources in the medulla, or alternatively, because the limiting factor is DC-derived IL-2, and dendritic cell numbers in the thymus are unaffected. The former point may be supported by the finding that splenic T-Reg – unaltered in numerical terms in *Tnfrsf11b*$^{-/-}$ mice – are increased when OPG-deficient thymic lobes are grafted under the kidney capsule of nude mice, in

which the periphery is otherwise absent of αβ T-cells (Akiyama et al., 2014). Equally, the generation of thymic T-Reg has been shown to be enhanced in cultured *Tnfrsf11b*$^{-/-}$ lobes (Akiyama et al., 2014), in which the confounding problem of recirculation to the thymus is removed.

When induced in mature T-cells via TCR triggering, iNOS expression is suggested to limit the formation of immunomodulatory cell types, including T-Reg and Th17 cells (Lee et al., 2011, Jianjun et al., 2013), which are known to originate in vivo through both peripheral induction, as well as generation in the thymic medulla. Studies using mTEC-deficient *Relb*$^{-/-}$ models have shown medullary interactions to be essential for the generation of both T-Reg and Th17 cells in the thymus (Lee et al., 2011, Jianjun et al., 2013), and hence we were interested to determine whether these processes were similarly limited through mTEC expression of iNOS. However, we found *Nos2*$^{-/-}$ thymus to contain normal numbers of natural Th17s and T-Regs, in addition to T-Reg precursor populations. Prior identification of iNOS^{+} thymic APCs led to speculation that iNOS-induced production of nitric oxide was a mechanism for the negative selection of DP thymocytes, as the nitric oxide donor SNAP potentiates the induction of apoptosis in this population caused by *in vitro* TCR triggering (Fehsel et al., 1995, Tai et al., 1997). Upon repeating these experiments, we found NO to induce apoptosis potently in DP thymocytes, but also to a lesser extent in mature SP4s. This, together with our finding that iNOS expression is restricted to the medulla, suggested that iNOS would more likely play a later role in negative selection of cells that have already migrated from the cortex. However, we saw no increase in thymic cellularity, nor the numbers of DP and SP4 thymocytes in *Nos2*$^{-/-}$ mice, and rates of apoptosis were normal as

determined by annexin V staining. Lastly, two recent studies identified a key role for FRC-derived iNOS in constraining the proliferation of mature T-cells for the resolution of adaptive immune responses (Lukacs-Kornek et al., 2011, Siegert et al., 2011). Again, we found no differences in the rates of proliferation of thymocytes, and no increase in the populations of re-circulating peripheral T-cells within the medulla of *Nos2*$^{-/-}$ mice. It therefore again seems unlikely that iNOS plays a major role in the development of conventional and immunomodulatory T-cell subsets in the thymus in quantitative terms.

Although our data together are suggestive that tolerance induction in terms of both negative selection and the generation of regulatory T-cells is not significantly altered in the absence of either OPG or iNOS, it remains possible that this only applies in quantitative terms. Some evidence hints that iNOS may play a part in shaping the TCR repertoire of developing thymocytes. Despite iNOS playing a role in tissue damage in autoimmunity, *Nos2*$^{-/-}$ mice have exacerbated disease symptoms in some autoimmune mouse models, including experimental autoimmune encephalomyelitis (Fenyk-Melody et al., 1998) and experimental autoimmune uveoretinitis (Silver et al., 1999). There is also some evidence to suggest that nitrosylation of the tyrosine residue of peptide antigens can alter their capacity to activate antigen-specific T-cells (Birnboim et al., 2003). It is therefore plausible that iNOS may play a role in shaping the pool of TRAs available for selection through their direct nitrosylation. Alternatively, as NO can activate transcription factors and intermediates in major signalling pathways (Serafini et al., 2006), it is possible that iNOS plays a minor role by modulating the expression levels of some TRAs in mTEC^{hi}. Equally, although negative selection as determined by the number of SP4 thymocytes is unchanged in OPG-

deficient mice, it may be that any effect is masked by the rarity of autoreactive T-cell clones post-selection in wildtype mice. The capacity for negative selection and T-Reg induction could hence be better assessed by the following measures. At a basic level, the TCR repertoire of wildtype, *Nos2*$^{-/-}$ and *Tnfrsf11b*$^{-/-}$ thymocytes could be compared through profiling of the Vβ usage, although this technique has revealed only minor alterations in *Aire*$^{-/-}$ mice (Takaba et al., 2015, Liston et al., 2003), despite the profound differences in TRA expression. Alternatively, the capacity for negative selection of monoclonal T-cells through the generation of bone marrow chimeras could be achieved, although a range of TCR transgenic strains reactive against Aire-dependent and Aire-independent self-antigens would likely need to be tested. Lastly, it has previously been shown that reconstitution of mice with Foxp3-DTR (diphtheria toxin receptor) bone marrow - in which T-Reg selectively express DTR, and can be ablated by DT treatment - can be used as an assessment of the efficiency of negative selection (Hauri-Hohl et al., 2014). This model has recently been used to assess the impact of medullary expansion in TGFβ receptor 2 conditional knockout mice, as the severity of autoimmunity caused by T-Reg ablation acts as a readout of the efficiency of negative selection of autoreactive T-cells (Hauri-Hohl et al., 2014).

5.4. The effect of OPG and iNOS on T-cell development and maturation

It is beginning to become clear that the medulla plays an important role not just in the establishment of central tolerance, but also in the maturation of SP thymocytes, both phenotypically and functionally. Previous studies have

observed phenotypic maturation of medullary thymocytes through the up-regulation of markers such as Qa2 and CD62L, and the loss of expression of CD69 and HSA, both initially acquired after positive selection in the cortex (Li et al., 2007, Dave et al., 1999). It has been reported that *Aire*$^{-/-}$ mice lack the most mature, Qa2^{hi} subset of SP4 thymocytes (Li et al., 2007), which is suggested to represent a stalling in the development of these cells. Having found SP4s derived from *Nos2*$^{-/-}$ thymi to have higher levels of Qa2, we hypothesized iNOS expression, which is increased in *Aire*$^{-/-}$ TEC, to restrict intrathymic maturational processes. However, *Aire*$^{-/-}$ mice have a profoundly normal peripheral T-cell pool, suggesting the formation of Qa2^{hi} thymocytes to be a redundant step in T-cell production. Xing et al. have contributed to our understanding of this contradiction through their assessment of phenotypic maturation in different parameters, where they have found SP4s to successively up-regulate MHC-I, and lose expression of CD69, giving three distinct maturational phases (SM, M1 and M2) that correlate strongly with changes in gene expression relating to functional maturation (Xing et al., 2016). More-so, their finding that phenotypic maturation by these new parameters is unperturbed in *Ifnar*$^{-/-}$ mice, in which thymocytes similarly fail to up-regulate Qa2 expression, suggests Qa2 up-regulation to be an event uncoupled from progressive T-cell development, instead relating to tonic type I interferon signalling in the medulla (Xing et al., 2016). Indeed, we found SM, M1 and M2 development to be grossly normal in *Aire*$^{-/-}$ mice, as well as *Nos2*$^{-/-}$ and DKO strains, the former two of which also had normal numbers of RTE. This strongly suggests that T-cell development is not dependent on Aire or iNOS expression by mTEC; instead the up-regulation of Qa2 expression appeared to correlate with mTEC-derived IFNβ, which was lost

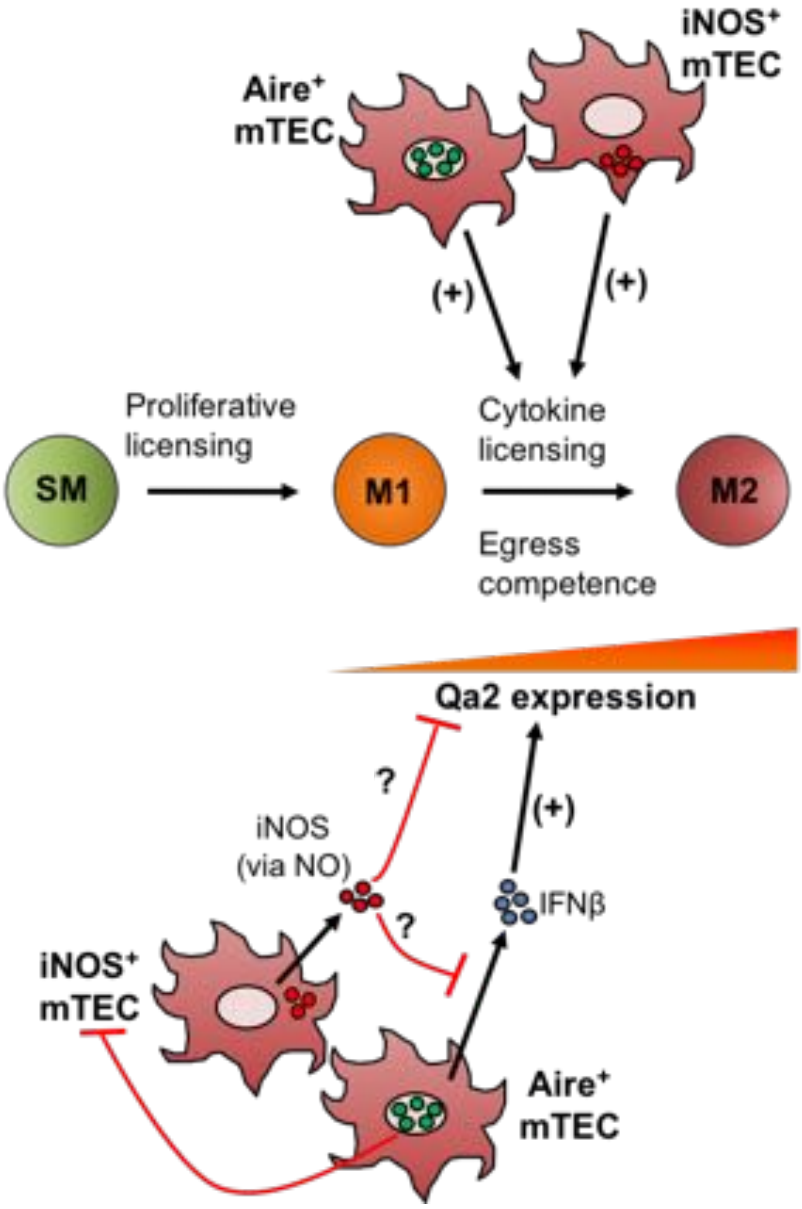
iNOS+
mTEC
Aire+
mTEC
(+)
(+)
Proliferative
licensing
Cytokine
licensing
SM
M1
M2
Egress
competence
Qa2 expression
?
(+)
iNOS
(via NO)
IFNβ
?
iNOS+
mTEC
Aire+
mTEC

Figure 5.3: Aire and iNOS impact on the processes of cytokine licensing and Qa2 up-regulation by SP4 thymocytes

SP thymocytes mature phenotypically through the following sequential stages; semi-mature (SM) – $CD69^{+}MHC\text{-}I^{-}$, mature 1 (M1) - $CD69^{+}MHC\text{-}I^{+}$ and mature 2 (M2) - $CD69^{-}MHC\text{-}I^{+}$. Progress from M1 to M2 is defined by cytokine licensing, and coincides with the IFNβ-driven process of Qa2 up-regulation. Cytokine licensing, in which cells acquire the capacity to express TNFα upon TCR ligation, is positively regulated by both Aire and iNOS expression by mTEC.

In contrast, Qa2 up-regulation requires Aire-dependent mTEC expression of IFNβ. iNOS inhibits Qa2 expression either directly (via NO), or indirectly, by negatively regulation IFNβ expression. Qa2 is hence lost in *Aire*$^{-/-}$ TEC, as Aire blocks the formation of $iNOS^{+}$ mTEC, which accumulate in the *Aire*$^{-/-}$ medula.

in *Aire*$^{-/-}$ TEC, and increased in the absence of iNOS. However, exposure of sorted thymocyte populations to recombinant IFNβ in vitro did not cause up-regulated Qa2 expression, and hence it is possible that this process requires a secondary signal, such as TCR-triggering, to occur (potential model summarized in Figure 5.3). Qa2 expression by developing thymocytes was also enhanced in *Tnfrsf11b*$^{-/-}$ mice (not shown), however it is unclear how this finding may relate to Aire^{+}/iNOS^{+} mTEC, or whether the maturation is effected in terms of SM, M1 and M2 development.

In addition to redefining phenotypic maturation, Xing et al. also suggested licensing of proliferation, cytokine production and the acquisition of egress competence to be distinct events in the development of medullary thymocytes. Hence, in spite of the normality of development in *Aire*$^{-/-}$ and *Nos2*$^{-/-}$ mice in quantitative terms, we were keen to begin to assess functional development. Both *Aire*$^{-/-}$ and *Nos2*$^{-/-}$ thymocytes had a reduction in TNFα production relative to wildtype cells, which was marginally compounded by the absence of both factors in DKO mice. Sorted *Aire*$^{-/-}$ populations were tested for their capacity to proliferate in response to TCR-triggering in vitro, and thymocytes from the mature M1 and M2 subsets underwent the same number of divisions as those isolated from wildtype mice over three days in culture, suggesting proliferative licensing to occur independently of Aire, and Aire-dependent TRA expression, and any defect to relate only to the latest stage of functional maturation in cytokine licensing. This is interesting, as recent publications have alluded to the essential nature of TCR-pMHC interactions in priming T-cells for activation in the periphery. The absence of thymic expression of the proteasomal subunit β5t (Takada et al., 2015) or the C-type lectin family member Clec16A (Schuster et al.,

2015) negatively impact on the development of CD8 and CD4 T-cells respectively in quantitative terms, as both differentially impact antigen availability for presentation by TEC. However, T-cells developing in both of these models have been shown to be functionally defective, and hyporeactive to TCR triggering, failing to fully up-regulate activation markers such as CD69 and CD25. This is true in a polyclonal setting, and in the case of β5t-deficient *Psmb11*$^{-/-}$ mice, has been demonstrated in monoclonal OT-I TCR^{+} T-cells which are generated in normal numbers in the absence of β5t (Takada et al., 2015). OT-I T-cells selected in *Psmb11*$^{-/-}$ thymi were also poorly responsive to infection by an OVA-expressing strain of Listeria Monocytogenes, and couldn't form long-lived memory cells (Takada et al., 2015). As thymocytes already express CD69 and CD5, it is difficult to conclude whether *Aire*$^{-/-}$ and *Nos2*$^{-/-}$ SP4s are similarly sub-responsive, however SP thymocytes from *Aire*$^{-/-}$ mice, like *Psmb11*$^{-/-}$ SP8s have been shown to have low CD5 expression *in vivo* (Liston et al., 2003), suggestive of receipt of only low affinity TCR-ligation in the medulla. Recent evidence also alludes to the importance of post-thymic maturational events in generating fully responsive T-cells. Recent thymic emigrants express higher levels of anergy-associated markers than mature naïve peripheral T-cells, and respond poorly to TCR triggering *in vitro* in terms of both proliferation and IL-2 (Friesen et al., 2016)/IL-4 (Berkley et al., 2013) production in the absence of inflammatory cytokines. It is therefore likely that a combination of thymic TCR:pMHC interactions and undescribed peripheral events that are likely to be MHC-independent (Houston and Fink, 2009) act to confer full functional maturation to developing T-cells. It is unclear from our data whether cytokine licensing is restored to *Nos2*$^{-/-}$ and *Aire*$^{-/-}$ T-cells on further maturation in the periphery;

however, this is not the case in *Psmb11*$^{-/-}$ mice – cells not cultured by specific TCR:pMHC interactions in the thymic cortex remain hyporesponsive to TCR triggering as mature naïve T-cells (Takada et al., 2015). If this holds true for T-cells that have developed within the medulla in the absence of Aire-dependent TRAs, this may explain the mild auto-immune phenotype we and others (Bouneaud et al., 2000, Hubert et al., 2009) have observed in *Aire*$^{-/-}$ mice on the C57BL/6 background, compared to the severe autoimmune consequences of mutations in the human Aire gene, as manifested by the disease APECED (Ramsey et al., 2002). Equally, TCR sub-responsiveness may offer an alternative explanation as to why lineage commitment of *Nos2*$^{-/-}$ T-cells is dramatically skewed under polarising conditions (Jianjun et al., 2013). It is hence possible that interaction with Aire- and iNOS-expressing mTEC acts as an important step in the functional maturation of medullary thymocytes that may impact on their responsiveness in the periphery, however the importance of OPG in dictating functional and phenotypic maturation of SP thymocytes by restricting mTEC availability has yet to be addressed. In summary, we have highlighted the importance of heterogeneic expression of two newly identified functional molecules by mTEC, wherein we have shown OPG to act as a major regulator of mTEC pool size, indirectly controlling the re-circulation of peripheral lymphocytes to the thymus, and iNOS to have a potentially important role in intrathymic maturation of SP thymocytes.

6. APPENDIX

6.1 References

ADEREM, A. & UNDERHILL, D. M. 1999. Mechanisms of phagocytosis in macrophages. *Annu Rev Immunol,* 17**,** 593-623.

ADOLFSSON, J., MANSSON, R., BUZA-VIDAS, N., HULTQUIST, A., LIUBA, K., JENSEN, C. T., BRYDER, D., YANG, L., BORGE, O. J., THOREN, L. A., ANDERSON, K., SITNICKA, E., SASAKI, Y., SIGVARDSSON, M. & JACOBSEN, S. E. 2005. Identification of Flt3+ lympho-myeloid stem cells lacking erythro-megakaryocytic potential a revised road map for adult blood lineage commitment. *Cell,* 121**,** 295-306.

AHMED, R. & GRAY, D. 1996. Immunological memory and protective immunity: understanding their relation. *Science,* 272**,** 54-60.

AICHINGER, M., WU, C., NEDJIC, J. & KLEIN, L. 2013. Macroautophagy substrates are loaded onto MHC class II of medullary thymic epithelial cells for central tolerance. *J Exp Med,* 210**,** 287-300.

AIELLO, S., NORIS, M., PICCININI, G., TOMASONI, S., CASIRAGHI, F., BONAZZOLA, S., MISTER, M., SAYEGH, M. H. & REMUZZI, G. 2000. Thymic dendritic cells express inducible nitric oxide synthase and generate nitric oxide in response to self- and alloantigens. *J Immunol,* 164**,** 4649-58.

AIFANTIS, I., AZOGUI, O., FEINBERG, J., SAINT-RUF, C., BUER, J. & VON BOEHMER, H. 1998. On the role of the pre-T cell receptor in alphabeta versus gammadelta T lineage commitment. *Immunity,* 9**,** 649-55.

AKIYAMA, N., SHINZAWA, M., MIYAUCHI, M., YANAI, H., TATEISHI, R., SHIMO, Y., OHSHIMA, D., MATSUO, K., SASAKI, I., HOSHINO, K., WU, G., YAGI, S., INOUE, J., KAISHO, T. & AKIYAMA, T. 2014. Limitation of immune tolerance-inducing thymic epithelial cell development by Spi-B-mediated negative feedback regulation. *J Exp Med,* 211**,** 2425-38.

AKIYAMA, T., MAEDA, S., YAMANE, S., OGINO, K., KASAI, M., KAJIURA, F., MATSUMOTO, M. & INOUE, J. 2005. Dependence of self-tolerance on TRAF6-directed development of thymic stroma. *Science,* 308**,** 248-51.

AKIYAMA, T., SHIMO, Y., YANAI, H., QIN, J., OHSHIMA, D., MARUYAMA, Y., ASAUMI, Y., KITAZAWA, J., TAKAYANAGI, H., PENNINGER, J. M., MATSUMOTO, M., NITTA, T., TAKAHAMA, Y. & INOUE, J. 2008. The tumor necrosis factor family receptors RANK and CD40 cooperatively establish the thymic medullary microenvironment and self-tolerance. *Immunity,* 29**,** 423-37.

AMIT, A. G., MARIUZZA, R. A., PHILLIPS, S. E. & POLJAK, R. J. 1986. Three-dimensional structure of an antigen-antibody complex at 2.8 A resolution. *Science,* 233**,** 747-53.

ANDERSON, G., JENKINSON, E. J., MOORE, N. C. & OWEN, J. J. 1993. MHC class II-positive epithelium and mesenchyme cells are both required for T-cell development in the thymus. *Nature,* 362**,** 70-3.

ANDERSON, M. S., VENANZI, E. S., CHEN, Z., BERZINS, S. P., BENOIST, C. & MATHIS, D. 2005. The cellular mechanism of Aire control of T cell tolerance. *Immunity,* 23**,** 227-39.

ANDERSON, M. S., VENANZI, E. S., KLEIN, L., CHEN, Z., BERZINS, S. P., TURLEY, S. J., VON BOEHMER, H., BRONSON, R., DIERICH, A., BENOIST, C. & MATHIS, D. 2002. Projection of an immunological self shadow within the thymus by the aire protein. *Science,* 298**,** 1395-401.

ANDERSON, R. M. & MAY, R. M. 1985. Vaccination and herd immunity to infectious diseases. *Nature,* 318**,** 323-9.

ARAI, K. I., LEE, F., MIYAJIMA, A., MIYATAKE, S., ARAI, N. & YOKOTA, T. 1990. Cytokines: coordinators of immune and inflammatory responses. *Annu Rev Biochem,* 59**,** 783-836.

ARSTILA, T. P., CASROUGE, A., BARON, V., EVEN, J., KANELLOPOULOS, J. & KOURILSKY, P. 1999. A direct estimate of the human alphabeta T cell receptor diversity. *Science,* 286**,** 958-61.

AYABE, T., SATCHELL, D. P., WILSON, C. L., PARKS, W. C., SELSTED, M. E. & OUELLETTE, A. J. 2000. Secretion of microbicidal alpha-defensins by intestinal Paneth cells in response to bacteria. *Nat Immunol,* 1**,** 113-8.

BAIK, S., JENKINSON, E. J., LANE, P. J., ANDERSON, G. & JENKINSON, W. E. 2013. Generation of both cortical and Aire(+) medullary thymic epithelial compartments from CD205(+) progenitors. *Eur J Immunol,* 43**,** 589-94.

BAIK, S., SEKAI, M., HAMAZAKI, Y., JENKINSON, W. E. & ANDERSON, G. 2016. Relb acts downstream of medullary thymic epithelial stem cells and is essential for the emergence of RANK(+) medullary epithelial progenitors. *Eur J Immunol,* 46**,** 857-62.

BALCIUNAITE, G., CEREDIG, R. & ROLINK, A. G. 2005. The earliest subpopulation of mouse thymocytes contains potent T, significant macrophage, and natural killer cell but no B-lymphocyte potential. *Blood,* 105**,** 1930-6.

BASSING, C. H., SWAT, W. & ALT, F. W. 2002. The mechanism and regulation of chromosomal V(D)J recombination. *Cell,* 109 Suppl**,** S45-55.

BERKLEY, A. M., HENDRICKS, D. W., SIMMONS, K. B. & FINK, P. J. 2013. Recent thymic emigrants and mature naive T cells exhibit differential DNA methylation at key cytokine loci. *J Immunol,* 190**,** 6180-6.

BERNARD, O., HOZUMI, N. & TONEGAWA, S. 1978. Sequences of mouse immunoglobulin light chain genes before and after somatic changes. *Cell,* 15**,** 1133-44.

BEUTLER, B. 2004. Innate immunity: an overview. *Mol Immunol,* 40**,** 845-59.

BIANCHI, M. E. 2007. DAMPs, PAMPs and alarmins: all we need to know about danger. *J Leukoc Biol,* 81**,** 1-5.

BIN, G., JIARONG, Z., SHIHAO, W., XIULI, S., CHENG, X., LIANGBIAO, C. & MING, Z. 2012. Aire promotes the self-renewal of embryonic stem cells through Lin28. *Stem Cells Dev,* 21**,** 2878-90.

BIRNBOIM, H. C., LEMAY, A. M., LAM, D. K., GOLDSTEIN, R. & WEBB, J. R. 2003. Cutting edge: MHC class II-restricted peptides containing the inflammation-associated marker 3-nitrotyrosine evade central tolerance and elicit a robust cell-mediated immune response. *J Immunol,* 171**,** 528-32.

BLEUL, C. C., CORBEAUX, T., REUTER, A., FISCH, P., MONTING, J. S. & BOEHM, T. 2006. Formation of a functional thymus initiated by a postnatal epithelial progenitor cell. *Nature,* 441**,** 992-6.

BODMER, H., VIVILLE, S., BENOIST, C. & MATHIS, D. 1994. Diversity of endogenous epitopes bound to MHC class II molecules limited by invariant chain. *Science,* 263**,** 1284-6.

BOES, M., CERNY, J., MASSOL, R., OP DEN BROUW, M., KIRCHHAUSEN, T., CHEN, J. & PLOEGH, H. L. 2002. T-cell engagement of dendritic cells rapidly rearranges MHC class II transport. *Nature,* 418**,** 983-8.

BOGDAN, C. 2001. Nitric oxide and the immune response. *Nat Immunol,* 2**,** 907-16.

BOGDAN, C. 2015. Nitric oxide synthase in innate and adaptive immunity: an update. *Trends Immunol,* 36**,** 161-78.

BOUNEAUD, C., KOURILSKY, P. & BOUSSO, P. 2000. Impact of negative selection on the T cell repertoire reactive to a self-peptide: a large fraction of T cell clones escapes clonal deletion. *Immunity,* 13**,** 829-40.

BOURSALIAN, T. E., GOLOB, J., SOPER, D. M., COOPER, C. J. & FINK, P. J. 2004. Continued maturation of thymic emigrants in the periphery. *Nat Immunol,* 5**,** 418-25.

BOUSSO, P., BHAKTA, N. R., LEWIS, R. S. & ROBEY, E. 2002. Dynamics of thymocyte-stromal cell interactions visualized by two-photon microscopy. *Science,* 296**,** 1876-80.

BREDT, D. S., HWANG, P. M. & SNYDER, S. H. 1990. Localization of nitric oxide synthase indicating a neural role for nitric oxide. *Nature,* 347**,** 768-70.

BREDT, D. S. & SNYDER, S. H. 1989. Nitric oxide mediates glutamate-linked enhancement of cGMP levels in the cerebellum. *Proc Natl Acad Sci U S A,* 86**,** 9030-3.

BRENNECKE, P., REYES, A., PINTO, S., RATTAY, K., NGUYEN, M., KUCHLER, R., HUBER, W., KYEWSKI, B. & STEINMETZ, L. M. 2015. Single-cell transcriptome analysis reveals coordinated ectopic gene-expression patterns in medullary thymic epithelial cells. *Nat Immunol,* 16**,** 933-41.

BREZINSCHEK, H. P., BREZINSCHEK, R. I. & LIPSKY, P. E. 1995. Analysis of the heavy chain repertoire of human peripheral B cells using single-cell polymerase chain reaction. *J Immunol,* 155**,** 190-202.

BRINKMANN, V., REICHARD, U., GOOSMANN, C., FAULER, B., UHLEMANN, Y., WEISS, D. S., WEINRAUCH, Y. & ZYCHLINSKY, A. 2004. Neutrophil extracellular traps kill bacteria. *Science,* 303**,** 1532-5.

BURKLY, L., HESSION, C., OGATA, L., REILLY, C., MARCONI, L. A., OLSON, D., TIZARD, R., CATE, R. & LO, D. 1995. Expression of relB is required for the development of thymic medulla and dendritic cells. *Nature,* 373**,** 531-6.

CALDERON, L. & BOEHM, T. 2011. Three chemokine receptors cooperatively regulate homing of hematopoietic progenitors to the embryonic mouse thymus. *Proc Natl Acad Sci U S A,* 108**,** 7517-22.

CALFON, M., ZENG, H., URANO, F., TILL, J. H., HUBBARD, S. R., HARDING, H. P., CLARK, S. G. & RON, D. 2002. IRE1 couples endoplasmic reticulum load to secretory capacity by processing the XBP-1 mRNA. *Nature,* 415**,** 92-6.

CAMPBELL, J. J., PAN, J. & BUTCHER, E. C. 1999. Cutting edge: developmental switches in chemokine responses during T cell maturation. *J Immunol,* 163**,** 2353-7.

CANTRELL, D. 1996. T cell antigen receptor signal transduction pathways. *Annu Rev Immunol,* 14**,** 259-74.

CAO, S. S. & KAUFMAN, R. J. 2012. Unfolded protein response. *Curr Biol,* 22**,** R622-6.

CAPONE, M., HOCKETT, R. D., JR. & ZLOTNIK, A. 1998. Kinetics of T cell receptor beta, gamma, and delta rearrangements during adult thymic development: T cell receptor rearrangements are present in CD44(+)CD25(+) Pro-T thymocytes. *Proc Natl Acad Sci U S A,* 95**,** 12522-7.

CARRIER, A., NGUYEN, C., VICTORERO, G., GRANJEAUD, S., ROCHA, D., BERNARD, K., MIAZEK, A., FERRIER, P., MALISSEN, M., NAQUET, P., MALISSEN, B. & JORDAN, B. R. 1999. Differential gene expression in CD3epsilon- and RAG1-deficient thymuses: definition of a set of genes potentially involved in thymocyte maturation. *Immunogenetics,* 50**,** 255-70.

CAZENAVE, P. A., MARCHE, P. N., JOUVIN-MARCHE, E., VOEGTLE, D., BONHOMME, F., BANDEIRA, A. & COUTINHO, A. 1990. V beta 17 gene polymorphism in wild-derived mouse strains: two amino acid substitutions in the V beta 17 region greatly alter T cell receptor specificity. *Cell,* 63**,** 717-28.

CELLA, M., ENGERING, A., PINET, V., PIETERS, J. & LANZAVECCHIA, A. 1997. Inflammatory stimuli induce accumulation of MHC class II complexes on dendritic cells. *Nature,* 388**,** 782-7.

CHAN, A. C., IWASHIMA, M., TURCK, C. W. & WEISS, A. 1992. ZAP-70: a 70 kd protein-tyrosine kinase that associates with the TCR zeta chain. *Cell,* 71**,** 649-62.

CHAPLIN, D. D. 2010. Overview of the immune response. *J Allergy Clin Immunol,* 125**,** S3-23.

CHEN, G., SHAW, M. H., KIM, Y. G. & NUNEZ, G. 2009. NOD-like receptors: role in innate immunity and inflammatory disease. *Annu Rev Pathol,* 4**,** 365-98.

CHEN, W., JIN, W., HARDEGEN, N., LEI, K. J., LI, L., MARINOS, N., MCGRADY, G. & WAHL, S. M. 2003. Conversion of peripheral CD4+CD25- naive T cells to CD4+CD25+ regulatory T cells by TGF-beta induction of transcription factor Foxp3. *J Exp Med,* 198**,** 1875-86.

CHONG, M. M., CORNISH, A. L., DARWICHE, R., STANLEY, E. G., PURTON, J. F., GODFREY, D. I., HILTON, D. J., STARR, R., ALEXANDER, W. S. & KAY, T. W. 2003. Suppressor of cytokine signaling-1 is a critical regulator of interleukin-7-dependent CD8+ T cell differentiation. *Immunity,* 18**,** 475-87.

CIOFANI, M., KNOWLES, G. C., WIEST, D. L., VON BOEHMER, H. & ZUNIGA-PFLUCKER, J. C. 2006. Stage-specific and differential notch dependency at the alphabeta and gammadelta T lineage bifurcation. *Immunity,* 25**,** 105-16.

CLEVERS, H., ALARCON, B., WILEMAN, T. & TERHORST, C. 1988. The T cell receptor/CD3 complex: a dynamic protein ensemble. *Annu Rev Immunol,* 6**,** 629-62.

COHEN, O., KFIR-ERENFELD, S., SPOKOINI, R., ZILBERMAN, Y., YEFENOF, E. & SIONOV, R. V. 2009. Nitric oxide cooperates with glucocorticoids in thymic epithelial cell-mediated apoptosis of double positive thymocytes. *Int Immunol,* 21**,** 1113-23.

COOMBES, J. L., SIDDIQUI, K. R., ARANCIBIA-CARCAMO, C. V., HALL, J., SUN, C. M., BELKAID, Y. & POWRIE, F. 2007. A functionally specialized population of

mucosal CD103+ DCs induces Foxp3+ regulatory T cells via a TGF-beta and retinoic acid-dependent mechanism. *J Exp Med,* 204**,** 1757-64.

COQUET, J. M., RIBOT, J. C., BABALA, N., MIDDENDORP, S., VAN DER HORST, G., XIAO, Y., NEVES, J. F., FONSECA-PEREIRA, D., JACOBS, H., PENNINGTON, D. J., SILVA-SANTOS, B. & BORST, J. 2013. Epithelial and dendritic cells in the thymic medulla promote CD4+Foxp3+ regulatory T cell development via the CD27-CD70 pathway. *J Exp Med,* 210**,** 715-28.

COWAN, J. E., JENKINSON, W. E. & ANDERSON, G. 2015. Thymus medulla fosters generation of natural Treg cells, invariant gammadelta T cells, and invariant NKT cells: what we learn from intrathymic migration. *Eur J Immunol,* 45**,** 652-60.

COWAN, J. E., MCCARTHY, N. I. & ANDERSON, G. 2016. CCR7 Controls Thymus Recirculation, but Not Production and Emigration, of Foxp3(+) T Cells. *Cell Rep,* 14**,** 1041-8.

COWAN, J. E., MCCARTHY, N. I., PARNELL, S. M., WHITE, A. J., BACON, A., SERGE, A., IRLA, M., LANE, P. J., JENKINSON, E. J., JENKINSON, W. E. & ANDERSON, G. 2014. Differential requirement for CCR4 and CCR7 during the development of innate and adaptive alphabetaT cells in the adult thymus. *J Immunol,* 193**,** 1204-12.

COWAN, J. E., PARNELL, S. M., NAKAMURA, K., CAAMANO, J. H., LANE, P. J., JENKINSON, E. J., JENKINSON, W. E. & ANDERSON, G. 2013. The thymic medulla is required for Foxp3+ regulatory but not conventional CD4+ thymocyte development. *J Exp Med,* 210**,** 675-81.

CUSS, S. M. & GREEN, E. A. 2012. Abrogation of CD40-CD154 signaling impedes the homeostasis of thymic resident regulatory T cells by altering the levels of IL-2, but does not affect regulatory T cell development. *J Immunol,* 189**,** 1717-25.

D'AUTREAUX, B., TUCKER, N. P., DIXON, R. & SPIRO, S. 2005. A non-haem iron centre in the transcription factor NorR senses nitric oxide. *Nature,* 437**,** 769-72.

DAL PORTO, J. M., HABERMAN, A. M., SHLOMCHIK, M. J. & KELSOE, G. 1998. Antigen drives very low affinity B cells to become plasmacytes and enter germinal centers. *J Immunol,* 161**,** 5373-81.

DANIELS, M. A., TEIXEIRO, E., GILL, J., HAUSMANN, B., ROUBATY, D., HOLMBERG, K., WERLEN, G., HOLLANDER, G. A., GASCOIGNE, N. R. & PALMER, E. 2006. Thymic selection threshold defined by compartmentalization of Ras/MAPK signalling. *Nature,* 444**,** 724-9.

DAVE, V. P., ALLMAN, D., WIEST, D. L. & KAPPES, D. J. 1999. Limiting TCR expression leads to quantitative but not qualitative changes in thymic selection. *J Immunol,* 162**,** 5764-74.

DAVIS, C. B., KILLEEN, N., CROOKS, M. E., RAULET, D. & LITTMAN, D. R. 1993. Evidence for a stochastic mechanism in the differentiation of mature subsets of T lymphocytes. *Cell,* 73**,** 237-47.

DAVIS, M. M. & BJORKMAN, P. J. 1988. T-cell antigen receptor genes and T-cell recognition. *Nature,* 334**,** 395-402.

DE SANTO, C., SERAFINI, P., MARIGO, I., DOLCETTI, L., BOLLA, M., DEL SOLDATO, P., MELANI, C., GUIDUCCI, C., COLOMBO, M. P., IEZZI, M., MUSIANI, P., ZANOVELLO, P. & BRONTE, V. 2005. Nitroaspirin corrects immune

dysfunction in tumor-bearing hosts and promotes tumor eradication by cancer vaccination. *Proc Natl Acad Sci U S A,* 102**,** 4185-90.

DEKONING, J., DIMOLFETTO, L., REILLY, C., WEI, Q., HAVRAN, W. L. & LO, D. 1997. Thymic cortical epithelium is sufficient for the development of mature T cells in relB-deficient mice. *J Immunol,* 158**,** 2558-66.

DENZIN, L. K., FALLAS, J. L., PRENDES, M. & YI, W. 2005. Right place, right time, right peptide: DO keeps DM focused. *Immunol Rev,* 207**,** 279-92.

DERBINSKI, J., GABLER, J., BRORS, B., TIERLING, S., JONNAKUTY, S., HERGENHAHN, M., PELTONEN, L., WALTER, J. & KYEWSKI, B. 2005. Promiscuous gene expression in thymic epithelial cells is regulated at multiple levels. *J Exp Med,* 202**,** 33-45.

DERBINSKI, J., PINTO, S., ROSCH, S., HEXEL, K. & KYEWSKI, B. 2008. Promiscuous gene expression patterns in single medullary thymic epithelial cells argue for a stochastic mechanism. *Proc Natl Acad Sci U S A,* 105**,** 657-62.

DESANTI, G. E., COWAN, J. E., BAIK, S., PARNELL, S. M., WHITE, A. J., PENNINGER, J. M., LANE, P. J., JENKINSON, E. J., JENKINSON, W. E. & ANDERSON, G. 2012. Developmentally regulated availability of RANKL and CD40 ligand reveals distinct mechanisms of fetal and adult cross-talk in the thymus medulla. *J Immunol,* 189**,** 5519-26.

DINARELLO, C. A. 1997. Proinflammatory and anti-inflammatory cytokines as mediators in the pathogenesis of septic shock. *Chest,* 112**,** 321S-329S.

DINARELLO, C. A. 2000. Proinflammatory cytokines. *Chest,* 118**,** 503-8.

DONG, J., CHEN, Y., XU, X., JIN, R., TENG, F., YAN, F., TANG, H., LI, P., SUN, X., LI, Y., WU, H., ZHANG, Y. & GE, Q. 2013. Homeostatic properties and phenotypic maturation of murine CD4+ pre-thymic emigrants in the thymus. *PLoS One,* 8**,** e56378.

DORSHKIND, K., MONTECINO-RODRIGUEZ, E. & SIGNER, R. A. 2009. The ageing immune system: is it ever too old to become young again? *Nat Rev Immunol,* 9**,** 57-62.

DZHAGALOV, I. L., CHEN, K. G., HERZMARK, P. & ROBEY, E. A. 2013. Elimination of self-reactive T cells in the thymus: a timeline for negative selection. *PLoS Biol,* 11**,** e1001566.

EBERT, P. J., JIANG, S., XIE, J., LI, Q. J. & DAVIS, M. M. 2009. An endogenous positively selecting peptide enhances mature T cell responses and becomes an autoantigen in the absence of microRNA miR-181a. *Nat Immunol,* 10**,** 1162-9.

EGAWA, T. 2015. Regulation of CD4 and CD8 coreceptor expression and CD4 versus CD8 lineage decisions. *Adv Immunol,* 125**,** 1-40.

ELGUETA, R., BENSON, M. J., DE VRIES, V. C., WASIUK, A., GUO, Y. & NOELLE, R. J. 2009. Molecular mechanism and function of CD40/CD40L engagement in the immune system. *Immunol Rev,* 229**,** 152-72.

ELIAS, P. M. 2007. The skin barrier as an innate immune element. *Semin Immunopathol,* 29**,** 3-14.

ENGELHARD, V. H. 1994. Structure of peptides associated with class I and class II MHC molecules. *Annu Rev Immunol,* 12**,** 181-207.

ESHEL, I., SAVION, N. & SHOHAM, J. 1990. Analysis of thymic stromal cell subpopulations grown in vitro on extracellular matrix in defined medium. I. Growth conditions and morphology of murine thymic epithelial and mesenchymal cells. *J Immunol,* 144**,** 1554-62.

FABRE, S., CARRETTE, F., CHEN, J., LANG, V., SEMICHON, M., DENOYELLE, C., LAZAR, V., CAGNARD, N., DUBART-KUPPERSCHMITT, A., MANGENEY, M., FRUMAN, D. A. & BISMUTH, G. 2008. FOXO1 regulates L-Selectin and a network of human T cell homing molecules downstream of phosphatidylinositol 3-kinase. *J Immunol,* 181**,** 2980-9.

FALK, I., NERZ, G., HAIDL, I., KROTKOVA, A. & EICHMANN, K. 2001. Immature thymocytes that fail to express TCRbeta and/or TCRgamma delta proteins die by apoptotic cell death in the CD44(-)CD25(-) (DN4) subset. *Eur J Immunol,* 31**,** 3308-17.

FALK, K., ROTZSCHKE, O., STEVANOVIC, S., JUNG, G. & RAMMENSEE, H. G. 1991. Allele-specific motifs revealed by sequencing of self-peptides eluted from MHC molecules. *Nature,* 351**,** 290-6.

FARR, A., DEROOS, P. C., EASTMAN, S. & RUDENSKY, A. Y. 1996. Differential expression of CLIP:MHC class II and conventional endogenous peptide:MHC class II complexes by thymic epithelial cells and peripheral antigen-presenting cells. *Eur J Immunol,* 26**,** 3185-93.

FARR, A. G. & ANDERSON, S. K. 1985. Epithelial heterogeneity in the murine thymus: fucose-specific lectins bind medullary epithelial cells. *J Immunol,* 134**,** 2971-7.

FARR, A. G. & BRADDY, S. C. 1989. Patterns of keratin expression in the murine thymus. *Anat Rec,* 224**,** 374-8.

FEHLING, H. J., KROTKOVA, A., SAINT-RUF, C. & VON BOEHMER, H. 1995. Crucial role of the pre-T-cell receptor alpha gene in development of alpha beta but not gamma delta T cells. *Nature,* 375**,** 795-8.

FEHSEL, K., KRONCKE, K. D., MEYER, K. L., HUBER, H., WAHN, V. & KOLB-BACHOFEN, V. 1995. Nitric oxide induces apoptosis in mouse thymocytes. *J Immunol,* 155**,** 2858-65.

FELLEY-BOSCO, E., AMBS, S., LOWENSTEIN, C. J., KEEFER, L. K. & HARRIS, C. C. 1994. Constitutive expression of inducible nitric oxide synthase in human bronchial epithelial cells induces c-fos and stimulates the cGMP pathway. *Am J Respir Cell Mol Biol,* 11**,** 159-64.

FENYK-MELODY, J. E., GARRISON, A. E., BRUNNERT, S. R., WEIDNER, J. R., SHEN, F., SHELTON, B. A. & MUDGETT, J. S. 1998. Experimental autoimmune encephalomyelitis is exacerbated in mice lacking the NOS2 gene. *J Immunol,* 160**,** 2940-6.

FERREIRA, C., PALMER, D., BLAKE, K., GARDEN, O. A. & DYSON, J. 2014. Reduced regulatory T cell diversity in NOD mice is linked to early events in the thymus. *J Immunol,* 192**,** 4145-52.

FIGUEROA, X. F., LILLO, M. A., GAETE, P. S., RIQUELME, M. A. & SAEZ, J. C. 2013. Diffusion of nitric oxide across cell membranes of the vascular wall requires specific connexin-based channels. *Neuropharmacology,* 75**,** 471-8.

FIORINI, E., FERRERO, I., MERCK, E., FAVRE, S., PIERRES, M., LUTHER, S. A. & MACDONALD, H. R. 2008. Cutting edge: thymic crosstalk regulates delta-like 4 expression on cortical epithelial cells. *J Immunol,* 181**,** 8199-203.

FLANAGAN, S. P. 1966. 'Nude', a new hairless gene with pleiotropic effects in the mouse. *Genet Res,* 8**,** 295-309.

FONTENOT, J. D., GAVIN, M. A. & RUDENSKY, A. Y. 2003. Foxp3 programs the development and function of CD4+CD25+ regulatory T cells. *Nat Immunol,* 4**,** 330-6.

FONTENOT, J. D. & RUDENSKY, A. Y. 2005. A well adapted regulatory contrivance: regulatory T cell development and the forkhead family transcription factor Foxp3. *Nat Immunol,* 6**,** 331-7.

FORMAN, H. J. & TORRES, M. 2002. Reactive oxygen species and cell signaling: respiratory burst in macrophage signaling. *Am J Respir Crit Care Med,* 166**,** S4-8.

FORSTER, R., SCHUBEL, A., BREITFELD, D., KREMMER, E., RENNER-MULLER, I., WOLF, E. & LIPP, M. 1999. CCR7 coordinates the primary immune response by establishing functional microenvironments in secondary lymphoid organs. *Cell,* 99**,** 23-33.

FOSS, D. L., DONSKOY, E. & GOLDSCHNEIDER, I. 2001. The importation of hematogenous precursors by the thymus is a gated phenomenon in normal adult mice. *J Exp Med,* 193**,** 365-74.

FRIESEN, T. J., JI, Q. & FINK, P. J. 2016. Recent thymic emigrants are tolerized in the absence of inflammation. *J Exp Med,* 213**,** 913-20.

FUNG-LEUNG, W. P., WALLACE, V. A., GRAY, D., SHA, W. C., PIRCHER, H., TEH, H. S., LOH, D. Y. & MAK, T. W. 1993. CD8 is needed for positive selection but differentially required for negative selection of T cells during thymic ontogeny. *Eur J Immunol,* 23**,** 212-6.

GALLEGOS, A. M. & BEVAN, M. J. 2004. Central tolerance to tissue-specific antigens mediated by direct and indirect antigen presentation. *J Exp Med,* 200**,** 1039-49.

GANZ, T. 2003. Defensins: antimicrobial peptides of innate immunity. *Nat Rev Immunol,* 3**,** 710-20.

GARDNER, J. M., METZGER, T. C., MCMAHON, E. J., AU-YEUNG, B. B., KRAWISZ, A. K., LU, W., PRICE, J. D., JOHANNES, K. P., SATPATHY, A. T., MURPHY, K. M., TARBELL, K. V., WEISS, A. & ANDERSON, M. S. 2013. Extrathymic Aire-expressing cells are a distinct bone marrow-derived population that induce functional inactivation of CD4(+) T cells. *Immunity,* 39**,** 560-72.

GERMAIN, R. N. 2001. The art of the probable: system control in the adaptive immune system. *Science,* 293**,** 240-5.

GERMAIN, R. N. 2002. T-cell development and the CD4-CD8 lineage decision. *Nat Rev Immunol,* 2**,** 309-22.

GILFILLAN, S., DIERICH, A., LEMEUR, M., BENOIST, C. & MATHIS, D. 1993. Mice lacking TdT: mature animals with an immature lymphocyte repertoire. *Science,* 261**,** 1175-8.

GILLARD, G. O., DOOLEY, J., ERICKSON, M., PELTONEN, L. & FARR, A. G. 2007. Aire-dependent alterations in medullary thymic epithelium indicate a role for Aire in thymic epithelial differentiation. *J Immunol,* 178**,** 3007-15.

GODFREY, D. I., KENNEDY, J., SUDA, T. & ZLOTNIK, A. 1993. A developmental pathway involving four phenotypically and functionally distinct subsets of CD3-CD4-CD8- triple-negative adult mouse thymocytes defined by CD44 and CD25 expression. *J Immunol,* 150**,** 4244-52.

GODFREY, V. L., WILKINSON, J. E., RINCHIK, E. M. & RUSSELL, L. B. 1991a. Fatal lymphoreticular disease in the scurfy (sf) mouse requires T cells that

mature in a sf thymic environment: potential model for thymic education. *Proc Natl Acad Sci U S A,* 88**,** 5528-32.

GODFREY, V. L., WILKINSON, J. E. & RUSSELL, L. B. 1991b. X-linked lymphoreticular disease in the scurfy (sf) mutant mouse. *Am J Pathol,* 138**,** 1379-87.

GOMMEAUX, J., GREGOIRE, C., NGUESSAN, P., RICHELME, M., MALISSEN, M., GUERDER, S., MALISSEN, B. & CARRIER, A. 2009. Thymus-specific serine protease regulates positive selection of a subset of CD4+ thymocytes. *Eur J Immunol,* 39**,** 956-64.

GOSSENS, K., NAUS, S., CORBEL, S. Y., LIN, S., ROSSI, F. M., KAST, J. & ZILTENER, H. J. 2009. Thymic progenitor homing and lymphocyte homeostasis are linked via S1P-controlled expression of thymic P-selectin/CCL25. *J Exp Med,* 206**,** 761-78.

GRAY, D. 1993. Immunological memory. *Annu Rev Immunol,* 11**,** 49-77.

GRAY, D., ABRAMSON, J., BENOIST, C. & MATHIS, D. 2007. Proliferative arrest and rapid turnover of thymic epithelial cells expressing Aire. *J Exp Med,* 204**,** 2521-8.

GROLL, M., DITZEL, L., LOWE, J., STOCK, D., BOCHTLER, M., BARTUNIK, H. D. & HUBER, R. 1997. Structure of 20S proteasome from yeast at 2.4 A resolution. *Nature,* 386**,** 463-71.

GU, L., TSENG, S., HORNER, R. M., TAM, C., LODA, M. & ROLLINS, B. J. 2000. Control of TH2 polarization by the chemokine monocyte chemoattractant protein-1. *Nature,* 404**,** 407-11.

HAGER-THEODORIDES, A. L., FURMANSKI, A. L., ROSS, S. E., OUTRAM, S. V., ROWBOTHAM, N. J. & CROMPTON, T. 2009. The Gli3 transcription factor expressed in the thymus stroma controls thymocyte negative selection via Hedgehog-dependent and -independent mechanisms. *J Immunol,* 183**,** 3023-32.

HAJI-GHASSEMI, O., BLACKLER, R. J., MARTIN YOUNG, N. & EVANS, S. V. 2015. Antibody recognition of carbohydrate epitopesdagger. *Glycobiology,* 25**,** 920-52.

HAMAZAKI, Y., FUJITA, H., KOBAYASHI, T., CHOI, Y., SCOTT, H. S., MATSUMOTO, M. & MINATO, N. 2007. Medullary thymic epithelial cells expressing Aire represent a unique lineage derived from cells expressing claudin. *Nat Immunol,* 8**,** 304-11.

HARA, M., KINGSLEY, C. I., NIIMI, M., READ, S., TURVEY, S. E., BUSHELL, A. R., MORRIS, P. J., POWRIE, F. & WOOD, K. J. 2001. IL-10 is required for regulatory T cells to mediate tolerance to alloantigens in vivo. *J Immunol,* 166**,** 3789-96.

HAURI-HOHL, M., ZUKLYS, S., HOLLANDER, G. A. & ZIEGLER, S. F. 2014. A regulatory role for TGF-beta signaling in the establishment and function of the thymic medulla. *Nat Immunol,* 15**,** 554-61.

HAYASHI, F., SMITH, K. D., OZINSKY, A., HAWN, T. R., YI, E. C., GOODLETT, D. R., ENG, J. K., AKIRA, S., UNDERHILL, D. M. & ADEREM, A. 2001. The innate immune response to bacterial flagellin is mediated by Toll-like receptor 5. *Nature,* 410**,** 1099-103.

HEMMI, H., TAKEUCHI, O., KAWAI, T., KAISHO, T., SATO, S., SANJO, H., MATSUMOTO, M., HOSHINO, K., WAGNER, H., TAKEDA, K. & AKIRA, S. 2000. A Toll-like receptor recognizes bacterial DNA. *Nature,* 408**,** 740-5.

HERNANDEZ-HOYOS, G., SOHN, S. J., ROTHENBERG, E. V. & ALBEROLA-ILA, J. 2000. Lck activity controls CD4/CD8 T cell lineage commitment. *Immunity,* 12**,** 313-22.

HIKOSAKA, Y., NITTA, T., OHIGASHI, I., YANO, K., ISHIMARU, N., HAYASHI, Y., MATSUMOTO, M., MATSUO, K., PENNINGER, J. M., TAKAYANAGI, H., YOKOTA, Y., YAMADA, H., YOSHIKAI, Y., INOUE, J., AKIYAMA, T. & TAKAHAMA, Y. 2008. The cytokine RANKL produced by positively selected thymocytes fosters medullary thymic epithelial cells that express autoimmune regulator. *Immunity,* 29**,** 438-50.

HOFFMAN, E. S., PASSONI, L., CROMPTON, T., LEU, T. M., SCHATZ, D. G., KOFF, A., OWEN, M. J. & HAYDAY, A. C. 1996. Productive T-cell receptor beta-chain gene rearrangement: coincident regulation of cell cycle and clonality during development in vivo. *Genes Dev,* 10**,** 948-62.

HOGQUIST, K. A., JAMESON, S. C., HEATH, W. R., HOWARD, J. L., BEVAN, M. J. & CARBONE, F. R. 1994. T cell receptor antagonist peptides induce positive selection. *Cell,* 76**,** 17-27.

HONEY, K., NAKAGAWA, T., PETERS, C. & RUDENSKY, A. 2002. Cathepsin L regulates CD4+ T cell selection independently of its effect on invariant chain: a role in the generation of positively selecting peptide ligands. *J Exp Med,* 195**,** 1349-58.

HONJO, T. 1983. Immunoglobulin genes. *Annu Rev Immunol,* 1**,** 499-528.

HOOPER, L. V., LITTMAN, D. R. & MACPHERSON, A. J. 2012. Interactions between the microbiota and the immune system. *Science,* 336**,** 1268-73.

HORI, S., NOMURA, T. & SAKAGUCHI, S. 2003. Control of regulatory T cell development by the transcription factor Foxp3. *Science,* 299**,** 1057-61.

HOSHINO, K., TAKEUCHI, O., KAWAI, T., SANJO, H., OGAWA, T., TAKEDA, Y., TAKEDA, K. & AKIRA, S. 1999. Cutting edge: Toll-like receptor 4 (TLR4)-deficient mice are hyporesponsive to lipopolysaccharide: evidence for TLR4 as the Lps gene product. *J Immunol,* 162**,** 3749-52.

HOUSTON, E. G., JR. & FINK, P. J. 2009. MHC drives TCR repertoire shaping, but not maturation, in recent thymic emigrants. *J Immunol,* 183**,** 7244-9.

HSIEH, C. S., MACATONIA, S. E., TRIPP, C. S., WOLF, S. F., O'GARRA, A. & MURPHY, K. M. 1993. Development of TH1 CD4+ T cells through IL-12 produced by Listeria-induced macrophages. *Science,* 260**,** 547-9.

HSING, L. C. & RUDENSKY, A. Y. 2005. The lysosomal cysteine proteases in MHC class II antigen presentation. *Immunol Rev,* 207**,** 229-41.

HU, Q., BAZEMORE WALKER, C. R., GIRAO, C., OPFERMAN, J. T., SUN, J., SHABANOWITZ, J., HUNT, D. F. & ASHTON-RICKARDT, P. G. 1997. Specific recognition of thymic self-peptides induces the positive selection of cytotoxic T lymphocytes. *Immunity,* 7**,** 221-31.

HUANG, D., CAI, D. T., CHUA, R. Y., KEMENY, D. M. & WONG, S. H. 2008. Nitric-oxide synthase 2 interacts with CD74 and inhibits its cleavage by caspase during dendritic cell development. *J Biol Chem,* 283**,** 1713-22.

HUANG, P. L., HUANG, Z., MASHIMO, H., BLOCH, K. D., MOSKOWITZ, M. A., BEVAN, J. A. & FISHMAN, M. C. 1995. Hypertension in mice lacking the gene for endothelial nitric oxide synthase. *Nature,* 377**,** 239-42.

HUBERT, F. X., KINKEL, S. A., CREWTHER, P. E., CANNON, P. Z., WEBSTER, K. E., LINK, M., UIBO, R., O'BRYAN, M. K., MEAGER, A., FOREHAN, S. P., SMYTH, G. K., MITTAZ, L., ANTONARAKIS, S. E., PETERSON, P., HEATH, W. R. &

SCOTT, H. S. 2009. Aire-deficient C57BL/6 mice mimicking the common human 13-base pair deletion mutation present with only a mild autoimmune phenotype. *J Immunol,* 182**,** 3902-18.

HUBERT, F. X., KINKEL, S. A., WEBSTER, K. E., CANNON, P., CREWTHER, P. E., PROEITTO, A. I., WU, L., HEATH, W. R. & SCOTT, H. S. 2008. A specific anti-Aire antibody reveals aire expression is restricted to medullary thymic epithelial cells and not expressed in periphery. *J Immunol,* 180**,** 3824-32.

HUESMANN, M., SCOTT, B., KISIELOW, P. & VON BOEHMER, H. 1991. Kinetics and efficacy of positive selection in the thymus of normal and T cell receptor transgenic mice. *Cell,* 66**,** 533-40.

IRVING, B. A. & WEISS, A. 1991. The cytoplasmic domain of the T cell receptor zeta chain is sufficient to couple to receptor-associated signal transduction pathways. *Cell,* 64**,** 891-901.

ITANO, A. & ROBEY, E. 2000. Highly efficient selection of CD4 and CD8 lineage thymocytes supports an instructive model of lineage commitment. *Immunity,* 12**,** 383-9.

ITO, T., WANG, Y. H., DURAMAD, O., HORI, T., DELESPESSE, G. J., WATANABE, N., QIN, F. X., YAO, Z., CAO, W. & LIU, Y. J. 2005. TSLP-activated dendritic cells induce an inflammatory T helper type 2 cell response through OX40 ligand. *J Exp Med,* 202**,** 1213-23.

IWASAKI, A. & MEDZHITOV, R. 2004. Toll-like receptor control of the adaptive immune responses. *Nat Immunol,* 5**,** 987-95.

IWASAKI, A. & MEDZHITOV, R. 2010. Regulation of adaptive immunity by the innate immune system. *Science,* 327**,** 291-5.

JANAS, M. L., VARANO, G., GUDMUNDSSON, K., NODA, M., NAGASAWA, T. & TURNER, M. 2010. Thymic development beyond beta-selection requires phosphatidylinositol 3-kinase activation by CXCR4. *J Exp Med,* 207**,** 247-61.

JANEWAY, C. A., JR. 1992. The T cell receptor as a multicomponent signalling machine: CD4/CD8 coreceptors and CD45 in T cell activation. *Annu Rev Immunol,* 10**,** 645-74.

JANEWAY, C. A., JR. & MEDZHITOV, R. 2002. Innate immune recognition. *Annu Rev Immunol,* 20**,** 197-216.

JENKINSON, E. J. & ANDERSON, G. 1994. Fetal Thymic Organ-Cultures. *Current Opinion in Immunology,* 6**,** 293-297.

JENKINSON, W. E., MCCARTHY, N. I., DUTTON, E. E., COWAN, J. E., PARNELL, S. M., WHITE, A. J. & ANDERSON, G. 2015. Natural Th17 cells are critically regulated by functional medullary thymic microenvironments. *J Autoimmun,* 63**,** 13-22.

JIANJUN, Y., ZHANG, R., LU, G., SHEN, Y., PENG, L., ZHU, C., CUI, M., WANG, W., ARNABOLDI, P., TANG, M., GUPTA, M., QI, C. F., JAYARAMAN, P., ZHU, H., JIANG, B., CHEN, S. H., HE, J. C., TING, A. T., ZHOU, M. M., KUCHROO, V. K., MORSE, H. C., 3RD, OZATO, K., SIKORA, A. G. & XIONG, H. 2013. T cell-derived inducible nitric oxide synthase switches off Th17 cell differentiation. *J Exp Med,* 210**,** 1447-62.

JIN, R., WANG, W., YAO, J. Y., ZHOU, Y. B., QIAN, X. P., ZHANG, J., ZHANG, Y. & CHEN, W. F. 2008. Characterization of the in vivo dynamics of medullary CD4+CD8- thymocyte development. *J Immunol,* 180**,** 2256-63.

JOLICOEUR, C., HANAHAN, D. & SMITH, K. M. 1994. T-cell tolerance toward a transgenic beta-cell antigen and transcription of endogenous pancreatic genes in thymus. *Proc Natl Acad Sci U S A,* 91**,** 6707-11.

JUNE, C. H., LEDBETTER, J. A., LINSLEY, P. S. & THOMPSON, C. B. 1990. Role of the CD28 receptor in T-cell activation. *Immunol Today,* 11**,** 211-6.

JUNG, S., RAJEWSKY, K. & RADBRUCH, A. 1993. Shutdown of class switch recombination by deletion of a switch region control element. *Science,* 259**,** 984-7.

KAJIURA, F., SUN, S., NOMURA, T., IZUMI, K., UENO, T., BANDO, Y., KURODA, N., HAN, H., LI, Y., MATSUSHIMA, A., TAKAHAMA, Y., SAKAGUCHI, S., MITANI, T. & MATSUMOTO, M. 2004. NF-kappa B-inducing kinase establishes self-tolerance in a thymic stroma-dependent manner. *J Immunol,* 172**,** 2067-75.

KARUPIAH, G., XIE, Q. W., BULLER, R. M., NATHAN, C., DUARTE, C. & MACMICKING, J. D. 1993. Inhibition of viral replication by interferon-gamma-induced nitric oxide synthase. *Science,* 261**,** 1445-8.

KASER, A., LEE, A. H., FRANKE, A., GLICKMAN, J. N., ZEISSIG, S., TILG, H., NIEUWENHUIS, E. E., HIGGINS, D. E., SCHREIBER, S., GLIMCHER, L. H. & BLUMBERG, R. S. 2008. XBP1 links ER stress to intestinal inflammation and confers genetic risk for human inflammatory bowel disease. *Cell,* 134**,** 743-56.

KATZ, J. F., STEBBINS, C., APPELLA, E. & SANT, A. J. 1996. Invariant chain and DM edit self-peptide presentation by major histocompatibility complex (MHC) class II molecules. *J Exp Med,* 184**,** 1747-53.

KAUFMAN, J. F., AUFFRAY, C., KORMAN, A. J., SHACKELFORD, D. A. & STROMINGER, J. 1984. The class II molecules of the human and murine major histocompatibility complex. *Cell,* 36**,** 1-13.

KAWABE, T., NAKA, T., YOSHIDA, K., TANAKA, T., FUJIWARA, H., SUEMATSU, S., YOSHIDA, N., KISHIMOTO, T. & KIKUTANI, H. 1994. The immune responses in CD40-deficient mice: impaired immunoglobulin class switching and germinal center formation. *Immunity,* 1**,** 167-78.

KAWANO, H., NISHIJIMA, H., MORIMOTO, J., HIROTA, F., MORITA, R., MOURI, Y., NISHIOKA, Y. & MATSUMOTO, M. 2015. Aire Expression Is Inherent to Most Medullary Thymic Epithelial Cells during Their Differentiation Program. *J Immunol,* 195**,** 5149-58.

KAY, H. D., BONNARD, G. D., WEST, W. H. & HERBERMAN, R. B. 1977. A functional comparison of human Fc-receptor-bearing lymphocytes active in natural cytotoxicity and antibody-dependent cellular cytotoxicity. *J Immunol,* 118**,** 2058-66.

KERDILES, Y. M., BEISNER, D. R., TINOCO, R., DEJEAN, A. S., CASTRILLON, D. H., DEPINHO, R. A. & HEDRICK, S. M. 2009. Foxo1 links homing and survival of naive T cells by regulating L-selectin, CCR7 and interleukin 7 receptor. *Nat Immunol,* 10**,** 176-84.

KERN, P. S., TENG, M. K., SMOLYAR, A., LIU, J. H., LIU, J., HUSSEY, R. E., SPOERL, R., CHANG, H. C., REINHERZ, E. L. & WANG, J. H. 1998. Structural basis of CD8 coreceptor function revealed by crystallographic analysis of a murine CD8alphaalpha ectodomain fragment in complex with H-2Kb. *Immunity,* 9**,** 519-30.

KHAN, I. S., MOUCHESS, M. L., ZHU, M. L., CONLEY, B., FASANO, K. J., HOU, Y., FONG, L., SU, M. A. & ANDERSON, M. S. 2014. Enhancement of an anti-tumor immune response by transient blockade of central T cell tolerance. *J Exp Med,* 211**,** 761-8.

KIMBRELL, D. A. & BEUTLER, B. 2001. The evolution and genetics of innate immunity. *Nat Rev Genet,* 2**,** 256-67.

KISHIMOTO, H. & SPRENT, J. 1997. Negative selection in the thymus includes semimature T cells. *J Exp Med,* 185**,** 263-71.

KISIELOW, P., TEH, H. S., BLUTHMANN, H. & VON BOEHMER, H. 1988. Positive selection of antigen-specific T cells in thymus by restricting MHC molecules. *Nature,* 335**,** 730-3.

KLEIN, L., HINTERBERGER, M., WIRNSBERGER, G. & KYEWSKI, B. 2009. Antigen presentation in the thymus for positive selection and central tolerance induction. *Nat Rev Immunol,* 9**,** 833-44.

KLEIN, L., KYEWSKI, B., ALLEN, P. M. & HOGQUIST, K. A. 2014. Positive and negative selection of the T cell repertoire: what thymocytes see (and don't see). *Nat Rev Immunol,* 14**,** 377-91.

KOBLE, C. & KYEWSKI, B. 2009. The thymic medulla: a unique microenvironment for intercellular self-antigen transfer. *J Exp Med,* 206**,** 1505-13.

KOLLER, B. H., MARRACK, P., KAPPLER, J. W. & SMITHIES, O. 1990. Normal development of mice deficient in beta 2M, MHC class I proteins, and CD8+ T cells. *Science,* 248**,** 1227-30.

KRAAL, G., BREEL, M., JANSE, M. & BRUIN, G. 1986. Langerhans' cells, veiled cells, and interdigitating cells in the mouse recognized by a monoclonal antibody. *J Exp Med,* 163**,** 981-97.

KRUEGER, A., WILLENZON, S., LYSZKIEWICZ, M., KREMMER, E. & FORSTER, R. 2010. CC chemokine receptor 7 and 9 double-deficient hematopoietic progenitors are severely impaired in seeding the adult thymus. *Blood,* 115**,** 1906-12.

KUROBE, H., LIU, C., UENO, T., SAITO, F., OHIGASHI, I., SEACH, N., ARAKAKI, R., HAYASHI, Y., KITAGAWA, T., LIPP, M., BOYD, R. L. & TAKAHAMA, Y. 2006. CCR7-dependent cortex-to-medulla migration of positively selected thymocytes is essential for establishing central tolerance. *Immunity,* 24**,** 165-77.

KYEWSKI, B. A. 1987. Seeding of thymic microenvironments defined by distinct thymocyte-stromal cell interactions is developmentally controlled. *J Exp Med,* 166**,** 520-38.

LAAN, M., KISAND, K., KONT, V., MOLL, K., TSEREL, L., SCOTT, H. S. & PETERSON, P. 2009. Autoimmune regulator deficiency results in decreased expression of CCR4 and CCR7 ligands and in delayed migration of CD4+ thymocytes. *J Immunol,* 183**,** 7682-91.

LANCASTER, J. R., JR. 1994. Simulation of the diffusion and reaction of endogenously produced nitric oxide. *Proc Natl Acad Sci U S A,* 91**,** 8137-41.

LAUFER, T. M., DEKONING, J., MARKOWITZ, J. S., LO, D. & GLIMCHER, L. H. 1996. Unopposed positive selection and autoreactivity in mice expressing class II MHC only on thymic cortex. *Nature,* 383**,** 81-5.

LEAVY, O. 2013. Regulatory T cells: the thymic medulla - a cradle for TReg cell development. *Nat Rev Immunol,* 13**,** 304.

LEE, C. & MCCONNELL, H. M. 1995. A general model of invariant chain association with class II major histocompatibility complex proteins. *Proc Natl Acad Sci U S A,* 92**,** 8269-73.

LEE, S. C., DICKSON, D. W., LIU, W. & BROSNAN, C. F. 1993. Induction of nitric oxide synthase activity in human astrocytes by interleukin-1 beta and interferon-gamma. *J Neuroimmunol,* 46**,** 19-24.

LEE, S. W., CHOI, H., EUN, S. Y., FUKUYAMA, S. & CROFT, M. 2011. Nitric oxide modulates TGF-beta-directive signals to suppress Foxp3+ regulatory T cell differentiation and potentiate Th1 development. *J Immunol,* 186**,** 6972-80.

LEI, Y., RIPEN, A. M., ISHIMARU, N., OHIGASHI, I., NAGASAWA, T., JEKER, L. T., BOSL, M. R., HOLLANDER, G. A., HAYASHI, Y., MALEFYT RDE, W., NITTA, T. & TAKAHAMA, Y. 2011. Aire-dependent production of XCL1 mediates medullary accumulation of thymic dendritic cells and contributes to regulatory T cell development. *J Exp Med,* 208**,** 383-94.

LENSCHOW, D. J., WALUNAS, T. L. & BLUESTONE, J. A. 1996. CD28/B7 system of T cell costimulation. *Annu Rev Immunol,* 14**,** 233-58.

LEVELT, C. N., WANG, B., EHRFELD, A., TERHORST, C. & EICHMANN, K. 1995. Regulation of T cell receptor (TCR)-beta locus allelic exclusion and initiation of TCR-alpha locus rearrangement in immature thymocytes by signaling through the CD3 complex. *Eur J Immunol,* 25**,** 1257-61.

LEY, K. & KANSAS, G. S. 2004. Selectins in T-cell recruitment to non-lymphoid tissues and sites of inflammation. *Nat Rev Immunol,* 4**,** 325-35.

LI, J., LI, Y., YAO, J. Y., JIN, R., ZHU, M. Z., QIAN, X. P., ZHANG, J., FU, Y. X., WU, L., ZHANG, Y. & CHEN, W. F. 2007. Developmental pathway of CD4+CD8- medullary thymocytes during mouse ontogeny and its defect in Aire-/- mice. *Proc Natl Acad Sci U S A,* 104**,** 18175-80.

LICHTMAN, A. H., CHIN, J., SCHMIDT, J. A. & ABBAS, A. K. 1988. Role of interleukin 1 in the activation of T lymphocytes. *Proc Natl Acad Sci U S A,* 85**,** 9699-703.

LIEBER, M. R., HESSE, J. E., LEWIS, S., BOSMA, G. C., ROSENBERG, N., MIZUUCHI, K., BOSMA, M. J. & GELLERT, M. 1988. The defect in murine severe combined immune deficiency: joining of signal sequences but not coding segments in V(D)J recombination. *Cell,* 55**,** 7-16.

LIN, J., YANG, L., SILVA, H. M., TRZECIAK, A., CHOI, Y., SCHWAB, S. R., DUSTIN, M. L. & LAFAILLE, J. J. 2016. Increased generation of Foxp3(+) regulatory T cells by manipulating antigen presentation in the thymus. *Nat Commun,* 7**,** 10562.

LIND, E. F., PROCKOP, S. E., PORRITT, H. E. & PETRIE, H. T. 2001. Mapping precursor movement through the postnatal thymus reveals specific microenvironments supporting defined stages of early lymphoid development. *J Exp Med,* 194**,** 127-34.

LIO, C. W., DODSON, L. F., DEPPONG, C. M., HSIEH, C. S. & GREEN, J. M. 2010. CD28 facilitates the generation of Foxp3(-) cytokine responsive regulatory T cell precursors. *J Immunol,* 184**,** 6007-13.

LIO, C. W. & HSIEH, C. S. 2008. A two-step process for thymic regulatory T cell development. *Immunity,* 28**,** 100-11.

LISTON, A., LESAGE, S., WILSON, J., PELTONEN, L. & GOODNOW, C. C. 2003. Aire regulates negative selection of organ-specific T cells. *Nat Immunol,* 4**,** 350-4.

LIU, C., SAITO, F., LIU, Z., LEI, Y., UEHARA, S., LOVE, P., LIPP, M., KONDO, S., MANLEY, N. & TAKAHAMA, Y. 2006. Coordination between CCR7- and CCR9-mediated chemokine signals in prevascular fetal thymus colonization. *Blood,* 108**,** 2531-9.

LKHAGVASUREN, E., SAKATA, M., OHIGASHI, I. & TAKAHAMA, Y. 2013. Lymphotoxin beta receptor regulates the development of CCL21-expressing subset of postnatal medullary thymic epithelial cells. *J Immunol,* 190**,** 5110-7.

LO, W. L., FELIX, N. J., WALTERS, J. J., ROHRS, H., GROSS, M. L. & ALLEN, P. M. 2009. An endogenous peptide positively selects and augments the activation and survival of peripheral CD4+ T cells. *Nat Immunol,* 10**,** 1155-61.

LOVE, P. E. & HAYES, S. M. 2010. ITAM-mediated signaling by the T-cell antigen receptor. *Cold Spring Harb Perspect Biol,* 2**,** a002485.

LU, F. T., YANG, W., WANG, Y. H., MA, H. D., TANG, W., YANG, J. B., LI, L., ANSARI, A. A. & LIAN, Z. X. 2015. Thymic B cells promote thymus-derived regulatory T cell development and proliferation. *J Autoimmun,* 61**,** 62-72.

LUKACS-KORNEK, V., MALHOTRA, D., FLETCHER, A. L., ACTON, S. E., ELPEK, K. G., TAYALIA, P., COLLIER, A. R. & TURLEY, S. J. 2011. Regulated release of nitric oxide by nonhematopoietic stroma controls expansion of the activated T cell pool in lymph nodes. *Nat Immunol,* 12**,** 1096-104.

LUSTER, A. D. 1998. Chemokines--chemotactic cytokines that mediate inflammation. *N Engl J Med,* 338**,** 436-45.

MACMICKING, J., XIE, Q. W. & NATHAN, C. 1997. Nitric oxide and macrophage function. *Annu Rev Immunol,* 15**,** 323-50.

MACMICKING, J. D., NATHAN, C., HOM, G., CHARTRAIN, N., FLETCHER, D. S., TRUMBAUER, M., STEVENS, K., XIE, Q. W., SOKOL, K., HUTCHINSON, N. & ET AL. 1995. Altered responses to bacterial infection and endotoxic shock in mice lacking inducible nitric oxide synthase. *Cell,* 81**,** 641-50.

MAGRI, M., YATIM, A., BENNE, C., BALBO, M., HENRY, A., SERRAF, A., SAKANO, S., GAZZOLO, L., LEVY, Y. & LELIEVRE, J. D. 2009. Notch ligands potentiate IL-7-driven proliferation and survival of human thymocyte precursors. *Eur J Immunol,* 39**,** 1231-40.

MAHMUD, S. A., MANLOVE, L. S., SCHMITZ, H. M., XING, Y., WANG, Y., OWEN, D. L., SCHENKEL, J. M., BOOMER, J. S., GREEN, J. M., YAGITA, H., CHI, H., HOGQUIST, K. A. & FARRAR, M. A. 2014. Costimulation via the tumor-necrosis factor receptor superfamily couples TCR signal strength to the thymic differentiation of regulatory T cells. *Nat Immunol,* 15**,** 473-81.

MAILLARD, I., KOCH, U., DUMORTIER, A., SHESTOVA, O., XU, L., SAI, H., PROSS, S. E., ASTER, J. C., BHANDOOLA, A., RADTKE, F. & PEAR, W. S. 2008. Canonical notch signaling is dispensable for the maintenance of adult hematopoietic stem cells. *Cell Stem Cell,* 2**,** 356-66.

MALCHOW, S., LEVENTHAL, D. S., NISHI, S., FISCHER, B. I., SHEN, L., PANER, G. P., AMIT, A. S., KANG, C., GEDDES, J. E., ALLISON, J. P., SOCCI, N. D. & SAVAGE, P. A. 2013. Aire-dependent thymic development of tumor-associated regulatory T cells. *Science,* 339**,** 1219-24.

MALISSEN, M., MINARD, K., MJOLSNESS, S., KRONENBERG, M., GOVERMAN, J., HUNKAPILLER, T., PRYSTOWSKY, M. B., YOSHIKAI, Y., FITCH, F., MAK, T. W. & ET AL. 1984. Mouse T cell antigen receptor: structure and organization of constant and joining gene segments encoding the beta polypeptide. *Cell,* 37**,** 1101-10.

MALISSEN, M., TRUCY, J., JOUVIN-MARCHE, E., CAZENAVE, P. A., SCOLLAY, R. & MALISSEN, B. 1992. Regulation of TCR alpha and beta gene allelic exclusion during T-cell development. *Immunol Today,* 13**,** 315-22.

MARRACK, P. & KAPPLER, J. 1987. The T cell receptor. *Science,* 238**,** 1073-9.

MASUDA, K., KAKUGAWA, K., NAKAYAMA, T., MINATO, N., KATSURA, Y. & KAWAMOTO, H. 2007. T cell lineage determination precedes the initiation of TCR beta gene rearrangement. *J Immunol,* 179**,** 3699-706.

MAYER, C. E., ZUKLYS, S., ZHANYBEKOVA, S., OHIGASHI, I., TEH, H. Y., SANSOM, S. N., SHIKAMA-DORN, N., HAFEN, K., MACAULAY, I. C., DEADMAN, M. E., PONTING, C. P., TAKAHAMA, Y. & HOLLANDER, G. A. 2016. Dynamic spatio-temporal contribution of single beta5t+ cortical epithelial precursors to the thymus medulla. *Eur J Immunol,* 46**,** 846-56.

MCCARTHY, N. I., COWAN, J. E., NAKAMURA, K., BACON, A., BAIK, S., WHITE, A. J., PARNELL, S. M., JENKINSON, E. J., JENKINSON, W. E. & ANDERSON, G. 2015. Osteoprotegerin-Mediated Homeostasis of Rank+ Thymic Epithelial Cells Does Not Limit Foxp3+ Regulatory T Cell Development. *J Immunol,* 195**,** 2675-82.

MCCARTNEY-FRANCIS, N., ALLEN, J. B., MIZEL, D. E., ALBINA, J. E., XIE, Q. W., NATHAN, C. F. & WAHL, S. M. 1993. Suppression of arthritis by an inhibitor of nitric oxide synthase. *J Exp Med,* 178**,** 749-54.

MCCAUGHTRY, T. M., ETZENSPERGER, R., ALAG, A., TAI, X., KURTULUS, S., PARK, J. H., GRINBERG, A., LOVE, P., FEIGENBAUM, L., ERMAN, B. & SINGER, A. 2012. Conditional deletion of cytokine receptor chains reveals that IL-7 and IL-15 specify CD8 cytotoxic lineage fate in the thymus. *J Exp Med,* 209**,** 2263-76.

MCCAUGHTRY, T. M., WILKEN, M. S. & HOGQUIST, K. A. 2007. Thymic emigration revisited. *J Exp Med,* 204**,** 2513-20.

MCHEYZER-WILLIAMS, L. J. & MCHEYZER-WILLIAMS, M. G. 2005. Antigen-specific memory B cell development. *Annu Rev Immunol,* 23**,** 487-513.

MCKEITHAN, T. W. 1995. Kinetic proofreading in T-cell receptor signal transduction. *Proc Natl Acad Sci U S A,* 92**,** 5042-6.

MEREDITH, M., ZEMMOUR, D., MATHIS, D. & BENOIST, C. 2015. Aire controls gene expression in the thymic epithelium with ordered stochasticity. *Nat Immunol,* 16**,** 942-9.

METZGER, T. C., KHAN, I. S., GARDNER, J. M., MOUCHESS, M. L., JOHANNES, K. P., KRAWISZ, A. K., SKRZYPCZYNSKA, K. M. & ANDERSON, M. S. 2013. Lineage tracing and cell ablation identify a post-Aire-expressing thymic epithelial cell population. *Cell Rep,* 5**,** 166-79.

MICHIE, A. M. & ZUNIGA-PFLUCKER, J. C. 2002. Regulation of thymocyte differentiation: pre-TCR signals and beta-selection. *Semin Immunol,* 14**,** 311-23.

MILLAR, D. G. & OHASHI, P. S. 2016. Central tolerance: what you see is what you don't get! *Nat Immunol,* 17**,** 115-6.

MILLER, R. A. 1996. The aging immune system: primer and prospectus. *Science,* 273**,** 70-4.

MISSLITZ, A., PABST, O., HINTZEN, G., OHL, L., KREMMER, E., PETRIE, H. T. & FORSTER, R. 2004. Thymic T cell development and progenitor localization depend on CCR7. *J Exp Med,* 200**,** 481-91.

MIYASAKA, M. & TANAKA, T. 2004. Lymphocyte trafficking across high endothelial venules: dogmas and enigmas. *Nat Rev Immunol,* 4**,** 360-70.

MOMBAERTS, P., CLARKE, A. R., RUDNICKI, M. A., IACOMINI, J., ITOHARA, S., LAFAILLE, J. J., WANG, L., ICHIKAWA, Y., JAENISCH, R., HOOPER, M. L. & ET AL. 1992. Mutations in T-cell antigen receptor genes alpha and beta block thymocyte development at different stages. *Nature,* 360**,** 225-31.

MONCADA, S., PALMER, R. M. & HIGGS, E. A. 1989. Biosynthesis of nitric oxide from L-arginine. A pathway for the regulation of cell function and communication. *Biochem Pharmacol,* 38**,** 1709-15.

MONROE, R. J., SEIDL, K. J., GAERTNER, F., HAN, S., CHEN, F., SEKIGUCHI, J., WANG, J., FERRINI, R., DAVIDSON, L., KELSOE, G. & ALT, F. W. 1999. RAG2:GFP knockin mice reveal novel aspects of RAG2 expression in primary and peripheral lymphoid tissues. *Immunity,* 11**,** 201-12.

MOORE, T. A., VON FREEDEN-JEFFRY, U., MURRAY, R. & ZLOTNIK, A. 1996. Inhibition of gamma delta T cell development and early thymocyte maturation in IL-7 -/- mice. *J Immunol,* 157**,** 2366-73.

MORAN, A. E., HOLZAPFEL, K. L., XING, Y., CUNNINGHAM, N. R., MALTZMAN, J. S., PUNT, J. & HOGQUIST, K. A. 2011. T cell receptor signal strength in Treg and iNKT cell development demonstrated by a novel fluorescent reporter mouse. *J Exp Med,* 208**,** 1279-89.

MORI, S., NAKANO, H., ARITOMI, K., WANG, C. R., GUNN, M. D. & KAKIUCHI, T. 2001. Mice lacking expression of the chemokines CCL21-ser and CCL19 (plt mice) demonstrate delayed but enhanced T cell immune responses. *J Exp Med,* 193**,** 207-18.

MOSMANN, T. R. & COFFMAN, R. L. 1989. TH1 and TH2 cells: different patterns of lymphokine secretion lead to different functional properties. *Annu Rev Immunol,* 7**,** 145-73.

MOSMANN, T. R. & SAD, S. 1996. The expanding universe of T-cell subsets: Th1, Th2 and more. *Immunol Today,* 17**,** 138-46.

MOURI, Y., YANO, M., SHINZAWA, M., SHIMO, Y., HIROTA, F., NISHIKAWA, Y., NII, T., KIYONARI, H., ABE, T., UEHARA, H., IZUMI, K., TAMADA, K., CHEN, L., PENNINGER, J. M., INOUE, J., AKIYAMA, T. & MATSUMOTO, M. 2011. Lymphotoxin signal promotes thymic organogenesis by eliciting RANK expression in the embryonic thymic stroma. *J Immunol,* 186**,** 5047-57.

MOVAHEDI, K., GUILLIAMS, M., VAN DEN BOSSCHE, J., VAN DEN BERGH, R., GYSEMANS, C., BESCHIN, A., DE BAETSELIER, P. & VAN GINDERACHTER, J. A. 2008. Identification of discrete tumor-induced myeloid-derived suppressor cell subpopulations with distinct T cell-suppressive activity. *Blood,* 111**,** 4233-44.

MURAMATSU, M., KINOSHITA, K., FAGARASAN, S., YAMADA, S., SHINKAI, Y. & HONJO, T. 2000. Class switch recombination and hypermutation require activation-induced cytidine deaminase (AID), a potential RNA editing enzyme. *Cell,* 102**,** 553-63.

MURATA, S., SASAKI, K., KISHIMOTO, T., NIWA, S., HAYASHI, H., TAKAHAMA, Y. & TANAKA, K. 2007. Regulation of CD8+ T cell development by thymus-specific proteasomes. *Science,* 316**,** 1349-53.

NAGAMINE, K., PETERSON, P., SCOTT, H. S., KUDOH, J., MINOSHIMA, S., HEINO, M., KROHN, K. J., LALIOTI, M. D., MULLIS, P. E., ANTONARAKIS, S. E., KAWASAKI, K., ASAKAWA, S., ITO, F. & SHIMIZU, N. 1997. Positional cloning of the APECED gene. *Nat Genet,* 17**,** 393-8.

NAGL, M., KACANI, L., MULLAUER, B., LEMBERGER, E. M., STOIBER, H., SPRINZL, G. M., SCHENNACH, H. & DIERICH, M. P. 2002. Phagocytosis and killing of bacteria by professional phagocytes and dendritic cells. *Clin Diagn Lab Immunol,* 9**,** 1165-8.

NAKAGAWA, T., ROTH, W., WONG, P., NELSON, A., FARR, A., DEUSSING, J., VILLADANGOS, J. A., PLOEGH, H., PETERS, C. & RUDENSKY, A. Y. 1998. Cathepsin L: critical role in Ii degradation and CD4 T cell selection in the thymus. *Science,* 280**,** 450-3.

NATARAJAN, K., LI, H., MARIUZZA, R. A. & MARGULIES, D. H. 1999. MHC class I molecules, structure and function. *Rev Immunogenet,* 1**,** 32-46.

NEDJIC, J., AICHINGER, M., EMMERICH, J., MIZUSHIMA, N. & KLEIN, L. 2008. Autophagy in thymic epithelium shapes the T-cell repertoire and is essential for tolerance. *Nature,* 455**,** 396-400.

NEEFJES, J., JONGSMA, M. L., PAUL, P. & BAKKE, O. 2011. Towards a systems understanding of MHC class I and MHC class II antigen presentation. *Nat Rev Immunol,* 11**,** 823-36.

NITTA, T., MURATA, S., SASAKI, K., FUJII, H., RIPEN, A. M., ISHIMARU, N., KOYASU, S., TANAKA, K. & TAKAHAMA, Y. 2010. Thymoproteasome shapes immunocompetent repertoire of CD8+ T cells. *Immunity,* 32**,** 29-40.

NJAU, M. N. & JACOB, J. 2014. Inducible nitric oxide synthase is crucial for plasma cell survival. *Nat Immunol,* 15**,** 219-21.

NOWELL, C. S., BREDENKAMP, N., TETELIN, S., JIN, X., TISCHNER, C., VAIDYA, H., SHERIDAN, J. M., STENHOUSE, F. H., HEUSSEN, R., SMITH, A. J. & BLACKBURN, C. C. 2011. Foxn1 regulates lineage progression in cortical and medullary thymic epithelial cells but is dispensable for medullary sublineage divergence. *PLoS Genet,* 7**,** e1002348.

NUSSBAUM, A. K., DICK, T. P., KEILHOLZ, W., SCHIRLE, M., STEVANOVIC, S., DIETZ, K., HEINEMEYER, W., GROLL, M., WOLF, D. H., HUBER, R., RAMMENSEE, H. G. & SCHILD, H. 1998. Cleavage motifs of the yeast 20S proteasome beta subunits deduced from digests of enolase 1. *Proc Natl Acad Sci U S A,* 95**,** 12504-9.

O'NEILL, L. A. & BOWIE, A. G. 2007. The family of five: TIR-domain-containing adaptors in Toll-like receptor signalling. *Nat Rev Immunol,* 7**,** 353-64.

OHIGASHI, I., ZUKLYS, S., SAKATA, M., MAYER, C. E., HAMAZAKI, Y., MINATO, N., HOLLANDER, G. A. & TAKAHAMA, Y. 2015. Adult Thymic Medullary Epithelium Is Maintained and Regenerated by Lineage-Restricted Cells Rather Than Bipotent Progenitors. *Cell Rep,* 13**,** 1432-43.

OHIGASHI, I., ZUKLYS, S., SAKATA, M., MAYER, C. E., ZHANYBEKOVA, S., MURATA, S., TANAKA, K., HOLLANDER, G. A. & TAKAHAMA, Y. 2013. Aire-expressing thymic medullary epithelial cells originate from beta5t-expressing progenitor cells. *Proc Natl Acad Sci U S A,* 110**,** 9885-90.

OPPMANN, B., LESLEY, R., BLOM, B., TIMANS, J. C., XU, Y., HUNTE, B., VEGA, F., YU, N., WANG, J., SINGH, K., ZONIN, F., VAISBERG, E., CHURAKOVA, T., LIU, M., GORMAN, D., WAGNER, J., ZURAWSKI, S., LIU, Y., ABRAMS, J. S., MOORE, K. W., RENNICK, D., DE WAAL-MALEFYT, R., HANNUM, C., BAZAN, J. F. & KASTELEIN, R. A. 2000. Novel p19 protein engages IL-12p40 to form a cytokine, IL-23, with biological activities similar as well as distinct from IL-12. *Immunity,* 13**,** 715-25.

ORG, T., REBANE, A., KISAND, K., LAAN, M., HALJASORG, U., ANDRESON, R. & PETERSON, P. 2009. AIRE activated tissue specific genes have histone modifications associated with inactive chromatin. *Hum Mol Genet,* 18**,** 4699-710.

ORTMANN, B., ANDROLEWICZ, M. J. & CRESSWELL, P. 1994. MHC class I/beta 2-microglobulin complexes associate with TAP transporters before peptide binding. *Nature,* 368**,** 864-7.

OSORIO, F., TAVERNIER, S. J., HOFFMANN, E., SAEYS, Y., MARTENS, L., VETTERS, J., DELRUE, I., DE RYCKE, R., PARTHOENS, E., POULIOT, P., IWAWAKI, T., JANSSENS, S. & LAMBRECHT, B. N. 2014. The unfolded-protein-response sensor IRE-1alpha regulates the function of CD8alpha+ dendritic cells. *Nat Immunol,* 15**,** 248-57.

OWEN, J. J. & RAFF, M. C. 1970. Studies on the differentiation of thymus-derived lymphocytes. *J Exp Med,* 132**,** 1216-32.

OYADOMARI, S. & MORI, M. 2004. Roles of CHOP/GADD153 in endoplasmic reticulum stress. *Cell Death Differ,* 11**,** 381-9.

PAIVA, R. S., LINO, A. C., BERGMAN, M. L., CARAMALHO, I., SOUSA, A. E., ZELENAY, S. & DEMENGEOT, J. 2013. Recent thymic emigrants are the preferential precursors of regulatory T cells differentiated in the periphery. *Proc Natl Acad Sci U S A,* 110**,** 6494-9.

PALACIOS, E. H. & WEISS, A. 2007. Distinct roles for Syk and ZAP-70 during early thymocyte development. *J Exp Med,* 204**,** 1703-15.

PALMER, E. & NAEHER, D. 2009. Affinity threshold for thymic selection through a T-cell receptor-co-receptor zipper. *Nat Rev Immunol,* 9**,** 207-13.

PANTELOURIS, E. M. 1968. Absence of thymus in a mouse mutant. *Nature,* 217**,** 370-1.

PAOLUCCI, C., BURASTERO, S. E., ROVERE-QUERINI, P., DE PALMA, C., FALCONE, S., PERROTTA, C., CAPOBIANCO, A., MANFREDI, A. A. & CLEMENTI, E. 2003. Synergism of nitric oxide and maturation signals on human dendritic cells occurs through a cyclic GMP-dependent pathway. *J Leukoc Biol,* 73**,** 253-62.

PARKER, D. C. 1993. T cell-dependent B cell activation. *Annu Rev Immunol,* 11**,** 331-60.

PAUL, W. E. 2011. Bridging innate and adaptive immunity. *Cell,* 147**,** 1212-5.

PAUL, W. E. & SEDER, R. A. 1994. Lymphocyte responses and cytokines. *Cell,* 76**,** 241-51.

PERERA, J., MENG, L., MENG, F. & HUANG, H. 2013. Autoreactive thymic B cells are efficient antigen-presenting cells of cognate self-antigens for T cell negative selection. *Proc Natl Acad Sci U S A,* 110**,** 17011-6.

PERNER, A., ANDRESEN, L., NORMARK, M. & RASK-MADSEN, J. 2002. Constitutive expression of inducible nitric oxide synthase in the normal human colonic epithelium. *Scand J Gastroenterol,* 37**,** 944-8.

PERRY, J. S., LIO, C. W., KAU, A. L., NUTSCH, K., YANG, Z., GORDON, J. I., MURPHY, K. M. & HSIEH, C. S. 2014. Distinct contributions of Aire and antigen-presenting-cell subsets to the generation of self-tolerance in the thymus. *Immunity,* 41**,** 414-26.

PETERS, P. J., NEEFJES, J. J., OORSCHOT, V., PLOEGH, H. L. & GEUZE, H. J. 1991. Segregation of MHC class II molecules from MHC class I molecules in the Golgi complex for transport to lysosomal compartments. *Nature,* 349**,** 669-76.

PETERSON, L. W. & ARTIS, D. 2014. Intestinal epithelial cells: regulators of barrier function and immune homeostasis. *Nat Rev Immunol,* 14**,** 141-53.

PFAFFL, M. W. 2001. A new mathematical model for relative quantification in real-time RT-PCR. *Nucleic Acids Res,* 29**,** e45.

PFLANZ, S., TIMANS, J. C., CHEUNG, J., ROSALES, R., KANZLER, H., GILBERT, J., HIBBERT, L., CHURAKOVA, T., TRAVIS, M., VAISBERG, E., BLUMENSCHEIN, W. M., MATTSON, J. D., WAGNER, J. L., TO, W., ZURAWSKI, S., MCCLANAHAN, T. K., GORMAN, D. M., BAZAN, J. F., DE WAAL MALEFYT, R., RENNICK, D. & KASTELEIN, R. A. 2002. IL-27, a heterodimeric cytokine composed of EBI3 and p28 protein, induces proliferation of naive CD4+ T cells. *Immunity,* 16**,** 779-90.

PICKART, C. M. 2001. Mechanisms underlying ubiquitination. *Annu Rev Biochem,* 70**,** 503-33.

PILLEMER, E., WHITLOCK, C. & WEISSMAN, I. L. 1984. Transformation-associated proteins in murine B-cell lymphomas that are distinct from Abelson virus gene products. *Proc Natl Acad Sci U S A,* 81**,** 4434-8.

PLOTKIN, J., PROCKOP, S. E., LEPIQUE, A. & PETRIE, H. T. 2003. Critical role for CXCR4 signaling in progenitor localization and T cell differentiation in the postnatal thymus. *J Immunol,* 171**,** 4521-7.

PLOTKIN, S. A. 2010. Correlates of protection induced by vaccination. *Clin Vaccine Immunol,* 17**,** 1055-65.

QURESHI, O. S., ZHENG, Y., NAKAMURA, K., ATTRIDGE, K., MANZOTTI, C., SCHMIDT, E. M., BAKER, J., JEFFERY, L. E., KAUR, S., BRIGGS, Z., HOU, T. Z., FUTTER, C. E., ANDERSON, G., WALKER, L. S. & SANSOM, D. M. 2011. Trans-endocytosis of CD80 and CD86: a molecular basis for the cell-extrinsic function of CTLA-4. *Science,* 332**,** 600-3.

RAHEMTULLA, A., FUNG-LEUNG, W. P., SCHILHAM, M. W., KUNDIG, T. M., SAMBHARA, S. R., NARENDRAN, A., ARABIAN, A., WAKEHAM, A., PAIGE, C. J., ZINKERNAGEL, R. M. & ET AL. 1991. Normal development and function of CD8+ cells but markedly decreased helper cell activity in mice lacking CD4. *Nature,* 353**,** 180-4.

RAMSEY, C., WINQVIST, O., PUHAKKA, L., HALONEN, M., MORO, A., KAMPE, O., ESKELIN, P., PELTO-HUIKKO, M. & PELTONEN, L. 2002. Aire deficient mice develop multiple features of APECED phenotype and show altered immune response. *Hum Mol Genet,* 11**,** 397-409.

RATTAY, K., MEYER, H. V., HERRMANN, C., BRORS, B. & KYEWSKI, B. 2016. Evolutionary conserved gene co-expression drives generation of self-antigen diversity in medullary thymic epithelial cells. *J Autoimmun,* 67**,** 65-75.

RAULET, D. H. 1989. The structure, function, and molecular genetics of the gamma/delta T cell receptor. *Annu Rev Immunol,* 7**,** 175-207.

REIMOLD, A. M., IWAKOSHI, N. N., MANIS, J., VALLABHAJOSYULA, P., SZOMOLANYI-TSUDA, E., GRAVALLESE, E. M., FRIEND, D., GRUSBY, M. J., ALT, F. & GLIMCHER, L. H. 2001. Plasma cell differentiation requires the transcription factor XBP-1. *Nature,* 412**,** 300-7.

REINHERZ, E. L., TAN, K., TANG, L., KERN, P., LIU, J., XIONG, Y., HUSSEY, R. E., SMOLYAR, A., HARE, B., ZHANG, R., JOACHIMIAK, A., CHANG, H. C., WAGNER, G. & WANG, J. 1999. The crystal structure of a T cell receptor in complex with peptide and MHC class II. *Science,* 286**,** 1913-21.

RETH, M. 1992. Antigen receptors on B lymphocytes. *Annu Rev Immunol,* 10**,** 97-121.

RIPEN, A. M., NITTA, T., MURATA, S., TANAKA, K. & TAKAHAMA, Y. 2011. Ontogeny of thymic cortical epithelial cells expressing the thymoproteasome subunit beta5t. *Eur J Immunol,* 41**,** 1278-87.

ROBERTS, N. A., WHITE, A. J., JENKINSON, W. E., TURCHINOVICH, G., NAKAMURA, K., WITHERS, D. R., MCCONNELL, F. M., DESANTI, G. E., BENEZECH, C., PARNELL, S. M., CUNNINGHAM, A. F., PAOLINO, M., PENNINGER, J. M., SIMON, A. K., NITTA, T., OHIGASHI, I., TAKAHAMA, Y., CAAMANO, J. H., HAYDAY, A. C., LANE, P. J., JENKINSON, E. J. & ANDERSON, G. 2012. Rank signaling links the development of invariant gammadelta T cell progenitors and Aire(+) medullary epithelium. *Immunity,* 36**,** 427-37.

ROBINSON, J. M. 2009. Phagocytic leukocytes and reactive oxygen species. *Histochem Cell Biol,* 131**,** 465-9.

ROCK, K. L., GRAMM, C., ROTHSTEIN, L., CLARK, K., STEIN, R., DICK, L., HWANG, D. & GOLDBERG, A. L. 1994. Inhibitors of the proteasome block the degradation of most cell proteins and the generation of peptides presented on MHC class I molecules. *Cell,* 78**,** 761-71.

RODE, I., MARTINS, V. C., KUBLBECK, G., MALTRY, N., TESSMER, C. & RODEWALD, H. R. 2015. Foxn1 Protein Expression in the Developing, Aging, and Regenerating Thymus. *J Immunol,* 195**,** 5678-87.

RODEWALD, H. R. 2008. Thymus organogenesis. *Annu Rev Immunol,* 26**,** 355-88.

ROGERS, D. F. 2003. The airway goblet cell. *Int J Biochem Cell Biol,* 35**,** 1-6.

ROGOZIN, I. B. & KOLCHANOV, N. A. 1992. Somatic hypermutagenesis in immunoglobulin genes. II. Influence of neighbouring base sequences on mutagenesis. *Biochim Biophys Acta,* 1171**,** 11-8.

ROMAGNANI, S. 2000. T-cell subsets (Th1 versus Th2). *Ann Allergy Asthma Immunol,* 85**,** 9-18; quiz 18, 21.

ROSENBLUM, M. D., GRATZ, I. K., PAW, J. S., LEE, K., MARSHAK-ROTHSTEIN, A. & ABBAS, A. K. 2011. Response to self antigen imprints regulatory memory in tissues. *Nature,* 480**,** 538-42.

ROSSI, F. M., CORBEL, S. Y., MERZABAN, J. S., CARLOW, D. A., GOSSENS, K., DUENAS, J., SO, L., YI, L. & ZILTENER, H. J. 2005. Recruitment of adult thymic progenitors is regulated by P-selectin and its ligand PSGL-1. *Nat Immunol,* 6**,** 626-34.

ROSSI, S. W., JENKINSON, W. E., ANDERSON, G. & JENKINSON, E. J. 2006. Clonal analysis reveals a common progenitor for thymic cortical and medullary epithelium. *Nature,* 441**,** 988-91.

ROSSI, S. W., KIM, M. Y., LEIBBRANDT, A., PARNELL, S. M., JENKINSON, W. E., GLANVILLE, S. H., MCCONNELL, F. M., SCOTT, H. S., PENNINGER, J. M., JENKINSON, E. J., LANE, P. J. & ANDERSON, G. 2007. RANK signals from

CD4(+)3(-) inducer cells regulate development of Aire-expressing epithelial cells in the thymic medulla. *J Exp Med,* 204**,** 1267-72.
ROT, A. & VON ANDRIAN, U. H. 2004. Chemokines in innate and adaptive host defense: basic chemokinese grammar for immune cells. *Annu Rev Immunol,* 22**,** 891-928.
ROTHENBERG, E. V., MOORE, J. E. & YUI, M. A. 2008. Launching the T-cell-lineage developmental programme. *Nat Rev Immunol,* 8**,** 9-21.
ROUND, J. L. & MAZMANIAN, S. K. 2010. Inducible Foxp3+ regulatory T-cell development by a commensal bacterium of the intestinal microbiota. *Proc Natl Acad Sci U S A,* 107**,** 12204-9.
SAINI, A. S., SHENOY, G. N., RATH, S., BAL, V. & GEORGE, A. 2014. Inducible nitric oxide synthase is a major intermediate in signaling pathways for the survival of plasma cells. *Nat Immunol,* 15**,** 275-82.
SAINT-RUF, C., PANIGADA, M., AZOGUI, O., DEBEY, P., VON BOEHMER, H. & GRASSI, F. 2000. Different initiation of pre-TCR and gammadeltaTCR signalling. *Nature,* 406**,** 524-7.
SAKAGUCHI, S., SAKAGUCHI, N., ASANO, M., ITOH, M. & TODA, M. 1995. Immunologic self-tolerance maintained by activated T cells expressing IL-2 receptor alpha-chains (CD25). Breakdown of a single mechanism of self-tolerance causes various autoimmune diseases. *J Immunol,* 155**,** 1151-64.
SAKAGUCHI, S., YAMAGUCHI, T., NOMURA, T. & ONO, M. 2008. Regulatory T cells and immune tolerance. *Cell,* 133**,** 775-87.
SALDANA, J. I., SOLANKI, A., LAU, C. I., SAHNI, H., ROSS, S., FURMANSKI, A. L., ONO, M., HOLLANDER, G. & CROMPTON, T. 2016. Sonic Hedgehog regulates thymic epithelial cell differentiation. *J Autoimmun,* 68**,** 86-97.
SALLUSTO, F., CELLA, M., DANIELI, C. & LANZAVECCHIA, A. 1995. Dendritic cells use macropinocytosis and the mannose receptor to concentrate macromolecules in the major histocompatibility complex class II compartment: downregulation by cytokines and bacterial products. *J Exp Med,* 182**,** 389-400.
SARAFOVA, S. D., ERMAN, B., YU, Q., VAN LAETHEM, F., GUINTER, T., SHARROW, S. O., FEIGENBAUM, L., WILDT, K. F., ELLMEIER, W. & SINGER, A. 2005. Modulation of coreceptor transcription during positive selection dictates lineage fate independently of TCR/coreceptor specificity. *Immunity,* 23**,** 75-87.
SAVINO, W., DARDENNE, M. & CARNAUD, C. 1996. The conveyor belt model for intrathymic T-cell migration. *Immunol Today,* 17**,** 97-8.
SAVINO, W., MENDES-DA-CRUZ, D. A., SMANIOTTO, S., SILVA-MONTEIRO, E. & VILLA-VERDE, D. M. 2004. Molecular mechanisms governing thymocyte migration: combined role of chemokines and extracellular matrix. *J Leukoc Biol,* 75**,** 951-61.
SCHATZ, D. G. 2004. Antigen receptor genes and the evolution of a recombinase. *Semin Immunol,* 16**,** 245-56.
SCHEDI, M. P., GOLDSTEIN, G. & BOYCE, E. A. 1975. Differentiation of T cells in nude mice. *Science,* 190**,** 1211-3.
SCHILHAM, M. W., WILSON, A., MOERER, P., BENAISSA-TROUW, B. J., CUMANO, A. & CLEVERS, H. C. 1998. Critical involvement of Tcf-1 in expansion of thymocytes. *Journal of Immunology,* 161**,** 3984-3991.

SCHUSTER, C., GEROLD, K. D., SCHOBER, K., PROBST, L., BOERNER, K., KIM, M. J., RUCKDESCHEL, A., SERWOLD, T. & KISSLER, S. 2015. The Autoimmunity-Associated Gene CLEC16A Modulates Thymic Epithelial Cell Autophagy and Alters T Cell Selection. *Immunity,* 42**,** 942-52.

SCHWARTZ, R. H. 1985. T-lymphocyte recognition of antigen in association with gene products of the major histocompatibility complex. *Annu Rev Immunol,* 3**,** 237-61.

SCOTT, B., BLUTHMANN, H., TEH, H. S. & VON BOEHMER, H. 1989. The generation of mature T cells requires interaction of the alpha beta T-cell receptor with major histocompatibility antigens. *Nature,* 338**,** 591-3.

SEACH, N., UENO, T., FLETCHER, A. L., LOWEN, T., MATTESICH, M., ENGWERDA, C. R., SCOTT, H. S., WARE, C. F., CHIDGEY, A. P., GRAY, D. H. & BOYD, R. L. 2008. The lymphotoxin pathway regulates Aire-independent expression of ectopic genes and chemokines in thymic stromal cells. *J Immunol,* 180**,** 5384-92.

SEKAI, M., HAMAZAKI, Y. & MINATO, N. 2014. Medullary thymic epithelial stem cells maintain a functional thymus to ensure lifelong central T cell tolerance. *Immunity,* 41**,** 753-61.

SEKIROV, I. & FINLAY, B. B. 2009. The role of the intestinal microbiota in enteric infection. *J Physiol,* 587**,** 4159-67.

SERAFINI, P., MECKEL, K., KELSO, M., NOONAN, K., CALIFANO, J., KOCH, W., DOLCETTI, L., BRONTE, V. & BORRELLO, I. 2006. Phosphodiesterase-5 inhibition augments endogenous antitumor immunity by reducing myeloid-derived suppressor cell function. *J Exp Med,* 203**,** 2691-702.

SERBINA, N. V., SALAZAR-MATHER, T. P., BIRON, C. A., KUZIEL, W. A. & PAMER, E. G. 2003. TNF/iNOS-producing dendritic cells mediate innate immune defense against bacterial infection. *Immunity,* 19**,** 59-70.

SHAW, A. C., JOSHI, S., GREENWOOD, H., PANDA, A. & LORD, J. M. 2010. Aging of the innate immune system. *Curr Opin Immunol,* 22**,** 507-13.

SHAW, S. & LUCE, G. E. 1987. The lymphocyte function-associated antigen (LFA)-1 and CD2/LFA-3 pathways of antigen-independent human T cell adhesion. *J Immunol,* 139**,** 1037-45.

SHINKAI, Y., KOYASU, S., NAKAYAMA, K., MURPHY, K. M., LOH, D. Y., REINHERZ, E. L. & ALT, F. W. 1993. Restoration of T cell development in RAG-2-deficient mice by functional TCR transgenes. *Science,* 259**,** 822-5.

SHIOW, L. R., ROSEN, D. B., BRDICKOVA, N., XU, Y., AN, J., LANIER, L. L., CYSTER, J. G. & MATLOUBIAN, M. 2006. CD69 acts downstream of interferon-alpha/beta to inhibit S1P1 and lymphocyte egress from lymphoid organs. *Nature,* 440**,** 540-4.

SIEGERT, S., HUANG, H. Y., YANG, C. Y., SCARPELLINO, L., CARRIE, L., ESSEX, S., NELSON, P. J., HEIKENWALDER, M., ACHA-ORBEA, H., BUCKLEY, C. D., MARSLAND, B. J., ZEHN, D. & LUTHER, S. A. 2011. Fibroblastic reticular cells from lymph nodes attenuate T cell expansion by producing nitric oxide. *PLoS One,* 6**,** e27618.

SILVER, P. B., TARRANT, T. K., CHAN, C. C., WIGGERT, B. & CASPI, R. R. 1999. Mice deficient in inducible nitric oxide synthase are susceptible to experimental autoimmune uveoretinitis. *Invest Ophthalmol Vis Sci,* 40**,** 1280-4.

SINGER, A., ADORO, S. & PARK, J. H. 2008. Lineage fate and intense debate: myths, models and mechanisms of CD4- versus CD8-lineage choice. *Nat Rev Immunol,* 8**,** 788-801.

STAMLER, J. S., SIMON, D. I., OSBORNE, J. A., MULLINS, M. E., JARAKI, O., MICHEL, T., SINGEL, D. J. & LOSCALZO, J. 1992. S-nitrosylation of proteins with nitric oxide: synthesis and characterization of biologically active compounds. *Proc Natl Acad Sci U S A,* 89**,** 444-8.

STARR, T. K., JAMESON, S. C. & HOGQUIST, K. A. 2003. Positive and negative selection of T cells. *Annu Rev Immunol,* 21**,** 139-76.

STEIN, K. E. 1992. Thymus-independent and thymus-dependent responses to polysaccharide antigens. *J Infect Dis,* 165 Suppl 1**,** S49-52.

STEPANEK, O., PRABHAKAR, A. S., OSSWALD, C., KING, C. G., BULEK, A., NAEHER, D., BEAUFILS-HUGOT, M., ABANTO, M. L., GALATI, V., HAUSMANN, B., LANG, R., COLE, D. K., HUSEBY, E. S., SEWELL, A. K., CHAKRABORTY, A. K. & PALMER, E. 2014. Coreceptor scanning by the T cell receptor provides a mechanism for T cell tolerance. *Cell,* 159**,** 333-45.

STRITESKY, G. L., XING, Y., ERICKSON, J. R., KALEKAR, L. A., WANG, X., MUELLER, D. L., JAMESON, S. C. & HOGQUIST, K. A. 2013. Murine thymic selection quantified using a unique method to capture deleted T cells. *Proc Natl Acad Sci U S A,* 110**,** 4679-84.

SUN, C. M., HALL, J. A., BLANK, R. B., BOULADOUX, N., OUKKA, M., MORA, J. R. & BELKAID, Y. 2007. Small intestine lamina propria dendritic cells promote de novo generation of Foxp3 T reg cells via retinoic acid. *J Exp Med,* 204**,** 1775-85.

SUN, L., LI, H., LUO, H. & ZHAO, Y. 2014. Thymic epithelial cell development and its dysfunction in human diseases. *Biomed Res Int,* 2014**,** 206929.

SURH, C. D. & SPRENT, J. 1994. T-cell apoptosis detected in situ during positive and negative selection in the thymus. *Nature,* 372**,** 100-3.

TAGHON, T., YUI, M. A., PANT, R., DIAMOND, R. A. & ROTHENBERG, E. V. 2006. Developmental and molecular characterization of emerging beta- and gammadelta-selected pre-T cells in the adult mouse thymus. *Immunity,* 24**,** 53-64.

TAGHON, T. N., DAVID, E. S., ZUNIGA-PFLUCKER, J. C. & ROTHENBERG, E. V. 2005. Delayed, asynchronous, and reversible T-lineage specification induced by Notch/Delta signaling. *Genes Dev,* 19**,** 965-78.

TAI, X., COWAN, M., FEIGENBAUM, L. & SINGER, A. 2005. CD28 costimulation of developing thymocytes induces Foxp3 expression and regulatory T cell differentiation independently of interleukin 2. *Nat Immunol,* 6**,** 152-62.

TAI, X., ERMAN, B., ALAG, A., MU, J., KIMURA, M., KATZ, G., GUINTER, T., MCCAUGHTRY, T., ETZENSPERGER, R., FEIGENBAUM, L., SINGER, D. S. & SINGER, A. 2013. Foxp3 transcription factor is proapoptotic and lethal to developing regulatory T cells unless counterbalanced by cytokine survival signals. *Immunity,* 38**,** 1116-28.

TAI, X. G., TOYO-OKA, K., YAMAMOTO, N., YASHIRO, Y., MU, J., HAMAOKA, T. & FUJIWARA, H. 1997. Expression of an inducible type of nitric oxide (NO) synthase in the thymus and involvement of NO in deletion of TCR-stimulated double-positive thymocytes. *J Immunol,* 158**,** 4696-703.

TAKABA, H., MORISHITA, Y., TOMOFUJI, Y., DANKS, L., NITTA, T., KOMATSU, N., KODAMA, T. & TAKAYANAGI, H. 2015. Fezf2 Orchestrates a Thymic

Program of Self-Antigen Expression for Immune Tolerance. *Cell,* 163**,** 975-87.

TAKADA, K. & TAKAHAMA, Y. 2015. Positive-selection-inducing self-peptides displayed by cortical thymic epithelial cells. *Adv Immunol,* 125**,** 87-110.

TAKADA, K., VAN LAETHEM, F., XING, Y., AKANE, K., SUZUKI, H., MURATA, S., TANAKA, K., JAMESON, S. C., SINGER, A. & TAKAHAMA, Y. 2015. TCR affinity for thymoproteasome-dependent positively selecting peptides conditions antigen responsiveness in CD8(+) T cells. *Nat Immunol,* 16**,** 1069-76.

TAKAHAMA, Y. 2006. Journey through the thymus: stromal guides for T-cell development and selection. *Nat Rev Immunol,* 6**,** 127-35.

TAKEUCHI, O., KAWAI, T., SANJO, H., COPELAND, N. G., GILBERT, D. J., JENKINS, N. A., TAKEDA, K. & AKIRA, S. 1999. TLR6: A novel member of an expanding toll-like receptor family. *Gene,* 231**,** 59-65.

TALMADGE, J. E. 2007. Pathways mediating the expansion and immunosuppressive activity of myeloid-derived suppressor cells and their relevance to cancer therapy. *Clin Cancer Res,* 13**,** 5243-8.

TANAKA, K. 1994. Role of proteasomes modified by interferon-gamma in antigen processing. *J Leukoc Biol,* 56**,** 571-5.

TESMER, L. A., LUNDY, S. K., SARKAR, S. & FOX, D. A. 2008. Th17 cells in human disease. *Immunol Rev,* 223**,** 87-113.

THIAULT, N., DARRIGUES, J., ADOUE, V., GROS, M., BINET, B., PERALS, C., LEOBON, B., FAZILLEAU, N., JOFFRE, O. P., ROBEY, E. A., VAN MEERWIJK, J. P. & ROMAGNOLI, P. 2015. Peripheral regulatory T lymphocytes recirculating to the thymus suppress the development of their precursors. *Nat Immunol,* 16**,** 628-34.

THORNTON, A. M. & SHEVACH, E. M. 2000. Suppressor effector function of CD4+CD25+ immunoregulatory T cells is antigen nonspecific. *J Immunol,* 164**,** 183-90.

TONEGAWA, S. 1983. Somatic generation of antibody diversity. *Nature,* 302**,** 575-81.

TOUGH, D. F. & SPRENT, J. 1994. Turnover of naive- and memory-phenotype T cells. *J Exp Med,* 179**,** 1127-35.

TRAMPONT, P. C., TOSELLO-TRAMPONT, A. C., SHEN, Y., DULEY, A. K., SUTHERLAND, A. E., BENDER, T. P., LITTMAN, D. R. & RAVICHANDRAN, K. S. 2010. CXCR4 acts as a costimulator during thymic beta-selection. *Nat Immunol,* 11**,** 162-70.

TRIGUEROS, C., HOZUMI, K., SILVA-SANTOS, B., BRUNO, L., HAYDAY, A. C., OWEN, M. J. & PENNINGTON, D. J. 2003. Pre-TCR signaling regulates IL-7 receptor alpha expression promoting thymocyte survival at the transition from the double-negative to double-positive stage. *Eur J Immunol,* 33**,** 1968-77.

TRINCHIERI, G. 1995. Interleukin-12: a proinflammatory cytokine with immunoregulatory functions that bridge innate resistance and antigen-specific adaptive immunity. *Annu Rev Immunol,* 13**,** 251-76.

TURNER, J. M., BRODSKY, M. H., IRVING, B. A., LEVIN, S. D., PERLMUTTER, R. M. & LITTMAN, D. R. 1990. Interaction of the unique N-terminal region of tyrosine kinase p56lck with cytoplasmic domains of CD4 and CD8 is mediated by cysteine motifs. *Cell,* 60**,** 755-65.

UCAR, A., UCAR, O., KLUG, P., MATT, S., BRUNK, F., HOFMANN, T. G. & KYEWSKI, B. 2014. Adult thymus contains FoxN1(-) epithelial stem cells that are bipotent for medullary and cortical thymic epithelial lineages. *Immunity,* 41**,** 257-69.

UENO, T., HARA, K., WILLIS, M. S., MALIN, M. A., HOPKEN, U. E., GRAY, D. H., MATSUSHIMA, K., LIPP, M., SPRINGER, T. A., BOYD, R. L., YOSHIE, O. & TAKAHAMA, Y. 2002. Role for CCR7 ligands in the emigration of newly generated T lymphocytes from the neonatal thymus. *Immunity,* 16**,** 205-18.

UENO, T., SAITO, F., GRAY, D. H., KUSE, S., HIESHIMA, K., NAKANO, H., KAKIUCHI, T., LIPP, M., BOYD, R. L. & TAKAHAMA, Y. 2004. CCR7 signals are essential for cortex-medulla migration of developing thymocytes. *J Exp Med,* 200**,** 493-505.

ULYANCHENKO, S., O'NEILL, K. E., MEDLEY, T., FARLEY, A. M., VAIDYA, H. J., COOK, A. M., BLAIR, N. F. & BLACKBURN, C. C. 2016. Identification of a Bipotent Epithelial Progenitor Population in the Adult Thymus. *Cell Rep,* 14**,** 2819-32.

VALITUTTI, S. & LANZAVECCHIA, A. 1997. Serial triggering of TCRs: a basis for the sensitivity and specificity of antigen recognition. *Immunol Today,* 18**,** 299-304.

VAN BERGEN, J., SCHOENBERGER, S. P., VERRECK, F., AMONS, R., OFFRINGA, R. & KONING, F. 1997. Efficient loading of HLA-DR with a T helper epitope by genetic exchange of CLIP. *Proc Natl Acad Sci U S A,* 94**,** 7499-502.

VAN DER MERWE, P. A. & DUSHEK, O. 2011. Mechanisms for T cell receptor triggering. *Nat Rev Immunol,* 11**,** 47-55.

VELDHOEN, M., HOCKING, R. J., ATKINS, C. J., LOCKSLEY, R. M. & STOCKINGER, B. 2006. TGFbeta in the context of an inflammatory cytokine milieu supports de novo differentiation of IL-17-producing T cells. *Immunity,* 24**,** 179-89.

VIRET, C., LAMARE, C., GUIRAUD, M., FAZILLEAU, N., BOUR, A., MALISSEN, B., CARRIER, A. & GUERDER, S. 2011a. Thymus-specific serine protease contributes to the diversification of the functional endogenous CD4 T cell receptor repertoire. *J Exp Med,* 208**,** 3-11.

VIRET, C., LEUNG-THEUNG-LONG, S., SERRE, L., LAMARE, C., VIGNALI, D. A., MALISSEN, B., CARRIER, A. & GUERDER, S. 2011b. Thymus-specific serine protease controls autoreactive CD4 T cell development and autoimmune diabetes in mice. *J Clin Invest,* 121**,** 1810-21.

WALTERS, S. N., WEBSTER, K. E., DALEY, S. & GREY, S. T. 2014. A role for intrathymic B cells in the generation of natural regulatory T cells. *J Immunol,* 193**,** 170-6.

WANG, X., LAAN, M., BICHELE, R., KISAND, K., SCOTT, H. S. & PETERSON, P. 2012. Post-Aire maturation of thymic medullary epithelial cells involves selective expression of keratinocyte-specific autoantigens. *Front Immunol,* 3**,** 19.

WEI, X. Q., CHARLES, I. G., SMITH, A., URE, J., FENG, G. J., HUANG, F. P., XU, D., MULLER, W., MONCADA, S. & LIEW, F. Y. 1995. Altered immune responses in mice lacking inducible nitric oxide synthase. *Nature,* 375**,** 408-11.

WEIH, F., CARRASCO, D., DURHAM, S. K., BARTON, D. S., RIZZO, C. A., RYSECK, R. P., LIRA, S. A. & BRAVO, R. 1995. Multiorgan inflammation and

hematopoietic abnormalities in mice with a targeted disruption of RelB, a member of the NF-kappa B/Rel family. *Cell,* 80**,** 331-40.

WEISS, A. & LITTMAN, D. R. 1994. Signal transduction by lymphocyte antigen receptors. *Cell,* 76**,** 263-74.

WEIST, B. M., KURD, N., BOUSSIER, J., CHAN, S. W. & ROBEY, E. A. 2015. Thymic regulatory T cell niche size is dictated by limiting IL-2 from antigen-bearing dendritic cells and feedback competition. *Nat Immunol,* 16**,** 635-41.

WHITE, A. J., NAKAMURA, K., JENKINSON, W. E., SAINI, M., SINCLAIR, C., SEDDON, B., NARENDRAN, P., PFEFFER, K., NITTA, T., TAKAHAMA, Y., CAAMANO, J. H., LANE, P. J., JENKINSON, E. J. & ANDERSON, G. 2010. Lymphotoxin signals from positively selected thymocytes regulate the terminal differentiation of medullary thymic epithelial cells. *J Immunol,* 185**,** 4769-76.

WHITE, A. J., WITHERS, D. R., PARNELL, S. M., SCOTT, H. S., FINKE, D., LANE, P. J., JENKINSON, E. J. & ANDERSON, G. 2008. Sequential phases in the development of Aire-expressing medullary thymic epithelial cells involve distinct cellular input. *Eur J Immunol,* 38**,** 942-7.

WILLERFORD, D. M., CHEN, J., FERRY, J. A., DAVIDSON, L., MA, A. & ALT, F. W. 1995. Interleukin-2 receptor alpha chain regulates the size and content of the peripheral lymphoid compartment. *Immunity,* 3**,** 521-30.

WILLIAMS, A. F. & BARCLAY, A. N. 1988. The immunoglobulin superfamily--domains for cell surface recognition. *Annu Rev Immunol,* 6**,** 381-405.

WILLIAMS, J. A., ZHANG, J., JEON, H., NITTA, T., OHIGASHI, I., KLUG, D., KRUHLAK, M. J., CHOUDHURY, B., SHARROW, S. O., GRANGER, L., ADAMS, A., ECKHAUS, M. A., JENKINSON, S. R., RICHIE, E. R., GRESS, R. E., TAKAHAMA, Y. & HODES, R. J. 2014. Thymic medullary epithelium and thymocyte self-tolerance require cooperation between CD28-CD80/86 and CD40-CD40L costimulatory pathways. *J Immunol,* 192**,** 630-40.

WILLIAMS, O. W., SHARAFKHANEH, A., KIM, V., DICKEY, B. F. & EVANS, C. M. 2006. Airway mucus: From production to secretion. *Am J Respir Cell Mol Biol,* 34**,** 527-36.

WILSON, A., MACDONALD, H. R. & RADTKE, F. 2001. Notch 1-deficient common lymphoid precursors adopt a B cell fate in the thymus. *J Exp Med,* 194**,** 1003-12.

WONG, K., LISTER, N. L., BARSANTI, M., LIM, J. M., HAMMETT, M. V., KHONG, D. M., SIATSKAS, C., GRAY, D. H., BOYD, R. L. & CHIDGEY, A. P. 2014. Multilineage potential and self-renewal define an epithelial progenitor cell population in the adult thymus. *Cell Rep,* 8**,** 1198-209.

WONG, S. H., SANTAMBROGIO, L. & STROMINGER, J. L. 2004. Caspases and nitric oxide broadly regulate dendritic cell maturation and surface expression of class II MHC proteins. *Proc Natl Acad Sci U S A,* 101**,** 17783-8.

WU, L., D'AMICO, A., HOCHREIN, H., O'KEEFFE, M., SHORTMAN, K. & LUCAS, K. 2001. Development of thymic and splenic dendritic cell populations from different hemopoietic precursors. *Blood,* 98**,** 3376-82.

XIE, Q. W., CHO, H. J., CALAYCAY, J., MUMFORD, R. A., SWIDEREK, K. M., LEE, T. D., DING, A., TROSO, T. & NATHAN, C. 1992. Cloning and characterization of inducible nitric oxide synthase from mouse macrophages. *Science,* 256**,** 225-8.

XING, Y., JAMESON, S. C. & HOGQUIST, K. A. 2013. Thymoproteasome subunit-beta5T generates peptide-MHC complexes specialized for positive selection. *Proc Natl Acad Sci U S A,* 110**,** 6979-84.

XING, Y., WANG, X., JAMESON, S. C. & HOGQUIST, K. A. 2016. Late stages of T cell maturation in the thymus involve NF-kappaB and tonic type I interferon signaling. *Nat Immunol,* 17**,** 565-73.

YACHI, P. P., AMPUDIA, J., ZAL, T. & GASCOIGNE, N. R. 2006. Altered peptide ligands induce delayed CD8-T cell receptor interaction--a role for CD8 in distinguishing antigen quality. *Immunity,* 25**,** 203-11.

YAMANO, T., NEDJIC, J., HINTERBERGER, M., STEINERT, M., KOSER, S., PINTO, S., GERDES, N., LUTGENS, E., ISHIMARU, N., BUSSLINGER, M., BRORS, B., KYEWSKI, B. & KLEIN, L. 2015. Thymic B Cells Are Licensed to Present Self Antigens for Central T Cell Tolerance Induction. *Immunity,* 42**,** 1048-61.

YAMASHITA, I., NAGATA, T., TADA, T. & NAKAYAMA, T. 1993. CD69 cell surface expression identifies developing thymocytes which audition for T cell antigen receptor-mediated positive selection. *Int Immunol,* 5**,** 1139-50.

YAN, J. & MAMULA, M. J. 2002. Autoreactive T cells revealed in the normal repertoire: escape from negative selection and peripheral tolerance. *J Immunol,* 168**,** 3188-94.

YANG, Z. & KLIONSKY, D. J. 2010. Eaten alive: a history of macroautophagy. *Nat Cell Biol,* 12**,** 814-22.

YANO, M., KURODA, N., HAN, H., MEGURO-HORIKE, M., NISHIKAWA, Y., KIYONARI, H., MAEMURA, K., YANAGAWA, Y., OBATA, K., TAKAHASHI, S., IKAWA, T., SATOH, R., KAWAMOTO, H., MOURI, Y. & MATSUMOTO, M. 2008. Aire controls the differentiation program of thymic epithelial cells in the medulla for the establishment of self-tolerance. *J Exp Med,* 205**,** 2827-38.

YAZDANBAKHSH, M., KREMSNER, P. G. & VAN REE, R. 2002. Allergy, parasites, and the hygiene hypothesis. *Science,* 296**,** 490-4.

YONEYAMA, M. & FUJITA, T. 2007. RIG-I family RNA helicases: cytoplasmic sensor for antiviral innate immunity. *Cytokine Growth Factor Rev,* 18**,** 545-51.

YONEYAMA, M., KIKUCHI, M., NATSUKAWA, T., SHINOBU, N., IMAIZUMI, T., MIYAGISHI, M., TAIRA, K., AKIRA, S. & FUJITA, T. 2004. The RNA helicase RIG-I has an essential function in double-stranded RNA-induced innate antiviral responses. *Nat Immunol,* 5**,** 730-7.

YOSHIDA, T., NG, S. Y., ZUNIGA-PFLUCKER, J. C. & GEORGOPOULOS, K. 2006. Early hematopoietic lineage restrictions directed by Ikaros. *Nat Immunol,* 7**,** 382-91.

YUI, M. A. & ROTHENBERG, E. V. 2014. Developmental gene networks: a triathlon on the course to T cell identity. *Nat Rev Immunol,* 14**,** 529-45.

ZANKER, D., WAITHMAN, J., YEWDELL, J. W. & CHEN, W. 2013. Mixed proteasomes function to increase viral peptide diversity and broaden antiviral CD8+ T cell responses. *J Immunol,* 191**,** 52-9.

ZHU, M., CHIN, R. K., TUMANOV, A. V., LIU, X. & FU, Y. X. 2007. Lymphotoxin beta receptor is required for the migration and selection of autoreactive T cells in thymic medulla. *J Immunol,* 179**,** 8069-75.

ZIJLSTRA, M., BIX, M., SIMISTER, N. E., LORING, J. M., RAULET, D. H. & JAENISCH, R. 1990. Beta 2-microglobulin deficient mice lack CD4-8+ cytolytic T cells. *Nature,* 344**,** 742-6.

ZINKERNAGEL, R. M. & DOHERTY, P. C. 1979. MHC-restricted cytotoxic T cells: studies on the biological role of polymorphic major transplantation antigens determining T-cell restriction-specificity, function, and responsiveness. *Adv Immunol,* 27**,** 51-177.

ZINKERNAGEL, R. M. & DOHERTY, P. C. 1997. The discovery of MHC restriction. *Immunol Today,* 18**,** 14-7.

ZLOTOFF, D. A., SAMBANDAM, A., LOGAN, T. D., BELL, J. J., SCHWARZ, B. A. & BHANDOOLA, A. 2010. CCR7 and CCR9 together recruit hematopoietic progenitors to the adult thymus. *Blood,* 115**,** 1897-905.

ZOU, Y. R., SUNSHINE, M. J., TANIUCHI, I., HATAM, F., KILLEEN, N. & LITTMAN, D. R. 2001. Epigenetic silencing of CD4 in T cells committed to the cytotoxic lineage. *Nat Genet,* 29**,** 332-6.

ZUKLYS, S., BALCIUNAITE, G., AGARWAL, A., FASLER-KAN, E., PALMER, E. & HOLLANDER, G. A. 2000. Normal thymic architecture and negative selection are associated with Aire expression, the gene defective in the autoimmune-polyendocrinopathy-candidiasis-ectodermal dystrophy (APECED). *J Immunol,* 165**,** 1976-83.

ZUNIGA-PFLUCKER, J. C., LONGO, D. L. & KRUISBEEK, A. M. 1989. Positive selection of CD4-CD8+ T cells in the thymus of normal mice. *Nature,* 338**,** 76-8.

6.2 Papers arising from thesis

MCCARTHY, N. I., COWAN, J. E., NAKAMURA, K., BACON, A., BAIK, S., WHITE, A. J., PARNELL, S. M., JENKINSON, E. J., JENKINSON, W. E. & ANDERSON, G. 2015. Osteoprotegerin-Mediated Homeostasis of Rank+ Thymic Epithelial Cells Does Not Limit Foxp3+ Regulatory T Cell Development. *J Immunol,* 195**,** 2675-82.

COWAN, J. E., MCCARTHY, N. I. & ANDERSON, G. 2016. CCR7 Controls Thymus Recirculation, but Not Production and Emigration, of Foxp3(+) T Cells. *Cell Rep,* 14**,** 1041-8.

COWAN, J. E., MCCARTHY, N. I., PARNELL, S. M., WHITE, A. J., BACON, A., SERGE, A., IRLA, M., LANE, P. J., JENKINSON, E. J., JENKINSON, W. E. & ANDERSON, G. 2014. Differential requirement for CCR4 and CCR7 during the development of innate and adaptive alphabetaT cells in the adult thymus. *J Immunol,* 193**,** 1204-12.

JENKINSON, W. E., MCCARTHY, N. I., DUTTON, E. E., COWAN, J. E., PARNELL, S. M., WHITE, A. J. & ANDERSON, G. 2015. Natural Th17 cells are critically regulated by functional medullary thymic microenvironments. *J Autoimmun,* 63**,** 13-22.

COWAN, J. E. & MCCARTHY, N. I. & ANDERSON, G. 2016. . to be submitted to *J Immunol.* (manuscript assembled, pre-submission).

Additional journal publications

WYSS, L., STADINSKI, B.D., KING, C.G., SCHALLENBURG, S., MCCARTHY, N.I., LEE, J.Y., KRETSCHMER, K., TERRACCIANO, LM., ANDERSON, G., SURH, C.D., HUSEBY, E.S. & PALMER, E. 2016 Affinity for self antigen selects Treg cells with distinct functional properties. *Nature Imm*, 17, 1093-101.